THE STUDY AND CHARACTERISATION OF WATER-BASED LATICES USED FOR CAN COATING INTERIORS

Paul Wright

A thesis submitted for the degree of

Doctor of Philosophy

THE UNIVERSITY OF ASTON IN BIRMINGHAM

March 1995

THE UNIVERSITY OF ASTON IN BIRMINGHAM

The Study and Characterisation of Water Based Latices used for Can Coating Interiors

A thesis submitted for the degree of Doctor of Philosophy

Paul Wright

1995

SUMMARY

Water-based latices, used in the production of internal liners for beer/ beverage cans, were investigated using a number of analytical techniques. The epoxy-graft-acrylic polymers, used to prepare the latices, and films, produced from those latices, were also examined.

It was confirmed that acrylic polymer preferentially grafts onto higher molecular weight portions of the epoxy polymer. The amount of epoxy remaining ungrafted was determined to be 80%. This figure is higher than was previously thought. Molecular weight distribution studies were carried out on the epoxy and epoxy-g-acrylic resins. A quantitative method for determining copolymer composition using GPC was evaluated. The GPC method was also used to determine polymer composition as a function of molecular weight. IR spectroscopy was used to determine the total level of acrylic modification of the polymers and NMR was used to determine the level of grafting.

Particle size determinations were carried out using transmission electron microscopy and dynamic light scattering. Levels of stabilising amine greatly affected the viscosity of the latex, particle size and amount of soluble polymer but the core particle size, as determined using TEM, was unaffected. NMR spectra of the latices produced spectra only from solvents and amine modifiers. Using solid-state CP/MAS/ freezing techniques spectra from the epoxy component could be observed. FT-IR spectra of the latices were obtained after spectral subtraction of water. The only difference between the spectra of the latices and those of the dry film were due to the presence of the solvents in the former.

A distinctive morphology in the films produced from the latices was observed. This suggested that the micelle structure of the latex survives the film forming process. If insufficient acrylic is present, large epoxy domains are produced which gives rise to poor film characteristics. Casting the polymers from organic solutions failed to produce similar morphology.

Key words: Epoxy-graft-acrylic polymers, latices, can coatings, nuclear magnetic resonance spectroscopy, gel permeation chromatography, dynamic light scattering.

Acknowledgments

The author wishes to express his gratitude to Dr M. Beevers of the University of Aston in Birmingham and Dr R.Good of Holden Surface Coatings for their considerable help. I would also like to thank my employer Holden Surface Coatings for allowing me day release to attend the course and paying all of the fees.

My thanks also to Lesley Tomkins of Birmingham University for recording the electron micrographs and to Mike Perry of Aston University for recording the NMR spectra.

My final thanks are to my wife, Gail, who has supported me through all of my studies.

Contents **Page**

Thesis Summary 2

Acknowledgements 3

List of Tables 11

List of Figures 15

Chapter 1. Introduction

1.1 Can Coatings 17

1.2 Aims of the project 17

Chapter 2. Review

2.1 Coatings introduction 20

2.1.1 Epoxy-graft-acrylic 21

2.1.2 Epoxy-acrylic esters and phosphates 22

2.1.3 Epoxy-acrylic monomers 23

2.1.4 Epoxy-amine anhydrides 23

2.1.5 Epoxy-poly (ethylene glycol) 25

2.1.6 Acrylic and acrylic modified polymers 26

2.1.7 Epoxy ester polymers 27

2.2 Polymer characterisation

2.2.1 Nuclear Magnetic Resonance Spectroscopy

(a) Epoxy resins 28

(b) Phenolic resins 28

(c) Amino resins 30

(d) Polyester resins 31

(e) Acrylic resins 31

(f) Solid state and mobility studies 32

2.2.2 Gel Permeation Chromatography 35

(a) Calibration for molecular weight distribution analysis 36

(b) Polymer characterisation 38

(c) Copolymer characterisation 39

(d) Multi-wavelength UV detectors 43
(e) Multi-component analysis 44
(f). Liquid Chromatography 46

2.3 Colloidal studies

2.3.1 Transmission electron microscopy 47
2.3.2 Dynamic light scattering 49
2.3.3 Infra-red Spectroscopy 54

2.4 Film characterisation

2.4.1 Film formation

(a) Evaporation of water from films 55
(b) Mechanisim of film formation 56
2.4.2 Transmission electron microscopy 60

Chapter 3. Sample preparation

3.1 Introduction 64

3.2 Sample preparation

3.2.1 Experimental resins PW1 and PW2 65
3.2.2 Experimental resins WRB621, 622, 623 and 624 67
3.2.3 46900 type latices (phenolic cross-linking) 68

Chapter 4. Polymer characterisation: Experimental

4.1 Infra-red Spectroscopy

4.1.1 Introduction 69
4.1.2 Assignment of IR absorbance bands 69
4.1.3 Calibration 70
4.1.4 Sample analysis 70

4.2 Nuclear magnetic resonance spectroscopy

4.2.1 Epoxy resins 71
4.2.2 epoxy-graft-acrylic 71
4.2.3 Epoxy-PMMA mixtures 71

4.3 Solvent fractionation

4.3.1 Introduction 72

4.3.2 Soxhlet extraction 72

4.3.3 Liquid-liquid extraction 73

4.4 Gel Permeation Chromatography

4.4.1 Introduction 73

4.4.2 GPC instrumentation

(a) GPC system 1 74

(b) GPC system 2 75

4.4.3 Customised data station

(a) System requirements 75

(b) Data reprocessing: a procedure 75

(c) Flow time corrections 76

4.4.4 Molecular weight distribution analysis

(a) Column calibration 77

(b) Sample analysis 77

4.4.5 Copolymer analysis

(a) Sample response factors using GPC 78

(b) Injection reproducibility 79

(c) Simple polymers system 79

(d) Epoxy-graft-acrylic polymers 80

4.4.6 Derivatization

(a) Introduction 81

(b) Analysis of a simple system 81

(c) Epoxy-g-Acrylic polymers 82

Chapter 5. Polymer Characterisation: Results

5.1 Infra-red spectroscopy

5.1.1 Characteristic absorbance bands 83

5.1.2 Calibration for 'acrylic' determination 85

5.1.3 Sample analysis 86

5.2 Nuclear magnetic resonance spectroscopy

5.2.1 Proton NMR spectra of epoxy resins 88

5.2.2 Carbon-13 NMR spectra of epoxy resins 91

5.2.3 Effect of solvent on the Carbon-13 NMR spectrum 94

5.2.4 Proton NMR spectra of epoxy-g-acrylic samples 94

5.2.5 Carbon-13 NMR spectra of epoxy-g-acrylic samples 95

5.3 Solvent fractionation

5.3.1 Soxhlet extractions 97

5.3.2 Liquid-liquid extractions 101

5.4 Gel permeation chromatography: Molecular Weight Distribution Analysis

5.4.1 Instrument conditions 105

5.4.2 Calibration 105

5.4.3 Sample analysis 109

5.5 Gel permeation Chromatography: Copolymer analysis

5.5.1 Introduction 111

5.5.2 Determination of response factors 112

5.5.3 Injection reproducibility 113

5.5.4 Simple systems

(a) Epoxy:polystyrene 116

(b) Epoxy:polystyrene:poly(methyl methacrylate) 118

(c) Epoxy:polyester 121

(d) Epoxy:phenolic 123

5.5.5 Epoxy-g-acrylic analysis 126

5.5.6 Derivatization 131

5.5.7 DMF system 134

Chapter 6. Colloid studies: Experimental

6.1 Determination of particle size: Comparison of techniques

6.1.1 Dynamic light scattering 137

6.1.2 Transmission electron microscopy 139

6.2 Rheology 139

6.3 Nuclear magnetic resonance spectroscopy 140

6.4 Infra-red spectroscopy

6.4.1 Introduction 141

6.4.2 Latex and polymer solutions 141

6.4.3 Cast films 142

6.5 Centrifuge

6.5.1 Introduction 143

6.5.2 Sample preparation 143

6.5.3 Polymer content determinations 143

6.5.4 IR analysis 144

6.5.5 GPC analysis 144

Chapter 7. Colloid studies: Results

7.1 Particle size determinations

7.1.1 Dynamic light scattering 145

7.1.2 Transmission electron microscopy 152

7.2 Rheology

7.2.1 Initial samples 157

7.2.2 Effect of pH upon viscosity 158

7.2.3 Effect of concentration upon viscosity 162

7.3 NMR 164

7.4 Infra-red 168

7.5 Centrifuge

7.5.1 Determination of soluble polymer 173

7.5.2 Chemical composition 176

7.5.3 GPC analysis of soluble polymer 180

7.5.4 46900 latex (phenolic cross-linked polymer) 181

Chapter 8. Film characterisation: Experimental

8.1 Introduction 186

8.2 Film application and stoving conditions 187

8.3 **Removal of films from substrate** 188
8.4 **TEM analysis** 188

Chapter 9. Film characterisation: Results

9.1 **Introduction** 189
9.2 **Examination of films cast from latices** 189
9.3 **Examination of films cast from solution** 191

Chapter 10. Discussion

10.1 **Determination of grafting levels** 194
10.2 **Grafting of acrylic upon high molecular weight epoxy resin** 198
10.2.1 GPC using selective detection 200
10.2.2 Non-size exclusion GPC separation 202
10.2.3 Solvent extraction 202
10.3 **Particle size data** 203
10.4 **Rheology and soluble polymer data** 207
10.5 **Latex stability and film morphology** 210

Chapter 11. Conclusions and proposed further work 212

Appendices

Appendix 1 Coupling constants for epoxy resins 215
Appendix 2 Empirical parameters for chemical shift calculations 218
Appendix 3 Basic matrix algebra
3.1 Multiplication 220
3.2 Definitions 220
3.3 Inversion 222

(a) 2x2 Matrix 222
(b) 3x3 Matrix 222
3.4 K-matrix approach 222
3.5 Over-determination 223

Appendix 4 Equations used in copolymers analysis

4.1 Two-component system
(a) Calibration 225
(b) Analysis 226
4.2 Three-component system
(a) Calibration using simultaneous equations 227
(b) Analysis using simultaneous equations 228
(c) Calibration using matrices 230
(d) Analysis using matrices 231
4.3 Four component system using matrices 233

Appendix 5 Errors

5.1 Source of errors
(a) Calibration step using standard mixtures 237
(b) Calibration using single standards 240
5.2 Error minimisation 240
(a) Sum of errors: 2 component system 241
(b) Sum of errors: 3 component system 244

Appendix 6 MWD calibration curves 246
Appendix 7 Particle size determination using TEM: raw data 252
Appendix 8 Particle size using the DLS from autocorrelation function 255

Abbreviations 260

References 261

Index of Tables

Chapter 3. Sample preparation

3.1	Molecular weight data of epoxy resins	64
3.2	Latex formulations	65
3.3	PW1 and PW2 base-polymer composition	66
3.4	PW1 and PW2 latex composition	66
3.5	Composition of epoxy-graft-acrylic formulations	68

Chapter 5. Polymer characterisation: Results

5.1	Assigned IR absorbance bands from spectra of polymers and latices	83
5.2	Composition of mixtures used for IR calibration	85
5.3	Linear regression data from IR calibration data	86
5.4	IR absorbance ratios for base-polymers and latices	86
5.5	Calculated composition of epoxy-g-acrylic polymers using IR data	87
5.6	Assignment of proton chemical shifts for epoxy resins	90
5.7	Proton NMR peak intensities for various epoxy resins	90
5.8	Assignment of carbon-13 chemical shifts for epoxy resins	93
5.9	Data from carbon-13 NMR spectra of epoxy resins	93
5.10	Effect of solvent upon carbon-13 NMR spectra of epoxy resins	94
5.11	Data from proton NMR spectra of epoxy resins	95
5.12	Data from carbon-13 NMR for various epoxy-g-acrylic formulations	95
5.13	MWD results from Soxhlet extracted '9' type epoxy resin	97
5.14	Soxhlet and liquid-liquid extraction efficiencies	98
5.15	MWD results from Soxhlet extraction of epoxy-g-acrylic polymer	100
5.16	MWD results from liquid/liquid extraction of epoxy-g-acrylic polymer	101
5.17	Composition of aqueous layer from liquid/liquid extraction using IR data	103
5.18	Retention time of standards used in GPC calibration curves	107
5.19	Calculated Mp values of standards using linear regression.	108
5.20	Residuals between actual and calculated Mp values	109
5.21	MWD analysis of polymers using GPC	110
5.22	Calculated response factors of various polymers using GPC	113
5.23	Peak area data for injection reproducibility studies	115
5.24	GPC injection reproducibility studies	115

5.25 Calculated composition of epoxy/ polystyrene blend 116
5.26 GPC response factors of epoxy, polystyrene and PMMA 119
5.27 Calculated composition of epoxy/ polystyrene/ PMMA blends 119
5.28 Calculated response factors of epoxy and polyester polymers 121
5.29 Calculated composition of epoxy/ polyester systems 123
5.30 Calculated response factors of epoxy and phenolic polymers 124
5.31 Calculated composition of epoxy/ phenolic blend and copolymer 124
5.32 Response factors of epoxy/ polystyrene/ PMMA 126
5.33 Calculated composition of epoxy-graft-acrylic polymers 127
5.34 Calculated composition of graft polymers using 'acrylic' response factor 128
5.35 GPC response factors used in 'two component' calculation 128
5.36 Composition of graft polymers using 'two component' calculation 129
5.37 Response factors of derivatized and non-derivatized components 132
5.38 Calculated composition using GPC derivatization techniques 132
5.39 GPC peak area data for polymers analysed using 'DMF' system 136

Chapter 7. Colloid studies : Results

7.1 Particle size data of polystyrene sulphonate standard using DLS 145
7.2 Particle size data of WRB625 latex using DLS 147
7.3 Particle size data of latex samples using DLS 148
7.4 Particle size data of latices in different diluents using DLS 149
7.5 Particle size data of WRB633 using DLS. Effect of addition of DMAE 151
7.6 Particle size data of WRB633 using DLS. Effect of addition of HCl 151
7.7 Particle size data of WRB633 using DLS. Effect of addition of HCl to a sample neutralised with DMAE 152
7.8 Particle size data of various latices using TEM. 154
7.9 Particle size data using TEM. Dilution in DMAE solution 154
7.10 Composition and viscosity data of latex formulations. 157
7.11 Viscosity data for diluted latex samples. 158
7.12 Viscosity data for WRB625 diluted in various DMAE concentrations. 159
7.13 Viscosity data for WRB633 diluted in various DMAE concentrations. 161
7.14 Effect of Latex concentration upon viscosity 162
7.15 Assignment of bands in carbon-13 NMR spectrum of GEN 1 latex 164
7.16 Assignment of bands in carbon-13 NMR spectrum of solvents and amines 166

7.17 IR C-H str. frequencies of various samples 170
7.18 Soluble polymer determinations using centrifugation 174
7.19 Effect of pH upon soluble polymer levels 176
7.20 Preparation details of polymer blends used in IR calibration 178
7.21 Calculated compositions of latex samples using IR data 178
7.22 MWD results for initial latex and soluble polymers 180
7.23 Soluble polymer determinations of 46900 latex using centrifugation 181
7.24 GPC peak area peak area data for 46900 latex 182

Chapter 8. Film formation: Experimental

8.1 Polymer formulations 186

Chapter 9. Film formation: Results

9.1 Measured particle size of latices using TEM 190

Chapter 10. Discussion

10.1 Levels of ungrafted epoxy 194
10.2 MWD results from toluene Soxhlet 195
10.3 MWD results from GPC data 196
10.4 MWD results from liquid-liquid extractions 197
10.5 Particle size data of latex samples 204
10.6 Particle size data of diluted samples 206
10.7 Effect of DMAE upon particle size of WRB633 207
10.8 Latex composition and viscosity 208
10.9 Viscosity of latices 209
10.10 Effect of neutralisation upon viscosity 209

Appendices

A1 Peak assignments in proton NMR spectra of a 'liquid' epoxy 215
A2 Chemical shift changes for substituted aromatic carbon atoms 218
A3 Carbon-13 NMR chemical shifts for aromatic carbon atoms 219
A4 GPC response factors of epoxy and polystyrene using UV detection. 223
A5 GPC 'over-determination' calculation. 223
A6 GPC response factors. Worked example for a three component system. 229

A7	GPC response factors. Worked example for a four component system.	234
A8	Error analysis: Example 1	238
A9	Error analysis: Example 2	239
A10	Error analysis: Example 3	240
A11	Sum of errors for a 2-component system. Example data 1.	242
A12	Sum of errors for a 2-component system. Example data 2	243
A13	Sum of errors for a 2-component system. Example data 3.	244
A14	GPC response factors. Example data for a 3-component sum of errors.	244
A15	Sum of errors for a 3-component system.	245
A16	GPC retention times of polystyrene molecular weight standards	246
A17	Calculation of ΣX_i, ΣY_i, ΣX_i^2, ΣX_i^3, etc for regression analysis	251
A18	Calculated particle diameter for latices diluted in water	253
A19	Particle diameter for latices diluted in water and 2% aq. DMAE	254
A20	DLS spreadsheet, particle size standard	258

Index of Figures

Chapter 2. Can coatings

2.1 Micelle structure of latex 20

2.2 Reaction of epoxy-amine adduct with succinic anhydride 24

2.3 Acid catalysed cleavage of epoxide groups 25

2.4 Carbon-13 NMR assignments for 4-(1'-heptanonyl) benzene sulphonate 34

2.5 Proton NMR assignments for 4-(1'-heptanonyl) benzene sulphonate 34

2.6 Hydrazine/osmium tetroxide reaction 61

Chapter 3. Sample Preparation

3.1 Chemical Structure of epoxy resins 64

Chapter 4. Polymer characterisation: Experimental

4.1 Structure of o-[p-nitrobenzyl]-N,N(diisopropyl) isourea (NBDI) 81

Chapter 5. Polymer characterisation: Results

5.1 IR spectra (a) WRB621 epoxy-g-acrylic resin and (b) WRB625 latex 84

5.2 Structure of epoxy resin with proton atoms labelled 88

5.3 Proton NMR spectra of Epikote's (i) 828, (ii) 1001 and (iii) 1009 89

5.4 Carbon-13 NMR spectra of Epikote's (i) 828, (ii) 1001 and (iii) 1009 92

5.5 Structure of epoxy resin with carbon atoms labelled 91

5.6 IR spectra of toluene Soxhlet extracts from WRB621 99

5.7 GPC profiles of (a) WRB621 and (b) organic layer from L/L extract 102

5.8 IR spectra of liquid-liquid extractions of WRB621 104

5.9 (a) GPC chromatogram of polystyrene molecular weight standards and (b) GPC molecular weight calibration curve 106

5.10 GPC UV response factors of various polymers 114

5.11 GPC profiles from epoxy plus polystyrene blends 117

5.12 GPC profiles from epoxy, polystyrene and PMMA blends 120

5.13 GPC profiles from epoxy-polyester copolymers 122

5.14 GPC profiles from epoxy-phenolic copolymers 125

5.15 GPC profiles of epoxy-g-acrylic polymers 130

5.16 GPC profiles of derivatized epoxy-g-acrylic samples 133

5.17 GPC profiles from DMF system 135

Chapter 7. Colloid Studies, Results

7.1 DLS results for polystyrene sulphonate particle size standard 146
7.2 Effect of neutralisation on particle size of latices 150
7.3 TEM micrographs of latices 155
7.4 Histogram plots of particle size data from TEM results 156
7.5 Effect of neutralisation on viscosity of latices 160
7.6 Effect of concentration upon the viscosity of latices 163
7.7 Carbon-13 NMR spectra of (a) latex and (b) epoxy resin in solution 165
7.8 Carbon-13 NMR spectra of DMAE and CP-MAS spectrum of latex 167
7.9 IR Spectra of water and latex 171
7.10 IR spectra of latex after spectral subtraction of water 172
7.11 Effect of degree of neutralisation upon level of soluble polymer 175
7.12 IR calibration data 175
7.13 IR spectra of WRB625 latex and centrifuged soluble portion 179
7.14 GPC profiles of WRB625 latex and centrifuged soluble portion/46900 184
7.15 GPC profiles of ML97 (phenolic) at various UV wavelengths 185

Chapter 9. Film Characterisation, Results

9.1 TEM micrographs of films produced from latices 192
9.2 TEM micrographs of films produced from latices and from solution 193

Chapter 10. Discussion

10.1 GPC profiles of WRB621 and deconvoluted data 199
10.2 GPC profiles of samples (a) using 'DMF system' (b) GPC profiles of centrifuged latex samples and (c) & (d) liquid-liquid extracted samples 201

Appendices

A1 Chemical structure of epoxy resin with proton atoms labelled 215
A2 Proton NMR spectrum of epoxy resin 217
A3 Chemical structure of the repeat unit of an epoxy resin 218
A4 DLS data from particle sze standard 257

CHAPTER 1. INTRODUCTION

1.1 Can Coatings

A major use of epoxy resins has been as a component in surface coating formulations. They provide the coating with toughness, flexibility and chemical resistance. Such coating systems, have been prepared as solutions in organic solvents and formulated with curing agents and flow additives. The internal coating applied to beer/beverage cans are examples of such formulations. The lacquers are sprayed onto the interior walls of the cans which are then passed through a conveyer oven to cross-link the coating releasing the volatile constituents into the atmosphere.

The Control of Substances Hazardous to Health (COSHH) [1] Regulations require control and monitoring of harmful substances in the atmosphere. Some low volatile organic content (VOC) systems have lead to less expensive coated articles with no effects upon performance. The means of achieving low VOC systems include use of powder coatings, high 'solid-content' coatings, reactive diluent coatings and water-borne coatings.

1.2 Aims of the project

The ability of surface coatings to prevent physical contact between metal containers and their contents, so as to reduce undesirable interactions is an important requisite of the food and packaging industry. The effectiveness of surface coatings depends not only on the mechanical and chemical properties of the coatings, but also depends on the nature of the physico-chemical interactions at the surface between the metal and the coating and at the interface between the can contents and the coating. Properties of a surface coating lacquer for use as an internal coating for beer and beverage cans should include good wetting of the metal substrate, a known minimum film forming temperature, good adhesion of the cured coating to the substrate and provide an effective barrier against

chemical attack and migration through the film. Migration through the coating may occur in either direction. Components from the can contents may migrate through to the substrate. Oil and other lubricants used during manufacture and process of the substrate but still present during the coating of the can may affect the wetting performance of the lacquer and migrate through the film contaminating the can contents.

In recent years there has been an increasing desire to move away from coating formulations that contain high proportions of organic solvents to those based on water dispersible polymers in the form of emulsions. Although it is known that these emulsions are micellar in nature much work still remains to be done in determining the structure and properties of the micelles and establishing how the physical properties of the micelles and the resultant coatings are governed by the structures of their constituent molecules.

The proposed research project was divided into three areas.

1. Characterisation of the polymers

This area of the project was concerned with the characterisation of an existing water-dispersible formulation, the Glidden patented epoxy-acrylic-graft polymer, known as ' GEN 1' [2]. Analytical techniques used for this work included;

(a) Gel permeation chromatography (GPC) which provided basic molecular weight data of the various components in the lacquer.

(b) Infra-red and nuclear magnetic resonance spectroscopy (NMR) which determined chemical composition and structural information, and

(c) Selective solvent precipitation to physically separate the various resin components followed by spectroscopic analysis.

Once the analytical methods had been established, results obtained from the GEN 1 material were compared to results obtained from formulations based on ICI World Packaging Group technology.

2. Structural studies of the dispersed latex

The objective of this second area of the project was to determine the structure and macroscopic organisation of the micelles. Again analytical results obtained from GEN 1 material was compared to results from modified versions of the basic formulation.

Particle size determinations were carried out using dynamic light-scattering equipment based at Aston University. Rheological studies on the latex were also carried out.

3.Film formation

The effect of chemical composition and micellar structure on the appearance of the cured film and its effectiveness as a barrier was examined. The films were initially examined using transmission electron microscopy (TEM) with prior staining to show any fine structure which may be present. Films were also cast from solution and compared with those films cast from dispersion.

CHAPTER 2. LITERATURE REVIEW

2.1 Introduction to coatings

Water-borne coatings are commonly used for lining cans which are to be filled with beer and beverages. To produce a water dilutable polymer, which forms an effective film barrier which is resistant to water, modified hydrophobic polymers are used. This has lead to a wide variety of approaches to achieve water soluble or water dilutable polymers [3]. Many of the formulations produced have the appearance of emulsions and it has been speculated that the droplets formed consist of micelles with a hydrophobic interior and an exterior coated with ionised carboxylic acid groups stabilised by counter ions in the water phase. This structure is depicted in Figure 2.1.

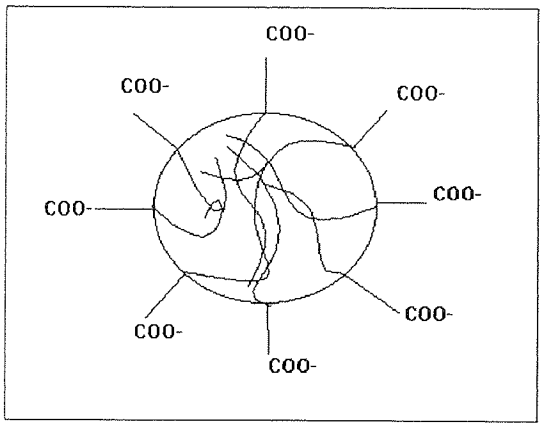

Figure 2.1. Micelle structure of typical water reducible polymers

Since 1979 patents have been published detailing formulations of water-dispersible materials for use as liners for the interiors of cans for beer and other beverages. The chemical composition of such formulations can be grouped into seven main types: epoxy-graft-acrylic polymers, epoxy-acrylic esters and epoxy-phosphates, polymers prepared using epoxy monomers with acrylic functionality, epoxy-amine-anhydride

formulations, epoxy-polyethylene glycol polymers, acrylics and epoxy-esters. Each of these will be discussed in more detail.

2.1.1 Epoxy-Graft-Acrylic

A typical formulation would consist of a high molecular weight epoxy resin with an acrylic addition polymer grafted onto the epoxy back-bone [2,4]. The acrylic addition polymer contains carboxylic acid at a sufficiently high level to produce a dispersion in a basic aqueous medium that would ionise the acid functional polymer. The site of the graft on the epoxy resin has been established, using NMR spectroscopy, as occurring on the aliphatic carbons of the epoxy resin [5]. After grafting, the product will consist of: epoxy-acrylic graft copolymer, ungrafted acrylic addition polymer and ungrafted epoxy resin.

To produce the required characteristics in the finished coating, it was found necessary for the molecular weight of the initial epoxy resin to be in the range 4000 to 10,000. The epoxy resin used was produced by reacting 4,4'-isopropylidene diphenol (commercial names include Bisphenol A, BPA and DPP) with a low molecular weight 'liquid' epoxy resin e.g. DER333 (a process commonly referred to as LUG i.e. liquid up-grade) or using preformed high molecular weight material. Acrylic monomers investigated include methacrylic acid, ethyl acrylate and styrene. The latter is generally used as an extender. To achieve stability in the final water dispersed product the Acid Number of the graft resin should be 85 i.e. 13% by weight of total solids. Benzoyl peroxide at a level of 6 to 7% was the catalyst used. Ester type grafting was found to occur if the level of catalyst is less than 3%. To eliminate the possibility of ester type grafting, part or all of the terminal epoxide groups may be capped [6]. Materials used for such a process include phenols, carboxylic acids, primary and secondary amines, thiols, alcohols and water.

To produce higher solid content dispersions, ethylenic monomers can be polymerised, after the dispersion has been formed, using benzoyl peroxide catalyst [7,8,9]. A grafting base resin can be produced by 'advancing' an epoxy resin in the presence of an extender resin, followed by addition of unsaturated monomers and grafting [10]. The proportion of organic solvent may be further reduced by in-situ polymerisation.

Soft drinks containing acid ingredients are particularly harsh on the coating for interiors for cans. Greater coating thickness are required for steel cans, to prevent tainting of the beverage, than for aluminium cans. Epoxy-graft-acrylic type dispersions blended with epoxy-phosphate ester dispersions have much improved corrosion resistance over the individual components [11,12].

Coating materials for can interiors have been prepared using ethyl acrylate/ methacrylic acid/styrene/N-isobutoxy methyl acrylamide copolymers grafted onto epoxy resins. The formulation is dispersed in dimethyl amino ethanol (DMAE)/ water mixtures and uses urea/formaldehyde and phenolic resins for cross-linking the coating [13].

2.1.2 Epoxy-Acrylic Esters and Epoxy Phosphates

A slightly different approach to grafting is to produce coatings based on self-emulsifiable epoxy ester resins [14]. An epoxy resin, or epoxy-phenolic [15], is reacted with carboxylic acid containing acrylic polymer using an amine catalyst. This polymer may then be dispersed in water. A variation of this formulation is to remove some of the oxirane functionality during the liquid up-grade process prior to reaction with the acrylic polymer [16]. The epoxy resin may be either reacted with acrylic copolymer or just physically blended. Typical acrylic formulations include ethyl acrylate /methacrylic acid /styrene[17-24], acrylic acid or methacrylic acid[25]/styrene/N-isobutoxy methyl acrylamide [26]

and acrylic acid/styrene/N-ethoxy methyl acrylamide [27]. Dimethyl amino ethanol and triethyl amine salts of acrylic copolymers have also been used [28,29].

A formulation based on n-butyl maleate modified epoxy resins followed by 'in-situ' polymerisation of styrene also produces materials suitable for can coatings [30,31].

Aqueous epoxy-phosphate dispersions have been formulated as coatings for container interiors [32]. The dispersions used hexamethoxymethyl melamine (HMMM) as the film cross-linker with n-butanol, n-hexanol and 2-butoxy ethanol as the solvents. Epoxy-phosphate copolymers can also be reacted with methacrylic acid/styrene/ ethyl acrylate copolymers [33] or blended with ethyl acrylate/methacrylic acid/styrene/N-iso butoxy methyl acrylamide copolymers [34]. Both of these formulations used an amino resin as the cross-linker and formed useful protective coatings.

2.1.3 Epoxy-Acrylic monomers

Emulsion polymers, useful as coatings, may be produced by polymerising an acrylic monomer mixture, containing an oxirane functional acrylic monomer, in an aqueous medium in the presence of a surfactant. Such dispersions were found to be capable of producing cross-linked coatings by either addition of amine[35] or low molecular weight epoxy resin[36]. A water-soluble formulation was produced by reacting the oxirane functional acrylic monomers in organic solvents, followed by reaction with 3-mercapto-1,2,4 triazole, prior to dilution in water [37].

2.1.4 Epoxy-Amine-Anhydrides

Polyepoxide resins are reacted with amines which are then further reacted with cyclic dicarboxylic acids [38,39]. The resulting resinous products can be dispersed in a basic aqueous medium. The epoxy-amine adduct is reacted with maleic or succinic anhydride

under such conditions where the anhydride-amine reaction is promoted and the anhydride-hydroxyl reaction minimised. This is achieved if the reaction is carried out between 20°C and 100°C, preferably 40°C. The anhydride ring opens forming an amide group and a pendant carboxylic acid group. The reactions are shown in Figure 2.2.

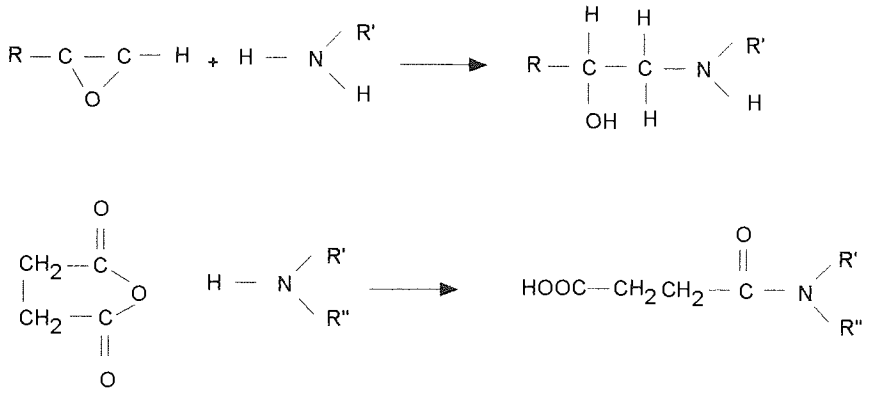

Figure 2.2. Reaction of epoxy-amine adduct with succinic anhydride

For optimum film performance it was determined that the epoxy resin, derived from a dihydric phenol and epichlorohydrin, should have a molecular weight between 450 and 4000. The amine is an alkyl primary mono-amine or a polyamide having at least two amine nitrogen atoms per molecule and at least three amine hydrogen atoms per molecule. The amine should have no other groups that could react with the epoxy. In the composition, about 1 mole of the amine is reacted with each epoxide equivalent of the epoxy resin and between 0.5 and 1.0 moles of maleic or succinic anhydride is reacted per amine nitrogen atom in the adduct.

This formulation may be modified to incorporate acrylic copolymer containing ethyl acrylate/ styrene/N-ethoxy methyl acrylamide /methacrylic acid. Amine, phenolic and amino resin cross-linkers are added before the final dispersion into water [40]. To

aminate and to provide carboxylic acid functionality the epoxy resin can be reacted with p-aminobenzoic acid. The polymer may then be dispersed into a water/amine medium [41].

The addition of a low molecular weight water insoluble epoxide cross-linker to a epoxy-amine adduct reportedly improves storage stability and film forming properties [42]. Excess amine is removed by distillation. When the two components are mixed with simple stirring the mix becomes opaque and viscous. However, with continuous stirring, after a minute or two, the mixture becomes translucent or transparent as a micro-emulsion forms. The micro-emulsions have the appearance of true solutions but exhibit light scattering. The solvent balance of the final latex should contain low boiling point solvents (<160^{0}C) to lower the surface tension and a high boiling point solvent (>160^{0}C) to aid coalescence of the film.

2.1.5 Epoxy-Polyethylene Glycol Formulations

Epoxy-polyethylene glycol formulations are prepared by the reaction between epoxy resins and polyethylene glycol using a phosphoric acid catalyst[43,44]. The composition of the formulations can be varied between: 55 to 90% Epoxy (MW 800 to 2500), 8 to 44% poly(ethylene glycol) (MW 300 to 2000) and between 1 to 2% phosphoric acid catalyst. The acid catalysed cleavage of epoxide groups is shown in Figure 2.3

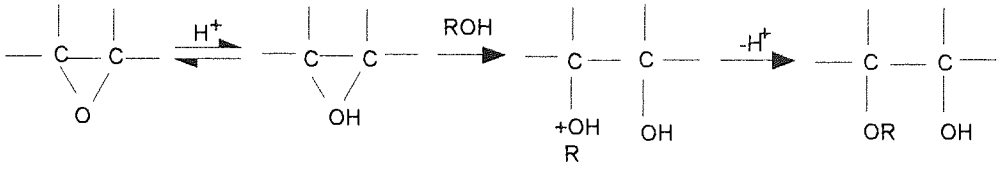

Figure 2.3. Acid catalysed cleavage of epoxide groups

The reaction is carried out at 100 to 150^{0}C. Most of the epoxide groups react either with the glycols to form ether groups or with the phosphoric acid to form monoesters. Water at a level between 0.6% and 2% is needed for the reaction to go to completion. Below this level there is insufficient hydrolysis of the di- and tri- phosphoric acid esters to mono-phosphoric acid esters. When di- and tri- esters are present there is insufficient acidity to catalyse the epoxide-hydroxyl reaction. If water is present at a higher level it competes with the glycol for reaction with the epoxide groups.

Amines e.g. DMAE can be used to salt the phosphoric acid ester terminated compositions. Preferably one to two moles of base are used per mole of reacted acid. To produce coating compositions amino resins can be added to the final dispersion at levels of 5 to 40% weight percent. Such formulations, although suitable for use on flexible substrates, cannot be deep drawn on metal substrates without some failure. The flexibility may be increased by addition of an aqueous dispersion of an epoxy resin produced by reacting 'liquid epoxy resin', Bisphenol A and polyoxyethylene glycol [45].

2.1.6 Acrylic and Acrylic modified Formulations

Water dispersible formulations may be prepared by dispersing N-iso butoxy methyl acrylamide /acrylonitrile/acrylic acid copolymers in a DMAE/water medium [46] or by dispersing a mixture of maleic acid/ vinyl acetate/vinyl chloride copolymer and glycidyl methacrylate/ vinyl acetate/vinyl chloride copolymer [47].

Water dispersible core-shell polymers prepared by a two stage process are useful as coatings for beverage-can ends. Styrene, ethyl acrylate, methacrylic acid and N-iso butoxy methacrylamide are polymerised in a pre-emulsion of styrene/ethyl acrylate [48].

Aqueous dispersions, useful for can liners may be prepared by polymerising acrylic monomers, containing some carboxylic acid functionality, in the presence of an amino resin solution [49]. Epoxy resin is then added. The carboxylic acid present is neutralised by

addition of amine e.g. DMAE followed by addition and dispersion in water. There is some evidence that during the course of the vinyl polymerisation reaction some interaction does occur between one or more of the monomer constituents and the amino resin. Acrylic monomers used include methacrylic acid, ethyl acrylate and styrene with benzoyl peroxide or tricersyl phosphate catalyst. The epoxy resin used had an epoxide equivalent weight of 2700.

2.1.7 Epoxy-Ester Formulations

An Epoxy resin prepared using the 'liquid up-grade' process is reacted with pelargonic acid ($CH_3(CH_2)_7CO_2H$). The polymer is then reacted with neo-pentyl glycol followed by trimellitic anhydride. The resultant epoxy-polyester is neutralised with ammonia and diluted in water [50].

2.2 Polymer Characterisation

2.2.1 Nuclear Magnetic Resonance Spectroscopy

Nuclear magnetic resonance was first used in the characterisation of polymers within a year of the first reports of the NMR phenomenon [51]. Proton NMR has been useful in both qualitative and quantitative analyses of materials used in the coatings industry [52]. Spectra of solvents e.g. acetone and 2-butanone, and polymers e.g. alkyd, acrylic and polyester resins were recorded. Mole ratios calculated from the integrated peak areas were in good agreement with theoretical values. The analysis of epoxy, phenolic, amino, polyester, alkyd and acrylic resins are of particular importance to the coatings industry and this project. The following review of the literature concentrates on these polymer systems.

(a) Epoxy resins

Carbon-13 NMR was used to study the curing of an epoxy resin using piperidine [53], dicyandiamide [54] and various amines and diamines [55]. In the latter reference the aromatic carbon atoms appear to be incorrectly assigned. Chemical shift values of all carbon nuclei were assigned [53]. Carbon-13 NMR was used to locate grafting sites during the reaction between a high molecular weight epoxy resin and acrylic monomers [5,56]. Using model compounds the location of grafting was identified as the methylene carbon α- to the hydroxyl carbon. A decrease in the signal of this carbon was observed with increasing levels of initiator. This decrease in signal was less obvious in the polymer samples and it should be noted that some of the aromatic carbons were incorrectly assigned. High temperature magic angle spinning was used to study the chain extension reaction of diglycydyl ether of Bisphenol A (DGEBPA) with Bisphenol A (4,4'-isopropylidene diphenol, BPA) [57]. When the mole ratios are equivalent the phenolic hydroxyl of BPA opens the epoxy end groups of DGEBPA to form linear polymers. If the reaction is deficient in BPA there are not enough phenolic hydroxyls to react with all the epoxy groups. This allows the epoxy groups to be ring opened by the secondary hydroxyl groups which are present along the polymer backbone. Each of these reactions constitutes a branch point. At 25^0C the amorphous polymer gives a poor spectrum. The spectrum sharpens at 100^0C. At 150^0C the spectrum degrades due to interference between polymer motion and either MAS or proton decoupling. At 200^0C the spectrum appears similar to that obtained in solution.

(b) Phenolic Resins

Phenol-formaldehyde resins fall into two main classes: novolaks, prepared in the presence of excess phenol and resoles prepared in the presence of excess formaldehyde.

Novolaks consist of phenolic nuclei linked by methylene bridges at ortho-, para and meta positions relative to the hydroxyl.

Proton NMR spectra of model compounds, phenol formaldehyde dimers and trimers, were used to interpret spectra of linear novolak phenol-formaldehyde polymers[58]. Chemical shifts of the methylene bridges of dimers and trimers were measured. In all cases there was a shift to lower field as the methylene bridge varied from p-p, o-p to o-o.

Analysis using carbon-13 NMR gives a quantitative measure of the isomer ratios as well as the average molecular weight [59]. This was achieved by measuring shifts due to end groups and those in the central repeat unit.

In order to understand carbon-13 NMR spectra of phenolic resins the spectra of purified oligomers were examined. The phenoxy region of the spectrum was found to yield information as to the amount of free phenol, concentration and types of end and middle groups and the concentration of branching centres [60]. Model compounds were prepared that represented the various types of methylene bridges that are possible during formation of novolak polymers [61]. The methylene bridges were characterised and assignments made to analyse spectra of cresol-formaldehyde polymers.

Resoles are more complex than novolaks containing methylene and methylene ether linkages as well as -CH_2OH and CH_2OCH_2OH groups. Proton signals from the methylene groups in the diphenyl methane linkages and methylene from the dibenzyl ether linkages can easily be resolved and quantitative information regarding the species present. Regions of chemical shifts for aromatic, methylene and methylene ether bridges were assigned [62].

Proton NMR was used to study the effect of catalyst on the structure of the phenol formaldehyde resin produced [63]. Triethyl amine was found to favour methylene ether bridges whilst sodium hydroxide favoured methylene bridges. GPC was used to determine the molecular weight distribution of the polymers produced.

(c) Amino Resins

Formaldehyde reacts with melamine in aqueous solution to give a mixture of methylolamines. Up to six molecules of formaldehyde can add to a molecule of melamine to make adducts ranging from mono- to hexa-methylolmelamine. In all, nine methylol-melamines are possible. Carbon-13 NMR spectra of mixtures of adducts exhibit several azine carbon peaks [64]. Peaks were assigned to six of the nine possible methylolmelamines. The areas of the peaks were used to estimate the relative proportions of mono-, di- and trimethylolmelamines in the mixtures.

Urea-Formaldehyde resins were examined using carbon-13 NMR, Low Field FT Proton NMR and Low and High Field continuous wave spectrometers [65]. To obtain quantitative measurements from the carbon-13 spectra 'chromium acac' was added to the samples to reduce the NOE and gated decoupling was then used to remove residual nuclear Overhauser enhancement (NOE). Signals due to mono-substituted amide, non-substituted amide, hydroxyl methylene and methoxyl were also identified and measured. Good agreement was found between the data derived from the carbon-13 NMR, proton High Field Continuous wave and Low Field FT NMR spectra. Low field continuous-wave proton spectra exhibit poorer resolution and provided inaccurate quantitative data.

Differences between the carbon-13 NMR spectra of commercial grades of urea-formaldehyde resins were observed [66]. It was thought that the technique could be used for quality control and monitoring the production of such polymers. The technique of cross polarisation and Magic Angle Spinning (CP MAS) provides a powerful technique for the analysis of polymers in the solid state [67]. At low field strength (1.41T) a spectrum of a urea-formaldehyde resin shows broad resonances. At higher fields, 2.35T and 4.70T, the spectra begin to show significant resolution.

Nitrogen-15 NMR spectra have been recorded of urea- and melamine-formaldehyde adducts [68]. All adducts were dissolved in DMSO prior to analysis. The

technique distinguishes between the unsubstituted amino groups, secondary and tertiary amino groups carrying methylol substituents and secondary and tertiary amino groups involved in methylene and methylene ether linkages in urea-formaldehyde resins.

(d) Polyester Resins

Proton NMR has been used for both qualitative and quantitative analyses of polyester resins [69]. Qualitative analysis was accomplished by comparison of sample spectra with spectra and charts obtained from known polyols, poly-functional acid monomers and known polyester resins. Quantitative results were also quoted for polyesters based on monomers including ethylene glycol, diethylene glycol, neopentyl glycol (2,2-dimethyl-1,3-propane diol), 1,2 propane diol, succinic acid, adipic acid, o-phthalic acid, maleic acid, fumaric acid and azelaic acid.

Carbon-13 NMR spectroscopy has also been used for the analysis of polyester resins [70]. Chemical shift values for an extensive range of polyols are quoted. Values were obtained from polyol acetates, aliphatic and aromatic systems.

A detailed structural analysis of a four component polyester resin based on adipic acid, iso-phthalic acid, neopentyl glycol and trimethylol propane (2-ethyl l-2- (hydroxy-methyl) -1,3-propane diol, TMP) [71] has been carried out. Resonances from the quaternary carbon of the TMP with all nine possible units were assigned.

(e) Acrylic Resins

Proton NMR has proved particularly useful in the study of the microstructure of acrylic polymers in solution [72,73]. The α-methyl group of poly(methyl methacrylate) is found to have different chemical shifts for each kind of triad: isotactic, sydiotactic and heterotactic. In a sample of mixed configuration the area under each peak will correspond

to the amount of each triad present. Obtaining spectra at 225 MHz has made it possible to assign pentad sequences in proton NMR spectra of poly(methyl methacrylate) [74].

Kozluk, Spychaj and Hamielc [75] used proton NMR to determine the composition of styrene-acrylic acid copolymers. Results based on the analysis of the carboxylic proton signal gave results with poor reproducibility. Formation of the ammonium salt gave satisfactory results for polymers with a high acrylic acid content. However, it was observed that for polymers with high styrene content, the ammonium proton signal shifts downfield and begins to overlap with the aromatic protons. Addition of D_2O to the polymer solution containing the ammonium salt derivative results in an exchange of ammonium protons with the D_2O giving a sharp DOH signal. This method gives good agreement between measured and theoretical compositions.

(f) Solid State NMR and mobility studies

There are many materials which will not dissolve in NMR compatible solvents and this has prevented analysis using high resolution NMR. In the recent past there has been a development of an NMR technique which has allowed structural information on a wide variety of solid materials [76,77].

In the solid state the peak line widths are broadened due to dipolar interactions between magnetic nuclei and the orientation dependence of shielding constants in the magnetic field which gives rise to a distribution of chemical shifts and hence broadening. Another problem encountered is due to the low sensitivity and long spin-lattice relaxation times (T_1) of carbon-13 nuclei leading to weak signals in repetitive pulse experiments [78]. High- Power decoupling, Cross-Polarisation (CP) and Magic Angle Spinning (MAS) can give high resolution spectra for powders or amorphous solids of comparable quality to those observed in solution. The application of a very high power proton decoupling field can reduce heteronuclear dipolar interactions to zero. The MAS technique involves

spinning the sample at an angle of $54^0 44'$ to the applied magnetic field at a rate of between 2 to 6 kHz. Organic solids will generally contain many nuclei in different environments resulting in broad resonances. The narrow lines observed in solution NMR experiments are the result of molecular motion which reduces the shielding to the isotropic value in addition to removing the dipolar interactions. The cross-polarisation technique makes use of the strong spin polarisation of the proton to enhance the inherently weaker spin polarisation of the carbon-13 nucleus.

CP-MAS NMR has shown that lamellar crystalline polyethylene consists of one crystalline and two noncrystalline phases. The two noncrystalline phases have different chemical shifts and spin-spin relaxation times but both have the same spin-lattice relaxation times [79].

Spin-lattice and pseudo-T_2 ($T_{1\rho}$) relaxation times were measured for polystyrene and poly (vinyl methyl ether) (PVME) blends [80]. It was observed that for the given polymer T_1 remained constant for various polymer blends. Values of T_{1P} however showed considerable differences depending upon sample preparation and thermal history of the samples. Changes in values of T_{1P} were then used to monitor changes in structure of methyl styrene / 2,6- dimethyl phenylene oxide polymers.

The width of the carbon-13 NMR carbonyl peak at 175 ppm in PES (poly(ethylene succinate)) /PVPh (poly(vinyl phenol)) blends shows an abrupt change at 55-60% PES [81]. At higher PES concentrations the peak is considerably broader and corresponds to a change from semi-crystalline blends to amorphous mixtures.

The effect of crosslinking upon the mobility of groups within a swollen styrene/ divinyl benzene gel has been investigated using single pulse and CP-MAS NMR [82]. Following cross-linking there appeared to be greater loss of aliphatic signals than the aromatic signals, indicating that the aliphatic backbone carbon atoms have a more

restricted motion and consequentially greater dipole coupling than the aromatic carbons which retain greater mobility due to rotational motion about the ring-backbone C-C bond.

The molecular motion and phase behaviour of sodium 4-(1'-heptylnonyl) benzene sulphonate (SHBS), a double tail sulphonate, has been investigated using NMR spectroscopy[83]. Carbon and proton nuclei were assigned as follows:

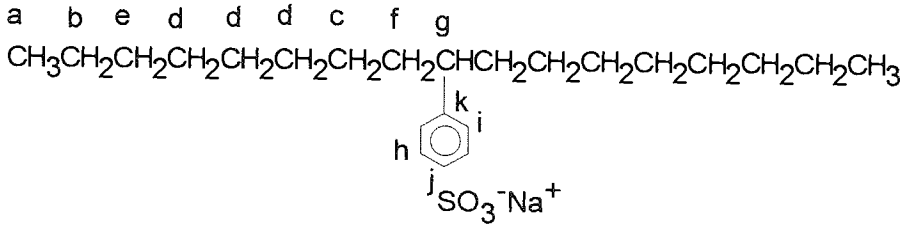

Figure 2.4 Carbon-13 NMR assignments of SHBS

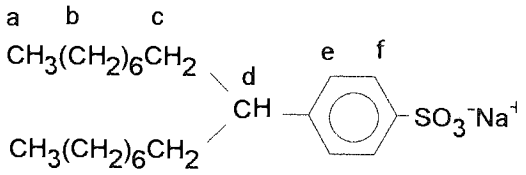

Figure 2.5 Proton NMR assignments of SHBS

The solubility of SHBS in chloroform at 25°C and 37°C is over 25 wt.%. Carbon-13 and proton spectra of 10% SHBS in chloroform show all resonances (a - f). The solubility of SHBS in water at 25°C is around 0.06% and 0.6% at 80°C. At 80°C the solution of 0.6% SHBS in D_2O the carbon-13 NMR spectrum again shows all resonances. At concentrations above 0.6% in water dispersed lamellar liquid crystals form. Only the peaks assigned A, B, D and E in carbon-13 spectra and A and B peaks in proton spectra are observed. The sharpness of these peaks suggests that the molecular motion of the corresponding segments is fairly fast and effectively isotropic. In contrast the segments

corresponding to the unobserved peaks must be restricted. The proton NMR of 14% SHBS in D_2O also shows a sharp HDO peak indicating that the water is quite mobile. The proton NMR spectrum of 70% SHBS in D_2O is dominated by a broad water resonance indicating little 'free' water and the 'A' and 'B' peaks are barely seen.

CP-MAS NMR spectra of 4-hydroxy benzoic acid polymer shows splitting of the peak due to the carbon ortho to the carboxyl [84]. This non-equivalency suggests that even at moderately high temperature there is little ring motion in this highly crystalline polymer. ^2H spectra at 140^0C suggest that a fraction of rings undergo rapid motion at this temperature which is not detected by carbon-13 NMR.

Studies of properties, including permeability, flexibility, enzymatic activity and lateral diffusion of embedded proteins [85], of phospholipid membranes have shown that the numerous physical properties depend upon the mobility of the fatty ester chains in the semi-ordered array that constitutes the hydrophobic interior of the bilayer. In principle the properties of NMR relaxation allow a very detailed, quantitative picture of phospholipid motion to be determined.

From a study of a series of relaxation techniques a detailed insight into the molecular dynamic processes of cyclic carbonates was obtained [86]. As the supercooled region is approached the rotational motion of the molecules becomes anisotropic.

To overcome the problem of detecting proton spectra of samples in the presence of water emphasis has been placed on hardware developments to improve the quality of water suppression [87].

2.2.2 Gel Permeation Chromatography

Gel permeation chromatography (GPC) separates the molecules present in a sample due to differences in the effective molecular size in solution. Separation occurs within a column containing packing material with a pore size distribution. Molecules too large to

penetrate any of the pores are not retained by the column and elute first. Such molecules are said to be totally excluded. Small molecules penetrate all of the pores and elute from the column last. Molecules with sizes between these limits are separated on the column.

a. Column Calibration

A GPC chromatogram can be viewed as a profile of the molecular size distribution of the sample polymer. However, with proper calibration the chromatogram can be converted into a molecular weight distribution (MWD) curve and molecular weight averages can be calculated. To determine the molecular weight distribution for a polymer it is necessary to establish a calibration curve relating elution volume (retention time) to molecular weight. This can be accomplished by relating the retention time to the peak molecular weight of a series of narrow disperse molecular weight polymer standards. However, narrow disperse molecular weight standards are generally not available for many synthetic polymers. Standards which are commercially available include polystyrene, poly(methyl methacrylate), poly(ethylene oxide), poly(ethylene glycol), poly(isoprene), poly(acrylic acid), poly(tetrahydrofuran), poly(butadiene) and poly(methyl styrene). These standards are usually characterised using so-called absolute techniques including NMR and light scattering. Characterisation using relative methods requires calibration with samples of known molecular weight. Such methods include viscosity and vapour pressure osmometry.

One method to determine the molecular weight of a polymer for which no standards are available involves the use of so-called 'Q- factors' which relates molecular weight to molecular size [88]. Q is defined as the molecular weight per extended chain length in angstroms.

A calibration curve may also be generated with the use of a broad disperse polymer standard [89]. Chromatograms of one or two broad standards are fitted with a set of linear

functions based on their true number- and weight-average molecular weights. The software adjusts the calibration functions until the computed values match the experimental values.

Differences in structure and solvent-polymer interactions lead to different hydrodynamic volumes for equivalent molecular weights. The hydrodynamic radius of the molecule is proportional to the logarithm of the product of molecular weight and intrinsic viscosity [η]. The Mark-Houwink equation $[\eta] = KM^a$ describes the relationship between intrinsic viscosity and molecular weight. A plot of the logarithms of the product of molecular weight and intrinsic viscosity versus peak elution volume or retention time will yield a single curve. This calibration technique is known as universal calibration [90,91]. Thus, for the determination of the molecular weight of a sample, its intrinsic viscosity must be measured[92]. A plot of log[η] versus log MW, for polystyrene in THF, will produce a straight line with a slope equal to the value of *a* and intercept logK [93]. The parameter K is a constant for a given polymer-solvent system. The parameter a depends upon the shape of the polymer in solution. For large rigid spheres the value of *a* is zero i.e. the viscosity is independent of molecular weight e.g. globular proteins [94]. For randomly coiled flexible chains *a* is usually in the range 0.5 (under theta conditions) to 0.8 (in good solvents). The value of a is 2 for rigid rods [95]. To calculate intrinsic viscosity, the viscosity of a series of sample solutions with varying concentrations are measured. A plot of reduced viscosity, which is the specific viscosity divided by concentration, versus concentration is extrapolated to zero concentration. The specific viscosity is given as :

$\eta_{sp} = \eta_{rel} - 1$, where the η_{rel} (relative viscosity) is equal to the measured sample viscosity divided by pure solvent viscosity.

Poly(ethylene oxide) does not follow a linear Mark-Houwink relationship. Molecular size and solvation studies of low molecular weight polyethylene oxide and phenol- formaldehyde Resols have been carried out in various solvents [96]. Calibration of

the GPC columns, using polyethylene oxide in various solvents, shows a non-linear viscosity-molecular weight log-log plot. The Mark-Houwink parameters (K,a) for poly(ethylene oxide) are similar in the presence or absence of salts i.e. are not affected by ionic strength. An Elias plot of (K) versus (*a*) obtained in various solvents shows (K) to be inversely proportional to (*a*). The calibration curves of PEO in both THF and DMF are found to be similar (PLGEL application note 107).

A low-angle laser light scattering (LALLS) detector used in series with a refractive index detector can be used for molecular weight determination [97]. Using LALLS it is possible to measure molecular weight distributions without using a calibration curve. This is especially useful for measuring molecular weights of novel polymers.

A triple detection system consisting of RI-VISC-RALLS (right-angle laser light scattering) is reported to be capable of determining accurate molecular weight and molecular size distributions over the widest range of molecular weights [98]. It is also reported to eliminate the need for band broadening correction and allows detection of highly branched structures.

Molar mass and radius of gyration of narrow distribution polystyrene standards have been determined using GPC with an on-line viscometer and multi-angle laser light scattering detector [99].

b. Polymer characterisation

Aggregation of phenolic polymers in solution is a problem when determining molecular weight values using GPC. The aggregation that is observed when using pure THF and DMF as the mobile phase, is removed by incorporation of trichloroacetic acid and lithium chloride or sodium nitrite [100].

Reaction rates and structures of phenolic polymers have been studied using carbon-13 NMR and GPC [101]. Aqueous GPC was used to determine the molecular weight

distribution (MWD) of water soluble phenolic resins. The aqueous mobile phase was modified using 0.1M sodium hydroxide. The columns were calibrated using phenol and 2,6,2',6'-tetra-bis (hydroxymethyl) 4,4'methylene bisphenol and drawing the resultant calibration curve parallel to that obtained using PEO molecular weight standards. Peaks corresponding to monomer, dimer, tetramer and octamer were observed.

Size exclusion chromatography has been used to study anionic polymers in aqueous solutions [102]. Universal calibration was carried out using polystyrene sulphonate (PSSNa) standards. The columns consisted of hydroxylated polymethacrylate packing with residual carboxyl groups. Adsorption onto the column was overcome by increasing the temperature to 60^0C and using a salt concentration of 0.1M. Apparent increase of the distribution of the PSSNa standards with increasing molecular weight was observed.

GPC has been used for the characterisation of poly(methyl methacrylate) (PMMA) and epoxy resins [103]. Values of dn/dc in THF were measured and show the refractive index detector to be most sensitive to polystyrene, to have a lower sensitivity for PMMA and lowest of all for PEO. Calibrations using polystyrene and PMMA were carried out. Calibration for the characterisation of epoxy resins was carried out using oligomers of low molecular weight epoxy resins.

MWD analysis for polystyrene produced by homopolymerisation and by graft polymerisation from polycarbonate has been carried out [104]. Comparison between the two polymerisation methods revealed differences which were attributed to a difference in the rate of the termination step.

c. Copolymer characterisation

An ultra-violet (UV) detector has been used in series with a refractive index detector to analyse the composition of styrene-butadiene copolymers [105]. Response factors of the styrene on the UV detector (at 260 nm) and styrene and butadiene on the RI

detectors were determined by comparison of the integrated areas under the chromatograms at given concentrations. The response of the polystyrene on the RI detector was determined to be a factor of 1.4 greater than that of polybutadiene and a factor of 35.6 greater than that of polystyrene on the UV detector i.e.

$$K_1 = K_{ps.ri} / K_{bd.ri} = 1.4 \quad \text{and} \quad K_2 = K_{ps.ri} / K_{ps.uv} = 35.6$$

Thus, the calculated response from the RI detector for polystyrene only is ($A_{ps.ri}$):

$$A_{ps.ri} = A_{uv} \times K_2 \tag{2.1}$$

and the calculated response from the RI detector for polybutadiene is:

$$A_{bd.ri} = 1.4x\ (A_{ri} - A_{ps.ri}) \tag{2.2}$$

Therefore percentage polybutadiene in the sample is:

$$\% \text{ polybutadiene} = \frac{A_{bd.ri}}{A_{bd.ri} + A_{ps.ri}} \times 100 \tag{2.3}$$

Using this approach to analyse a chromatogram a point-by- point composition of the copolymer can be calculated.

Molecular weight distribution values quoted for the polybutadiene component using the polystyrene calibration were calculated using:

$$\log M_c = W_s \log M_s + W_b \log M_b \tag{2.4}$$

where; M_c, M_s and M_b are the molecular weights of the copolymer, polystyrene and polybutadiene and W_s and W_b are the weight fractions of polystyrene and polybutadiene.

Equations have been derived to calculate the MWD values of linear block copolymers by utilising the calibration curves of the individual homopolymers [106]. An example is:

$$M_c = (M_a) / (1+[r-1]W_2) \qquad (2.5)$$

where: M_c is the molecular weight of the copolymer, M_a is the molecular weight of the copolymer using the calibration curve for homopolymer 'a', W_2 is the weight fraction of monomer 'b' and *r* is the ratio of molecular weights of 'a' and 'b' at elution volume V_0 obtained from the calibration curves.

GPC has been used to confirm the presence of block copolymers of polystyrene and poly(methyl methacrylate) [107]. Using dual detection i.e. a UV detector and an RI detector, the variation in composition of the copolymer with elution time may be calculated in a similar manner to that used by Runyon et al [105]. Thus the weight fraction of the component W_2 in a copolymer nay be calculated using:

$$W_2 = (A_2K_{11} - A_1K_{21}) / (K_{11}K_{22} - K_{21}K_{12}) \qquad (2.6)$$

where: W_2 is the weight fraction of component 2, A_1 and A_2 are the response from the UV and RI detectors at a given elution volume and K_{ij} are the response factors using detector i for component j.

Molecular weight distributions have been calculated for AB and ABA type copolymers using a new procedure for analysing GPC copolymer data applicable to systems where blocks of one component (A) are of uniform molecular weight [108]. The molecular weight of component b is given by the equation:

$$\ln M_b = (S_b [\ln\{10 (S_a V + I_a) - nM_a\} - I_a] + I_b)/ S_a \qquad (2.7)$$

where: S_a and S_b are the slopes of the homopolymer calibration curves, I_a and I_b are the intercepts of the calibration curves and n is the number of A blocks per copolymer.

Composition drift of a four component acrylic terpolymer has been monitored using GPC and a diode array UV detector [109]. Determination of the residual monomer levels as a function of process time was used to determine the actual drift in composition.

Chemical composition as a function of molecular weight was determined, using GPC, on a number of methyl acrylate-styrene copolymers [110]. The equations used to calculate the composition were similar to that of Runyon et al [105]. For low conversion polymers the methyl acrylate content was found to be constant with molecular weight. For high conversion polymers the methyl acrylate content was found to increase with increasing molecular weight.

A styrene/poly(methyl methacrylate) copolymer was analysed using a GPC system incorporating a RI detector and a UV detector monitoring at 260 nm [111]. The data from the detectors was collected using an IBM compatible PC and was transferred to a commercial spreadsheet package (EXCEL TM). Copolymer composition was calculated using equations developed by Runyon et al [105]and plotted as a function of elution time.

d. Multi-wavelength UV detectors

Using a specially designed flowcell, a UV spectrometer can be used to obtain UV spectra of components eluting from a HPLC column [112]. 'Stopped flow' hydraulics were used to trap chromatographic peaks, from a reverse phase separation of hydocarbons and analgesics, in the cell with minimum peak dilution. The UV spectra of individual components were then obtained.

The use of photodiode array detectors has enabled UV/Vis spectrometers to record full wavelength range spectra in seconds rather than minutes [113]. The multichannel detector contains a few hundred photodiodes in a linear array approximately one cm long. White light is passed through the sample and into the monochromator which disperses the light across the detector. Such instruments can be used as detectors for HPLC. A reverse phase separation of aromatic compounds was carried out and UV spectra of the separated components were obtained [114]. Spectra of overlapping peaks from a normal phase separation of mineral oil distillates were obtained from principal component analysis of data obtained from a photodiode detector [115].

The purity of a component separated on a HPLC column can be checked by measuring the ratio of absorbencies at a number of different wavelengths at points throughout the eluting peak. A pure component will give the same absorbance ratios over the range of the peak. Such confirmation of purity has been achieved using stopped flow techniques [116], using diode array detectors[117], scanning multi-wavelength detectors [119,120] and tandem detectors connected in series [118]. A multicomponent analysis procedure was developed to determine a mixture of extensively overlapped phenols during a HPLC separation [121]. Use was made of diode-array detector to generate data for a least squares linear regression calculation. It was recognised however that the limitation of the method was the need to have UV spectra of all the eluting substances.

e. Multicomponent analysis

Computers are increasingly being used to solve chemical problems [122,123] and a subdiscipline of chemistry called chemometrics has arisen. Chemometrics is the utilisation of mathematical and statistical methods for handling, interpreting and predicting data. A number of statistical software packages are available which includes techniques for chemometrics [124]. Composition analysis of multicomponent systems using spectroscopic techniques is ideal for matrix and chemomemtric methodologies.

Beers law relates the absorbance to quantity i.e.

$$A = kc \qquad (2.8)$$

where k is a constant which includes path length and absorbtivity terms, A is the measured absorbance and c is the concentration of the absorbing species.

Systems containing more than one component can be treated in a similar manner to single component analyses if an absorption band can be found for each constituent that does not overlap bands of other unknowns. Where overlap does occur the experimental procedure is changed and more complex methods of calculation are required. This involves deriving a set of simultaneous equations [125]. For a four component mixture the minimum requirement is the measurement of four absorbances at different wavelengths (or wavenumbers).

If A_i is the absorbance at wavelength i, K_{ij} is the response factor at wavelength i of component j and C_j = concentration of component j, then:

$$A_1 = K_{11}C_1 + K_{12}C_2 + K_{13}C_3 + K_{14}C_4$$

$$A_2 = K_{21}C_1 + K_{22}C_2 + K_{23}C_3 + K_{24}C_4$$

$$A_3 = K_{31}C_1 + K_{32}C_3 + K_{33}C_3 + K_{34}C_4$$

$$A_4 = K_{41}C_1 + K_{42}C_2 + K_{43}C_3 + K_{44}C_4 \qquad (2.9)$$

A simplification in notation can be achieved in matrix form:

$$\mathbf{A} = \mathbf{K}\,\mathbf{C} \qquad (2.10)$$

where: A = matrix or absorbances

K = matrix of response factors

C = matrix of concentrations

In this form the calculations have been referred to as the K-matrix approach [126]. The advantage of the K matrix method is that overdetermination can be carried out very easily. Care must be taken in the calibration step such that C or rather C multiplied by its trnsform (CC^t) is not nonsingular and that its determinant is non-zero.

An alternative is the P-matrix approach where:

$$\mathbf{C} = \mathbf{P}\,\mathbf{A} \qquad (2.11)$$

where: A = matrix or absorbances

P = matrix of response factors

C = matrix of concentrations

The advantage of the P matrix method is that analysis is possible even if impurities are present at varying levels in the calibration standards. The disadvantage is that the number of calibration standards limits the number of data points thereby making overdetermination more difficult.

(f) Liquid chromatography

Polymers and polymer fractions have been analysed using liquid chromatography. Styrene/ methyl acrylate polymers using normal phase chromatography [127] and styrene/ methyl methacrylate and styrene/ acrylonitrile polymers using normal and reverse phase chromatography [128,129]. Chemical composition distribution (CCD) plots as a function of molecular weight have been obtained by using liquid chromatography in conjunction with GPC for styrene/ methyl methacrylate copolymers [130,131] and for styrene/ 2-methoxyethyl methacrylate (MEMA) copolymers [132].

Methacrylate copolymers were studied using normal and reverse phase HPLC using purpose made polymeric packing materials [133]. Generally, for all types of column, although the resolution was different in each case, under normal phase conditions the higher the styrene content the earlier the peak eluted. Under reverse phase conditions the higher the styrene content the later the peak eluted. Under normal phase conditions with the acrylonitrile column the copolymer dissolves in the eluent, and is adsorbed onto the column retarding the elution. With the styrene gel column separation is governed by fractional dissolution. The opposite is true under reverse phase conditions. When the mechanism of separation is adsorption the effect of molecular weight on the separation is minimised.

Styrene-methyl acrylate copolymers were fractionated using GPC and each fraction was analysed according to chemical composition by means of gradient elution using thin layer chromatography with flame ionisation detection [134]. The use of on-line, coupled column chromatography, using exclusion chromatography as the first separation technique and reverse phase chromatography as the second technique, has been applied to various polymer systems [135]. Set at 215 nm the UV detector used was regarded as a 'universal' detector. A six port sampling valve with a 10 μl loop was used as the switching valve.

2.3 Colloidal Studies

2.3.1 Transmission Electron Microscopy

Transmission Electron Microscopy has been used to examine synthetic rubber lattices. Without fixing, soft rubber particles flatten and merge upon drying. Bromination can be used to stiffen poly(butadiene) particles but metal shadowing is still required prior to examination. Fixation using osmium tetroxide vapour [136] produces perfectly spherical particles and the latex does not require metal shadowing. Osmium tetroxide preferentially stains poly- (butadiene) in the presence of styrene- acrylonitrile copolymer [137]. Ruthenium tetroxide has also been used to examine poly(butadiene) and acrylonitrile-butadiene-styrene (ABS) particles [138].

TEM was used to show the dependence of the particle size distribution on the polymerization temperature in seed emulsion polymerization of styrene and acrylonitrile monomer mixture on polystyrene seed particles of 300 nm diameter[139]. At polymerization temperatures below 65^{0}C the larger fraction of new copolymer is in the new crop of particles. At temperatures above 65^{0}C the larger fraction of the new copolymer grafts onto seed particles.

TEM has been used to study decane/PMMA systems in which core-shell and hemispherical morphologies were observed [140].

Ruthenium tetroxide, generated using ruthenium trichloride and sodium hypochloride, preferentially stained polystyrene in iso-octyl acrylate/acrylic acid/polystyrene systems [141]. Solvent cast films produced distinct styrene domains whereas compression moulded films did not. Annealing these films at 90^{0}C produced more distinct domains. At higher styrene levels spherical domains changed to lamellar or cylindrical domains.

TEM was used to study the morphology of aqueous acrylamide inverse emulsions and latexes prepared by various stirring rates [142]. Conventional emulsion polymerization involves the emulsification of a water immiscible monomer in a water medium giving colloidal dispersion of polymer in water. Inverse emulsification polymerization involves the emulsification of a water- miscible monomer in an oil medium to give a colloidal dispersion of water-swollen particles in oil. TEM was also used to study the morphology of the emulsifier ethylene diamine tetrasubstituted with poly(propylene) oxide poly-ethylene oxide block copolymers [143]. In both the above experiments the microscope was fitted with a cold-stage sample holder.

Particle size determinations of vinyl acetate and butyl acrylate copolymers, prepared by batch and semi-continuous processes, have been determined by TEM [144]. Staining with uranyl acetate solutions was used to harden the soft copolymer particles for examination. Good agreement was found between light scattering results and weight average diameters determined by electron microscopy. The average particle size of the batch copolymer latexes was found to be almost independent of copolymer composition, whereas for the semi-continuous copolymer latexes the average diameter was found to decrease and the polydispersity to increase with increasing butyl acrylate content.

TEM has been used to monitor the inversion process in the manufacture of high impact polystyrene (HIPS). Initially black polystyrene droplets are observed in a lighter background of poly(butadiene) solution. During inversion both light and dark particles are observed in regions of dark and light backgrounds respectively. After inversion light butadiene particles are observed in a dark polystyrene solution [145].

A new staining technique for detecting crystalline and amorphous phases in poly-(tetrahydrofuran) has been developed for use with TEM [146]. Hexane is a non-solvent for crystalline PTHF but makes amorphous regions swell slightly. A section of PTHF deposited on a copper mesh is exposed to hexane containing 0.005% N-vinyl carbazole.

The specimen was then exposed to osmium tetroxide vapour. The amorphous regions were stained due to reaction between the osmium tetroxide and the N-vinyl carbazole. The percentage of unstained regions agreed well with the degree of crystallinity obtained using differential scanning calorimetry. Particle size data from TEM examination of poly (vinyl alcohol-co-vinyl acetate), poly (2-vinyl pyridene-co-butyl methacrylate) and poly (ethylene oxide) was compared with data using Charge Velocity Analysis [147], however CVA proved inaccurate for particles with a diameter less than 100 nm.

Examination of particles produced by evaporation from toluene of a blend of high molecular weight polystyrene and poly(methyl methacrylate) using TEM showed polystyrene particles encapsulated by PMMA on the surface [148]. For lower molecular weight polymers the reverse morphology was observed. It was also observed that agitation of the toluene swollen particles, formed from the higher molecular weight polymers, produced individual polymer particles. Particles produced from the lower molecular weight polymers resisted complete phase separation. This was thought to be due to the lower interfacial tension and better mixing at the interface between the polymers.

Poly(methyl methacrylate)/poly(dimethylsiloxane) copolymers were examined using TEM [149]. At lower PDMS contents the morphology was spherical domain texture but this changed to an ordered cylindrical texture when the PDMS content was increased to 45%.

2.3.2 Dynamic light scattering

In dynamic light scattering, a fine beam of laser light irradiates a sample solution. The particles in the solution are undergoing Brownian motion which causes the intensity of the scattered light to fluctuate due to interference effects. The intensity of the scattered light (I_s) is measured by a photomultiplier tube and the number of photons collected during

finite time intervals are counted using a correlator. The value of the time interval should be shorter than the highest diffusion coefficient of the particles present in the solution. Analysis of the fluctuations in I_s yields information regarding the diffusion coefficient from which the particle size can be calculated.

The autocorrelation function is obtained by multiplying an intensity at time (t) with the intensity at time (t-t'). When (t') is small compared to (t), Is(t) will be very similar to Is(t-t') because the particles have not had time to change positions significantly (compared with the wavelength of light) under diffusion.

$$C(t') = \langle Is(t) \times Is(t-t') \rangle \qquad (2.12)$$

The brackets <> indicates a summation over many values of t. This is a running sum of the many products of $I_s(t) \times I_s(t-t')$ all having the same separation in time (t') for many values of (t). Because $I_s(t)$ and $I_s(t-t')$ for small values of (t') are similar they are said to be highly correlated.

For a larger value of t' the quantity $I_s(t)$ and $I_s(t-t')$ will begin to lose correlation since the particles will have had time to change their positions.

For values of t', the extreme values will be as t' approaches zero and as t' approaches infinity. For the limit where (t') approaches zero Is(t) and Is(t-t') are essentially identical hence:

$$C_{(0')} = \langle Is^2(t) \rangle \qquad (2.13)$$

i.e. the value of C(t') for $t' \rightarrow 0$ ie $C_{(0)}$ is the sum, over many values of (t), of the square of the scattering intensity.

Where t' is large there will be no correlation between a pair of sampled intensities:

$$C(t' \rightarrow \text{infinity}) = \langle Is(t) \rangle^2. \qquad (2.14)$$

It is known that for any fluctuating quantity the average of the squares of that quantity is always larger than the square of the average. i.e $\langle Is^2(t) \rangle$ is greater than $\langle Is(t) \rangle^2$.

The lowest possible value for the correlation function is $\langle Is(t) \rangle^2$, all other values of C(t') for finite values of (t') must be larger. The function C(t') must fall from the value $\langle Is^2(t) \rangle$ at t'=0 to the baseline value $\langle Is(t) \rangle^2$ for large values of (t). For random diffusing non-interacting particles the auto-correlation function of the fluctuating scattered light intensity is an exponentially decaying function of time (t).

$$C(t) = A \exp^{-t/T} + B \qquad (2.15)$$

where $A = \langle Is^2(t) \rangle$, $B = \langle Is(t) \rangle^2$ and T is the decay time constant.

T is the decay time constant and is the speed with which the autocorrelation function decays. The larger the particles the slower their diffusion, the slower the fluctuations in I_s and the longer the decay time constant. To obtain a value for T, ln(t) is plotted versus (t). For uniform monodisperse particles a straight line of negative slope will result. The value of the slope is equal to the decay time constant T.

The diffusion coefficient can be calculated from the decay time constant using the equation:

$$D = 2/(2K^2T) \qquad (2.16)$$

where D is the diffusion coefficient, T is the decay time constant and K the scattering vector equal to $4\pi n\sin(\theta/2)/\lambda$ where: n is the refractive index of solvent, λ is the wavelength and θ = scattering angle.

The particle radius, r, can then be calculated from the diffusion coefficient using the Stokes-Einstein equation:

$$r = kT /6\pi\eta D \qquad (2.17)$$

where k is the Boltzman constant, T is the temperature (K) and η the viscosity.

The above approach has only limited usefulness since most samples differ appreciably from the uniform monodisperse case. Samples may contain a range of particle sizes, consisting of a smooth single peak or may be more complex resembling two discrete peaks or an even more complicated shape. Different mathematical algorithms have been developed to analyse the autocorrelation raw data.

The simplest kind of complexity is the smooth Gaussian-like population of sizes having a well defined mean diameter and half-width. A plot of $\ln C_{(t)}$ versus (t') will show a slight curvature. The method of cumulants attempts to find the quadratic function of t' which lies closest to the data points on a least squares basis [150].

More complex methods have been developed for use in the analysis of the autocorrelation raw data. These include the inverse Laplace transform and the so called CONTIN and DISCRETE computer programs [151].

Particle aggregation of a polystyrene latex was studied using dynamic light scattering [152], using a dilute solution of potassium chloride as the coagulant. The initial particle size determined using DLS was within 5% of the value determined using electron microscopy.

The aggregation of an aqueous solution of poly(methacrylic acid) using polyethylene glycol as the coagulant was investigated using DLS [153]. The technique was used to determine the average radius and radii distributions of the particles produced. The effect of pH upon the rate of aggregation was also studied. It was determined that under a pH of 1.9 the system was found to aggregate rapidly large particles.

A latex of polyalkylcyanacrylate particles were produced by a dispersion polymerization process in an aqueous phase at low pH [154]. DLS was used to determine the influence of temperature, type and concentration of electrolyte and stirring rate upon the resultant particle size and size distribution. The pH of the solution and to a lesser degree the initial monomer concentration were shown to be factors controlling the particle size whilst within the limits of the experiments a change in the other factors i.e. temperature, stirring rate and electrolyte, did not alter the particle size.

Colloid particles produced by the adsorption of narrow molecular weight distribution poly(ethylene oxide) onto silica particles were examined using DLS [155]. The particle diameters of the latex determined using DLS were in good agreement with measurements made using electron microscopy. At low latex concentrations the logarithmic plot of the correlation function $g^{(1)}(\tau)$ is linear. It is suggested that this indicates free diffusion of the latex. At higher concentrations the logarithmic plot of the correlation function can be divided into two regions. The low correlation time part of the plot corresponds to self-diffusion. The plot at higher correlation times has a similar slope to that produced at low concentrations. Good agreement between particle diameters were also obtained between TEM and DLS studies of poly(ethylene oxide) coated carboxylated poly(styrene) and poly(styrene- butadiene) particles[156]. The TEM values were found to be always lower than the DLS values and the diferences in particle diameter were attributed to the hydrodynamic layer thickness (HLT). TEM revealed the particles to have a relatively narrow distribution of particle sizes.

Examination of particles, produced by dispersing a poly(urethane)-graft-acrylic polymer in water, using DLS, revealed two types of particle [157]. The results, it was suggested, reveal the presence of swollen graft polymer particles together with compacted micelles.

2.3.3 Infra-Red Spectroscopy

Infra-red spectroscopy is an established technique for identifying polymers [158] and atlas's containing thousands of spectra of polymers are available [159,160].

The advent of computerised data handling systems and Fourier transform techniques has proved to be of great benefit in quantitative analyses [161]. The use of such systems has allowed FT-IR spectroscopy to be used in the investigation of colloids and interfacial phenomenon [162].

FT-IR spectroscopy coupled with attenuated total reflectance techniques has been used to study the kinetics of proteins, α-globulin and albumin, absorption in flowing systems [163]. The study included obtaining spectra of adsorbed and bulk proteins.

FT-IR spectroscopy has also been used to study micellar behaviour of aqueous sodium hexanoate ($C_6H_{11}O_2Na$) [164]. Transmission IR spectra were obtained by placing the aqueous samples in cells with barium fluoride windows with 12 μm spacers. The spectra of sodium hexanoate were obtained by subtracting a water spectrum from the solution spectra recorded under the same conditions. Spectra were recorded of solutions ranging from 0.1 M to 3.0 M and wavenumbers of bands due to $V_{as}CH_3$, $V_{as}CH_2$, $V_{as}COO$- and V_sCOO- were measured. After subtraction of water a weak band a 1655 cm^{-1} was observed. This was identified as the bending mode of bound water. With increasing concentration the wavenumber of $V_{as}CH_3$ and $V_{as}CH_2$ modes decrease from 2964.8 to 2959.4 and 2938.9 to 2933.0 cm^{-1} respectively. The $V_{as}COO^-$ mode shows an increase in

wavenumber with increasing concentration; 1544.8 to 1547.7 cm-1. The VsCOO- mode exhibits a minimum wavenumber value in the concentration region 1 to 2 M.

FT-IR spectroscopy has been used to study chemisorption and physisorption of poly(methyl siloxane) onto alumina [165]. The levels of adsorbed species were calculated from reduction in intensity and shifts in the Si-H bands. Chemisorption and physisorption were found to be temperature dependent and the balance between the rates determined the final surface conformation of the polymer.

IR spectra of perfluorosulphonate membranes were recorded [166]. The membranes studied were either in the dry state or hydrated and neutralised to various extents with sodium hydroxide or tertiarybutyl ammonium hydroxide. It was observed that with increasing neutralisation with sodium hydroxide the SO_3^- sym. stretch band increase in wavenumber; the dry state to a higher degree than the aqueous. This was explained in terms of formation of ionic contact pairs. In the dry state contact ion pairs are formed, the SO_3^- anion is polarised and the wavenumber increases. In the hydrated state the solvation inhibits the contact pair formation. With tertiary-butyl ammonium hydroxide neutralised samples, a decrease in wavenumber is observed to similar degrees in the dry and hydrated forms. Tight association of the ions and the lowering of the polarity of the environment by the presence of the large hydrophobic group cause a decrease in wavenumber with increasing neutralisation.

2.4 Film Characterisation

2.4.1 Film formation

(a) Evaporation and water-dilutable coatings

Evaporation of water is the first stage towards film formation after the latex has been applied to the substrate. Kornum [167] demonstrated that the drying rate of a water

containing polymer film is controlled by the diffusion of the volatile vapour through a boundary layer on the surface of the drying film.

Dodin suggested that there were three stages of drying: [168].

1. Evaporation from a free liquid surface. The principal movement of solvent to the evaporation surface is via convection. Since evaporation is slower than convective mass transfer the rate of evaporation during this stage is constant.

2. As the film begins to solidify, movement through the film by the solvent begins to change from convection to diffusion. The temperature of the film begins to increase and approaches that of the drying chamber.

3. The final stage is evaporation from the solid polymer film. Diffusion is slower than evaporation and the rate of diffusion limits the rate of evaporation. The temperature of the film is now equal to the temperature of the chamber.

(b) Mechanism of film formation

To achieve film formation the particles in the dispersion must coalesce. A number of mechanisms for this process have been suggested.

Bradford et al [169,170] suggested the process of sintering. Sintering is defined as the phenomenon of bonding particles with the action of heat at temperatures below the melting point of any component in the system. This coalescence of the particles is said to occur after the evaporation of water. When a film is produced no external stress is applied thus some internal mechanism must be responsible for the necessary shearing stress. The change of surface area and the minimisation of surface energy could provide the energy necessary to produce shearing stress of such magnitude that viscous flow results. There have been criticisms of this mechanism.

Brown [171] suggests that film formation is seen to occur concurrent with the evaporation of water. It is suggested that a capillary force (F_c) overcomes the resistance to

deformation of the particles. In order for films to be formed the capillary force F_c must be greater than the resistance to deformation F_g.

The third suggested mechanism [172] suggests a mechanism of mutual diffusion. Three steps are involved:

1. Initial evaporation of water leading to close packing of the particles,
2. increasing close approach, leading to deformation, of the particles' brought about by surface tension and capillary pressure as outlined above, and
3. diffusion of the dispersant away from the polymer- liquid interface leading to coalescence of polymer particles.

Sheetz [173] and Vanderhoff [174] also suggested that film formation is the result of several mechanisms. Capillarity, wet sintering and diffusion play complementary roles early in the process. At later stages the diffusion becomes the dominant mechanism. Such a model has been experimentally validated [175].

It is believed that enhancement of mechanical strength with annealing is a consequence of polymer diffusion across the particle-particle interface in the film. Fluorescence decay was used to measure polymer diffusion in films prepared from water based latices [176,177]. Direct non-radiative energy transfer requires a mixture of particles labelled with appropriate groups. One set of groups containing molecules which act as energy donors e.g. phenanthrene, the other set of groups requiring a molecule acting as energy acceptors e.g. anthracene. Latices were prepared using the butyl methacrylate derivative of these molecules. The volume fraction (f_m) of mixing between the two types of particle is given by the expression:

$$f_m(t) = f_m'(t) - f_m'(0) / f_m'(\alpha) - f_m'(0) \qquad (2.19)$$

Prior to coalescence and diffusion i.e. in the nascent film energy transfer can only occur across the particle interface. Values of $f_m'(0)$ obtained by experiment were found to be approximately 0.15. To obtain values of $f_m'(\alpha)$ solvent cast films were used. Values of $f_m(t)$ were found to increase with increased annealing. Rates of polymer diffusion were calculated from the degree of mixing. In the presence of coalescing solvents e.g. texanol (2,2,4 trimethyl pentanediol mono-iso butyrate) diffusion rates were found to increase.

The kinetics of coalescence of core (60:40 styrene: butyl acrylate) :shell (methacrylic acid:styrene: butyl acetate) latices were studied [178,179]. It was shown that the rate of coalescence decreased when interfacial tension decreased i.e. with increasing methacrylic acid content or when the methacrylic acid was neutralised with sodium hydroxide. The rates of coalescence were determined by measuring the solid contents of particle aggregates after immersion in water at a given temperature. As the particles coalesce the solid content of the aggregate increases.

The process of film formation during drying has been modelled using latices with known polymer weight fractions [180]. The influence of weight fraction, particle size, film thickness and particle size distribution on transmission spectra of acrylic latices was investigated. Spectra were obtained, in the range 200 nm to 1100 nm, by placing the latex between parallel quartz plates separated by spacers. At low polymer volume fractions the transmission was found to decrease with decreasing wavelength. At higher volume fractions a minimum is observed in the spectra. This is due to a better packing of polymer particles leading to interference. Such minima tended to flatten out for latices that have particles with broad distributions.

Film formation of latex particles, produced from PS / PBA polymers were studied [181]. Two types of latex were identified. The first type of latex having particles with a 'membrane' consisting of short chain zwitterionic surfactant molecules. The second type of latex consists of particles where the membrane consisted of hydrophilic polymers e.g.

poly(acrylic acid) grafted onto the core. During the drying process membranes from 'Type 1' latices may breakup and allow fusion of the particle cores. With 'Type 2' particles the membrane may remain intact until the film is completely dry.

The temperature below which a given polymer system does not produce coherent films is known as the 'minimum film formation temperature' (MFFT). Ellgood [182] showed a relationship between MFFT and Tg for vinyledene chloride/ methyl acrylate and vinyledene chloride/ ethyl acrylate copolymers. For the latter system the maximum Tg (approximately 25^{0}C) occurred at a composition of approximately 50% vinyledene chloride. The maximum MFFT (30^{0}C) however occurs at approximately 65% vinyledene chloride. Up to approximately 55% vinylidene chloride the MFFT is lower than Tg, greater than 55% the MFFT is greater than Tg. It was noted that the difference between MFFT and Tg appeared to shift from negative to positive as the hydrophilic nature of the copolymer decreased.

It has also been shown that MFFT increases with increasing particle size [175]. For MMA/ BA/MAA polymers the MFFT increases from 11.4^{0}C to 16.4^{0}C as the particle size increases from 150 nm to 1230 nm.

The MFFT of ethyl acrylate and methyl methacrylate copolymers [183] have been measured. It was observed that the higher the MMA content the higher the MFFT. For example for a copolymer containing 50% MMA the MFFT was 32^{0}C. The MFFT increased to 54^{0}C for a copolymer containing 65% MMA.

Minimum film formation temperatures have also been measured for core-shell particle latices [184,185]. When staged feeds of monomers are employed in emulsion polymerisation, the composition of the latex particle can be altered across the particle section. The copolymer compositions were classified, according to their Tg, as hard, medium or soft i.e. 60/40 MMA/BA = hard, 50:50 MMA/BA = medium and 40:60

MMA/BA = soft. The MFFT of the particles were expected to vary with core and shell characteristics in the following order: soft/hard > medium/medium > hard/soft. This order was observed only if the shell thickness was greater than a certain minimum value. The latter depends on the core polymer.

With unseeded particles MFFT did not show any effects of monomer sequencing only composition [186]. With seeded emulsion polymers of similar final composition the MFFT is observed to be greater (67°C) with a 'hard' (48.5:1.5 MMA:MAA) outer shell than (24°C) with a soft (48.5:1.5 EA:MAA) outer shell. Again this was only observed when the shell thickness is greater than a critical value. The MFFT of the seed particle (70:27:3 MMA/EA/MAA) was 63°C, for a copolymer with the average composition the MFFT was 25°C.

2.4.2 Transmission Electron Microscopy

The morphology of films cast from solutions of styrene/butadiene block copolymers have been studied [187,188]. Various compositions were cast from dilute toluene solution to give 0.2 mm thick films. The films were embedded in epoxy resin [189] and exposed to osmium tetroxide vapour. Ultra-thin sections were then produced, approximately 400 A thick, using an ultra-microtome. The structures obtained appeared to depend upon the overall composition and not the type of block chain arrangement. It was observed that as the butadiene fraction increases the butadiene phase changes from sphere through rod to sheet. At high butadiene compositions the styrene appears as domains in a black butadiene matrix [190].

The morphology of SBS copolymers cast from solution also depends upon rate of evaporation[191]. At low evaporation rates uniform domains are observed showing some grain structure [192]. At intermediate rates a parallel array of cylinders are observed. At high

rates of evaporation incomplete phase separation occurs with domains of various shapes and sizes. The particle size of the dispersed butadiene phase was found to increase with an increase in the molecular weight of the polybutadiene. For the preparation of 'high impact polystyrene' (HIPS) it was determined that the molecular weight should be over 110,000 (Mn) to achieve a particle size of greater than 2 microns.

Iso-butyl acrylate dispersions do not ordinarily take up osmium tetroxide stain but can be made to do so by prior reaction with hydrazine or hydroxylamine [193].

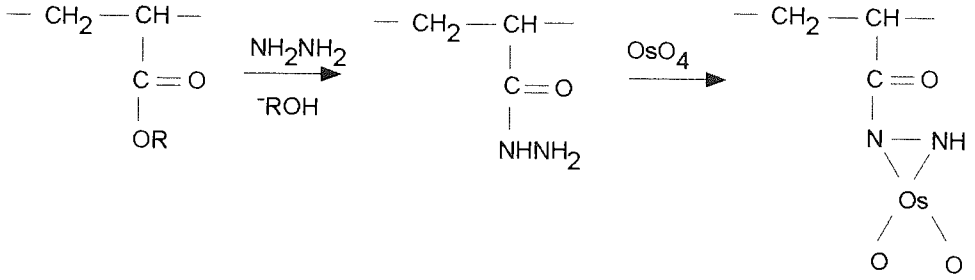

Figure 2.6 Hydrazine/osmium tetroxide reaction

The technique of prior reaction can be used on any polymer containing acrylate esters. The chemical reaction that takes place is shown in Figure 2.6.

Osmium tetroxide has been used to preferentially stain butyl acrylate domains in the presence of poly(vinyl acetate) [194]. Copolymers were prepared by both batch and semi- continuous processes. Butyl acrylate has a higher reactivity ratio than vinyl acetate, therefore in the batch process the polymer consists of relatively large dark butyl acrylate core surrounded by a vinyl acetate shell. In the semi-continuous process where monomers are added at a rate equal to or less than the rate it can polymerise, the particles have a smaller core i.e. a more homogeneous polymer. Batch prepared copolymers show two DSC peaks corresponding to Tg's of butyl acrylate and vinyl acetate homopolymers, whereas semi- continuous processed polymers show one peak [195].

A method of producing high contrast TEM photographs of polyethylene and polyolefins is to initially treat the polymer with chlorosulphonic acid [196-199]. This selectively reacts with amorphous zones in partially crystalline polyethylenes. Uranyl acetate is then reacted with the sulphonic acid groups anchored to the amorphous zones. Using this technique it is possible to make visible the crystalline lamellae and the amorphous layers.

Ruthenium tetroxide has been used as an alternative staining agent to osmium tetroxide. The reagent is chosen because of its high reactivity with some organic substances [200,201]. The morphology of an acrylonitrile/styrene resin was clearly determined after treatment with a 1% ruthenium tetroxide solution in water. Ruthenium tetroxide vapour is extremely effective in staining polymers containing polystyrene [202]. The reagent fails to stain poly(methyl methacrylate) and good morphological contrast can be obtained for their blends when examined using TEM. Ruthenium tetroxide is shown to stain both saturated and unsaturated polymer systems that contain ether, alcohol, aromatic or amide groups. Polyethylene, poly(vinyl methyl ketone) and polypropylene were also stained[203] whereas poly (methyl methacrylate), poly(vinyl chloride), poly(vinylidene fluoride) and poly- acrylonitrile were not stained.

The morphology of copolymers prepared by grafting styrene and acrylonitrile monomer mixtures onto mono-dispersed polystyrene seed latexes have been studied by TEM of thin sectioned ruthenium tetroxide stained films. The copolymers were prepared using batch, batch-with-equilibrium-swelling and semi-continuous processes [204]. When the degree of grafting was high, with low diameter seed particles, and the Tg was intermediate between that of the polystyrene and of the styrene-acrylonitrile copolymer the TEM shows two homogeneous interpenetrating polymer networks. Ruthenium tetroxide, generated using ruthenium trichloride and sodium hypochloride, preferentially stained polystyrene in iso-octyl acrylate/acrylic acid/polystyrene systems [205]. Solvent cast films

produced distinct styrene domains whereas compression moulded films did not. Annealing these films at 90°C produced more distinct domains. With increased styrene content the spherical domains changed to lamellar or cylindrical domains.

TEM micrographs of films, cast from dichloromethane, produced from several poly(dimethyl siloxane)-polystyrene (PDMS-PS) block copolymer were obtained. Changes in morphology were observed as the PDMS block length was varied [206]. At shorter block lengths spherical cell like domains surrounded by dark regions of PDMS matrix component. As the PDMS block length increases cell-like and lamellar PS domains are formed. With very large block lengths PS lamellae are observed.

Studies of the morphologies of poly(2,6-dimethyl-1,4-phenylene oxide)/SBS systems were carried out, with prior staining with mercuric trifluoroacetate using TEM[207]. No other selective staining method was currently available for such systems. The staining process involved immersing the ultra-microtomed section in a 10% solution of HgO in trifluoroacetic acid for up to one hour. The sample was washed in a dilute solution of trifluoroacetic acid followed by distilled water.

Blends of polyolefins (HDPE) and polyamides (PA6) have been investigated as engineering materials. Such mixtures are highly incompatible and annealing in the molten state leads to a coarse morphology with poor mechanical properties [208]. TEM has been used to investigate the effect of a 'compatibilizer' PA6/PB multiblock copolymer on the morphology of the system. The HDPE/PA6 blends show the typical appearance of an incompatible blend with large irregular shaped dispersed phases with distinct boundaries. Addition of the block copolymer reduces the size of the domains and improves the adhesion between the two phases.

CHAPTER 3. SAMPLE PREPARATION

3.1 Introduction

Two formulations were prepared by the author. PW1 was prepared to match GEN1[5]. GEN1 is a water-based latex developed for use as an internal liner for beer and beverage cans. PW1 was prepared without the addition of the cross-linker, as this could be added later. PW2 was a similar formulation to PW1 but was prepared using methyl methacrylate in place of styrene. Both formulations had an epoxy to acrylic weight ratio of 80:20 and the acid groups were both neutralised to 70% with N,N-dimethylethanolamine (dimethyl amino ethanol, DMAE). The epoxy resin used in these formulations was a commercially available '9' type epoxy, DOW XZ86762.

The chemical structure of an epoxy resin is shown in Figure 3.1.

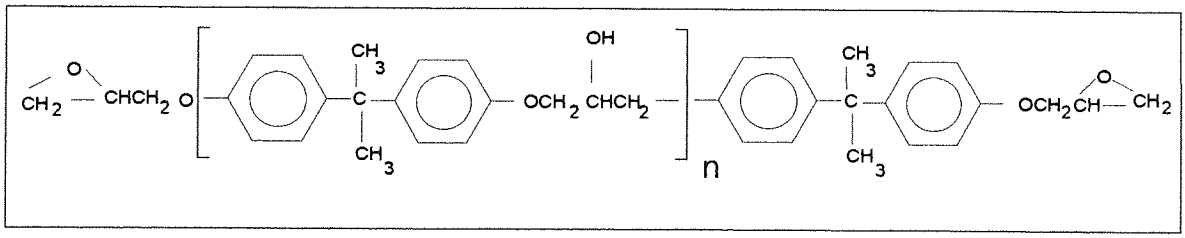

Figure 3.1 Structure of Epoxy resin

The commercial name, value of the repeat unit, n, and the approximate number average molecular weight are given in Table 3.1.

Table 3.1 Molecular Weight Vata of various commercial grade Epoxy Resins[209]

polymer	number of repeat units, n	molecular weight	Tg [210] (°C)
Epikote 828	0	380	-
Epikote 1001	2.0	900	30
Epikote 1004	3.7	1400	54
Epikote 1007	8.8	2900	69
Epikote 1009	12	3750	82

Four latices based on the GEN1 type formulation were prepared by Holden Surface Coating research laboratories. The formulations are given in Table 3.2.

Table 3.2 Polymer formulations used in water-based latices

Latex number	Base resin number	epoxy: acrylic	degree of neutralisation
WRB633	WRB622	60:40	35%
WRB624	WRB622	60:40	70%
WRB625	WRB621	80:20	70%
WRB626	WRB623	90:10	70%

The base epoxy resin used in these formulations were prepared via a 'liquid upgrade' process i.e. a low molecular weight liquid epoxy resin, DER333, was reacted with 4,4'-iso propyl- lidenediphenol (Bisphenol A, diphenylolpropane, DPP) to produce a high molecular weight epoxy resin.

3.2 Sample preparation

3.2.1 Experimental resins PW1 and PW2

2-Butoxy ethanol (1000 g) and n-butanol (1000 g) were added to a 3 litre flask fitted with a reflux condenser, stirrer, nitrogen line and addition funnel. The contents of the flask were heated to 100-110^{0}C and DOW XZ86762 (2000 g) was added over a period of 1 hour. The temperature was maintained until all the solid resin has dissolved. A quantity of the epoxy solution (600 g) was added to a 1 litre flask fitted with a reflux condenser, stirrer, nitrogen line and addition funnel. The contents of the flask was heated to 115-120^0 C. A mixture of methacrylic acid (48.74 g), styrene (21.38 g) and benzoyl peroxide (4.88 g) was added over a period of two hours. The temperature was held at 115-120^{0}C for a further 1 hour before cooling to 90^{0}C. De-ionised water (416 g), dimethyl amino ethanol (14 g) and 2-butoxy ethanol (14 g) were added to a separate 1 litre flask and

heated to 60°C. Graft polymer (250 g), held at a temperature of 90°C, was added over a period of 1 hour and stirred for a further 30 minutes.

The polymer PW2 was prepared using the above process but with the addition of methyl methacrylate in place of styrene.

Table 3.3 shows the compositions of the epoxy-graft-acrylic polymers PW1 and PW2.

Table 3.3 PW1 and PW2 epoxy-graft-acrylic polymer compositions

Component	% composition	
	PW1	**PW2**
epoxy resin	80.0	80.0
methacrylic acid	13.0	13.0
styrene	7.0	-
methyl methacrylate	-	7.0
benzoyl peroxide	1.3	1.3

Table 3.4 shows the composition of the latices prepared from the epoxy-graft-acrylic polymers PW1 and PW2.

Table 3.4 PW1 and PW2 latex composition

component	% composition
epoxy-graft-acrylic polymer	20.0
de-ionised water	60.0
2-butoxy ethanol	10.0
n-butanol	8.0
DMAE	2.0

3.2.2 Experimental resins WRB621, 622, 623 and 624.

Stage 1: Preparation of epoxy resin via 'liquid up-grade' (LUG process)

2-Butoxy ethanol (18.74 g) and DER333 (123.50 g) liquid epoxy resin were placed in a 2 litre flask. The contents of the flask were heated to 50^{0}C and Bisphenol A (65.10 g) followed by 2-butoxy ethanol (14.25 g) were added to the flask. The flask was heated to 70^{0}C and vacuum was applied. The vacuum was increased to 25-27" mercury and the distillate collected. By the time the temperature reached 120^{0}C approximately 3.0 g of distillate had been collected. The flask was set-up for direct reflux and heated to 150-160^{0}C. This temperature was maintained until the final epoxy molar mass (EMM) was between 4000-5000. At this point de-ionised water (0.50 g) and 2-butoxy ethanol (18.45 g) were added. When the temperature was below 150^{0}C n-butanol (88.61g) was added to the flask.

Stage 2 Acrylation

Methacrylic acid (30.45 g), styrene (15.90 g) and ethyl acrylate (0.41g) were placed into a beaker and warmed to 50^{0}C. Benzoyl peroxide catalyst (4.23 g) and 2-butoxy ethanol (11.90 g) were added to the beaker. The contents were stirred until the catalyst had dissolved. The monomer was transferred to an addition funnel and added at a uniform rate, to the epoxy solution prepared in stage 1 at 115-118^{0}C. This process took 2 hours 15 minutes. At the end of the monomer addition the temperature was held at 115-118^{0}C for one hour.

Stage 3:dispersion

De-ionised water (472.4 g), dimethylamino ethanol (22.19 g) and 2-butoxy ethanol (28.07 g) were added to a separate 2 litre flask fitted with a stirrer and a side arm and warmed to 50^{0}C. The acrylated polymer was added to the 2 litre flask over a period of 40

minutes during which time the temperature was expected to rise to 60-65^{0}C. After the addition of the polymer, the flask was stirred for 30 minutes. De-ionised water (78.61 g) was added and stirred for a further 30 minutes. The final characteristics of the latices were checked . The solid content is typically 22.5 ± 1% and the viscosity, as measured as a flow time through a BSS4 flow cup, range from 50 to 90 seconds.

Table 3.5 details the component weights of the four modifications.

Table 3.5 Composition of epoxy-graft-acrylic base-polymers

Stage	component	WRB625	WRB626	WRB633	WRB626
	epoxy:acrylic	**80:20**	**60:40**	**60:40**	**90:10**
Stage 1: Liquid Up-grade	2-butoxy ethanol	18.74	18.74	18.74	18.74
	DER331	123.50	92.96	92.96	139.44
	Bisphenol A (DPP)	65.10	49.01	49.01	73.50
	2-butoxy ethanol	14.25	14.25	14.25	14.25
	de-ionised water	0.50	0.50	0.50g	0.50
	2-butoxy ethanol	18.45	18.45	18.45	18.45
	n-butanol	88.61	88.61	88.61	88.61
Stage 2: Acrylation	methacrylic acid	30.45	60.02	60.02	15.01
	styrene	15.90	31.34	31.34	7.84
	ethyl acrylate	0.41	0.81	0.81	0.20
	benzoyl peroxide	4.23	8.33	8.33	2.08
	2-butoxy ethanol	11.90	11.90	11.90	11.90
	n-butanol	6.69	6.69	6.69	6.69
Stage 3: Dispersion	de-ionised water	472.40	472.40	472.40	472.40
	DMAE	22.19	43.74	21.86	10.94
	2-butoxy ethanol	28.07	28.07	28.07	28.07
	de-ionised water	78.61	78.61	78.61	78.61

3.2.3 Formulations of the 46900 type

The can coating latex 46900 is prepared in a similar manner to that of GEN 1. A phenolic resin is reacted with the epoxy-g-acrylic polymer prior to dispersion in water. The details of composition and preparation are restricted by the wishes of Holden Surface Coatings.

CHAPTER 4. POLYMER CHARACTERISATION: EXPERIMENTAL

4.1 Infra-red spectroscopy

4.1.1 Introduction

The samples analysed were variants of the standard epoxy-graft-acrylic type formulation known as GEN 1 [5]. The preparation of these samples is described in Chapter 3. Samples of the epoxy-graft-acrylic polymers and dispersed latices were examined using IR spectroscopy to determine both the chemical nature of the formulation and the level of acrylic polymer present in the samples.

In order to assign absorption bands, IR spectra of standard formulations were recorded. Samples with varying ratios of epoxy to acrylic and various cross-linking agents were examined. Commercial products as well as experimental formulations were included in the analyses. To determine the amount of acrylic polymer in the samples mixtures of epoxy resin and an acrylic copolymer, having a monomer composition similar to that used in the grafting process, were prepared.

All spectra were recorded using a Nicolet 5DX Fourier transform infra-red spectrometer.

4.1.2 Assignment of IR absorption bands

Infra-red spectra of epoxy resin (DOW XZ86762), poly(acrylic acid), poly (methyl methacrylate) and polystyrene were recorded and the characteristic IR absorption bands were assigned. Spectra of GEN1 which uses a melamine-formaldehyde cross-linking agent and a '46900' type latex which uses a phenolic resin cross-linking agent were also recorded. Spectra of the epoxy-graft-acrylic polymers WRB621, WRB622 and WRB633 and the latices WRB624, WRB625, WRB626 and WRB633 were also obtained. Details of the preparation of these materials are given in Chapter 3.

4.1.3 Determination of the epoxy and acrylic content: Calibration

Calibration was achieved by preparing mixtures of epoxy resin and an acrylic polymer (Holden internal number AT1140) with a composition similar to that used in the grafting process i.e. 65:35 methacrylic acid to styrene. The resin content of the acrylic polymer was 25% w/w, the remainder being solvent. Seven mixtures were prepared with an acrylic to epoxy ratios ranging from 0.10/ 1.0 to approximately 5.0 / 1.0. The polymer mixtures were dissolved in tetrahydrofuran, cast onto potassium bromide windows and vacuum dried at 90^{0}C for 20 minutes. IR spectra of the samples were recorded and plotted using a Nicolet 5DX Fourier transform infra-red spectrometer. For each spectrum ten scans were collected and plotted. The absorption values at 1730, 1600, 830 and 700 cm^{-1} were measured. These absorptions are characteristic of the epoxy, acrylic and styrene components present in the samples.

Graphs of total (i.e., acrylic plus styrene) acrylic to epoxy ratio versus the ratio of measured absorption values at 1730 cm^{-1} and 830 cm^{-1}, 1730 cm^{-1} and 1600 cm^{-1} and 830 cm^{-1} and 700 cm^{-1} were plotted and linear regression was used to calculate the slope and intercept values.

4.1.4 Sample analysis

Samples of epoxy-g-acrylic base polymers WRB621, WRB622 and WRB633 (see Chapter 3.1 for details of these formulations) were added to sample vials and diluted in tetrahydrofuran. The samples were shaken until completely dissolved. For each sample a drop of solution was then placed upon a potassium bromide IR window. The sample was then spread evenly across the window using another KBr window. The sample was allowed to dry at 90^{0}C under vacuum for 30 minutes and their IR spectra were then recorded. IR spectra of the latices were prepared by casting the samples onto silver chloride discs and drying in a vacuum oven at 90^{0}C for 20 minutes.

The spectra were plotted and absorption values at 1730, 1600, 830 and 700 cm^{-1} were measured. The ratio of absorption values, see previous chapter, were calculated and the acrylic content of the samples were determined.

4.2. Nuclear magnetic resonance spectroscopy

All spectra were recorded using a Bruker AC300 MHz spectrometer

4.2.1 Epoxy resins.

Samples of commercially available epoxy resins of various molecular weights were analysed to assign all proton and carbon-13 peaks and to determine the effect of molecular weight changes on the appearance of the spectra. The chemical structure of epoxy resins is shown in Figure 3.1. The commercial name, the repeat unit n and the approximate number average molecular weight are given in Table 3.1. Samples of Epikote's 828, 1001, 1004 1007 and 1009 were dissolved in deuterated chloroform and both proton and carbon-13 NMR spectra were recorded.

4.2.2 Epoxy-graft-acrylic resins

Samples of the epoxy-graft-acrylic polymers WRB621, WRB622 and WRB623 were dissolved in deuterated chloroform and both proton and carbon-13 NMR spectra were recorded.

4.2.3 Epoxy: Poly(methyl methacrylate) mixtures

Carbon-13 NMR spectra of mixtures of epoxy and poly(methyl methacrylate) polymers were recorded to ascertain the lower limits of detection for the acrylic component.

4.3 Solvent Fractionation

4.3.1 Introduction

Woo[5] suggests that epoxy homopolymer can be extracted from epoxy-graft-acrylic (e-g-a) polymers using a toluene Soxhlet extraction. DER669 was used to determine the extraction efficiency. This polymer was used since it was thought that it had a molecular weight distribution (MWD) similar to that of the epoxy used in the graft formulations. The extraction efficiency of the DER669 was found to be 100%. When the extraction was carried out on the e-g-a polymer only 47% was extracted. The GPC profile of the extracted epoxy indicated that it was lower molecular weight than the initial epoxy. This suggested that the graft was taking place preferentially on high molecular weight epoxy chains.

A program of work was undertaken to:

i. Compare molecular weight distribution of DER669 with epoxy resins used in current commercial formulations. The values quoted by Woo for DER669 and values determined by the author for the epoxy resins used in the current investigation are significantly different. The quoted values of Mn, Mw and Mz are 1610, 8050 and 25200 respectively. The base epoxy resin used in this study had Mn, Mw and Mz equal to 7000, 20000 and 40000 respectively,

ii. determine extraction efficiencies for epoxy resins of various molecular weights,

iii. determine the levels of ungrafted epoxy resin in epoxy-graft-acrylic polymers with various levels of acrylic, and

iv. determine the molecular weight distribution of the acrylic homopolymer.

4.3.2 Soxhlet extraction

All Soxhlet thimbles were preconditioned prior to use, using the following steps:

1. Warm in a box oven at 80^0C for 2 hours.

2. Soxhlet extract in toluene for 6 hours.

3. Warm in a box oven 80^{0}C for 2 hours and leave to cool for 1 hour prior to use.

The sample was weighed into a pre-weighed Soxhlet thimble and then extracted for two 8 hour periods. The thimble was then dried at 80^{0}C and allowed to cool prior to re-weighing.

The samples analysed included: a '7' type molecular weight epoxy resin, a '9' type molecular weight epoxy resin, and epoxy-g-acrylic resins with composition 90:10, 80:20 and 60:40 epoxy to acrylic.

4.3.3 Liquid-liquid extraction

A second method, to determine the level of un-grafted epoxy resin, was developed. This involves dissolving the sample (1 g, accurately weighed), in a mixture of toluene and tetrahydrofuran (80 cm^3 and 40 cm^3 respectively). The carboxylic acid rich component was then extracted using 1M sodium hydroxide (40 cm^3). Each of the separated layers was extracted a second time and the appropriate fractions combined.

The non-volatiles from the organic layer were weighed and kept for further analysis using IR spectroscopy and GPC. The aqueous extract was neutralised with hydrochloric acid prior to evaporation to dryness. This dried extract was then Soxhlet extracted in butanone in an attempt to extract the epoxy rich component.

4.4. Gel Permeation Chromatography

4.4.1 Introduction

Epoxy-graft-acrylic polymers used in 'GEN1' type water-based formulations have been characterised [5]. It was estimated that 47% of the epoxy component remains ungrafted, 61% of the acrylic monomer components undergo polymerization to form

acrylic copolymer leaving 39% of the acrylic monomers to graft onto the remaining 53% of the epoxy resin.

GPC was used to determine the increase in molecular weight of the epoxy backbone due to grafting and to obtain quantitative information regarding both the total composition i.e. epoxy to acrylic ratio and the composition as a function of molecular weight.

4.4.2 GPC instrumentation

(a) GPC System 1

The Waters 840 chromatograph consisted of a 510 pump, a 712 'WISP' auto-injector, column oven, temperature controlled at 35^0C, a variable-wavelength UV detector and a 410 refractive index detector, temperature controlled at 40^0C. The pump and auto-injector were controlled using a DEC 'pro 350' computer running Waters 'Expert' software. The computer could also collect data from both detectors.

The solvent used was inhibitor-free tetrahydrofuran which was degassed by bubbling helium gas through it. The flow rate of the mobile phase through the columns was set to 2.0 cm^3 min^{-1}. The column set consisted of two 30 cm by 7.2 mm, 10 μm 10^4A and two 30 cm by 7.2 mm, 10 μm 500A PLGEL columns connected in series. Data from the detectors could also be collected using the customised data station described in Chapter 4.4.3.

(b) GPC System 2

The Dupont chromatograph consisted of a 8800 pump, column oven fitted with a Rheodyne valve and temperature controlled at 35^0C, and variable-wavelength UV detector monitoring at 280 nm. The mobile phase consisted of dimethyl formamide degassed by bubbling helium through it. The flow rate of the DMF through the columns was set to 1.0

cm^3 min^{-1}. The column set consisted of two 30 cm by 7.2 mm 10 μm 10^4A and two 30 cm by 7.2 mm, 10 μm 500A PLGEL columns connected in series. Data was collected using the customised data- station described in Chapter 4.4.3.

4.4.3 GPC6000 Customised data-station

(a) System requirements

The system was designed to acquire data from two detectors simultaneously. The data-station was then able to carry out data processing. This included corrections for the time delay between the two detectors connected in series and flow rate deviations between injections. The data-station could also generate time-slice files needed for both molecular weight distribution calculations and copolymer analysis. The data acquisition, flow time corrections and time-slice file generation are carried out using the software in the customised GPC6000 data system. The molecular weight distribution calculations and copolymer analyses are carried out by importing the time-slice files into Lotus 1-2-3 spreadsheet software.

(b) Data reprocessing: a procedure

After the sample has been analysed and the data collected, the raw data file, containing the data from both detectors, is re-loaded into the software. The set retention time of the reference peak is entered into the software and the actual reference peak on the chromatograms from both detectors are manually located using a cursor. The software will then correct the data for the fixed delay time between detectors connected in series and for the difference in flow time, due to minor differences in flow rate and temperature, between the set retention time and the actual retention time of the reference peak. Using a cursor the start and stop times for data reprocessing are manually located. The required number of time-slices (usually 100) are then entered and the time-slice file (now in ASCII format)

containing a column of retention times and a column of time-slice areas is then automatically generated. After loading the spreadsheet software, the time-slice files are imported where the necessary calculations and graphical displays are carried out. The calculations necessary for the determination of the composition of the samples are shown in chapter 5.5.1.

(c) Correction for flow time variations

There will be a difference in the retention times of the reference peak on the chromatograms obtained from both detectors. This is due to the extra volume that the eluent must pass through to pass from the first detector to the second. There will also be differences in the retention times for the reference peaks between subsequent injections. This is due to minor flow rate and temperature deviations. A set retention time for the reference peak is obtained by averaging the retention times of the reference peak for a number of injections.

Let the actual difference in retention time between the two detectors be 'd' and let the variable error i.e. the difference between the actual retention time of the reference on detector 1 and the set time for the reference be equal to $(t_{1ref} - T)$.

The corrections required for each time slice for each detector are therefore:

1. for detector 1 : $t_{1corr} = (t_1 \times T)/(T_{1ref})$

2. for detector 2 : $t_{2corr} = ((t_2 \times T)/(t_{1ref})) - d$

where: t_{1corr} and t_{2corr} are the corrected time-slice retention times, t_1 and t_2 are the measured time slice retention times, T is the set retention time of the internal marker on detector 1, T_{1ref} is the measured retention time of the internal marker on detector 1 and d is the difference in retention time between the detectors.

4.4.4. Molecular weight distribution analysis

(a) Column calibration

The GPC column set was calibrated with polystyrene narrow distribution molecular weight standards (Polymer Laboratories). All molecular weight values produced using this calibration data are therefore polystyrene equivalents.

Three solutions containing 0.2% (w/v) of the following standards, dissolved in inhibitor-free tetrahydrofuran, were prepared.

Solution 1: 127000, 34500, 5100, 950, phenyl hexane (162) and toluene.

Solution 2: 675000, 82565, 10000, 950, 162 and toluene.

Solution 3: 165085, 34500, 2464, 162 and toluene.

The retention times of the peaks were measured and a calibration graph was constructed of ln Mp (peak molecular weight) versus retention time in seconds. The data was fitted using linear, second and third order regression. Residuals were calculated to determine which of the fits produced the lowest error.

(b) Sample analysis

Sample solutions were prepared by dissolving each polymer (0.1 g) into inhibitor-free tetrahydrofuran (10 cm^3). Toluene (10 µl) was added to each solution for use as an internal marker. Values of Mn, Mw, Mz and dispersity are defined as:

$$Mn = \frac{\Sigma NiMi}{\Sigma Ni} = \frac{\Sigma \text{ area}}{\Sigma(\text{area}/MW)}, \qquad (4.1)$$

$$Mw = \frac{\Sigma NiMi^2}{\Sigma NiMi} = \frac{\Sigma(\text{area} \times MW)}{\Sigma \text{ area}}, \qquad (4.2)$$

$$Mz = \frac{\Sigma NiMi^3}{\Sigma NiMi^2} = \frac{\Sigma(\text{area} \times MW^2)}{\Sigma(\text{area} \times MW)} \quad \text{and} \qquad (4.3)$$

$$D = \frac{Mw}{Mn} \qquad (4.4)$$

These calculations were carried out using Lotus 1-2-3.

4.4.5. Copolymer Analysis

(a) Sample response factors using GPC

For multi-component analysis to produce compositions with an acceptable degree of error, the various components present in the polymer systems must have different responses when analysed using different detectors. Details of error minimisation are discussed in Chapter 11.5. The two detectors used throughout this work were the refractive index detector (RI) and a variable wavelength ultra-violet (UV) spectrometer. The absorbance of the eluent from the GPC system is monitored using selected wavelengths of the UV detector. Rather than record complete UV spectra of the various components, the GPC profiles of standard polymer solutions are recorded at different wavelengths. Solutions with accurately known concentrations of phenol, phenolic polymer (Holden product ML97), epoxy resin (DOW XZ86762), polyester (Uralac 1735), polystyrene (10,000 molecular weight narrow distribution standard) and amino resin (Cymel 303) were prepared. Each solution was injected 15 times and for each run the sample was monitored using a different wavelength. The initial wavelength was 235 nm. This was increased by 5 nm for each subsequent injection up to a maximum of 305 nm. GPC profiles and peak areas were obtained for each injection.

(b) Injection reproducibility

By repeated injection of a single sample and by injection of different solutions the errors due to sampling and area measurement were determined. Six solutions, containing accurately known concentrations of DOW XZ86762, were prepared in tetrahydrofuran. One of the solutions was injected six times and the other five solutions each injected once. The areas under the peak for each injection was measured using the 'Waters expert' software. Mean values and population standard deviations were then calculated.

(c) Simple polymer systems

To initially investigate the data handling system and the analytical methodology, a number of simple polymer mixtures were analysed. Each sample was analysed on the chromatograph in two different ways. Firstly, by monitoring using the UV detector at 254 nm and the RI detector and secondly, by using the UV detector only monitoring at 280 nm. Data was collected using both 'Waters expert' and GPC6000 software. The peak areas quoted are those obtained from the 'expert' software. All data plots, unless otherwise stated, were obtained using the GPC6000 software. In all of the following cases the chromatograph was setup as described in Chapter 4.4.2. A quantity (0.01 g) of phenol was added to each solution for use as an internal marker.

i. Epoxy: Polystyrene blends

Solutions containing accurately known concentrations of epoxy resin (DOW XZ86762), polystyrene (5,000 molecular weight narrow distribution standard) and a mixture of these polymers, were prepared in tetrahydrofuran.

ii. Epoxy: polystyrene: poly(methyl methacrylate) blends

Solutions containing accurately known concentrations of epoxy resin (DOW XZ86762), polystyrene (narrow distribution molecular weight standard), poly (methyl methacrylate) (narrow distribution molecular weight standard) and a mixture of these components were prepared in tetrahydrofuran.

iii. Epoxy: polyester

Solutions containing accurately known concentrations of epoxy resin (DOW XZ86762), polyester (Uralac 1735), a mixture of these polymers and a reaction product of these polymers were prepared in tetrahydrofuran.

iv. Epoxy-phenolic

Solutions containing accurately known concentrations of epoxy resin (DOW XZ86762), a phenolic resin (Holden produced ML97), a mixture of these polymers and a reaction product of these polymers were prepared in tetrahydrofuran.

(d) Epoxy-graft-acrylic polymers

Samples of WRB621, WRB622, WRB623 and DLER100 (0.2 g) were weighed into 30 cm^3 sample vials and diluted in inhibitor- free tetrahydrofuran (10 cm^3). The vials were shaken until the polymer had completely dissolved. A quantity of phenol (0.01 g) was added to all of the vials. Each sample solution was injected (20 μl) onto the chromatograph with the UV detector initially monitoring at 280 nm and then a second injection with the UV detector monitoring at 254 nm. Each injection was also monitored using the RI detector. The areas under the polymer peaks were measured using the 'Waters expert' software. The raw data from the detectors was also collected using the GPC6000 software.

4.4.6 Derivatization

(a) Introduction

The compound o-[p-nitrobenzyl]-N,N[diisopropyl] isourea (NBDI) has been used for UV sensitization of carboxylic and fatty acids for HPLC detection. NBDI has a molecular weight of 279.3 and gives derivatives that have an absorbance λ_{max} at 265 nm.

NBDI has the following structure:

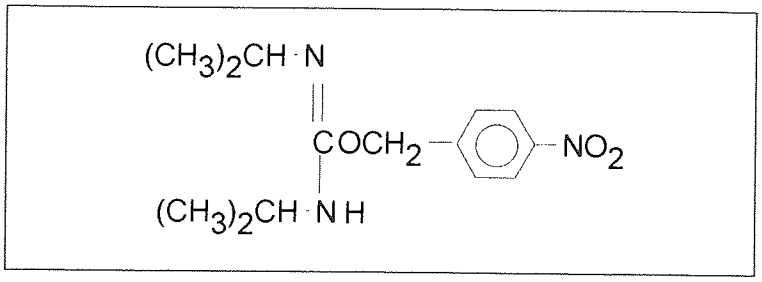

Figure 4.1 Structure of o-[p-nitrobenzyl]-N,N[diisopropyl] isourea (NBDI)

(b) Calibration using poly(acrylic acid)

Poly (acrylic acid) is insoluble in tetrahydrofuran and does not give a response on a UV detector monitoring at 254 or 280 nm. Derivatization with NBDI was used to render poly(acrylic acid) amenable to analysis using GPC. Poly (acrylic acid) (0.0114 g), with a molecular weight of 2000, was weighed into a 5 cm^3 'reactivial' and dissolved in dimethyl formamide (0.5 cm^3). A quantity of NBDI reagent (2 cm^3) was then added. The sample was heated for 2 hours at 80^{0}C in a box oven. After cooling, the solution was diluted to 10 cm^3 in tetrahydrofuran (THF). The sample was then analysed using the GPC under the conditions described in Chapter 4.4.2.

It is calculated that 2 cm^3 of the reagent contains 200 μM NBDI. The molecular weight of the acrylic acid repeat unit is 72. Therefore 72 g of poly (acrylic acid) contains 1 mole of carboxyl groups and 0.0114 g contains 158 μM carboxyl groups. By using the amounts of sample and reagent given above it follows that excess reagent is present in the

sample solutions. The final stage involved measuring the areas under the peaks, obtained using the UV detector monitoring at 254 nm and the RI detector.

(c) Epoxy-g-acrylic polymers

Samples of epoxy-graft-acrylic were derivatized using o-[p-nitrobenzyl]-N,N' [diisopropyl] isourea. A sample of the base epoxy resin was also treated with the reagent. Untreated sample solutions were also prepared. All of the samples were then analysed using GPC. Derivatized samples of WRB621, WRB622, WRB623 and DLER100 were prepared by weighing small amount (0.05g) into 5 cm^3 'reactivials'. Each sample was dissolved in THF (0.5 cm^3). NBDI reagent (2 cm^3) was added and the vials were then heated in a box oven at 80^0C for 2 hours. After cooling, the samples were diluted with THF (10 cm^3), in volumetric flasks. Untreated samples were prepared by diluting each sample (0.05 g) in THF (10 cm^3).

5.1 Infra-Red spectroscopy

5.1.1 Characteristic absorption bands

Infra-red spectra of epoxy, acrylic, amino and phenolic homopolymers as well as GEN 1 and 46900 water-based latex formulations were recorded. See Chapter 3 for details of the formulations. The peak assignments are shown in Table 5.1.

Table 5.1 Assigned IR Absorption Bands from Spectra of Polymers

wavenumber	functional group
3400	epoxy, -OH
3030	epoxy and polystyrene, C-H
3015	epoxy and polystyrene, C-H
2960	epoxy and polystyrene, C-H
2915	epoxy and polystyrene, C-H
2860	epoxy and polystyrene, C-H
1720	acrylic ester, C=O
1700	acrylic acid, C=O
1610	epoxy C=C,
1550	melamine/formaldehyde, N-H
1510	epoxy
830	p-p' disubstituted aromatic ring, epoxy
700	polystyrene
550	epoxy

Figure 5.1(a) shows the IR spectrum of the epoxy-graft-acrylic polymer WRB621. The absorption bands at 1700 cm^{-1} due to acrylic acid and ester and at 700 cm^{-1} due to styrene can be observed in the spectra. Figure 5.1(b) shows the IR spectrum of the same polymer after dispersion in water to produce the latex. The latex number of this material is WRB625. An IR absorption band can be observed at 1550 cm^{-1}, which is due to the amino resin cross-linking agent.

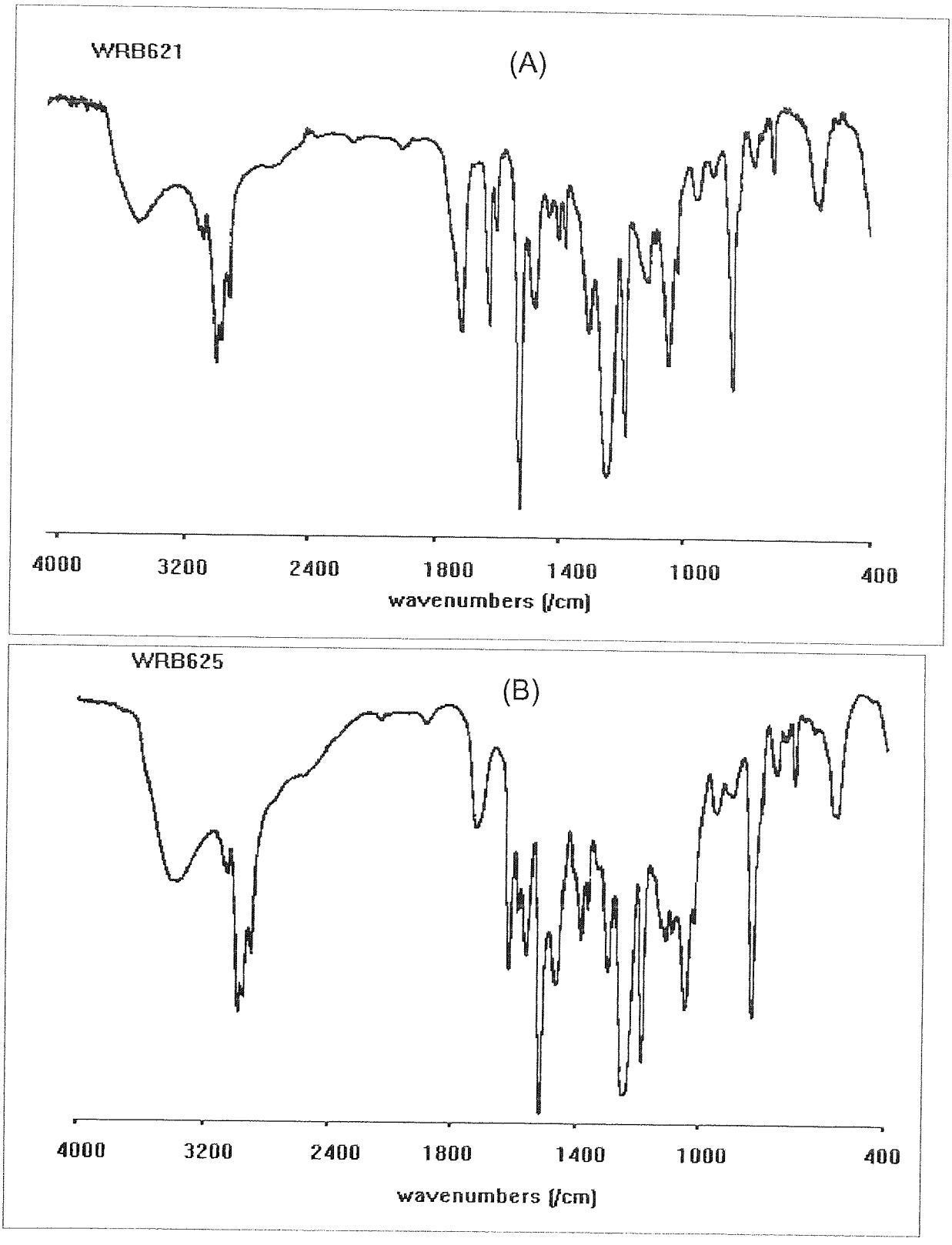

Figure 5.1 Transmission IR spectra of (A) WRB621 base epoxy-g-acrylic polymer with a composition of 80% epoxy and 20% acrylic and (B) water-based latex WRB625, produced from WRB621. WRB625 also contains an amino resin cross-linking agent.

5.1.2 Calibration to determine the level of acrylic modification

Mixtures of an epoxy resin and an acrylic resin, the latter having the same monomer composition as that used in the grafting process (see Chapter 3.1), were accurately prepared. Absorption values from the IR spectra of these standards were measured. The absorption band at 1700 cm^{-1} was the only band due to the acrylic acid and acrylic ester components observed in the spectra. However, the band at 700 cm^{-1}, due to the presence of styrene only, could also be used as a measure of the level of acrylic, since the styrene content of the acrylic polymer in all of the formulations is constant. Absorption bands at 1610 cm^{-1} and 830 cm^{-1} were used to determine levels of epoxy resin. Ratios of absorption values at 1700 cm^{-1}, due to ester to absorption values at 1610 cm^{-1} and 830 cm^{-1}, which are due to epoxy, were calculated. The ratio of the absorption values at 700 cm^{-1}, due to polystyrene to absorption values at 830 cm^{-1} again due to epoxy were also calculated.

Table 5.2 shows the composition of the mixtures and the ratio of absorption values from the IR spectra.

Table 5.2 Polymer Mixtures for IR Calibration

mixture number	composition		ratio of absorption values		
	epoxy:acrylic :polystyrene	total acrylic to epoxy ratio	1700/1610	1700/830	700/830
1	17.4:54.3:28.3	4.75	16.26	9.38	2.92
2	34.7:42.9:22.4	1.88	7.75	3.94	1.17
3	41.6:38.4:20.0	1.40	8.21	3.01	0.89
4	56.6:28.5:14.9	0.77	3.44	1.80	0.53
5	65.6:22.6:11.8	0.52	1.97	1.08	0.34
6	83.9:10.6: 5.5	0.19	0.74	0.41	0.11
7	91.0: 5.9: 3.1	0.10	0.42	0.24	0.07

Least-squares linear regression was applied to the above data. The ratio of acrylic to epoxy was used as the 'x' data and the absorption value ratios as the 'y' data. Table 5.3 shows the results from the regression analysis.

Table 5.3 Linear Regression Data from the IR Calibration Curves of Absorption Ratios versus Acrylic content

peak ratio	intercept	slope	R^2
1700/1610	0.3901	3.4155	0.993
1700/830	0.1378	1.9653	0.994
700/830	0.0202	0.613	0.995

5.1.3 Sample analysis

IR spectra of the polymers WRB621, WRB622 and WRB633, cast from THF solution and vacuum dried, were recorded. IR spectra of the latices WRB624, WRB625, WRB626 and WRB633, cast from dispersion and vacuum dried, were also recorded. Table 5.4 shows the ratios of the absorption values at 1700/1610 cm^{-1}, 1700/830 cm^{-1} and 700/830 cm^{-1}.

Table 5.4 IR Absorption value ratios for Base-Polymers and Latices

sample	ratio of absorption bands at various wavelengths (cm^{-1})		
	1700/1610	1700/ 830	1600/830
WRB621	1.36	0.64	0.17
WRB621/DMAE	0.92	0.38	0.16
WRB622	2.29	1.48	0.47
WRB623	0.85	0.33	0.1
WRB624	1.29	0.59	0.27
WRB625	0.86	0.29	0.15
WRB626	0.64	0.18	0.1
WRB633	1.5	0.77	0.32

From the 1730/1610, 1730/830 and 700/830 calibration curves, the level of epoxy in the epoxy-g-acrylic base polymers and dispersed latices were calculated. These calculated values are shown in Table 5.5.

It is evident that the composition of the graft polymers can be determined from the IR spectra and that reasonable agreement is obtained between calculated and known values.

Table 5.5 Calculated Composition of Epoxy-g-Acrylic Polymers using IR Data

sample	**sample type**	**% Epoxy**			
wavenumber ratio		**1700/1610**	**1710/830**	**700/830**	**known**
WRB621	base polymer	77.1	81.1	80.4	80
WRB621/DMAE	base polymer	86.6	89.1	81.4	80
WRB622	base polymer	64.3	59.4	59.4	60
WRB623	base polymer	88.2	91.1	88.5	90
WRB625	latex	88.1	92.8	82.5	80
WRB624	latex	79.2	81.3	71.1	60
WRB633	latex	75.5	75.7	67.2	60
WRB626	latex	93.3	97.9	88.5	90

However, for the latices, the calculated acrylic composition is approximately half the theoretical value. This can clearly be seen in the spectra of samples shown in Figure 5.1. WRB625 latex is produced from WRB621 i.e. both have identical polymer compositions. However, it can be observed that the ester carbonyl peak at 1725 cm^{-1} is approximately one half of the intensity in the WRB625 spectrum compared to that of the WRB621 spectrum. One of the differences between the samples is that in the latex sample WRB625, the acrylic acid, which gives rise to the carbonyl absorption band, is partially neutralised with dimethyl amino ethanol (DMAE).

To further investigate the reduction of this IR absorption band, a solution of WRB621 (80:20 epoxy:acrylic base- polymer) was prepared in tetrahydrofuran and an IR

spectrum of a cast film of the polymer was recorded. This was compared to a spectrum obtained from the solution after adding excess DMAE. It was observed that the ester carbonyl peak in the sample containing the DMAE was reduced by approximately half compared to the sample with no DMAE added. It would therefore appear that the neutralisation of the acrylic acid groups is the cause of the decrease in the intensity of the IR carbonyl peak. The intensities of the 700 and 830 cm^{-1} peaks appear to be less affected by the DMAE.

5.2 Nuclear Magnetic Resonance Spectroscopy

5.2.1 Proton NMR Spectra of Epoxy resins

The chemical structure of epoxy resins with emphasis on the proton environment is shown in Figure 5.2. The protons are labelled 'a' through to 'k'. The commercial name of the epoxy resins and the value of the repeat unit are given in Table 3.1.

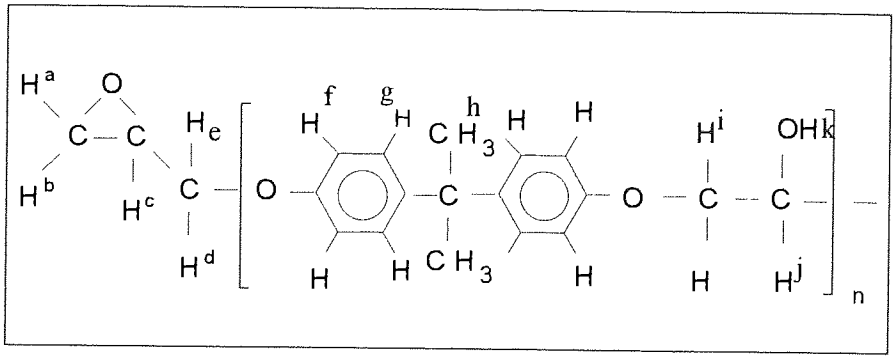

Figure 5.2 Structure of Epoxy Resin with Protons labelled 'a' to 'k'

Proton NMR spectra of epoxy resins with various molecular weights, dissolved in $CDCl_3$, were recorded and peaks assigned. The peak assignments are shown in Table 5.6.

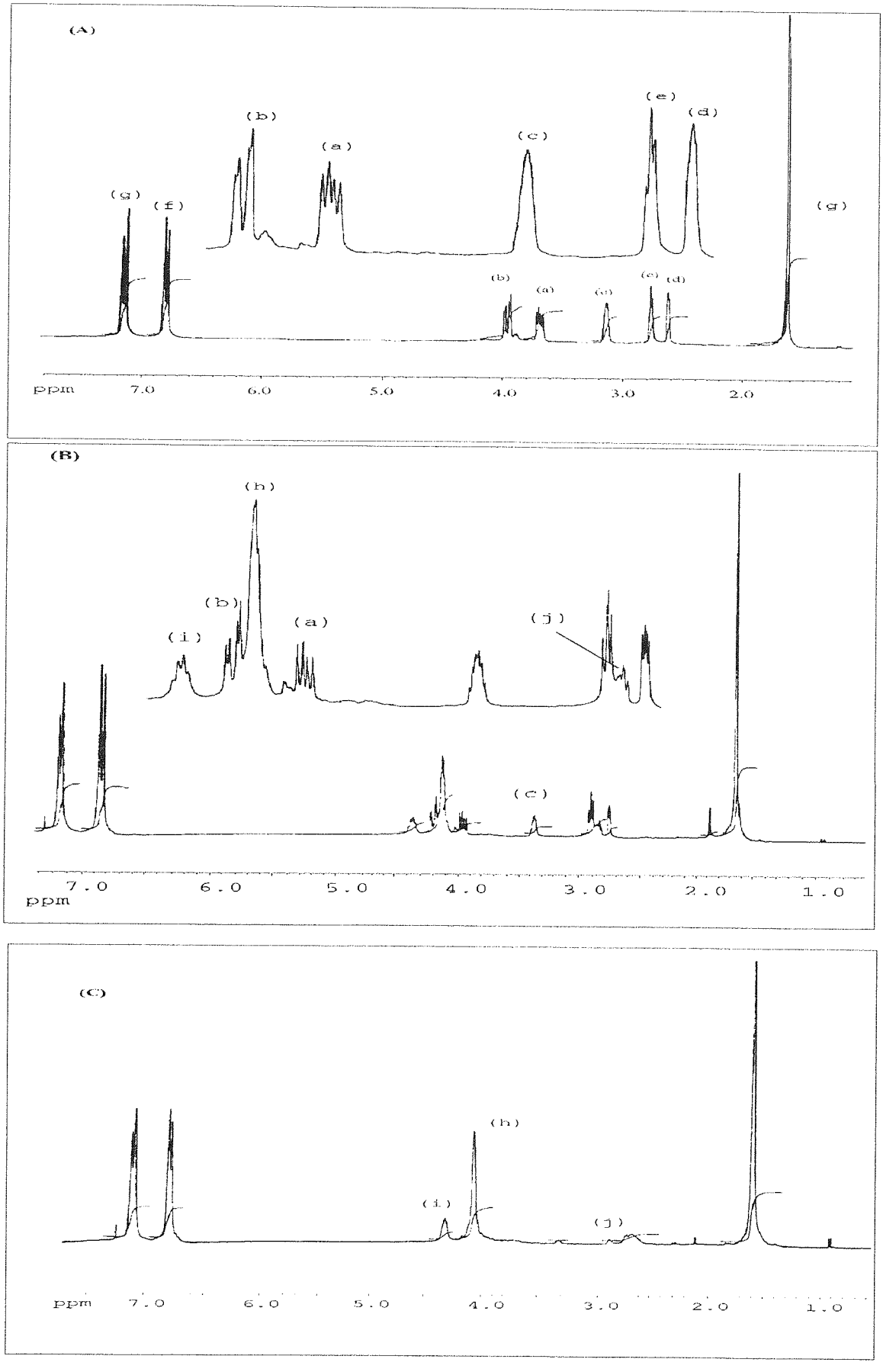

Figure 5.3 Proton NMR spectra of epoxy resins. (A) Epikote 828, (B) Epikote 1001 and (C) Epikote 1009. For peak assignments refer to Table 5.6 and Figure 5.2

Table 5.6 Assignment of Proton Chemical Shifts for Epoxy Resins

Peak	chemical shift (ppm)	Multiplicity	assignment
a	3.9	doublet of doublets	methine
b	4.3	doublet of doublets	methine
c	3.4	complex	methine
d	2.9	singlet, some structure	methine
e	2.7	singlet, some structure	methine
f	6.8	doublet	aromatic
g	7.1	doublet	aromatic
h	1.6	singlet	methyl group
i	4.2	broad (complex)	methylene
j	4.4	pentet?	methine
k	2.8	singlet	hydroxyl

Figure 5.3 (a), (b) and (c) show proton NMR spectra of epoxy resins: Epikote 828, Epikote 1001 and Epikote 1009. The intensity of the chemical shifts, relative to the aromatic protons labelled 'g', in the samples of epoxy resin with differing molecular weights are shown in Table 5.7.

Table 5.7 Proton NMR Peak Intensity Data from Samples of Epoxy Resin

peak	Epikote 828	Epikote 1001	Epikote 1004	Epikote 1007	Epikote 1009
a	0.52	0.22	0.11	-	-
b	0.58	0.23	-	-	-
c	0.43	0.15	0.04	-	-
d	0.45	0.15	0.06	-	
e	0.45	0.15	0.06		
f	0.99	0.92	0.88	0.93	0.94
g	1	1	1	1	1
h	1.5	1.52	1.4	1.59	1.65
i	-	0.61	0.71	0.96	1.06
j	-	0.22	0.19	0.28	0.23
k	-	0.19	0.15	-	-

From Table 5.7 it can be seen that as the chain length of the epoxy polymer increases the signals due to protons in the repeat unit increase relative to those outside of the repeat unit. For example, the intensities of the peaks labelled 'a' and 'b', which are due to the presence of the methylene epoxide group, decrease with increasing molecular weight. It can also be seen that the intensity of the proton labelled 'i' due to a proton of the repeat unit increases with increasing molecular weight.

The proton NMR spectrum of the Epikote 828 sample is further examined in Appendix 11.1 where coupling constants are measured.

5.2.2 Carbon-13 NMR Spectra of Epoxy Resins

Carbon-13 NMR spectra of the epoxy resins Epikote's 828, 1001, 1004, 1007 and 1009, all having different molecular weights, were recorded.

Figure 5.4 (a), (b) and (c) show carbon-13 NMR spectra of epoxy resins: Epikote 828, Epikote 1001 and Epikote 1009.

The chemical structure of epoxy resins with emphasis on the carbon atom environment is shown in Figure 5.5. The carbon atoms are labelled '1' through to '11'.

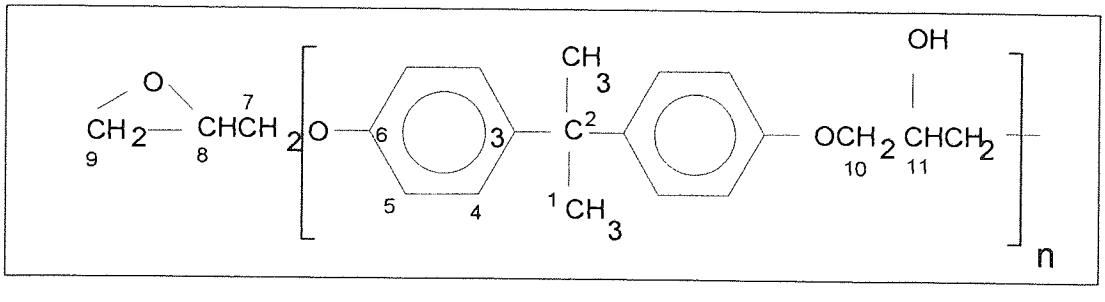

Figure 5.5 Structure of Epoxy Resin with Carbon Atoms Labelled

The spectra were recorded using an attached proton tests (APT) which uses gated decoupling [215]. Carbon atoms in groups with an odd number of protons will produce a positive signal and carbon atoms in groups with an even number of protons will produce a negative signal. The assignments of the peaks from the spectra are shown in Table 5.8.

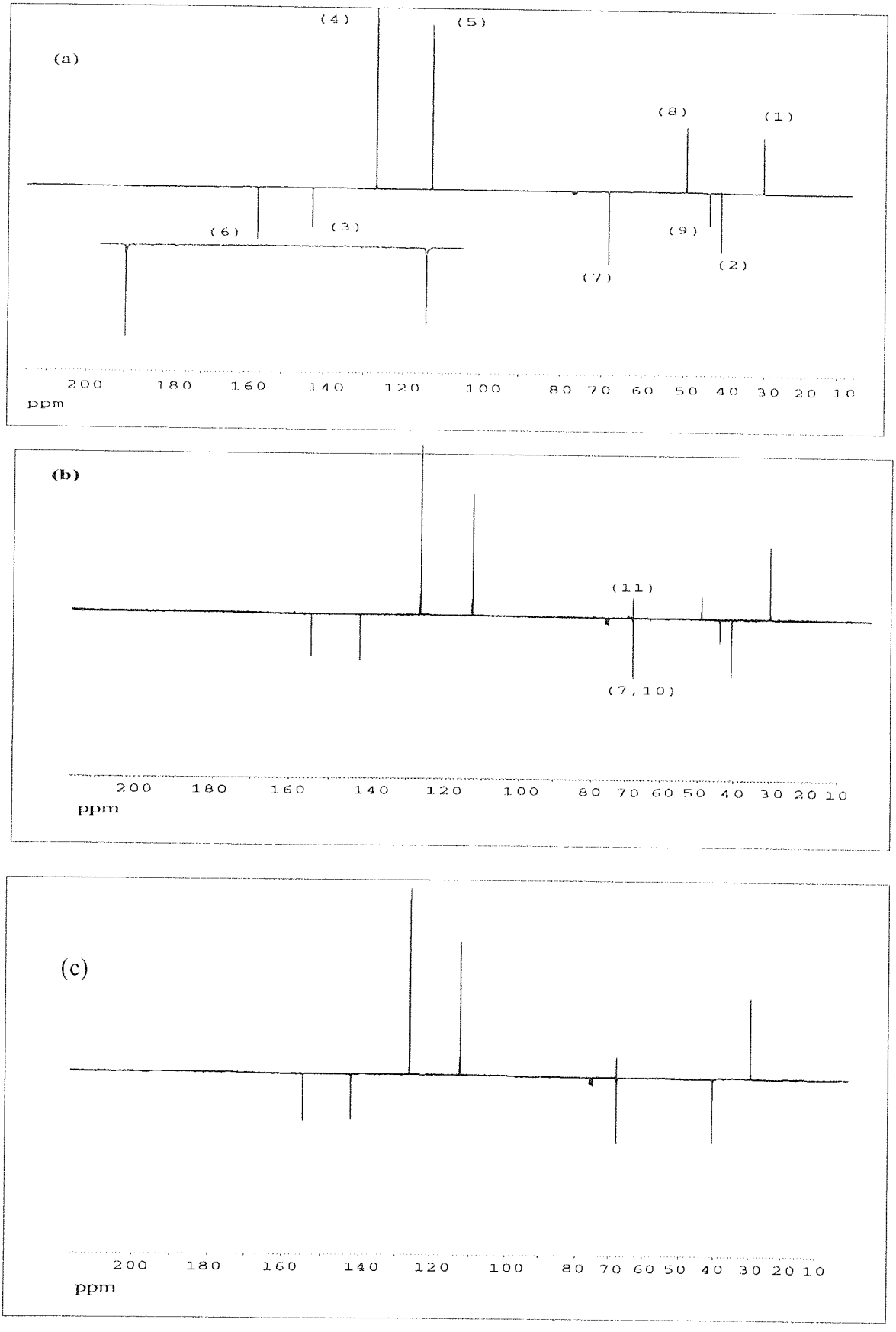

Figure 5.4 Carbon-13 NMR spectra of epoxy resins: (a) Epikote 828, (b) Epikote 1001 and (c) Epikote 1009. For peak assignments refer to Table 5.8 and Figure 5.4

Table 5.8 Assignment of Carbon-13 Chemical Shifts for Epoxy Resins

peak number	chemical shift (ppm)	intensity	description
1	31.1	+	methyl group from 'propane'
2	41.5	-	quaternary carbon from 'propane'
3	143.1	-	aromatic carbon
4	127.1	+	o-aromatic carbon
5	113.1	+	m-aromatic carbon
6	156.1	-	p-aromatic carbon
7	68.4	-	methylene next to 'O'
8	49.7	+	centre methine group
9	44.1	-	epoxide group methylene
10	68.4	-	methylene group in repeat unit
11	68.6	+	carbon attached to -OH group

Table 5.9 shows the variation in peak intensity for the range of epoxy resins. It can be seen, from both Table 5.9 and Figure 5.5, that with increasing molecular weight, the ratios of peaks numbers 1 to 6 are approximately constant. The peak comprising of 7+10 is slightly decreasing, peaks 8 and 9 are decreasing with molecular weight and peak 11 is increasing.

Table 5.9 Carbon-13 NMR Spectra of Various Molecular Weight Epoxy Resins

peak number	epikote 828	Epikote 1001	Epikote 1004	Epikote 1007	Epikote 1009
1	0.31	0.4	0.34	0.34	0.34
2	0.33	0.32	0.26	0.33	0.21
3	0.23	0.26	0.34	0.31	0.33
4	1	1	1	1	1
5	0.9	0.7	0.85	0.87	1
6	0.29	0.24	0.43	0.27	0.43
7+10	0.41	0.34	0.36	0.3	0.29
8	0.36	0.12	0.07	0.03	-
9	0.29	0.13	0.08	0.04	-
11	-	0.11	0.15	0.19	0.22

The ratios of the peaks may therefore be used as a guide to the molecular weight of the epoxy resin.

5.2.3 Effect of Solvent on Carbon-13 NMR Spectra of Epoxy Polymers

Carbon-13 NMR spectra of Epikote 1007 were recorded with the polymer dissolved in deuterated chloroform and in dimethyl sulphoxide (DMSO). Although some of the peaks observed in the spectra had identical chemical shifts, (see Table 5.10), some of the peaks were shifted. Peak assigned 1, 2, 3, 7 and 9 appeared to shift the most (all in a negative) direction when changing from $CDCl_3$ to DMSO. Extra peaks were observed in the 'DMSO' spectrum. These extra peaks are at 45 ppm (-), 49.8 ppm (+), 62 ppm (-) and 70.5 ppm (+).

Table 5.10 Effect of Solvent upon Carbon-13 NMR Spectra of Epoxy Resins

Peak number	description	Chemical shift (ppm)		
		$CDCl_3$	DMSO	difference
1	methyl group	31.1	30.7	-0.3
2	quaternary carbon	41.7	41.2	-0.5
3	aromatic C-1	143.6	142.7	-0.9
4	o-aromatic	127.3	127.4	0.1
5	m- aromatic	113.9	113.9	0
6	p-aromatic	156.2	156.6	0.1
7+10	CH_2-O	68.6	68.9	0.3
8	CH- group	*	49.9	*
9	end CH_2- group	41.7	41.2	-0.5
11	CH-OH	68.7	67.5	-1.2

5.2.4 Proton NMR Spectra of Epoxy-g-Acrylic Polymers

If grafting is taking place on the carbon designated 'h', (refer to Figure 5.2), then as the level of grafting increases the intensity of the signal from the protons on that carbon should decrease.

Table 5.11 shows the measured intensities for the aromatic protons, the 'h' methylene protons and the 'i' methine proton. The table also shows the intensity of 'h' and 'i' protons expressed as a percentage of the aromatic proton signal. There is no apparent decrease in the intensity of the methylene protons as grafting increases.

Table 5.11 Peak Intensities from Proton NMR Spectra

sample	aromatic 'e' + 'f'	$-CH_2-$ 'h'	-CH- 'i'	ratio 'h'	ratio 'i'
Epikote 1004	353.8	157.9	36.6	44.6	10.3
Epikote 1009	420.7	230.1	50.2	54.7	11.9
DLER100	169.1	77.8	16.7	46.0	9.9
WRB623 (90:10)	230.6	104.2	32.4	45.2	14.1
WRB622 (60:40)	109.2	49.5	11.8	45.3	10.8
WRB621 (80:20)	184.5	84.1	21.7	45.6	11.8

5.2.5 Carbon-13 Spectra of epoxy-graft-acrylic polymers

If grafting is taking place on the methylene carbon atom designated 10, refer to Figure 5.5, then as the level of grafting increases the intensity of this peak should decrease. However the ratio is found to remain constant.

Table 5.12 Carbon-13 Peak Intensity Data for Grafted and Ungrafted Epoxy Samples

sample	-C- '2'	$-CH_2-$'10'	-CH-'11'	ratio '10'	ratio '11'
Epikote 1004	3.262	4.480	1.940	1.373	0.595
Epikote 1009	2.621	3.616	2.738	1.380	1.045
DLER100	2.161	4.279	2.337	1.980	1.081
WRB623	2.481	4.271	2.324	1.721	0.937
WRB622	2.173	40.05	2.166	1.864	0.997
WRB621	2.300	3.989	1.933	1.730	0.840

Table 5.12 shows the measured intensities for the quaternary carbon , the '10' methylene carbon and the '11' methine carbon . The table also shows the intensity of '10' and

'11' carbons expressed as a percentage of the quaternary carbon signal. There is no apparent decrease in the intensity of the methylene carbon as grafting increases. If grafting is taking place at carbon 10, then as level of grafting increases the intensity of this peak should decrease. It is not seen to do so to any significant extent.

In order to calculate the theoretical decrease in signal due to grafting, the data determined by Woo[5] was used. Woo suggested that for the average molecule of epoxy-graft-acrylic polymer, there were two graft chains per molecule with an average molecular weight of 10,000. If the epoxy resin had 30 repeat units then the molecular weight would be 8520. In the ungrafted polymer there would be 60 $-CH_2-$ and 30 CH- units. In the grafted polymer 28 units would have the structure:

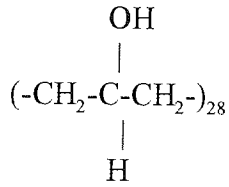

i.e. 56 $-CH_2-$ and 28 -CH- units

and 2 units would have the structure:

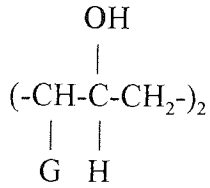

i.e. 2 $-CH_2-$ and 2 -CH- units , where G = graft polymer

The ratio of $-CH_2-$ to -CH- in the graft polymer would therefore be 58 $-CH_2-$ to 30 -CH- i.e. a ratio of 3.87:1.00 protons.

Although differences are observed between the initial epoxy and the graft polymers there does not appear to be a trend with increasing acrylic content.

5.3 Solvent Fractionation

5.3.1 Soxhlet Extraction

(a) Thimble preconditioning and sample preparation

The thimbles were conditioned by warming them in a box oven at 80°C for 1 hour. The thimbles were then left to cool in a desiccator for 24 hours prior to weighing. No further weight loss was observed after extracting for eight hours into toluene, 4-methyl-2-pentanone or 2-butanone. The samples were prepared for analysis by accurately weighing the sample (approximately 1g) into a conditioned and pre-weighed Soxhlet thimble. After the extraction, the thimble was allowed to drain, dry in a box oven at 80°C and then left for 24 hours in a desiccator before re-weighing.

(b) Extraction of epoxy resins

The toluene Soxhlet extraction was found to completely dissolve Epikote 1007, a 7 type epoxy resin, after two separate eight hour extraction periods. The level of epoxy resin extracted, expressed as extraction efficiencies in Table 5.13, is the weight of extract given as a percentage of the initial weight of the sample.

Table 5.13 Soxhlet and Liquid-Liquid Extraction Efficiencies for Samples of Epoxy Resins and Epoxy-graft-Acrylic Polymers

sample	Extraction Efficiency data (%)		
	toluene Soxhlet	2-butanone /toluene Soxhlet	Liquid/ Liquid extraction
Epikote 1007	99.9	100 .0	99.9
DLER100	91.1	99.1	99.3
DOW XZ86762	89.9	99.3	99.8
DER669	90.6	99.5	99.8
WRB621	69.4	81.8	81.0
WRB622	47.5	58.3	55.5
WRB623	78.3	92.6	88.1

The toluene Soxhlet however was found to only extract 90% of the '9' type epoxy resins, DOW XZ86762, DER669 and 'liquid up-grade resin' DLER100, even after eight consecutive eight hour extraction periods. GPC profiles were recorded of the original DLER100 sample and of the soluble and insoluble toluene Soxhlet extracted portions. Molecular weight distribution results were then calculated using the column calibration data from Chapter 5.4.2. The GPC data, shown in Table 5.14, indicates that the molecular weight of the toluene soluble portion of DLER100 is significantly lower than that of the initial sample. This indicates that the toluene Soxhlet is only extracting low molecular weight epoxy resin. The molecular weight of the insoluble portion is significantly higher molecular weight than the initial polymer.

Table 5.14 GPC MWD Results from Soxhlet Extraction of '9' type Epoxy Resin

sample	Mn	Mw	Mz
initial	7510	21400	43900
soluble portion	3450	12500	24300
insolubles	51700	66700	85000

When 2-butanone was used in place of toluene, the extractor was found to block with polymer. Therefore the procedure was modified whereby toluene was used for two eight hour extractions followed by one eight hour extraction in 2-butanone. Under these conditions all of the '9' type epoxy polymer was extracted.

(c) Extraction of epoxy-g-acrylic samples

Toluene and toluene/2-butanone Soxhlet extractions were carried out on the epoxy-graft acrylic formulations WRB621, WRB622 and WRB623. These formulations contain 20, 40 and 10% acrylic component respectively. A detailed composition of these materials can be found in Chapter 3.

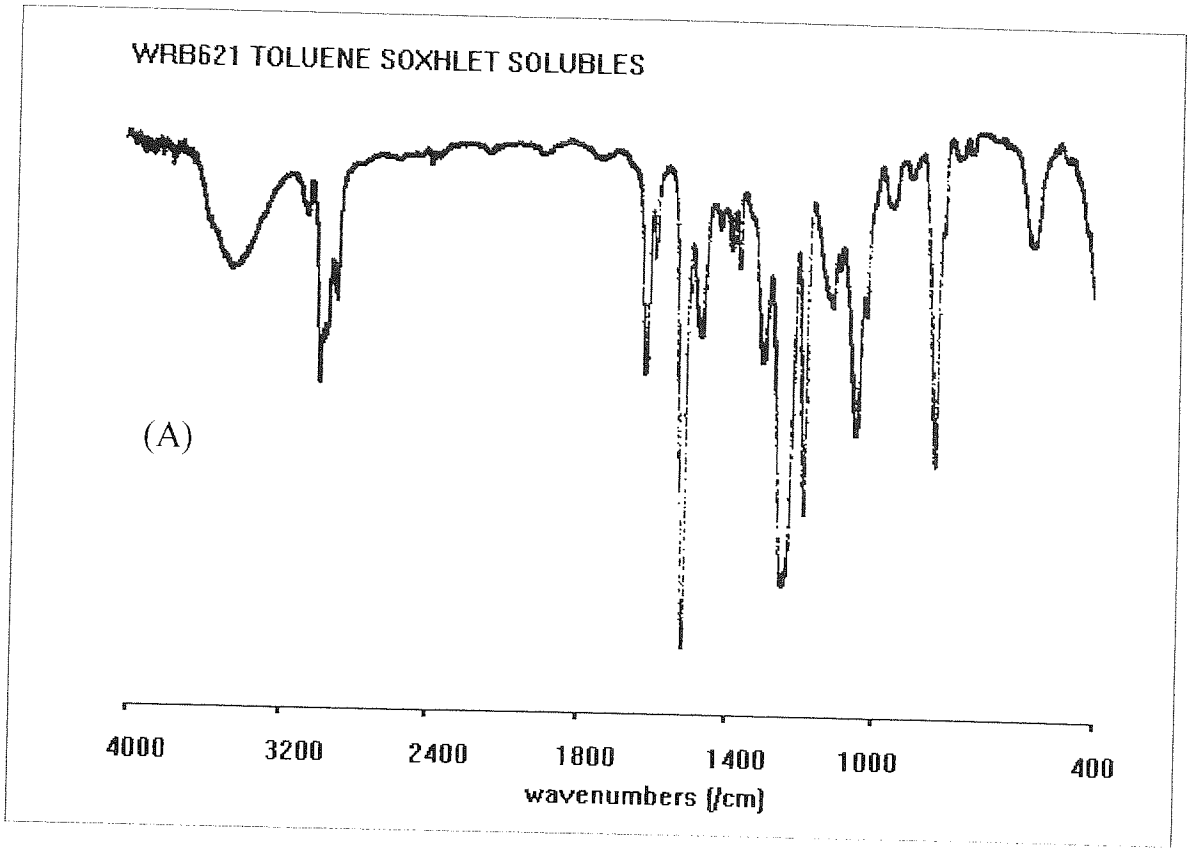

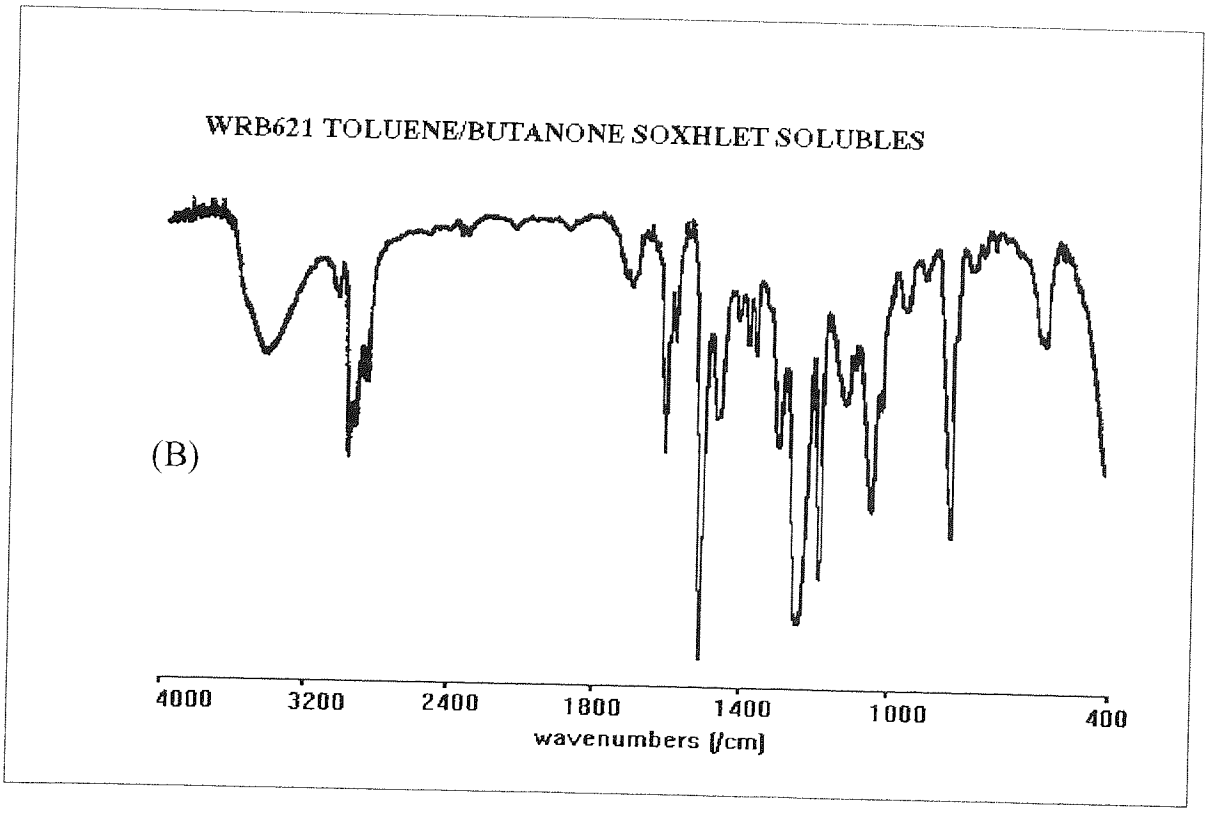

Figure 5.6. Transmission IR spectra of WRB621: (A) toluene Soxhlet soluble portion and (B) toluene/butanone Soxhlet soluble portion.

Table 5.13 shows the extraction efficiency data for both the liquid-liquid extraction and the Soxhlet extraction procedures. The extraction efficiencies quoted in the table are expressed as the weight of epoxy extracted as a percentage of the theoretical weight of epoxy component present in the sample. The IR spectrum of the toluene Soxhlet soluble portion of WRB621, shown in Figure 5.6(a), indicates that only epoxy resin is extracted. This IR spectrum, unlike that of the original epoxy-g-acrylic polymer shown in Figure 5.1(a), does not show the acrylic ester peak at 1720 cm^{-1}. The acrylic component is therefore not soluble in toluene.

GPC profiles of WRB621, DLER100 and the toluene Soxhlet soluble portion from WRB621 were recorded. Molecular weight distribution results were then calculated using the column calibration data from Chapter 5.4.2. The results, shown in Table 5.15, indicate that the soluble portion has a lower molecular weight than the initial epoxy. This observation was also recorded by Woo [5]. In the present case, however, the toluene is only extracting low molecular weight epoxy resin and this is the cause of the low molecular weight value.

Table 5.15 Molecular Weight Distribution Analysis of Epoxy-graft-Acrylic Sample WRB621 after Toluene Soxhlet Extractions

Sample	Mn	Mw	Mz
WRB621 (initial)	7570	23100	53900
DLER100	7510	21400	43900
soxhlet solubles	6300	13200	22300

The IR spectrum of the toluene/2-butanone Soxhlet soluble portion is shown in Figure 5.6(b). The spectrum indicates the presence of a significant quantity of ester functional material. Therefore, the weights of the soluble and insoluble portions, extracted using the toluene/2-butanone Soxhlet extraction, cannot be used to determine the level of ungrafted epoxy.

5.3.2 Liquid-liquid extraction

The composition of the extraction mixture was chosen to minimise the amount of water in the organic layer after separation from the aqueous phase. In a 2:1:1 mixture of toluene: tetrahydrofuran: water, the water content of the upper layer was determined using Karl Fischer titration method and found to be 0.6%. Using a 1:1:1 mixture the water content of the organic layer was 1.2%. To minimise the amount of water soluble polymer in the organic phase, the 2:1:1 ratio of solvents were used for all further extractions.

The liquid-liquid extractions were carried out on epoxy resins and on the epoxy-graft acrylic formulations WRB621, WRB622 and WRB623. These formulations contain 20, 40 and 10% acrylic component, respectively. The levels of epoxy resin extracted from the samples are shown in Table 5.13. The results indicate that for WRB621 (the polymer with a epoxy to acrylic composition of 80:20) the level of ungrafted epoxy is approximately 80%. The liquid-liquid extraction was found to extract all of a '9' type epoxy resin and only epoxy resin from the epoxy-graft-acrylic formulations. Figure 5.7(a) shows the IR spectrum of the organic layer from the extraction of WRB621. The spectrum shows no significant presence of the acrylic ester carbonyl peak.

The epoxy resin extracted from the graft polymer WRB621 was found to have a lower molecular weight distribution than that of the initial epoxy resin (DLER100). The results are shown in Table 5.16.

Table 5.16 Molecular Weight Distribution Analysis of Samples Extracted using the Liquid-Liquid Extraction Procedure

sample	Mn	Mw	Mz
DLER100	7510	21400	43900
DLER100 organic layer	6930	20300	41200
WRB621	7570	23100	53900
WRB621 organic layer	5580	17600	39000

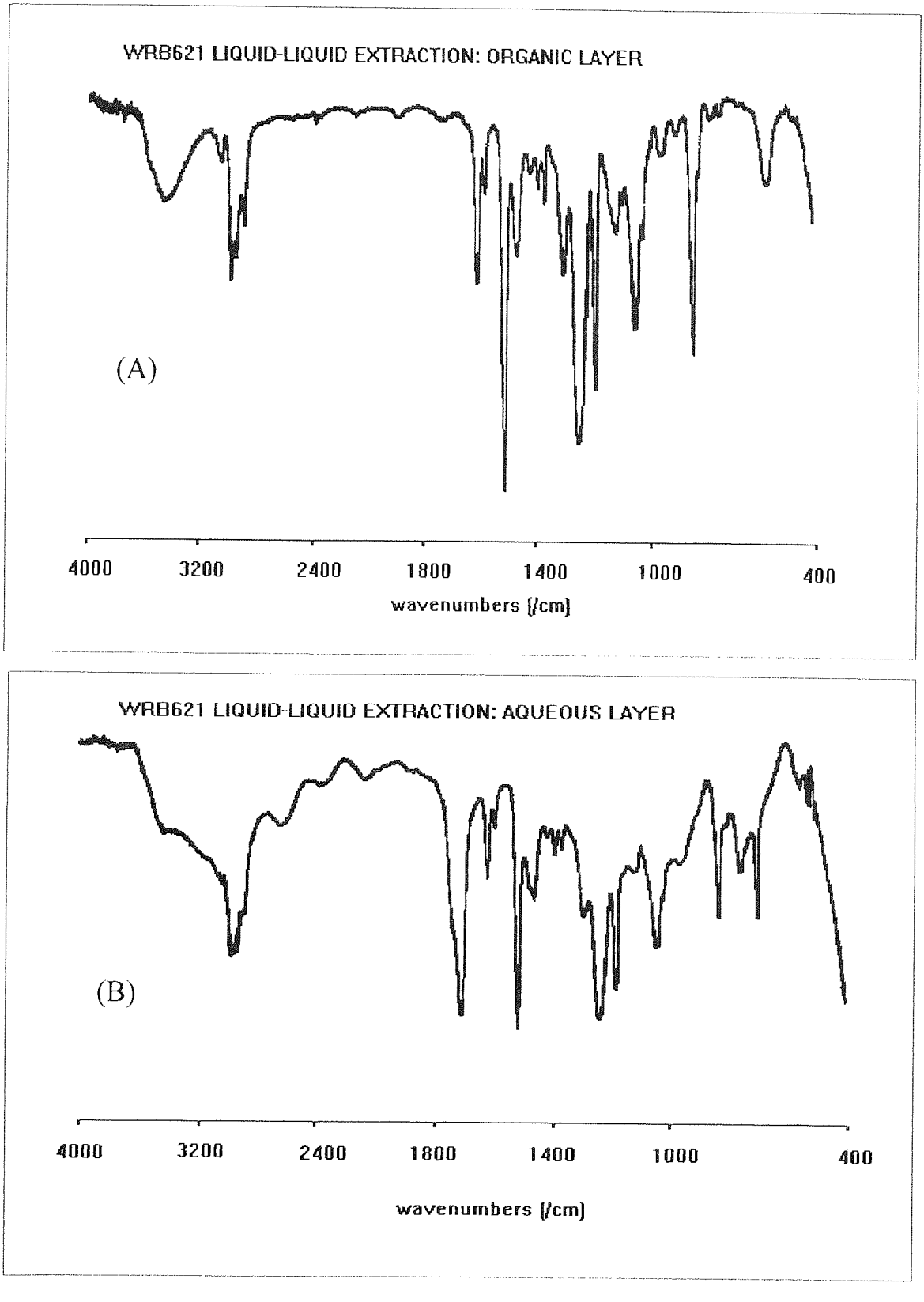

Figure 5.7. Transmission IR spectra of a liquid-liquid extraction of WRB621: (A) toluene soluble portion and (B) aqueous soluble portion Soxhlet extracted into THF.

The extraction procedure is not extracting high molecular weight polymer because this portion is undergoing preferential grafting, rendering it water soluble. This confirms the work carried out by Woo [5] which suggested that the graft was taking place on higher molecular weight epoxy backbone molecules. GPC profiles for WRB621, DLER100 and the polymer from the organic layer from the extract of WRB621 are shown in Figure 5.8.

The aqueous layers, from the liquid-liquid extraction, were neutralised with hydrochloric acid prior to evaporation to dryness. The residue was then Soxhlet extracted into tetrahydrofuran and IR spectra of the tetrahydrofuran soluble extracts were recorded. Figure 5.7(b) shows the IR spectrum of the extract from WRB621. The composition of the extracted polymers were calculated from the IR calibration data shown in Chapter 5.12. The theoretical composition of the polymer, remaining in the aqueous layer, for each epoxy-graft-acrylic sample can be calculated from the known initial composition of the samples and from the determined extraction efficiencies. Table 5.17 shows a comparison between the determined composition of the polymer remaining in the aqueous layer, as determined using IR, and the calculated theoretical composition.

Table 5.17 Composition of Aqueous Layer Determined using IR Calibration Data

sample	Epoxy content (%)	
	theoretical	determined
WRB621	43.2	41.3
WRB622	40.3	40.1
WRB623	51.7	47.1

The measured epoxy to acrylic ratios of the aqueous soluble polymers are close to the calculated values based on the measured ungrafted epoxy content.

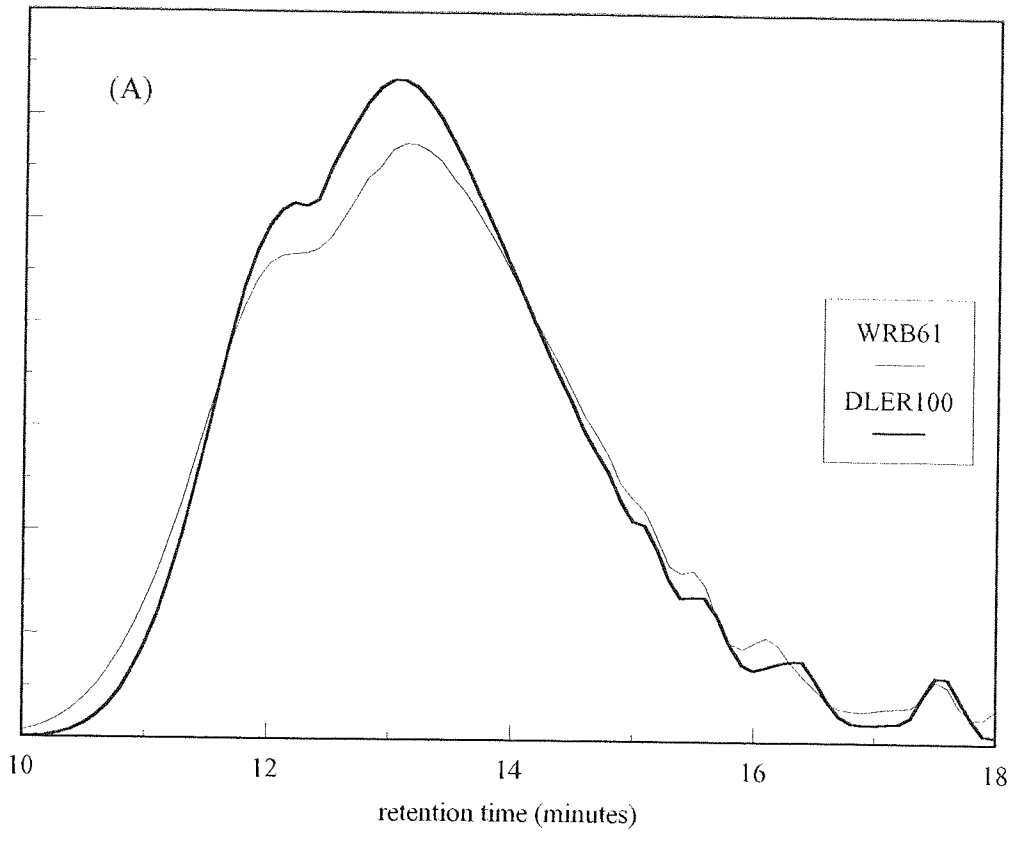

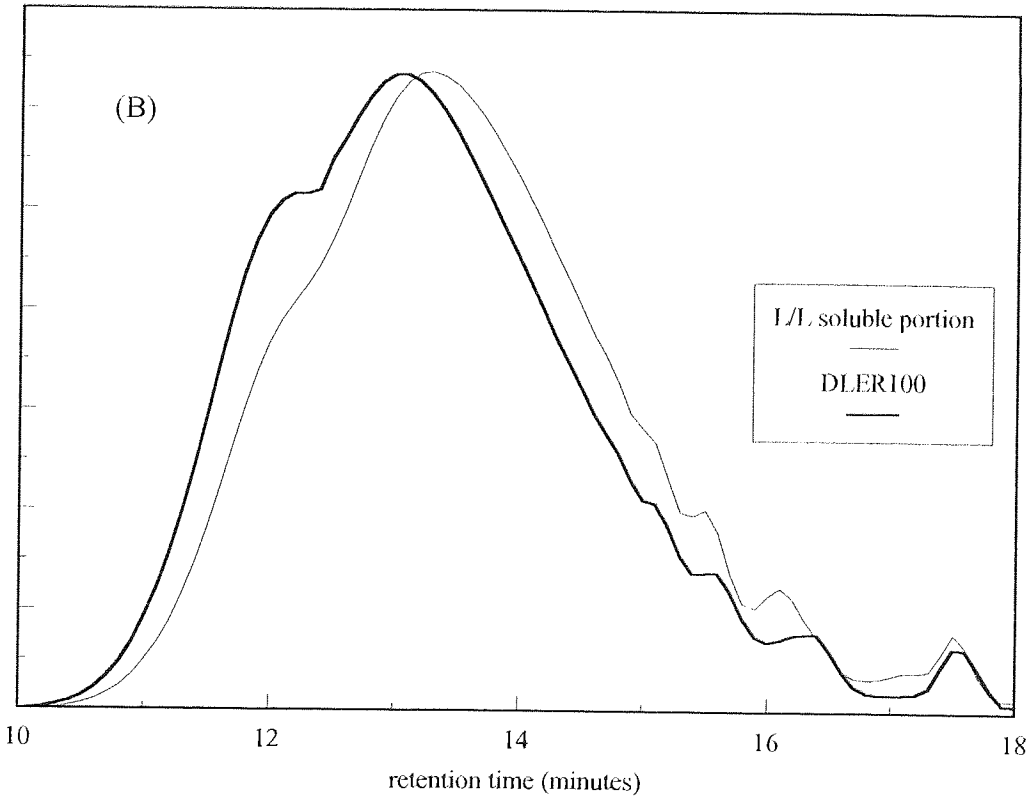

Figure 5.8 GPC profiles of (A) WRB621 epoxy-g-acrylic and base epoxy polymer DLER100 and (B) organic layer solubles from a liquid- liquid extract from WRB621 and DLER100.

If the extraction is carried out at neutral pH a complete separation of components does not occur. The Infra-red spectrum of the dried polymer, obtained from the organic layer, indicated the presence of a significant amount of acrylic ester.

5.4 Gel Permeation Chromatography: Molecular Weight Distribution Analysis

5.4.1 Instrument Conditions

The instrument was configured as described in Chapter 4.4.2. With a flow rate of 2.0 cm^3 min^{-1} the analysis time for each sample was 25 minutes. The results of the variance analysis of the volume injected using the auto-injector are shown in Chapter 5.5.3.

5.4.2 Calibration of the GPC columns

Three solutions of narrow distribution polystyrene molecular weight standards, prepared by diluting each standard (0.02 g) into tetrahydrofuran (10 cm^3), were injected onto the chromatograph. Toluene, which would be used by the GPC software as an internal marker, was added to each of the solutions. The three solutions prepared contained molecular weight standards with the following Mp values:

Standard 1: 127000, 34500, 5100, 950,162 (phenyl hexane) and toluene.

Standard 2: 675000, 82565, 10000, 950, 162 and toluene.

Standard 3: 165085, 34500, 2464, 162 and toluene.

The retention times obtained for each of the standards and the peak molecular weight (Mp) values are given in Table 5.18.

The chromatogram obtained from 'standard solution 1' is shown in Figure 5.9 (a). A graph of all the data points fitted with linear regression is shown in Figure 5.9 (b).

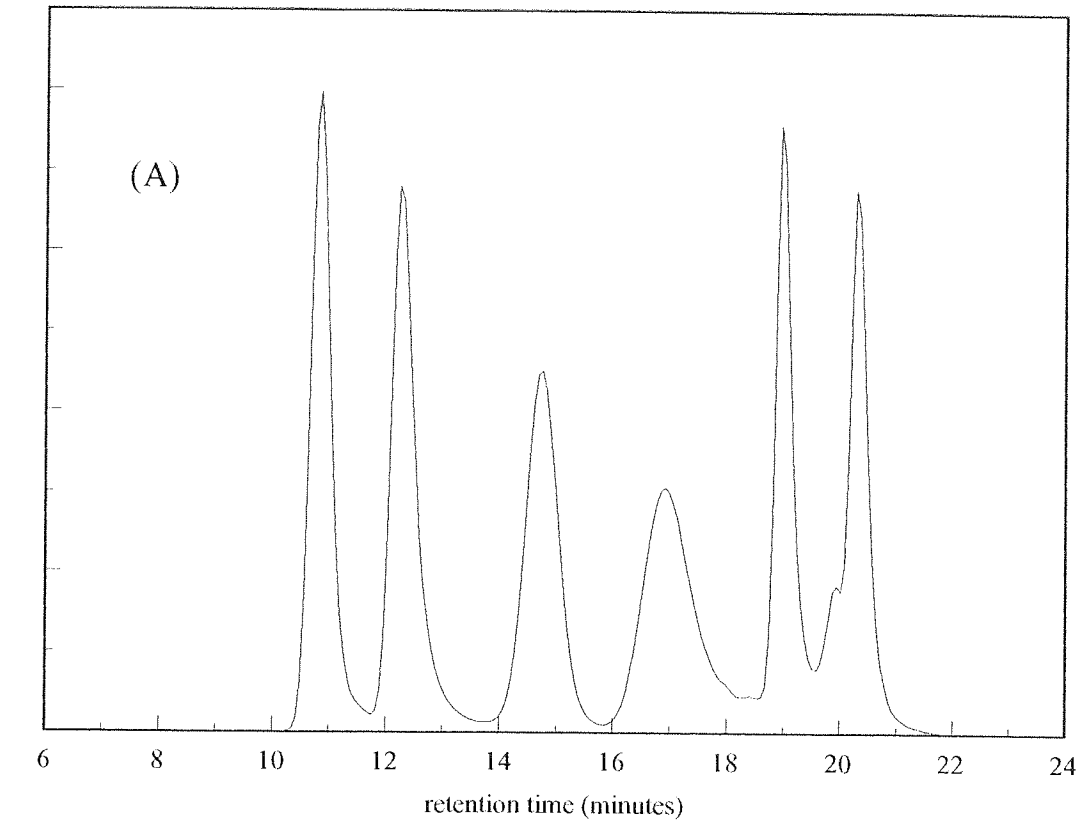

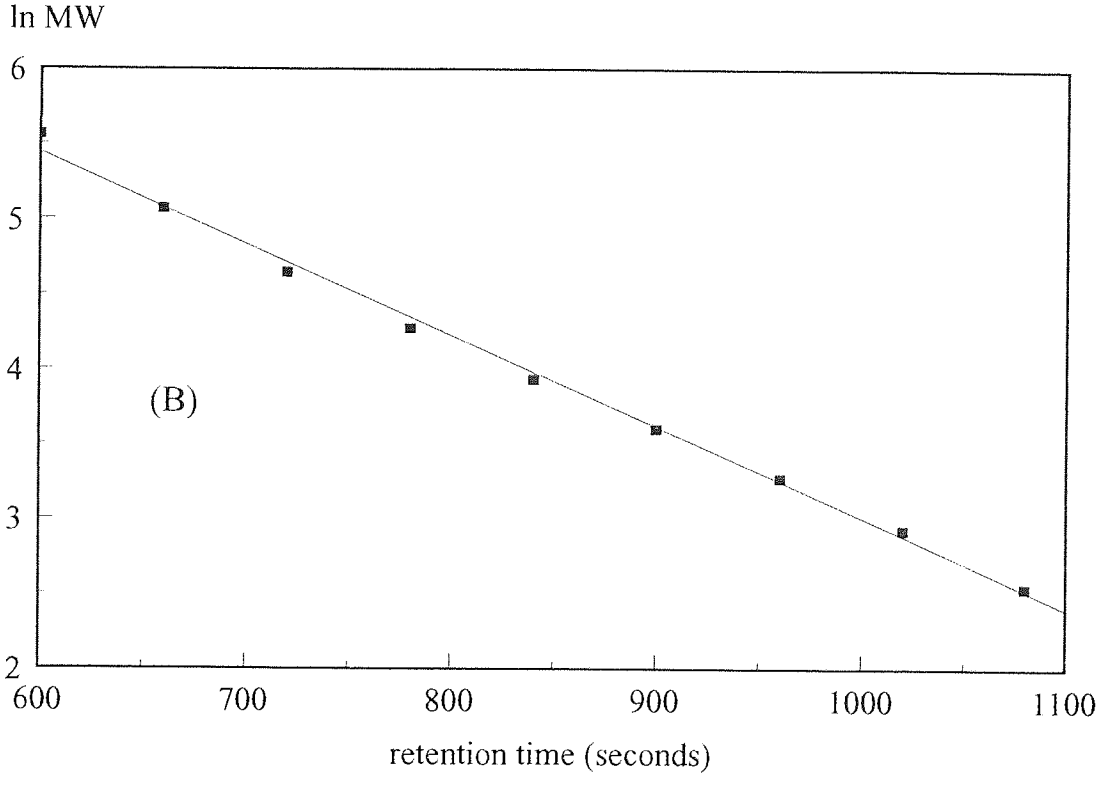

Figure 5.9. (A) GPC chromatogram of molecular weight polystyrene standards with Mp values of 127000, 34500, 5100, 950. Peaks with retention times of 19.1 and 20.5 minutes are due to phenyl hexane (Mp = 162) and toluene respectively. (B) GPC molecular weight calibration curve. Graph is derived from retention times of known molecular weight polystyrene standards. The straight line fit is for illustration only.

Table 5.18 Retention Time of Polystyrene Molecular Weight Standards

peak molecular weight (Mp)	retention time (minutes)
675000	9.66
165085	10.68
127000	10.91
82565	11.44
34500	12.35
10000	13.86
5100	14.82
2464	15.78
950	17.01
Phenyl hexane: 162	19.12
toluene	20.46

Regression analysis was used to calculate the linear, second and third order equations which would fit the above data. See Appendix 4 for further details of the calculations.

Linear regression

The linear equation fitted to the data is of the type:

$$\log (Mp) = B_1X + B_0 \qquad (5.1)$$

where B_1 is the slope, B_0 is the intercept and X is the retention time.

Using standard techniques the slope and intercept were calculated:

slope = -0.00608803, intercept = 9.143139395

Second order regression

A second order equation is of the type

$$\log(Mp) = B_0 + B_1X + B_2X^2 \qquad (5.2)$$

Using standard techniques the constants were determined to be:

$B_0 = 10.547561$

$B_1 = -0.009535$

$B_2 = 2.02 \times 10^{-6}$

Third order regression

A third order equation is of the type:

$$\log(Mp) = B_0 + B_1X + B_2X^2 + B_3X^3 \qquad (5.3)$$

Using standard techniques the constants were determined to be:

$B_0 = 18.739418$

$B_1 = -0.039428$

$B_2 = 3.7385 \times 10^{-5}$

$B_3 = -1.358 \times 10^{-8}$

The equation describing the third order fit is therefore:

$$\log Mw = 18.739418 - 0.039428R_T + 3.7385 \times 10^{-5}R_T^2 - 1.358 \times 10^{-8}R_T^3 \qquad (5.4)$$

where R_T is the retention time in seconds.

Table 5.19 Calculated Mp values from linear, 2nd and 3rd order regression

retention time (minutes)	actual (Mp)	calculated Mp values		
		linear	2nd order	3rd order
9.66	675000	411637	501024	632375
10.68	165000	174554	185033	178174
10.91	127000	143852	148522	137762
11.44	82565	92112	90106	78864
12.35	34500	42846	39052	33411
13.66	10000	12032	10368	9843
14.82	5100	5366	4643	4891
15.78	2464	2393	2144	2473
17.01	950	858	840	1008
19.12	162	144	186	159

To determine which of the equations best represented the data, the retention time of each molecular weight standard was entered to each of the equations given above and values of Mp were calculated. Table 5.19 shows the molecular weight calculated from the linear, second order and third order equations given above.

Values of residuals i.e. the calculated result minus measured peak molecular weight, expressed as a percentage of actual peak molecular weight are given in Table 5.20. It can be seen, from Table 5.20, that the 3rd order fit gives a lower sum of residuals than either the second order or linear regression. The third order fit will be used for all further calculations of molecular weight distributions.

Table 5.20 Calculation of Residuals for Molecular Weight Calibration

retention time minutes	actual Mp	linear residual	2nd order residual	3rd order residual
9.66	675000	39.1	25.8	6.3
10.68	165000	5.7	12.1	7.9
10.91	127000	13.3	16.9	8.5
11.44	82565	11.6	9.1	4.5
12.35	34500	24.2	13.2	3.2
13.66	10000	20.3	3.7	1.6
14.82	5100	5.2	9.1	4.1
15.78	2464	2.9	12.9	0.4
17.01	950	9.7	11.6	6.1
19.12	162	11.0	14.8	2.1
sum of residuals =		142.9	129.2	44.5

5.4.3 Sample analysis

Data was collected using the customised data-station described in Chapter 4.4.3. The interface and software was based on the Jones Chromatography GPC6000 system but specifically modified for the authors requirements. The software allows data to be

collected from two detectors simultaneously. The raw data is then corrected for retention time deviations by use of the toluene internal marker. The data is then converted into a time-slice file and imported into a Lotus 1-2-3 spreadsheet for molecular weight distribution calculations. The equations used to calculate Mn, Mw, Mz and the polydispersity D, are shown in Chapter 4.4.4.

Using the data handling system described above, the molecular weight distribution of the epoxy and epoxy-graft-acrylic polymers were determined. The values obtained are shown in Table 5.21.

Table 5.21 Molecular weight distribution analysis of epoxy and epoxy-graft-acrylic polymers using GPC

sample	Mn	Mw	Mz	D
DLER100	7510	21400	43900	2.9
WRB621	7570	23100	53900	3.1
WRB622	7510	23300	55800	3.1
WRB623	7530	22600	50700	3.1
Epikote 1007	3720	8770	15200	2.4
DER669	5720	18100	40900	3.2
DOW XZ86762	5640	17800	37400	3.2

The Mw and Mz values for the grafted samples are significantly higher than the base epoxy resin DOW XZ86762. The Mw values for the base epoxy resin DLER100 and the graft polymers WRB623, WRB621 and WRB622 with 10, 20 and 40% acrylic component, are 21400, 22600, 23100 and 23300 respectively. It therefore appears that the higher the level of the acrylic component the higher the molecular weight of the resultant graft polymer.

The higher molecular weight of the DER669 used in this study accounts for the observation that the toluene Soxhlet extraction only extracts 90% of the polymer. The

material used by Woo[5] is lower molecular weight and is completely extracted by the toluene Soxhlet. For further details refer to Chapter 10.1.

5.5 Gel Permeation Chromatography: Copolymer analysis

5.5.1 Introduction

GPC may be used to calculate the composition of copolymers and polymer blends. To achieve this the sample is analysed using a number of different detectors. The data obtained may be used to calculate both the total composition of the polymer and the composition as a function of molecular weight.

(a) Determination of Polymer Composition

To determine the composition of a two-component polymer using GPC, the data from two different detectors is required. Errors in the determination can be minimised when the response of the two components on each detector is significantly different. See error analysis in Appendix 6 for further discussion.

The composition of a two component mixture, can be calculated using the following equations:

$$W_1 = (A_1K_4 - A_2K_2) / (K_1K_4 - K_2K_3) \quad (5.5)$$

$$W_2 = (A_1K_3 - A_2K_1) / (K_2K_3 - K_1K_4) \quad (5.6)$$

where:

K_1 and K_2 = response factors for components 1 and 2 using detector 1,

K_3 and K_4 = response factors for components 1 and 2 using detector 2,

W_1 and W_2 = calculated weight fractions for components 1 and 2,

and A_1 and A_2 = measured areas/ responses for the sample using detectors 1 and 2.

The derivations of these equations are shown in Appendix 5.

(b) Polymer composition as a function of molecular weight.

Using the above approach to analyse the chromatogram a point by point composition of the copolymer can be calculated. However, to compare chromatograms from different injections the data must be corrected for (1) time delays between the detectors connected in series and (2) for minor flow rate differences. See Chapter 4.4.3c.

5.5.2 Determination of Response Factors

Solutions of phenol, a phenolic resin (Holden formulation ML97), an epoxy resin (DOW XZ86762), a polyester resin (a Holden formulation), a polystyrene molecular weight standard and an amino resin were prepared in tetrahydrofuran. Each solution was injected onto the chromatograph 15 times, each time monitoring at a different wavelength; starting at 235 nm and increasing at 5 nm intervals up to 305 nm.

The response factor of a component/ polymer is defined as the peak area per unit weight of material in 10 cm^3 solution. Therefore, to obtain the response factors the peak areas are divided by the weights used in the preparation the solutions. The calculated response factors are shown in Table 5.22.

Figure 5.10 shows the graphs obtained by plotting the response factor against wavelength. The result is essentially a UV spectrum for each component over the wavelength range 235 nm to 305 nm.

Table 5.22 Calculated GPC Response Factors

wavelength (nm)	phenol monomer	phenolic polymer	epoxy polymer	polyester polymer	poly-styrene	amino polymer
235	196.1	877.1	2640.9	1682.7	48.1	1978.1
240	60.7	536.6	1343.1	1548.5	42.1	1317.8
245	72.1	253.1	477.6	1300.9	53.5	811.9
250	133.7	100.7	185.4	991.1	68.4	446.3
255	215	72.6	156.6	730.9	83.9	244
260	418.9	104.6	228.4	367.7	104.7	67.2
265	649.6	163.9	336.8	211.2	101.4	20.1
270	918	248.4	481.1	157.8	76.5	5.9
275	1080.5	339.1	624.1	157.3	35.1	2.7
280	925.7	393.4	688.2	155.8	1.3	1.6
285	426.3	379.1	573.6	148.2	1.1	1.2
290	105.4	294	325.6	140.4	1.1	1.1
295	16.7	169.7	73.8	103.8	0.9	0.7
300	5.1	65.8	16.1	60.8	0.8	0.3
305	2.5	16.5	5.1	32.1	0.7	0.3

5.5.3 Injection reproducibility

Six solutions of epoxy resin (DOW XZ86762), labelled 1 to 6, were prepared. Solution 1 was injected six times and Solutions 2 to 5 were injected once only. By repeated injection of a single sample and by injection of different solutions the errors due to sampling and area measurement were determined.

The areas under the peaks were measured using the computer software. The areas and response factors, calculated by dividing the peak area by the sample weight, are shown in Table 5.23. An adjustment to the response factors of 25/10 was used since in all other experiments the samples were diluted to 10 cm^3 rather than 25 cm^3.

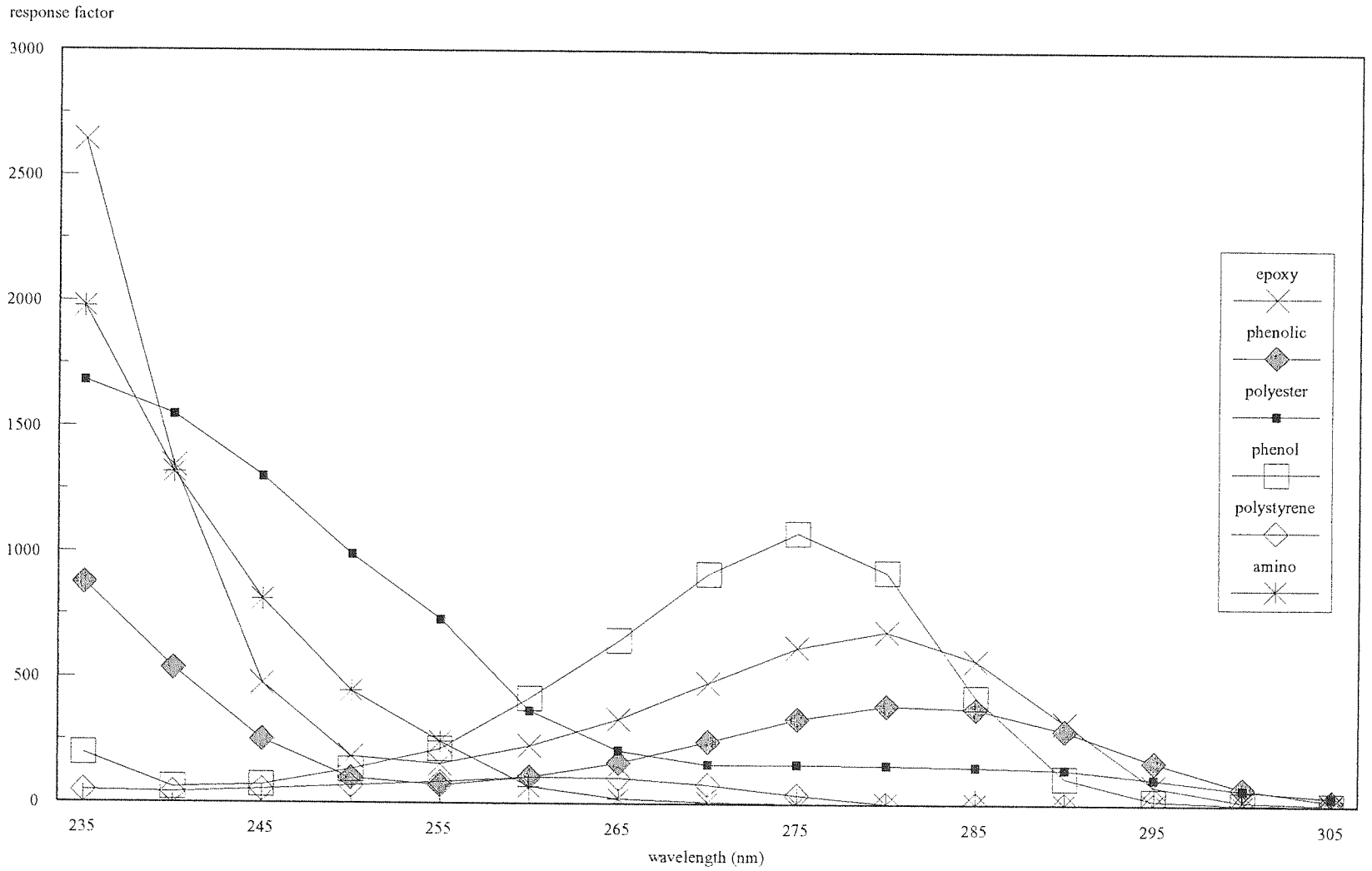

Figure 5.10. GPC UV response factors for various polymers.

Table 5.23 Injection Reproducibility: GPC Peak Areas and Calculated Response Factors

sample	concentration (g/ 25cm^3)	peak area (x10^6)		response factor	
		peak area (254nm)	peak area (RI)	UV detector 254nm	RI detector
1A	0.0249	16.059	0.8070	157.51	7.978
1B	"	16.066	0.8178	157.57	8.021
1C	"	16.176	0.8097	157.65	7.941
1D	"	16.279	0.8244	159.66	8.086
1E	"	16.356	0.8283	160.42	8.123
1F	"	16.391	0.8242	160.75	8.083
2	0.2352	14.876	0.8000	158.12	8.000
3	0.2565	15.969	0.8015	158.04	7.933
4	0.2777	17.583	0.8996	158.30	8.098
5	0.2408	15.345	0.7725	159.32	8.020
6	0.2172	13.916	0.7020	160.17	8.080

Table 5.24 shows the mean, sample and population standard deviations calculated from the response factors in Table 5.23. The results indicate that the error in the determination of the response factors should be less than 1%.

Table 5.24 Injection and Sample Preparation Reproducibility

	detector system	average response factor	sample std. dev.	population std. dev.
injection reproducibility	UV, 254 nm	159.09	1.41	0.89
	RI	8.04	0.06	0.07
preparation reproducibility	UV, 254 nm	158.58	0.98	0.62
	RI	8.02	0.06	0. 63

5.5.4 GPC analysis of simple polymer systems

(a) Epoxy: polystyrene polymer blends

Solutions of epoxy resin (a commercially available '9' type epoxy DOW XZ86762), a 10,000 molecular weight narrow disperse polystyrene standard and a mixture of these resins were prepared in tetrahydrofuran. The samples were analysed under the conditions given in Chapter 4.4.2a. The samples were injected onto the chromatograph and monitored using the RI detector and the UV detector monitoring at both 280 nm and 254 nm. Using the areas under the peaks for the two pure components and the known concentrations the response factors were calculated for that days analysis. See Table 5.26.

The composition of the mixture can be calculated using equations shown in Chapter 5.5.1. Three values can be calculated using the data from the three different detector combinations i.e. UV 280 nm plus UV 254 nm, UV 280 nm plus RI detector and finally UV 254 nm plus the RI detector. The experimentally determined composition of the epoxy/ polystyrene mixture are given in Table 5.25.

Table 5.25 Calculated Composition of the Epoxy/ Polystyrene Mixture

detector combination	% compostion	
	calculated epoxy	calculated polystyrene
UV 280 nm/ UV 254 nm	91.6	8.4
UV 280 nm/ RI	92.1	7.9
UV 254 nm /RI	92.7	7.3

The known starting composition of the mixture was 92.5:7.5 for epoxy and polystyrene respectively.

The composition may also be calculated by combining the data into a least squares or 'over-determination' type calculation. See Bauman [349] and Appendix 5. This procedure gives a calculated composition of 91.5% epoxy and 8.5% polystyrene.

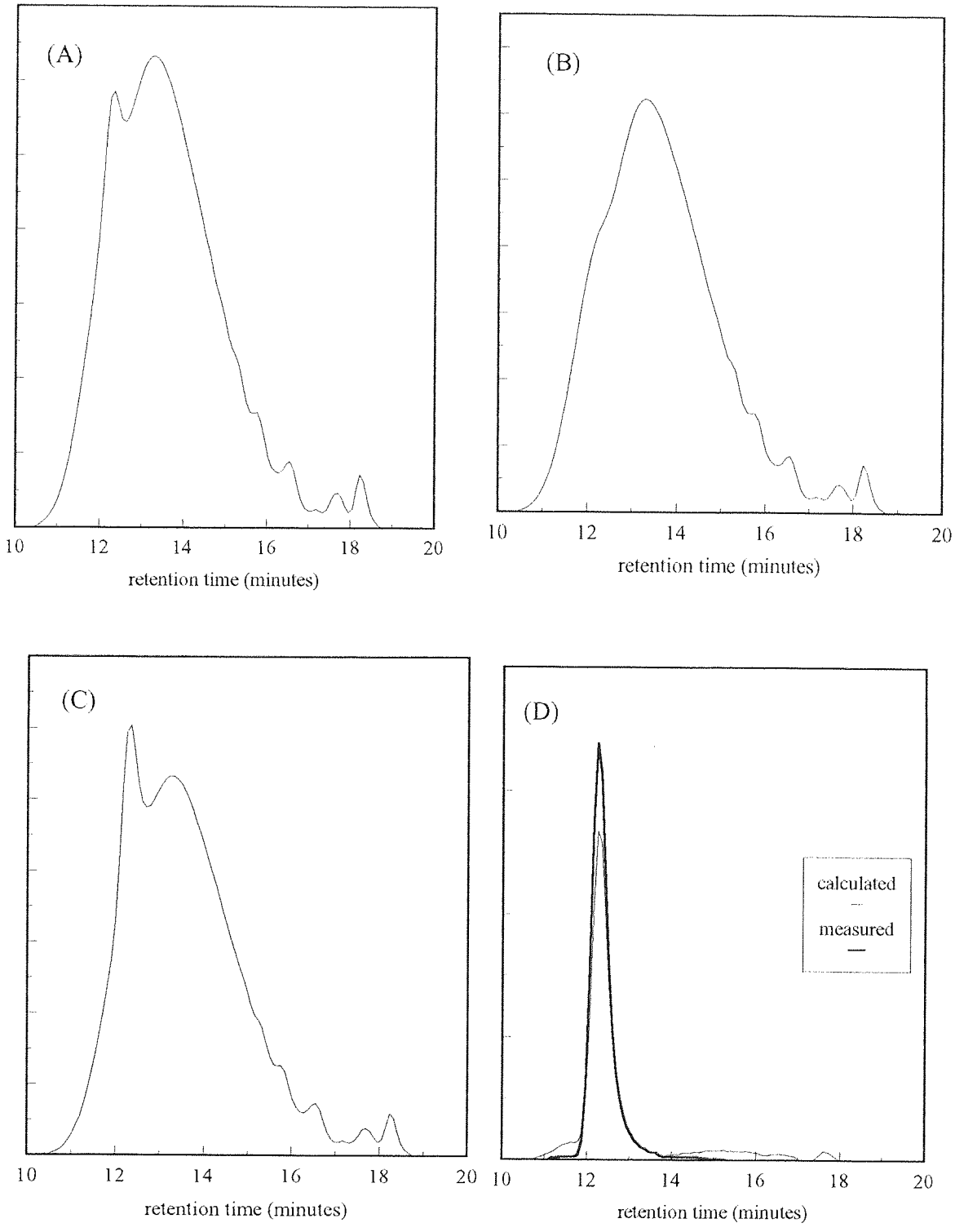

Figure 5.11 GPC profiles of the epoxy/polystyrene mixture monitored at (A) 254 nm, (B) 280 nm and (C) RI detector. Profiles (D) are the measured and calculated profiles of polystyrene.

Using the GPC6000 software data was corrected for flow rate deviations between the runs and time-slice files produced. The data was then imported into Lotus 1-2-3. Each data point from the three detectors were then analysed using the multi-component calculations and the data was then de-convoluted into the form of plots of relative detector response versus retention time.

Figures 5.11 (a), (b) and (c) show the chromatograms of the polymer mixture using the UV detector at 254 nm, 280 nm and using the RI detector. The chromatogram of the mixture obtained monitoring using the UV detector set at 280 nm (Figure 5.11(b)) shows the profile of the epoxy component only, since polystyrene does not absorb UV at this wavelength. At 254 nm (Figure 5.11(a)) the extra peak is due to the presence of the polystyrene which absorbs at this wavelength. The chromatogram obtained using the RI detector also shows both components. In this chromatogram the polystyrene peak is larger than in the chromatogram obtained at 254 nm since the response for the polystyrene component is similar to that of the epoxy. At 254 nm the polystyrene response is approximately one half of that of the epoxy. The response factors of these components are given in Table 5.26. Figure 5.11 (d) shows the deconvoluted polystyrene profile super-imposed upon the chromatogram of the 5100 molecular weight polystyrene standard.

(b) Epoxy:polystyrene:poly(methyl methacrylate)

Solutions of epoxy resin (a commercially available '9' type epoxy: DOW XZ86762), a 10,000 molecular weight narrow distribution polystyrene standard, a 5000 molecular weight narrow distribution standard poly(methyl methacrylate) (PMMA) and mixtures of these polymers were prepared in THF. Chromatograms were obtained using the UV detector monitoring at 254 nm and 280 nm and using a RI detector. The GPC profiles of the individual components were used to calculate response factors. Table 5.26

shows the response factors for the separate polymers calculated by dividing the area of the peak by the sample weight.

Table 5.26 Calculated Response Factors for the Epoxy/ Polystyrene/PMMA System

polymer	response factor UV 280 nm	response factor UV 254 nm	response factor RI
epoxy	658.1	158.6	7.95
polystyrene	4.5	80.0	7.51
PMMA	0	0	3.81

The composition of the mixtures can then be calculated by using either simultaneous equations or by using matrices. See Appendix 4.2. The calculated compositions for the three mixtures are shown in Table 5.27 alongside the known compositions.

Table 5.27 Calculated and known Compositions of Epoxy/Polystyrene/PMMA System

sample	calculated composition (%)			known composition (%)		
	epoxy	polystyrene	PMMA	epoxy	polystyrene	PMMA
Mixture 1	87.2	9.1	3.7	88.3	6.4	5.2
Mixture 2	87.5	6.1	5.4	89.6	5.1	5.3
Mixture 3	93.5	7.3	-0.3	93.9	6.1	0

Using the GPC6000 software the data was corrected for flow rate deviations between the runs and time slice files were produced . The data was then imported into Lotus 1-2-3. Each of the data points from the three detectors were then analysed using the multi-component calculations and plotted to give graphs of intensity versus retention time.

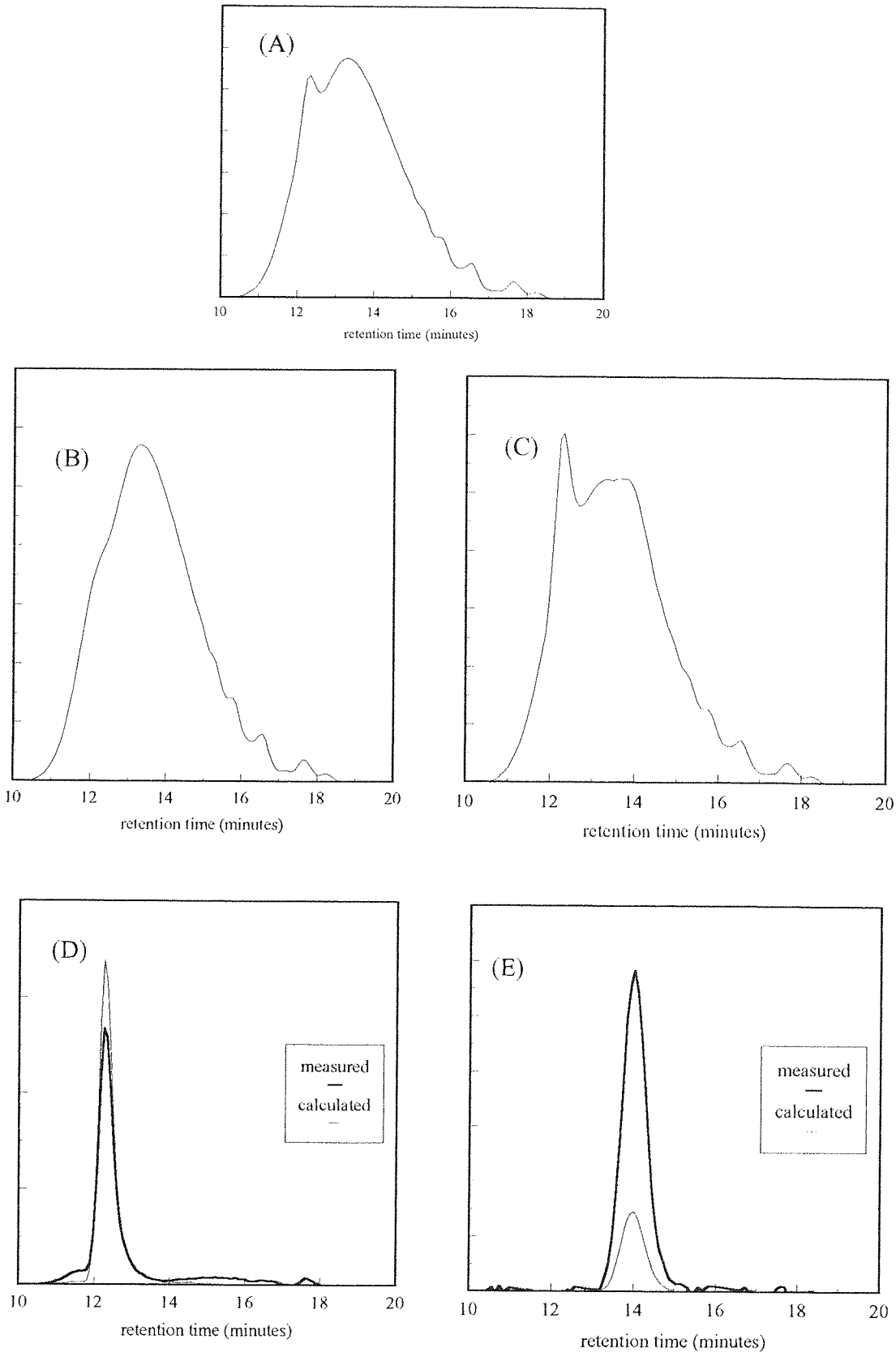

Figure 5.12 GPC profiles of the epoxy/polystyrene/ poly(methyl methacrylate) system using (A) UV 254 nm, (B) UV 280 nm and (C) RI detection, (D) measured and calculated polystyrene profiles and (E) measured and calculated poly (methyl methacrylate) profiles.

Figure 5.12(a), (b) and (c) show the chromatograms obtained by monitoring at 254 nm, monitoring at 280 nm and using the RI detector. Figure 5.12 (d) and (e) show the deconvoluted plots of the polystyrene component and the PMMA components respectively.

(c) Epoxy:polyester polymer system

Solutions of epoxy resin (DOW XZ86762), a polyester resin (Uralac), blends of the two polymers and a copolymer of epoxy-polyester were prepared in tetrahydrofuran. Chromatograms were obtained using the UV detector monitoring at 254 nm and 280 nm and using the RI detector.

Table 5.28 shows the response factors for the polymers calculated by dividing the area of the GPC profiles for the individual components by the sample weight.

Table 5.28 Calculated response factors for epoxy/polyester polymer system

polymer	response factor		
	UV 280 nm	UV 254 nm	RI
epoxy	659.9	165.5	8.20
polyester	157.8	817.9	3.35

The compositions of the mixtures can be calculated using the equations shown in Chapter 5.5.1. Since three detectors were used to determine two components, three values can be calculated from the three different detector combinations i.e. UV 280 nm / UV 254 nm, UV 280 nm/RI and finally UV 254 nm/RI. Table 5.29 shows the calculated compositions of the mixtures using the various detector combinations.

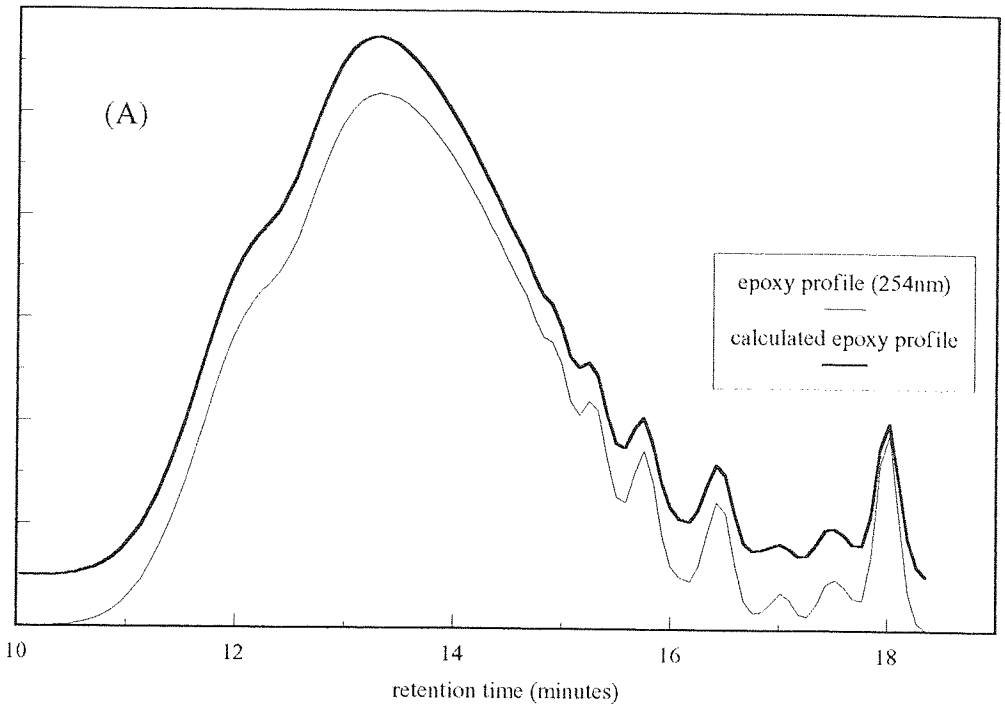

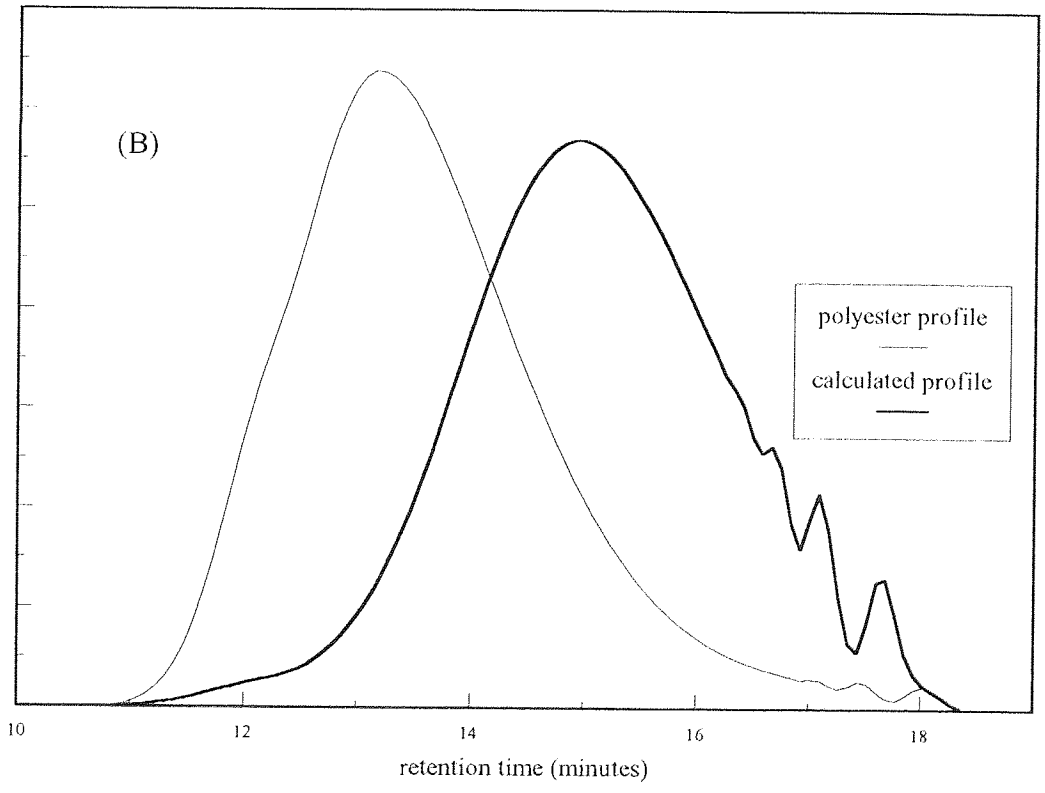

Figure 5.13 GPC profiles of the epoxy/polyester polymer system. Measured and calculated profiles of (A) epoxy and (B) polyester polymers.

Table 5.29 Calculated composition for the epoxy/polyster polymer system

Sample	280 nm/254 nm	280 nm/RI	254 nm/RI	known composition
Mixture 1	76.2:23.8	79.3:20.7	76.0:24.0	76.4:23.6
Mixture 2	50.1:49.9	49.3:50.7	50.3:49.7	49.1:50.9
Copolymer	48.2:51.8	49.6:50.4	48.0:52.0	50.6:49.4

The calculated values are in good agreement with the known composition.

The GPC6000 software was used to collect and to correct for flow rate variations and LOTUS 1-2-3 was used to plot the chromatograms. Figure 5.13(a) shows the chromatograms of both the epoxy polymer prior to polymerisation and the de-convoluted epoxy profile after copolymerisation. Figure 5.13(b) shows the chromatograms of the initial polyester resin and the de-convoluted polyester post-reaction profile. It is evident from the profiles that the epoxy resin is not reacting and that the polyester is depolymersing.

(d) Epoxy-phenolic

Solutions of epoxy resin (DOW XZ86762), phenolic resin (Holden produced ML97), a mixture of these polymers and an epoxy-phenolic reaction product were each prepared in tetrahydrofuran. The solutions were injected onto the chromatograph, under standard conditions given in Chapter 5.4.1. Each solution was injected twice, monitoring at a UV wavelength of 254 nm for the first run and then at 295 nm for the second run. The response factors for the epoxy and phenolic polymers, calculated by dividing the area of the peaks by the sample weight are shown in Table 5.30.

Table 5.30 Calculated Response Factors for the Epoxy-Phenolic System

polymer	response factor	
	UV 254 nm	UV 295 nm
epoxy	167.8	50.2
phenolic	49.4	129.9

It can be seen from the response factors in Table 5.30 that at 254 nm the epoxy component will give a greater response than the phenolic component. At 295 nm it is the phenolic that gives the greater response. Using the calculated response factors and the areas under the peaks for the polymer blend and the copolymer, the polymer composition of these samples can be calculated using the simultaneous equations developed in Chapter 5.5.1. The results of the calculation are shown in Table 5.31.

Table 5.31 Calculated Composition for the Epoxy/ Phenolic System

sample	composition (%) (epoxy to phenolic)	
	calculated	known
Blend	79.7:20.3	79.6:20.4
copolymer	54.0:46.0	80.0:20.0

The results indicate that for the cold blend, of epoxy and phenolic polymers the above analysis gives good agreement between calculated and known values. However the epoxy- phenolic copolymer sample has undergone a pre-condensation step where it is evident that a reaction has taken place which alters the response factors of the components and produces an erroneous result.

The GPC profiles for the phenolic resin component, the copolymer and polymer blend are shown in Figure 5.14. Figure 5.14(a) and (b) show the GPC profiles of the phenolic component monitored using UV detection at 254 nm and 295 nm respectively.

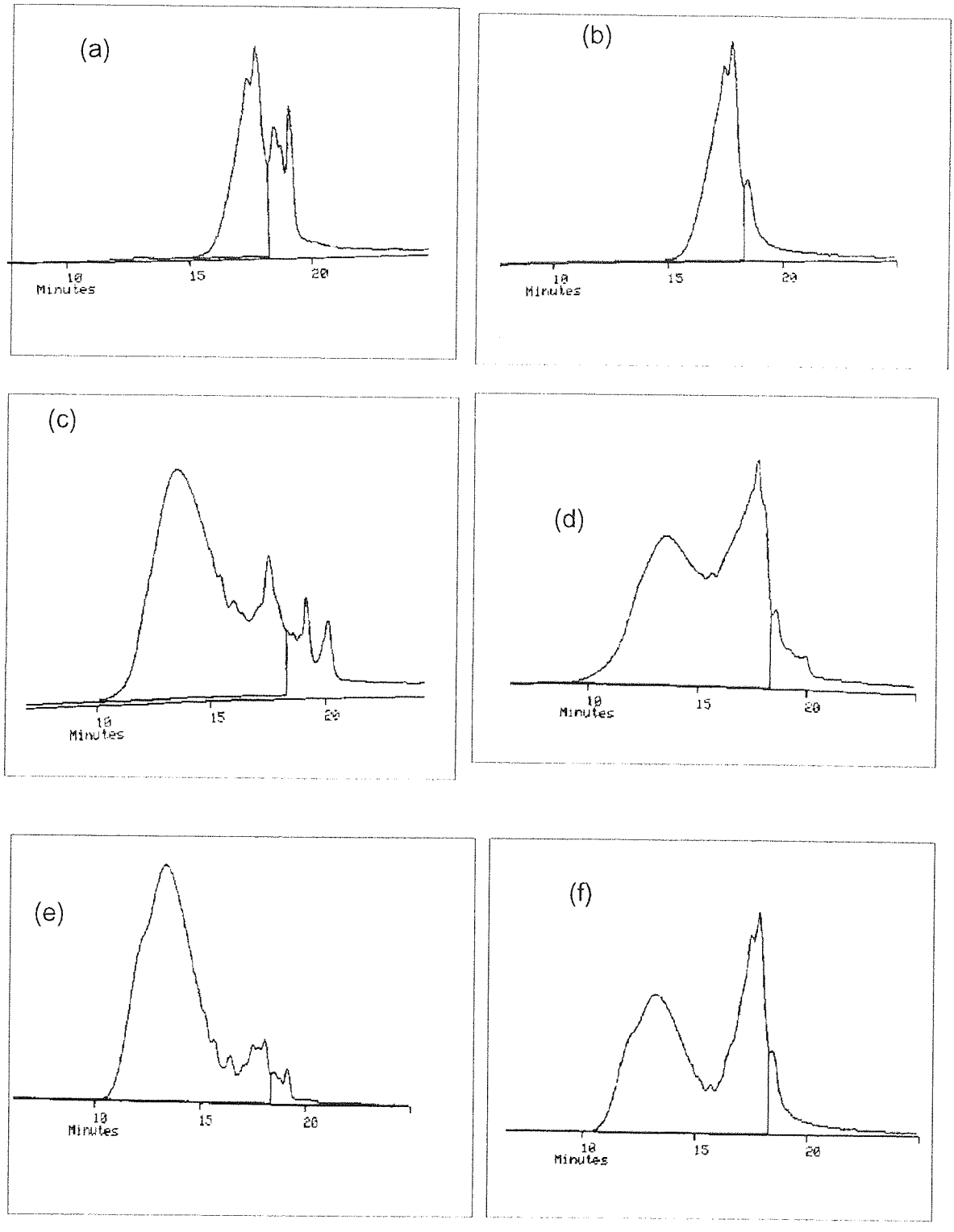

Figure 5.14 GPC profiles of epoxy-phenolic polymer system (a) and (b) phenolic component, (c) and (d) epoxy-phenolic condensate and (e) and (f) epoxy-phenolic blend monitored using UV detection at 254 nm and 295 nm respectively.

Comparison of the profiles suggest that the polymer does not have a constant chemical composition as a function of molecular weight. There are lower molecular weight components, eluting at the later retention times, which are detected at 254 nm but not at 295 nm. The GPC profiles of the polymer blend, at 254 and 280 nm in Figures 5.14 (e) and (f), respectively, are significantly different to those of the copolymer in figure 5.14 (c) and (d). This tends to confirm that some reaction has occurred between the two components in the copolymer system.

5.5.5 Epoxy-graft-acrylic polymers

Solutions of the epoxy-graft-acrylic polymers WRB621, WRB622 and WRB623 and the base epoxy resin, DLER100, were prepared in tetrahydrofuran. See Chapter 3 for details of the preparation of these materials. GPC profiles of the solutions were obtained. Each solution was injected twice, monitoring at a UV wavelength of 254 nm for the first run and then at 280 nm for the second run. During each run data was also collected from the RI detector. The response factors for epoxy, polystyrene and poly(methyl methacrylate) determined for this experiment, are shown in Table 5.32.

Table 5.32 Response Factors for Epoxy resin, PMMA and Polystyrene

polymer	response factors		
	UV 280 nm	**UV 254 nm**	**RI**
epoxy	659.90	165.50	8.20
polystyrene	4.50	80.0	7.95
PMMA	0.0	0.0	3.80

The calculated composition of the samples along with the known composition are listed in Table 5.33. From examination of this data it is concluded that there is a systematic error in the calculated values. For example, WRB623 has the largest epoxy content and is found to have the highest epoxy content of the three samples when determined using the methods described above.

Table 5.33 Calculated Composition of Epoxy-g-Acrylic Polymers

sample	composition (%)	
	calculated	known
DLER100	102.2:-0.5: -1.7	100 : 0.0 : 0.0
WRB621	93.0 :19.8:-12.1	78.6: 7.3:13.9
WRB622	64.2 :38.7:-12.9	58.4:14.1:27.1
WRB623	98.4 : 9.1: -7.5	89.4: 3.6: 6.9

Similarly WRB622 has the lowest theoretical epoxy content and is found experimentally to have the lowest epoxy content of the three samples. However, the calculated results and the known compositions show large differences.

It was suspected that the response factor for polystyrene at 254 nm may be the cause of the problem [216]. The response of styrene in a copolymer is different to that in the homopolymer. Therefore the response factor of polystyrene in the presence of acrylic comonomer with a composition similar to that of the monomer feed during the acrylation stage was determined. The response factor for the styrene component, at 254 nm, was calculated to be 150.84.

Using this new response factor for polystyrene at 254 nm the composition of the epoxy- graft-acrylic polymers were calculated. The results are shown in Table 5.34.

Table 5.34 Calculated Composition for Epoxy-g-Acrylic Polymers

sample	composition (%) (epoxy:polystyrene:acrylic)	
	calculated	**actual**
DLER100	102.5:-0.3:-2.2	100.0: 0.0: 0.0
WRB621	84.5: 9.5: 6.0	78.6: 7.3:13.9
WRB622	62.0:17.0:21.0	58.4:14.1:27.1
WRB623	94.1: 4.6: 1.3	89.4: 3.6: 6.9

Using the new response factor for polystyrene at 254 nm the calculated composition for the samples are closer to the known compositions than the initial results given in Table 5.31, but still show a degree of error. The author is of the opinion that the error is in the styrene response at 254 nm and that this response, if it could be calculated, may help to determine the chemical composition of the polymer.

The epoxy resin content of the graft polymers may also be calculated as a two component system i.e. epoxy resin plus acrylic, the latter including the styrene component. The composition of the polymers could be calculated from an 'over-determination' type calculation since we have two components and three detectors. However since the response of the UV detector at 254 nm is is thought to be incorrect, only the data from the UV detector monitoring at 280 nm and the RI detector will be used. The response factors for the epoxy and total acrylic components were calculated and are shown in Table 5.44.

Table 5.35 Response Factors used in the 'Two Component' Calculation

component	response factors	
	280 nm	**RI**
epoxy	659.90	8.20
total acrylic	0.38	5.41

The epoxy resin content of the graft copolymers can be calculated using the equations shown in Chapter 5.5.1. The results of the determination a shown in Table 5.36.

Table 5.36 Composition of Epoxy-graft-Acrylic polymers using the 'Two Component' Calculation

sample	calculated composition (%)		actual epoxy content (%)
	epoxy	acrylic	
DLER100	102.0	-2.0	100.0
WRB621	82.4	17.6	78.6
WRB622	61.1	38.9	58.4
WRB623	92.5	7.5	89.4

These results compare favourably with the theoretical values given in the final column of Table 5.36.

GPC profiles of WRB621 are shown in Figure 5.15. Figure 5.15(a) shows a deconvoluted profile of the calculated acrylic component superimposed on the WRB621 profile. Two differences between the profiles are observed.

There appears to be a low molecular weight component with an elution time of approximately 17.5 minutes which has a high acrylic content. The reason for its formation is not known at this time. The other difference between the two profiles appears as the shoulder on the leading edge of the high molecular weight peak, with a retention time of about 12 minutes, which is more pronounced in the deconvoluted profile. This may suggest that acrylic is preferentially grafting onto high molecular weight epoxy chains.

Figure 5.15(b) shows the deconvoluted profile of the calculated epoxy component superimposed on the WRB621 profile.

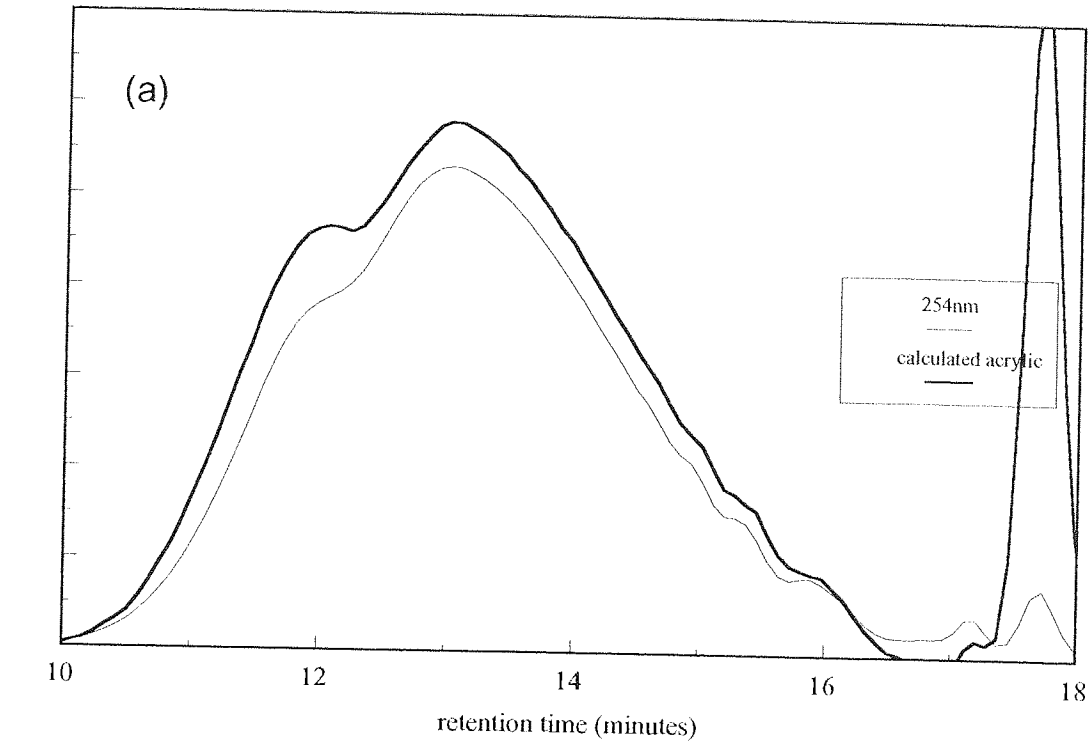

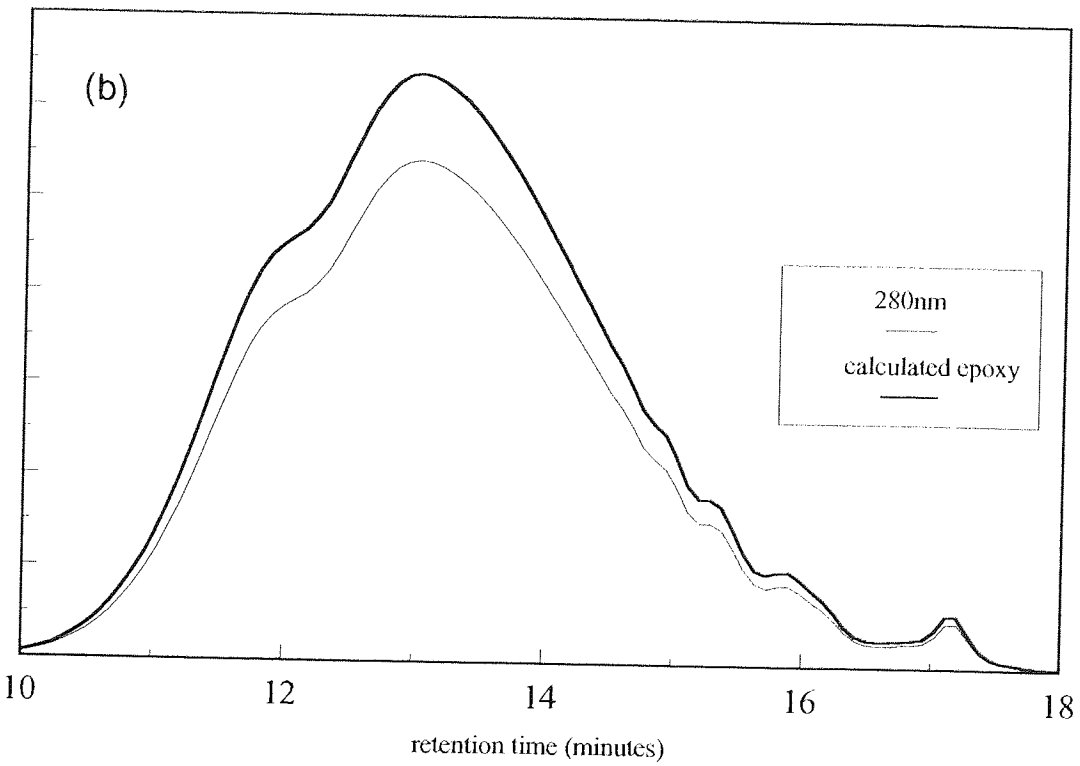

Figure 5.15. GPC profiles of epoxy-graft-acrylic sample WRB621. (a) at 254 nm superimposed onto the calculated profile for the acrylic component and (b) at 280 nm superimposed onto the calculated profile of the epoxy component.

5.5.6. Derivatization

(a) Derivatization of poly(acrylic acid)

A sample of poly(acrylic acid), with a reported molecular weight of 2000, was derivatized with (o-[p-nitrobenzyl]-N,N' [diisopropyl]isourea (NBDI). To prepare the sample for analysis, poly(acrylic acid) (0.01g), was accurately weighed into a 5 cm^3 'reactivial' and diluted in dimethyl formamide (0.5 cm^3). The vial was stoppered and shaken until all the polymer had dissolved. The NBDI reagent (2 cm^3) was then added. The sample was heated for 2 hours at 80^0C in a box-oven. After cooling, the solution was diluted with tetrahydrofuran (10 cm^3) in a volumetric flask. The resultant solution (20 μl) was injected onto the chromatograph which was set-up according to normal conditions as shown in Chapter 4.4.2 and the peak areas were measured. The response factors, calculated by dividing the peak area by the sample weight, were determined to be 4191.5 and 9.47 for the UV detector at 254 nm and the RI detector respectively. The observed polymer peak has an elution time of 904 seconds. The polystyrene calibration for the column used, see Chapter 5.4.2, is:

$$\log MW = 17.99725 - 0.03738R_T + 3.576x10^{-5}R_T^2 - 1.333x10^{-8}R_T^3$$

A retention time of 904 seconds corresponds to a polystyrene equivalent molecular weight of 3800.

(b) Epoxy-g-Acrylic polymers

Samples of epoxy-g-acrylic were derivatized using (o-[p-nitrobenzyl] -N,N' [diiso-propyl]isourea. A sample of the base epoxy resin was also derivatized. The derivatized and untreated samples were then analysed using GPC.

The response factors for the untreated and derivatized components using the UV detector at 254 nm and the RI detector are given in Table 5.37.

Table 5.37 Response Factors of Derivatized and Untreated Components

sample	untreated samples		derivatized samples	
	UV 254nm	RI	UV 254nm	RI
epoxy	158.6	7.95	158.6	7.95
acrylic acid	0.0	4.95	4191.5	9.47

The composition of the polymer samples can be calculated in either of two ways. Firstly both the UV and RI data from the derivatized samples only can be used. The results of this type of calculation are shown in Table 5.38 as 'calculation A'. Secondly the data from the UV detector only from both the untreated and derivatized samples can be used. Prior to calculating the composition of the samples, the areas for both untreated and derivatized samples must be adjusted to unit weight of sample. The results of this type of calculation are shown in Table 5.38 as 'calculation B'.

The determined compositions using calculation B show a higher degree of error when compared to the compositions calculated from the derivatized samples only. This is probably due to the data being calculated from two separate GPC injections.

Table 5.38 Calculated Epoxy-g-Acrylic Compositions using GPC and Derivatization Techniques

sample	acrylic acid content (%)		
	calculation A	calculation B	actual
WRB621	12.5	12.5	13.9
WRB622	22.8	23.4	27.1
WRB623	6.3	4.8	6.9
DLER100	0.1	-0.4	0.0

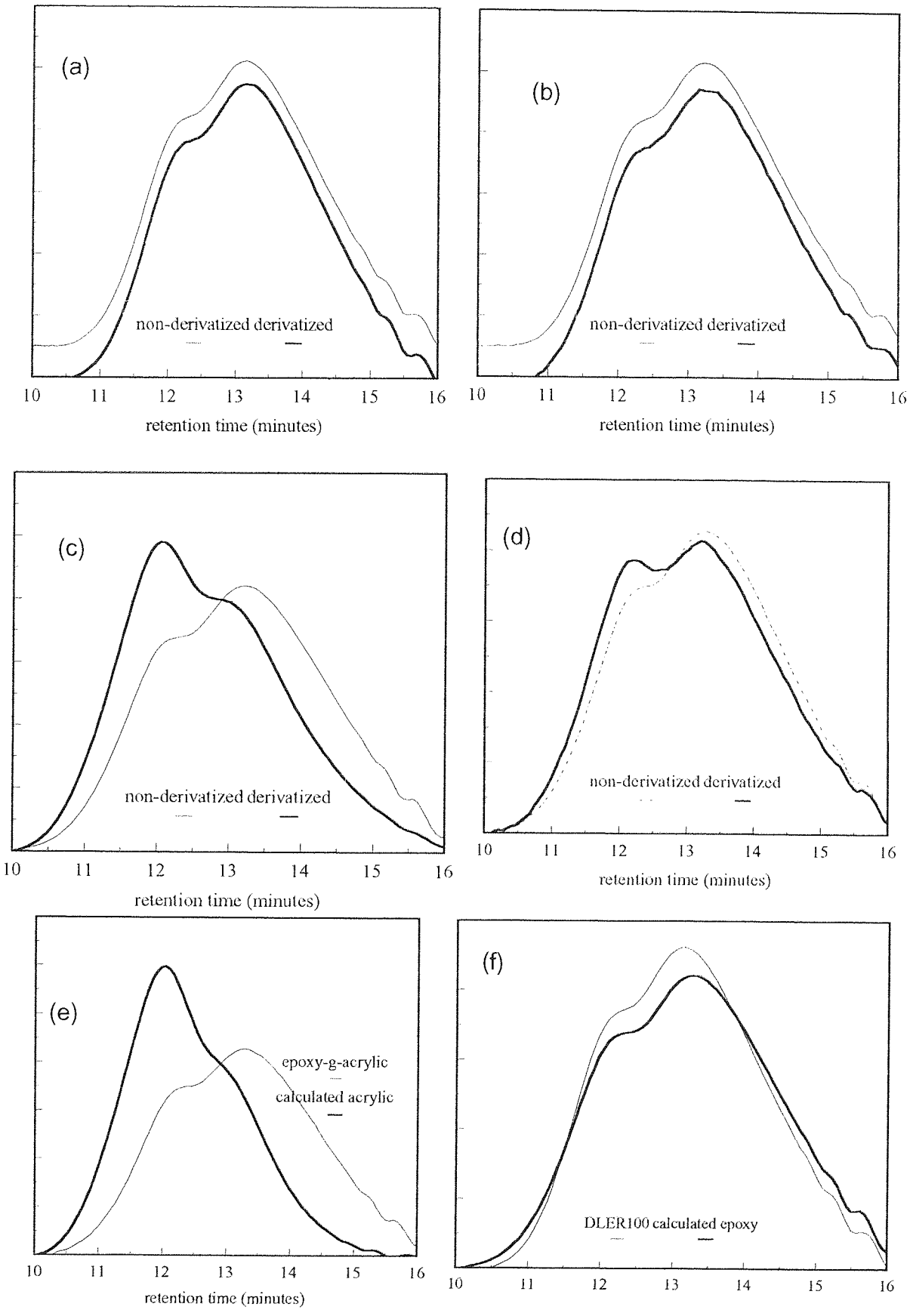

Figure 5.16 GPC profiles of derivatized and non-derivatized epoxy (DLER100) monitored using (a) UV detector at 254 nm and (b) RI detection. Derivatized and non-derivatized WRB621 monitored using (c) UV detector at 254 nm and (d) RI detection, (e) calculated acrylic component and (f) calculated epoxy component.

The GPC profiles of the base epoxy resin DLER100 with and without derivatization with NBDI using UV detection at 254 nm and using the RI detector are shown in Figures 5.16 (a) and (b). The derivatized profiles show no differences in molecular weight profile or response when using UV detection at 254 nm or RI detection when compared to the non-derivatized sample.

A change from a shoulder to a distinct peak at approximately 12 minutes retention time (Mp approximately 40,000) is observed for all the graft polymers. Figures 16(c) and (d) show normalised chromatograms obtained at 254 nm and RI respectively of WRB621 (80:20 epoxy:acrylic) in derivatized and non-derivatized forms.

Deconvoluted profiles of the acrylic and epoxy components were calculated using the UV GPC time-slice files of the derivatized and non-derivatized WRB621 and superimposed on the original WRB621 profile and on the base epoxy resin, respectively (see Figure 5.16(d) and (e)).

5.5.7 Analysis of epoxy-g-acrylic polymers using the 'DMF GPC system

Solutions of epoxy resins DOW XZ86762 and DLER100 and epoxy-graft-acrylic polymers WRB621, WRB622 and WRB623 were prepared in DMF. The solutions were then analysed using GPC system 2. The latter consisted of PLGEL columns similar to those employed in system 1, but dimethyl formamide was used as the mobile phase in place of tetrahydrofuran. The UV detector was set to monitor at 280 nm. See Chapter 4.4.2 for full details regarding the instrumentation. The samples were analysed on two different days in order to check the reproducibility of the method.

For the pure epoxy polymers, DOW XZ86762 and DLER100, a broad peak with a significantly smaller peak eluting earlier from the column, were observed. A chromatogram of DLER100 is shown in Figure 5.17(a). For the graft polymers the earlier eluting peak, observed in the epoxy samples, is significantly larger.

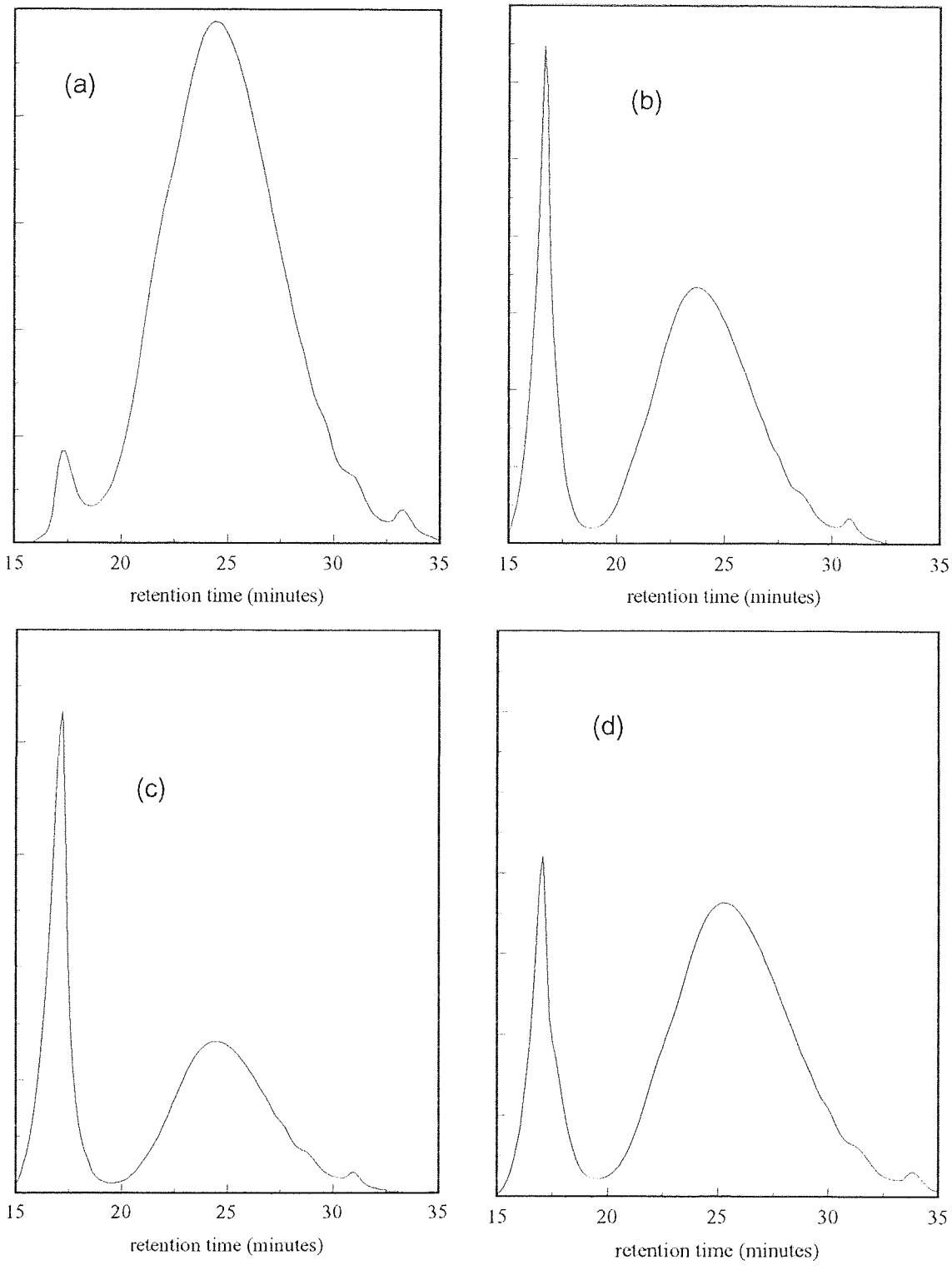

Figure 5.17 GPC profiles of epoxy and epoxy-graft-acrylic samples using the 'DMF' system. (a) DLER100 base epoxy resin, (b) WRB621, (c) WRB622 and (d) WRB623.

Chromatograms of WRB621, WRB622 and WRB623 are shown in Figures 5.17 (b) to (d). The first component eluting from the column is a relatively sharp peak. This peak (peak 1) is thought to be due to grafted polymer only. By monitoring at 280 nm the acrylic homopolymer would not be observed. The second, broad peak (peak 2), resembles the initial epoxy profile and is thought to be due to ungrafted epoxy. The area of the second peak expressed as a percentage of the total area are given in Table 5.39.

Table 5.39 Peak Areas of Samples Analysed using the DMF GPC System

Sample	Area under peak 2	
	day 1	day 2
DOW XZ86762	99.7	99.7
DLER100	96.9	97.3
WRB621	76.0	74.9
WRB622	60.7	60.2
WRB623	84.1	81.9

The areas of peak 2 expressed as a percentage of the total areas are similar to the levels of ungrafted epoxy resin determined by solvent extraction. For further discussion refer to Chapter 10.1.

CHAPTER 6. COLLOID STUDIES: EXPERIMENTAL

6.1 Particle size determinations

6.1.1 Photon Correlation Spectroscopy using the DLS700.

The Otsuka DLS700 photometer, used for all light scattering experiments, was set-up as described in the operation manual [215]. The incident wavelength from the 5 mW He-Ne laser was 632.8 nm. The bath pump and stirrer were switched on for 24 hours prior to using the equipment but both were turned off when the instrument was in use. The optical bath, filled with di-n-butyl phthalate, was temperature controlled at 25^0C, via an external water bath, and the goniometer was set to 90^0 for all measurements.

The particle size diameters reported in this manuscript were calculated automatically by the DLS700 from the second-order cumulant method [150]. For a graphical display of results the Non-Negative Least Squares (NNLS) [151] Histogram method 'AUTO1' [215] was chosen.

(a) Analysis of a particle size standard

Prior to the analysis of the samples, a polystyrene sulphonate standard (supplied by Polymer Laboratories) was analysed to check the reproducibility of the technique and to ensure the instrument was functioning correctly. The quoted particle size for this standard was 212 +/- 5 nm. The standard was also analysed six times on the same day and once each day on six separate days. The mean values and standard deviations were calculated.

(b) Analysis of latex samples

The latex samples were diluted prior to analysis such that the DLS700 detected approximately 8000 counts per second on pin-hole setting 2 (see operation manual). To achieve this the sample (2 g) was initially diluted in deionised water (25 cm^3). This

solution was usually prepared 24 hours prior to analysis. A quantity of this solution (0.4 cm^3) was then further diluted in deionised water (10 cm^3) in a clean sample vial. This diluted sample (0.4 cm^3) was then added directly to the DLS700 sample cell, containing 5 cm^3 of deionised water. The samples were re-analysed following the same dilution procedure as above but using 2% aqueous solution in place of deionised water.

(c) Effect of the degree of neutralisation upon particle size

Using the procedure described above, a sample of WRB633 was diluted, added to the sample cell and its particle size was measured. From the formulation of WRB633, (60:40 epoxy to acrylic, refer to Chapter 3), it can be shown that 100 g of latex contains 0.06 moles of methacrylic acid. Therefore the amount of acid groups added to the DLS700 sample cell, in the final 0.4 cm^3 aliquot, is 0.768 μmoles and since the latex has already been 35% neutralised, 0.269 μmoles of DMAE are also present. Aliquots (0.2 cm^3) of a 0.01% DMAE solution was added to the sample directly in the DLS700 cell. Each aliquot (0.2 cm^3) of DMAE solution contains 0.225 μmoles of DMAE. After each addition of DMAE the particle size was determined.

An aqueous solution of hydrochloric acid was prepared by diluting a 1M solution (2 cm^3) in water (50 cm^3). This solution was further diluted by taking an aliquot (2 cm^3) and diluting in water (50 cm^3). Aliquots of this solution (0.2 cm^3), which contains 0.32 μmoles of hydrochloric acid, were added to the sample cell containing the diluted latex. The dilute hydrochloric acid solution was also added to a sample of latex which had been neutralised with DMAE solution. After each addition of hydrochloric acid the particle size was determined.

6.1.2 Transmission Electron Microscopy

All of the micrographs reported in this manuscript were recorded at Birmingham University Biology Department. Prior to examination, the samples were diluted approximately 1 to 1000 in either deionised water or in a dilute solution of DMAE in water. Drops of each of the diluted samples were placed onto specimen copper grids. The volatiles i.e. water and solvents, were removed in a vacuum oven, controlled at a temperature of 40^{0}C. Three micrographs were taken of each sample. The latex particle diameters were calculated from the magnification factor and from the measured particle size on the micrographs. The latter was measured with a transparent ruler, taking an average of two readings at right-angles to each other.

6.2 Rheology

6.2.1 Initial Samples

All of the initial water-based latices in the present study have a polymer content of between 20 and 25% by weight. This is the composition when they are used as liners for can coatings. The composition of the latices are given in Chapter 3. The viscosity of these formulations were measured as flow times, in seconds, through a flow cup at a temperature of 25^{0}C. The type of cup used was a British Standard Specification cup number 3 (BSS3). A constant temperature was achieved by placing the cup in a purpose made water jacket through which water from a temperature controlled bath could be circulated.

6.2.2 Effect of the degree of neutralisation upon viscosity

To study the effect of the degree of neutralisation upon viscosity, the latices (2 g) were further diluted with water (25 cm^3) or with 2% solution of DMAE (25 cm^3). The viscosity of these diluted samples were measured as flow times through a suspended-level type viscometer placed in a water bath controlled at 25^{0}C. The viscometer chosen gave a

flow through time for water, at 25^0C, of around 80 seconds. To study the effect of the presence of the amino resin (used as the cross-linking agent) upon viscosity, samples of the latex PW1 were diluted, in either water or in 2% aqueous DMAE, with and without the addition of the polymer Cymel 303. To prepare the latex with cross-linker, Cymel 303 (0.2403 g) was added to PW1 (24.4392 g).

The viscosity of the latices WRB625 and WRB633 were measured as a function of pH. This was achieved by diluting the samples in various concentrations of di-methyl amino ethanol (DMAE). It can be shown that 2 g of WRB625 contains 0.6 $x10^{-3}$ moles of acid groups and 0.42 $x10^{-3}$ moles of DMAE and that 2g of WRB633 contains 1.2 $x10^{-3}$ moles of acid groups and 0.42 moles DMAE. Aliquots of a 2% DMAE aqueous solution (0 to 25 cm^3) were added to each latex (2 g) and diluted in water (25 cm^3). The viscosity of each solution was measured as a flow time through the suspended-level viscometer.

6.2.3 Effect of the latex concentration upon viscosity

Four solutions of each latex were prepared in water and in 2% aqueous DMAE, in the concentration range 0.1 to 2.0%. The viscosity of each solution was measured as a flow time through the suspended-level viscometer.

6.3 Nuclear Magnetic Resonance Spectroscopy

6.3.1. Introduction

Carbon-13 NMR spectra of various latices, additives and polymers were recorded. It was thought that the spectra could give insights in the mobility of epoxy chains within the micelle. TMS, placed in a capillary inside the sample cell, was used as a reference.

6.3.2. Sample analysis

Carbon-13 NMR spectra of the neat latex and samples diluted in water were recorded. Spectra of epoxy resin solutions in $CDCl_3$, with a similar resin content to those of the latex samples, were also recorded. Spectra were also obtained from dilute aqueous samples of n-butanol, 2-butoxy ethanol, triethyl amine, dimethyl aminoethanol (DMAE), and DMAE neutralised with poly(acrylic acid).

In another experiment the latex samples were cooled to -40^{0}C and CP-MAS spectra were recorded.

6.4 Infra-red Spectroscopy

6.4.1. Introduction

FT-IR analyses of aqueous sodium hexanoate [164] indicates that there is a decrease in the $\nu_{as}CH_3$ and $\nu_{as}CH_2$ values with increasing concentration. The increase in concentration leads to a progressive increase in aggregation.

In this present study FT-IR spectra of latices, solutions and dry films were recorded to determine the mobility of the epoxy chains.

A Nicolet 5DX Fourier transform infra-red spectrometer was used to record all spectra. After each opening and closing of the sample compartment 5 minutes was allowed to elapse to purge the sample compartment and optics with dry nitrogen before spectra were recorded.

6.4.2. Latex samples and polymer solutions

IR spectra of deionised water and PW1 were recorded using an attenuated total reflectance (ATR) unit collecting 10, 100, 1000 and 10 000 spectra. The ATR unit was set-up with a KRS5 crystal fitted with a liquid cell with a Teflon spacer on one side of the crystal only. When recording spectra with the ATR unit in place the 'detector gain' on the

Nicolet 5DX spectrometer was increased from its normal value of 1 to a value of 8. This was due to the limited amount of light reaching the detector with the ATR unit in place.

IR spectra of the latex samples were also recorded using a 0.012 mm fixed path length Calcium Fluoride cell. The 'detector gain' on the Nicolet 5DX spectrometer was set to 1 when recording all spectra. The samples of latices were diluted 1:1 in water and in 1:1 in D_20. A 1:1 mixture of water and D_2O was also prepared. Spectra of these samples were recorded. The spectrum of water was subtracted from that of the sample diluted in water and the $H_2O + D_2O$ spectrum was subtracted from that of the sample diluted in D_2O.

A sample of latex WRB625 was extracted in hexane to remove the solvents n-butanol and 2-butoxy ethanol. A quantity of the latex (10 cm^3) was added to a separating funnel. This was extracted twice using hexane (30 cm^3) each for 1 hour. An IR spectrum of this extracted sample was then recorded. The levels of solvent in the initial formulation and the extracted sample were determined using gas chromatography.

IR spectra of 5% solutions of n-butanol and 2-butoxy ethanol in water were recorded. IR spectra of carbon tetrachloride and a 5% solution of DER331 (a low molecular weight epoxy resin) in carbon tetrachloride, were also recorded.

6.4.3 Cast Films

Samples of latex were placed onto a silver chloride window. A second silver chloride window was drawn across the sample on the first window in order to produce an even liquid coat. Both windows were then dried at 80^0C under vacuum for 30 minutes. The windows were allowed to cool before recording the spectra.

IR spectra of epoxy resins DOW XZ86762 (high molecular weight '9' type epoxy) and DER331 (low molecular weight 'liquid' epoxy) were also recorded by casting onto potassium bromide windows from THF solution. The windows were vacuum dried at 80^0C for 30 minutes and allowed to cool prior to recording the spectra.

6.5 Soluble polymer determinations

6.5.1 Introduction

A centrifuge was used to separate soluble polymer from the latex particles. The effect of pH upon level of soluble polymer in the latex samples was determined. The chemical composition of the soluble and dispersed phases was determined using IR spectroscopy and gel permeation chromatography.

6.5.2 Sample preparation

The centrifuge used for all work was a Beckman J2-21. The tubes were 10 cm^3 capacity 'Nalgene' type, fitted into an eight position rotor.

The latex samples, with an initial polymer content of 20% by weight, were diluted in water, before the viscosity of the solution was low enough for separation in the centrifuge to occur. All samples, unless otherwise stated, were centrifuged at 15,000 rpm for 30 minutes at room temperature. If the solutions were more concentrated or a slower speed was used separation of the insoluble particles from solution was found not to occur.

For a typical analysis the latex (2 g), was diluted with the appropriate diluent i.e either de-ionised water (25 cm^3) or 2% DMAE in de-ionised water (25 cm^3). The samples were thoroughly shaken to ensure complete mixing. Prior to the separation, the pH of each sample was measured.

6.5.3 Polymer content determination

To determine the polymer content of each latex, an amount of sample (1 g) was accurately weighed onto a pre-weighed conditioned metal crucible and heated at 150^{0}C for 30 minutes. After cooling for 30 minutes the crucible, plus dry polymer, was re-weighed and polymer content determined of the latex determined. The polymer content of the

soluble portion was obtained in a similar manner except a larger amount (5 g) of sample was taken. The metal crucibles were conditioned by heating in a box oven at 150^{0}C for one hour prior to use.

6.5.4 **IR spectra of soluble and insoluble portions**

IR spectra of the latices, the soluble and insoluble polymer portions were recorded after casting the samples onto silver chloride windows and drying in a vacuum oven at 90^{0}C for 30 minutes.

6.5.5 GPC profiles of soluble and insoluble portions.

After separating the insoluble and soluble portions of the latex, the separated fractions were diluted in tetrahydrofuran (THF) and analysed using GPC. See Chapter 4.4.2 for GPC experimental details. The soluble portion was diluted 1:1 in THF and the insoluble portion and the original diluted samples were diluted 1:3 in THF prior to analysis.

CHAPTER 7. COLLOID STUDIES: RESULTS

7.1 Particle size determinations

7.1.1 Dynamic Light Scattering

The Otsuka DLS700 photometer was used for all light scattering experiments. The particle diameters quoted below were all calculated using a 286 PC running a data handling program supplied with the DLS700. The program calculates the diffusion coefficient from a second-order cumulant analysis of the autocorrelation function. The particle diameter is then calculated using the Stokes-Einstein equation. The AUTO1 Histogram method, used for plotting the data, uses the non-negative least squares (NNLS) algorithm [150].

(a) Analysis of a particle size standard

A poly(styrene sulphonate) particle size standard, from Polymer Laboratories (reported particle diameter 212 nm), was analysed a number of times to determine the reproducibility of the method. The sample was analysed on six different days and six times on the same day. The results of this determination are given in Table 7.1. The results indicate that for a sample with a mean particle diameter of 212 nm a sample standard deviation of 4 nm could be achieved.

Table 7.1 Particle Size Data of poly(styrene sulphonate) Standard

analysis number	particle diameter (nm)	
	same day	different day
1	227	219
2	227	213
3	229	218
4	229	223
5	229	223
6	230	224
mean value	229	220
sample standard deviation	1	4

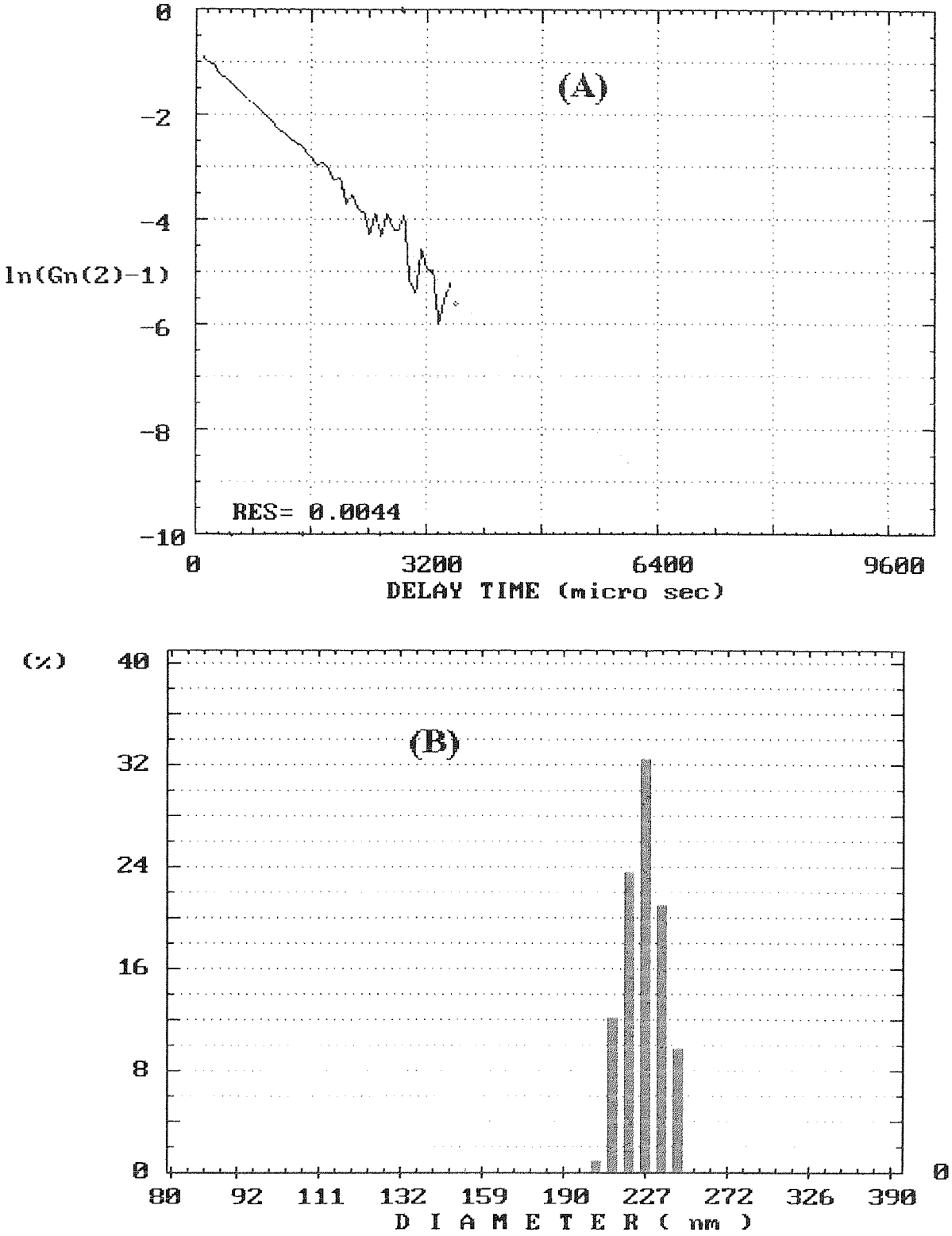

Figure 7.1 (A). ln plot of the autocorrelation function for the 212 nm particle size standard and (B) Histogram analysis of the 212 nm particle size standard

Figure 7.1(A) shows the log plot of the autocorrelation function. The linear nature indicates a narrow particle distribution. The histogram plot as calculated using 'AUTO1' is shown in Figure 7.1(B).

The particle diameter of the poly(styrene sulphonate) standard was also determined from data generated from the display of the autocorrelation function. The DLS700 software was run in the PC 'Windows' environment and bitmap file of the display of the auto-correlation function was copied into 'Windows paint-brush'. The 'x' and 'y' coordinates of each data point was entered into a spreadsheet. This data was then used to re-calculate the particle size. See Appendix 8 for all details. Good agreement between the calculated result and the DLS700 calculated results were obtained.

(b). Sample analysis

To determine the suitability of the method for the measurement of particle diameter of the latex samples, a test sample, WRB625 (80:20 epoxy:acrylic formulation with a 70% degree of neutralisation), was analysed a number of times on different days. The samples were prepared by diluting in deionised water. The determined particle size diameters are quoted in Table 7.2.

Table 7.2 Particle size analysis of WRB625 using DLS, carried out on different days

day	particle diameter (nm)
1	328
2	328
3	334
4	336
5	349
6	316
mean value	332
standard deviation	11

The calculated particle diameter for the sample appeared to be reproducible i.e. an average particle diameter of 332 nm with a standard deviation of 11 nm. Analysis of the samples using the histogram algorithms revealed a number of discrete peaks. However, the values of these peaks were not consistent and are not reported.

The particle size of the four epoxy-g-acrylic formulations, WRB624, WRB625, WRB626 and WRB633, were then determined. Details of the preparation of these materials is given in Chapter 3. Table 7.3 shows the results of the particle size determinations carried out on the latex samples.

Table 7.3 Particle size analysis of latex samples using DLS

sample	epoxy/acrylic ratio	degree of neutralisation	calculated diameter (nm)
WRB624	60:40	70%	320
WRB625	80:20	70%	340
WRB626	90:10	70%	220
WRB633	60:40	35%	130

The results obtained for the two latices WRB624 and WRB633 are markedly different i.e 320 nm and 130 nm, respectively. These latices have identical polymer compositions. The only differences between the samples is that WRB624 was neutralised to 70% with DMAE whilst WRB633 is neutralised to 35%.

(c) Effect of Degree of Neutralisation on Particle Size

The above samples were diluted prior to analysis using deionised water. The two 60:40 epoxy to acrylic formulations i.e. WRB624 and WRB633 were re-analysed following dilution of the samples in deionised water and in 2% aqueous DMAE. The results obtained from these experiments are given in Table 7.4.

Table 7.4 Effect of the Diluent on Particle Size Data measured using DLS

sample	particle diameter (nm) using the diluent:	
	de-ionised water	2% aq. DMAE
WRB624	390	320
WRB633	130	230

The particle size of WRB633 was found to increase from 130 nm to 230 nm in the presence of DMAE.

The decrease in measured particle size for WRB624 induced by the DMAE solution was thought to be due to the increased viscosity of the medium. The viscosity of water, as measured as a flow time through the suspended level viscometer was 78.3 seconds. The viscosity of the 2% aqueous solution of DMAE was 84.5 seconds. A solution of sodium chloride in water was prepared at the required concentration to produce a viscosity similar to that of the DMAE solution. The solution prepared was 10.0% w/v and gave a flow time of 85.9 seconds through the viscometer. The measured particle size of WRB624 in this medium was 330 nm. If the viscosity of the DMAE solution is introduced into the DLS700 software the measured particle diameter for WRB624 was determined to be 390 nm.

To further investigate the apparent increase in particle size of WRB633 with the addition of DMAE, the sample was diluted and the particle size measured in different DMAE concentrations. A sample of the diluted WRB633 was prepared and added to the DLS700 sample cell. Aliquots (0.2 cm^3) of a 0.01% DMAE solution were then added. After each addition of DMAE solution the particle size was measured. The results are shown in Table 7.5. A plot of mole ratio versus particle size is shown in Figure 7.2. The graph shows that the particle size reaches a maximum value around the DMAE to acid equivalence point.

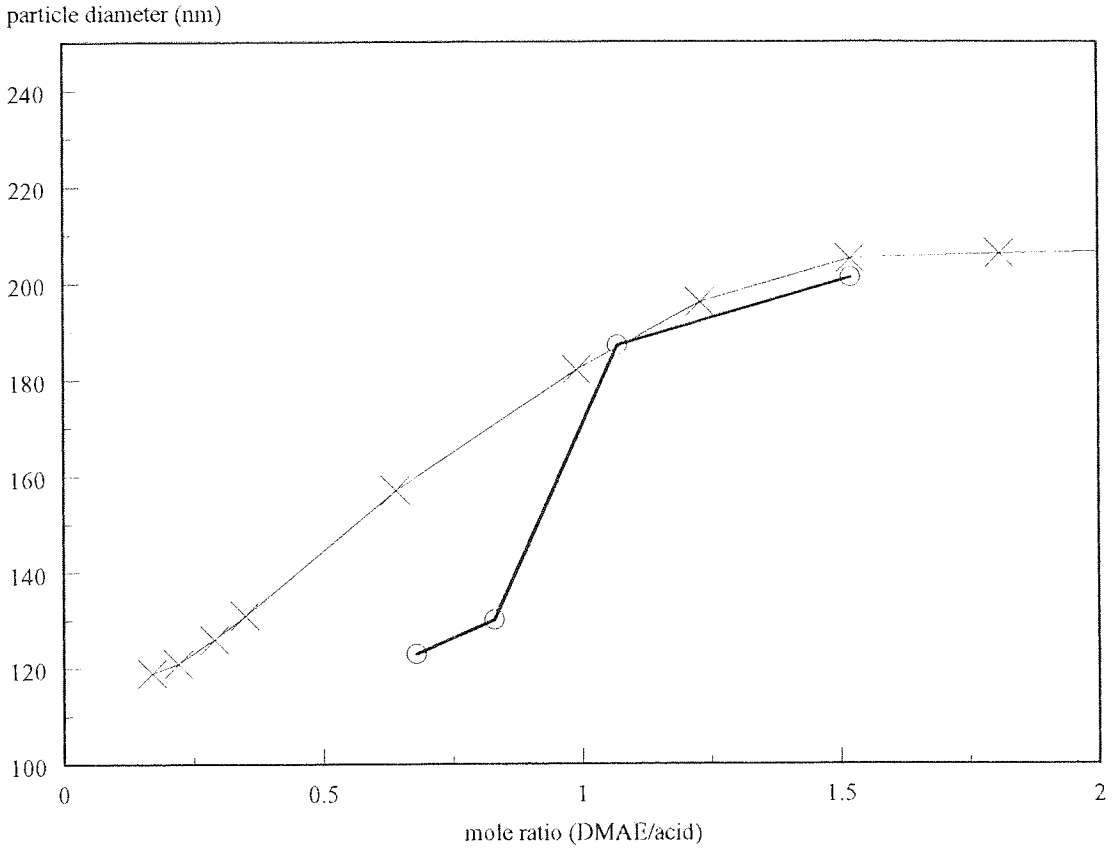

Figure 7.2 Effect of the mole ratio of DMAE to acid upon the particle size of WRB633 measured using Dynamic Light Scattering.

X:Neutralise carboxylic acid with DMAE. There is an increase in particle size with increasing DMAE/acid ratio.

O: Neutralise DMAE with HCl. If HCl is added to latex which has already been neutralised with DMAE there is a decrease in particle size but a minimum particle size is achieved at a higher DMAE/acid ratio.

Table 7.5 WRB633 Particle size data: effect of DMAE addition

volume of aq. DMAE added	moles of DMAE added (μmoles)	mole ratio DMAE/acid	particle size WRB633 (nm)
0	0	0.35	130
0.2	0.225	0.64	160
0.4	0.449	0.99	180
0.6	0.674	1.23	200
0.8	0.899	1.52	210
1	1.124	1.81	210
5	5.618	7.67	220

Aliquots (0.2 cm^3) of a dilute hydrochloric acid solution (0.00016M) was added to the DLS700 cell containing the diluted WRB633 latex and particle size measurements made. (Note: 0.2 cm^3 of this solution contains 0.32 $x10^{-6}$ moles HCl). Table 7.6 shows the effect of adding aliquots of the dilute HCl solution to a sample of WRB633.

Table 7.6 WRB633 Particle Size Data: Effect of the Addition of HCl

volume of dilute HCl solution added (cm^3)	moles of HCl added ($x10^{-6}$)	mole ratio DMAE/acid	particle size (nm)
0	0	0.35	130
0.10	0.16	0.29	130
0.30	0.48	0.22	120
0.50	0.8	0.17	120

Dilute hydrochloric acid was also added to diluted latex which had already neutralised with DMAE. The particle sizes listed in Table 7.7, show that, as previously observed, the measured particle size increases with addition of DMAE.

Table 7.7 WRB633 Particle size data: effect of addition of HCl to WRB633 neutralised with DMAE

volume of DMAE added (cm^3)	volume of HCl added (cm^3)	moles DMAE added ($x10^{-6}$)	moles HCl added($x10^{-6}$)	mole ratio DMAE/acid	particle size (nm)
0	0	0	0	0.35	130
0.8	0	0.90	0	1.52	200
0	0.20	0	0.32	1.07	190
0	0.40	0	0.64	0.83	130
0	0.60	0	0.96	0.68	120

In this case the rise is from 130 nm to 200 nm. Upon addition of dilute hydrochloric acid the measured particle size decreases from 200 nm to 120 nm. The effect of neutralisation upon particle diameter is shown graphically in Figure 7.2. The plot showing the neutralisation of the DMAE with hydrochloric acid does not follow the same path as the initial neutralisation of the carboxylic acid groups of the polymer with DMAE. This is probably due to hydrochloric acid being a stronger acid than the acrylic acids.

7.1.2 Particle Size Determinations: Transmission Electron Microscopy

All of the analyses using transmission electron microscopy were carried out at Birmingham University. Sample preparation involved placing the diluted samples onto copper grids. The samples were diluted approximately 1000:1 in either water or an aqueous solution of DMAE. The volatiles. i.e. water and organic solvents were then removed in a vacuum oven at 40^0C.

Two studies were carried out:

1. Particle size determinations of all latices diluted in water, and
2. particle size determinations of WRB624 and WRB633 diluted in water and 2% aqueous DMAE.

The studies were carried on different days thereby producing duplicate sets of data for WRB624 and 633 diluted in water.

Three micrographs for each sample were produced. The diameter of each particle was measured. The magnification on the print was obtained by measuring the same feature on the negative and on the print. The enlargement factor was then multiplied by the magnification given on the negative. The particle size distributions i.e. number of particles per particle size are listed in Appendix 8.

A spreadsheet was used to calculate number-average (D_n) and weight-average (D_w) particle diameters, which are defined, respectively, as:

$$D_n = \Sigma(d_i n_i)/N$$

$$D_w = (3 \times \Sigma(N_i V_i^2)/(8\pi \Sigma(N_i V_i)^{1/3})$$

where d_i is the diameter of each particle and n_i is the number of particles. N is the total number of particles and V_i is the volume of each particle.

(a) Study 1: Samples diluted in water

All samples were diluted approximately by 1000 in deionised water 24 hours before analysis. Micrographs of each latex are shown in Figure 7.3 (a) to (d). The micrograph of WRB625 shows a broad distribution of particle sizes. The micrograph of WRB626 shows a more polarised distribution of sizes i.e. A small number of very large particles and a large number of small particles. The particle sizes of WRB624 and 633 appear to be similar. The particle size distributions are shown in Figure 7.4 and Table 7.8 shows the number- and weight-average particle size distributions.

Table 7.8 TEM particle size data: samples diluted in water

sample	average particle size (nm)		
	D_n	D_w	D_w/D_n
WRB624	39	53	1.4
WRB625	44	129	2.9
WRB626	32	158	4.9
WRB633	42	60	1.4

The calculated values appear to be significantly different to those obtained from dynamic light scattering experiments, the results of which are summarised in Table 7.3. However, using DLS the values obtained may relate to a 'hydrodynamic' radius whereas the TEM data may relate to the size of the epoxy polymer core of the micelle. It is, therefore, not surprising that the TEM results for WRB624 and WRB633, both 60:40 epoxy to acrylic formulations, give similar particle size distributions.

(b) Study 2: samples diluted in water and aqueous DMAE

Samples of WRB624 and WRB633 were diluted by approximately 1000 in water and in a 2% aqueous DMAE solution, 24 hours prior to analysis.

Table 7.9 TEM particle size data: Samples diluted in 2% aqueous DMAE

sample	average particle size (nm)	
	D_n	D_w
WRB624 aq.	36	44
WRB624 DMAE	43	43
WRB633 aq.	43	55
WRB633 DMAE	37	46

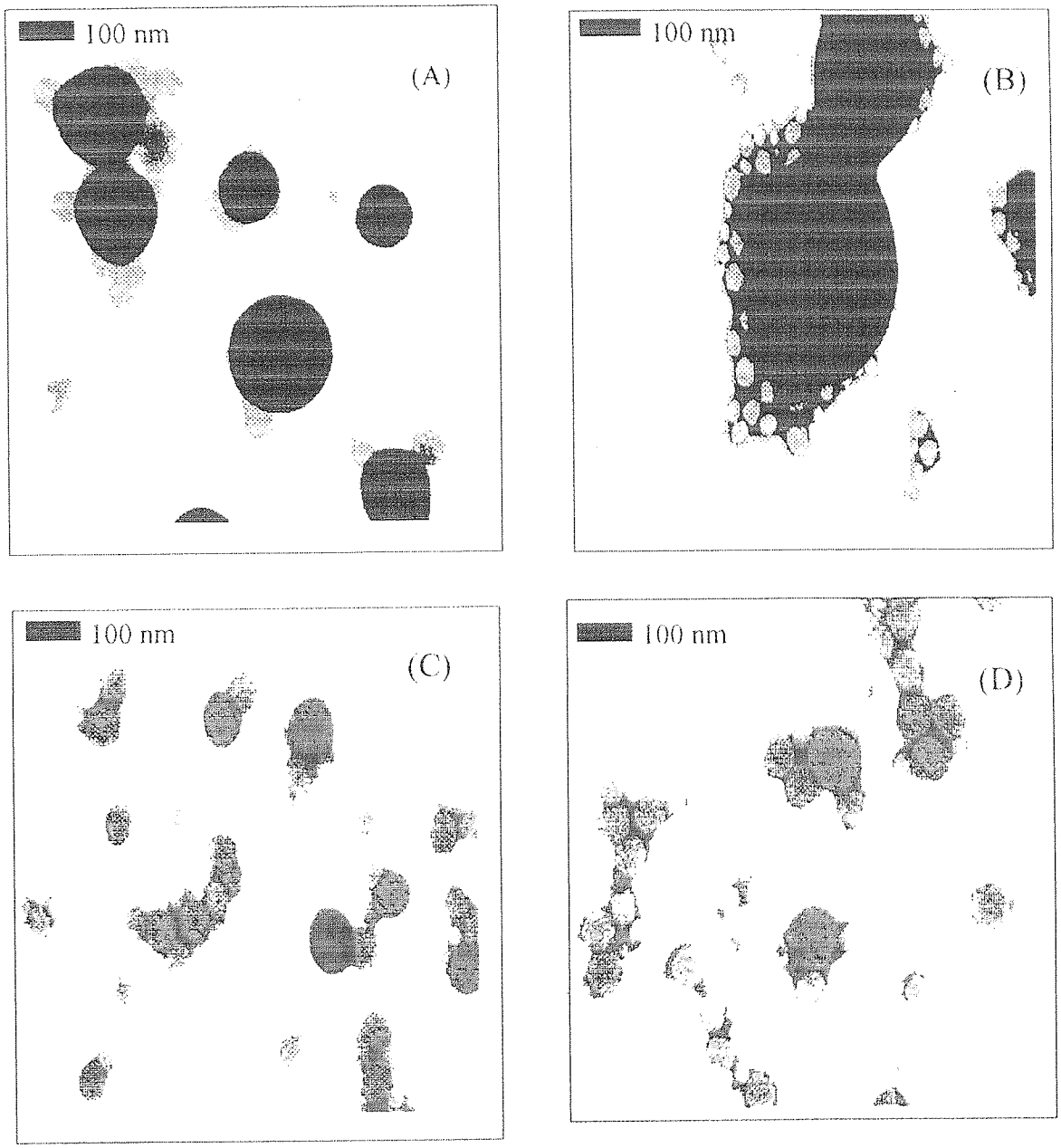

Figure 7.3. Examples of transmission electron micrographs from (A) WRB625, (B) WRB626, (C) WRB633 and (D) WRB624. The particle diameters were measured and number average and weight average values were calculated. Refer to Appendix 7 for full details. Particle size distributions, showing number of particles versus particle diameter, are shown in Figure 7.4.

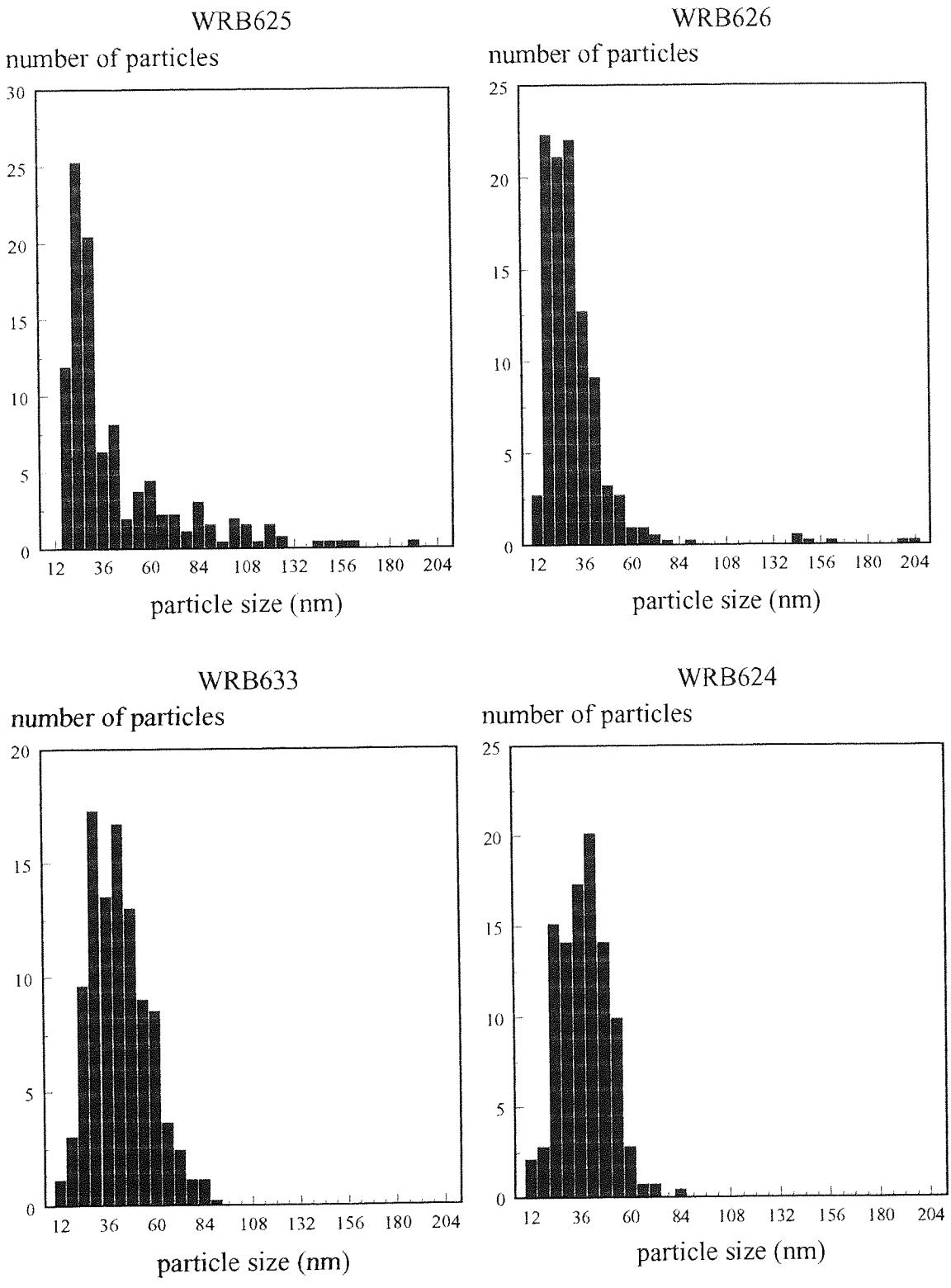

Figure 7.4 Particle size distributions from transmission electron micrographs of GEN1 type latices: WRB624, WRB625, WRB626 and WRB633. These distributions were obtained by measuring a number of particles from the micrographs of each latex. Examples of the micrographs are shown in Figure 7.3.

The particle size distributions, shown in Table 7.9 indicate that there are no significant differences between particle sizes of WRB624 and WRB633 diluted either in water or 2% aqueous DMAE solution. This is again in contrast with the DLS data where the presence of DMAE has a marked effect upon the measured particle size of the samples. This can be explained by the DMAE swelling the acrylic portion but not the epoxy core i.e. the hydrodynamic radii increases but the core diameter does not.

7.2 Rheology

7.2.1 Initial samples

The viscosity of all the latices prepared in this study were measured as flow times through a BSS3 flow cup. Table 7.10 shows the flow times of the samples, measured at 25^{0}C. The table also shows details of the sample composition. Details of the preparation of these latices are shown in Chapter 3.

Table 7.10 Viscosity of Latices Measured as a Flow Time through a 'Flow Cup'

sample	base-resin	epoxy:acrylic ratio	degree of neutralisation	Flow time (seconds)
WRB624	WRB622	60:40	70%	76
WRB625	WRB621	80:20	70%	71
WRB626	WRB623	90:10	70%	49
WRB633	WRB622	60:40	35%	225
PW1	PW1	80:20	70%	75
PW2	PW2	80:20	70%	77

The initial results show that levels of DMAE can markedly effect the viscosity of the samples. For example WRB633 has the same polymer composition as WRB624 but

have viscosities of 76 and 225 seconds respectively. The only differences between the samples being the amount of acrylic acid that has been neutralised by the addition of DMAE. In WRB633 35% of the methacrylic acid has been neutralised with DMAE whereas in WRB624 the level of neutralisation is 70%.

7.2.2 Effect of pH upon viscosity

To further investigate the effect of the degree of neutralisation upon viscosity, the samples were diluted to produce viscosities which could be measured through a suspended-level viscometer. The degree of dilution was the same as that used for the soluble polymer determinations, details of which are given in Chapter 7.5. Two aliquots of each sample (2 g) were diluted (25 cm^3) in either water or an aqueous solution of 2% DMAE. The viscosity of the solutions, measured as flow times through a suspended-level viscometer at 25^{0}C, are listed in Table 7.11. The flow times for water and 2% aqueous DMAE , through this viscometer were found to be 78.3 and 84.5 seconds respectively.

Table 7.11 Flow Times through a Suspended-Level Viscometer of Samples Diluted in Water and 2% Aqueous DMAE

sample	Flow time (seconds)	
	de-ionised water	2% aq. DMAE
WRB624	199.1	231.7
WRB625	139.2	156.1
WRB633	102.3	176.1
PW1	139.5	157.1
PW1 + cross-linker	138.4	156.2

The presence of the amino resin cross-linker has little effect upon the viscosity of the latex. In fact the measured viscosities of the samples containing the cross-linker are

slightly lower after dilution with either water or 2% DMAE solution than the samples with no added cross-linker but similarly diluted.

For all samples, it is apparent that the addition of DMAE results in solutions with higher viscosities. The sample which shows the greatest increase in viscosity is WRB633. The flow time of WRB633 diluted in water was 102.3 seconds. In 2% aqueous DMAE solution the flow time increases to 176.0 seconds. This is the sample with a polymer composition of 60:40 epoxy to acrylic with 35% of the acid neutralised with DMAE.

To further study the effect of the addition of DMAE to these samples, solutions of WRB625 were prepared that contained various concentrations of aqueous DMAE. Aliquots of the sample WRB625 (2 cm^3) was accurately weighed into 25 cm^3 volumetric flasks. Volumes of 2% aqueous DMAE (0, 1, 2.5, 5, 10, 15 and 25 cm^3) were then added. The volume was then made up to 25 cm^3 using de-ionised water. It can be shown that 2 g of WRB625 latex contains 0.6 mmoles of methacrylic acid and 0.42 mmoles of DMAE. The number of moles of DMAE added to each solution and the mole ratio of acid to DMAE were calculated. The viscosities of the solutions measured as flow times through the suspended-level viscometer are shown in Table 7.12.

Table 7.12 Flow Times through a Suspended-Level Viscometer of solutions of WRB625 containing various amounts of DMAE

sample	pH	mole ratio DMAE/acid	flow time (seconds)	corrected flow time
WRB625(1)	7.81	0.71	139.2	139.2
WRB625(2)	8.98	1.08	151.2	151.1
WRB624(3)	9.65	1.64	151.3	150.8
WRB625(4)	10.01	2.57	151.7	150.5
WRB625(5)	10.33	4.45	152.5	150.1
WRB625(6)	10.46	6.32	153.1	149.3
WRB625(7)	10.65	10.06	155.9	150.2

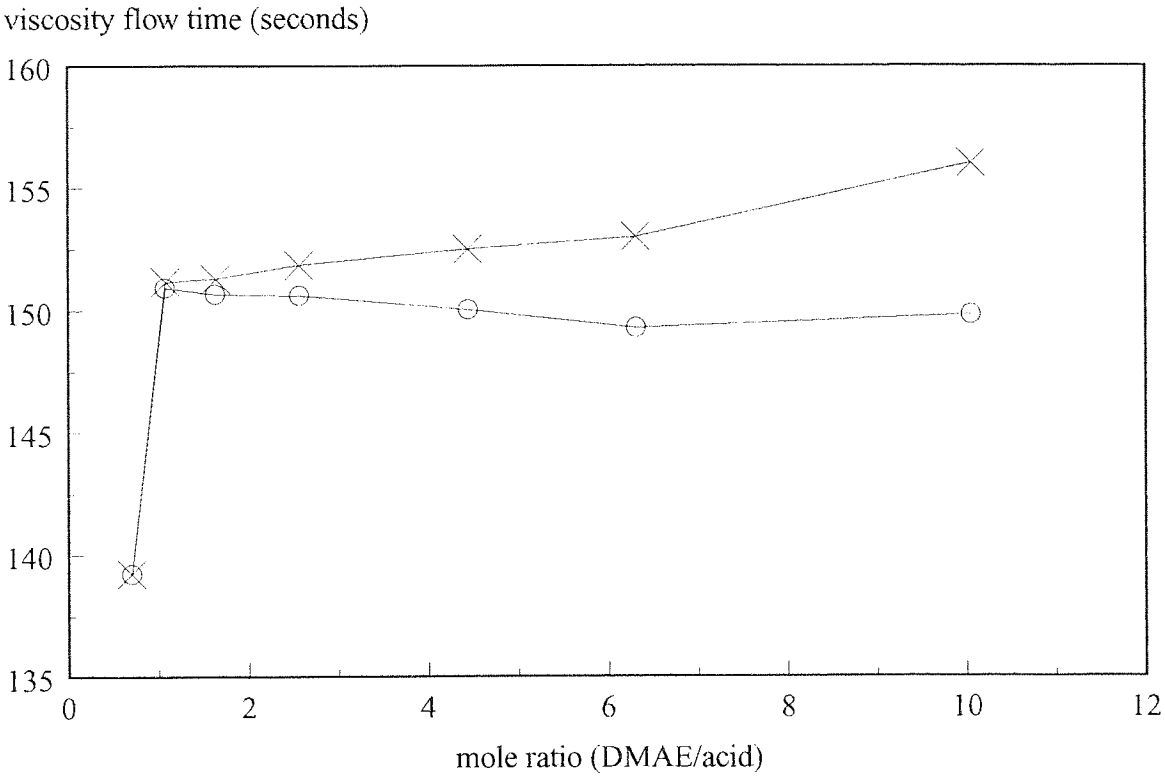

Figure 7.5(b). Effect of neutralisation upon the flow time viscosity of WRB625. **X** shows the measured flow time. **0** shows the flow time after the contribution due to DMAE has been subtracted.

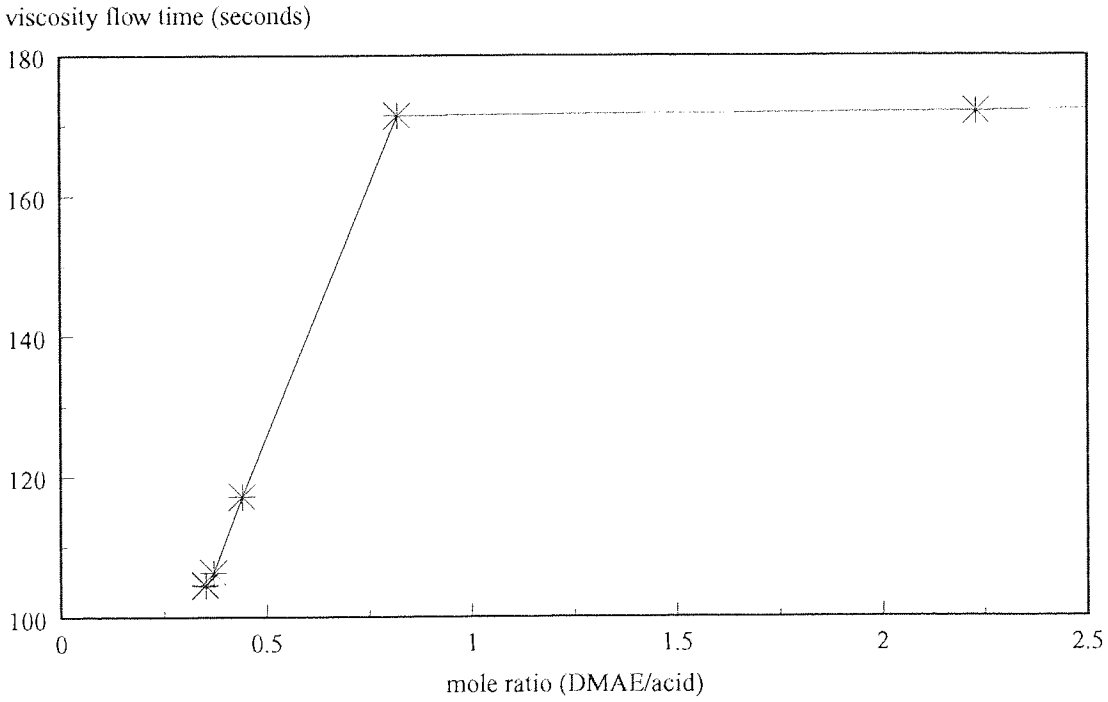

Figure 7.5(a). Effect of neutralisation upon the flow time viscosity of WRB633

The final column of Table 7.12 shows the viscosity of the sample after the contribution due to the presence of DMAE has been subtracted. The contribution due to the presence of DMAE at each concentration was determined by measuring the viscosity of DMAE solutions prepared in de-ionised water. From the results obtained it would appear that the viscosity increases after the first addition of DMAE but then remains constant. The results are shown graphically in Figure 7.5(b).

The experiment was repeated using the sample WRB633 and using more dilute DMAE solutions. It can be shown that 2 g of WRB633 already contains 1.2 mmoles of methacrylic acid and 0.42 mmoles of DMAE. Table 7.13 shows the flow times obtained for the samples and the DMAE to acid ratio.

The results indicate that the viscosity increases around the equivalence point for the DMAE to acid neutralisation. The results are displayed as a graph in Figure 7.5(a).

Table 7.13 Flow Times Through a Suspended-Level Viscometer of WRB633 Diluted in 2% Aqueous DMAE Solutions

sample	moles ($x10^{-3}$) of DMAE added	mole ratio DMAE /acid	corrected flow time (seconds)
WRB633(1)	0.0000	0.35	104.7
WRB633(2)	0.0010	0.35	104.5
WRB633(3)	0.0045	0.35	104.5
WRB633(4)	0.0225	0.37	106.3
WRB633(5)	0.1125	0.44	117.2
WRB633(6)	0.5625	0.82	171.5
WRB633(7)	2.2500	2.23	172.1
WRB633(8)	5.6250	5.04	175.2

7.2.3 Effect of concentration upon viscosity

A number of solutions of each latex were prepared, in either de-ionised water or 2% aqueous DMAE, in the concentration range 0.1 to 2.0%. The flow time viscosity of the solutions, through a suspended-level viscometer, were then measured. The concentration of the latices and flow time through the viscometer are shown in Table 7.14.

Table 7.14 Effect of Latex concentration upon viscosity

sample	Flow Time (seconds) through suspended level viscometer					
	WRB633		WRB625		WRB624	
conc/diluent	water	2% DMAE	water	2% DMAE	water	2% DMAE
2.0%	105.9	187.6	146.2	158.6	204.5	237.2
1.0%	95.1	132.5	113.9	118	144.6	155.3
0.5%	88.6	108.5	98.1	99.5	114.9	117.3
0.1%	81.9	89.8	84.2	87.8	87.9	91.6

The flow times of water and 2% aqueous DMAE were 79.5 and 85.2 seconds, respectively.

The flow time viscosity and reduced viscosity (viscosity number) are plotted on the same graph (Figure 7.6). The reduced viscosity or viscosity number is defined as the specific viscosity divided by the concentration, where the specific viscosity is the viscosity of the solution divided by the solvent viscosity minus 1. i.e. (η/η_0-1).

The samples diluted in the 2% aqueous DMAE solution are behaving as expected i.e the magnitude of the increase in viscosity is rising with increasing concentration [214]. This can be seen with in Figure 7.6 as the reduced viscosity increases with increasing concentration. The increase of viscosity of the samples diluted in water is decreasing with increasing concentration. The data presented in Figure 7.6 shows that the reduced viscosity decreases with increasing concentration.

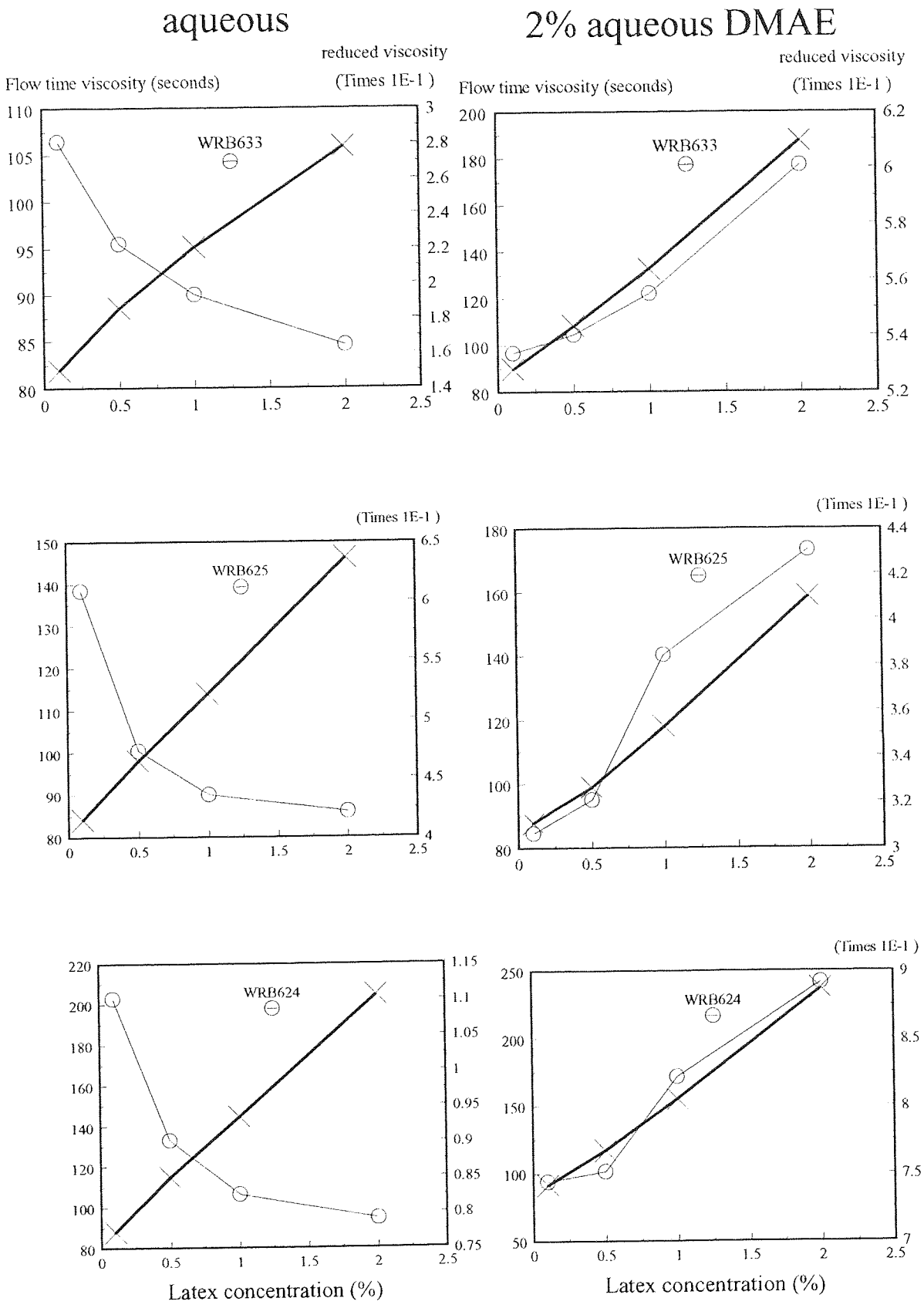

Figure 7.6. Effect of latex concentration upon viscosity. The graphs show viscosity measured as a flow time (**X**) and reduced viscosity (O) as a function of latex concentration diluted in water and in 2% aqueous DMAE, for the latices WRB633, WRB625 and WRB624.

7.3 NMR Spectroscopy

A carbon-13 NMR spectrum of the GEN1 latex is shown in Figure 7.7(a). Comparison of this spectrum with those of epoxy resins, see Chapter 5.2.2, indicates that none of the peaks from the epoxy resin component are observed in the spectrum of the latex. A spectrum of the base epoxy resin, in $CDCl_3$, solution is shown in Figure 7.7(b). The absence of peaks due to epoxy resin, in the spectrum of the latex, indicates that this component is either in solid form or in a solution environment that leads to viscosity broadening of the NMR peaks.

To identify the peaks that were observed in the latex spectrum, carbon-13 NMR spectra of aqueous solutions (5%) of the following were also recorded: n-butanol, 2-butoxy ethanol (BCS), triethyl amine, dimethyl amino ethanol (DMAE) and DMAE neutralised with poly(acrylic acid).

Table 7.15 Carbon-13 NMR peak assignments for solvents and amines

name and chemical structure	**carbon atom assignment**	**chemical shift (ppm)**
n-butanol a b e j CH_3-CH_2-CH_2-CH_2-OH	a b e j	15.6 20.9 36.1 64.2
2-butoxy ethanol (BCS) a c d i k l $CH_3CH_2CH_2CH_2OCH_2CH_3$	a c d i k l	15.5 20.7 33.0 62.6 72.1 73.1
triethyl amine m n $(CH_3CH_2)_3N$	m n	12.6 49.1
dimethyl amino ethanol (DMAE) f g h $(CH_3)_2N$-CH_2CH_2OH	f' g' h'	44.4 58.8 59.6
dimethyl amino ethanol (DMAE) plus poly(acrylic acid)	f g h	42.8 55.3 58.8

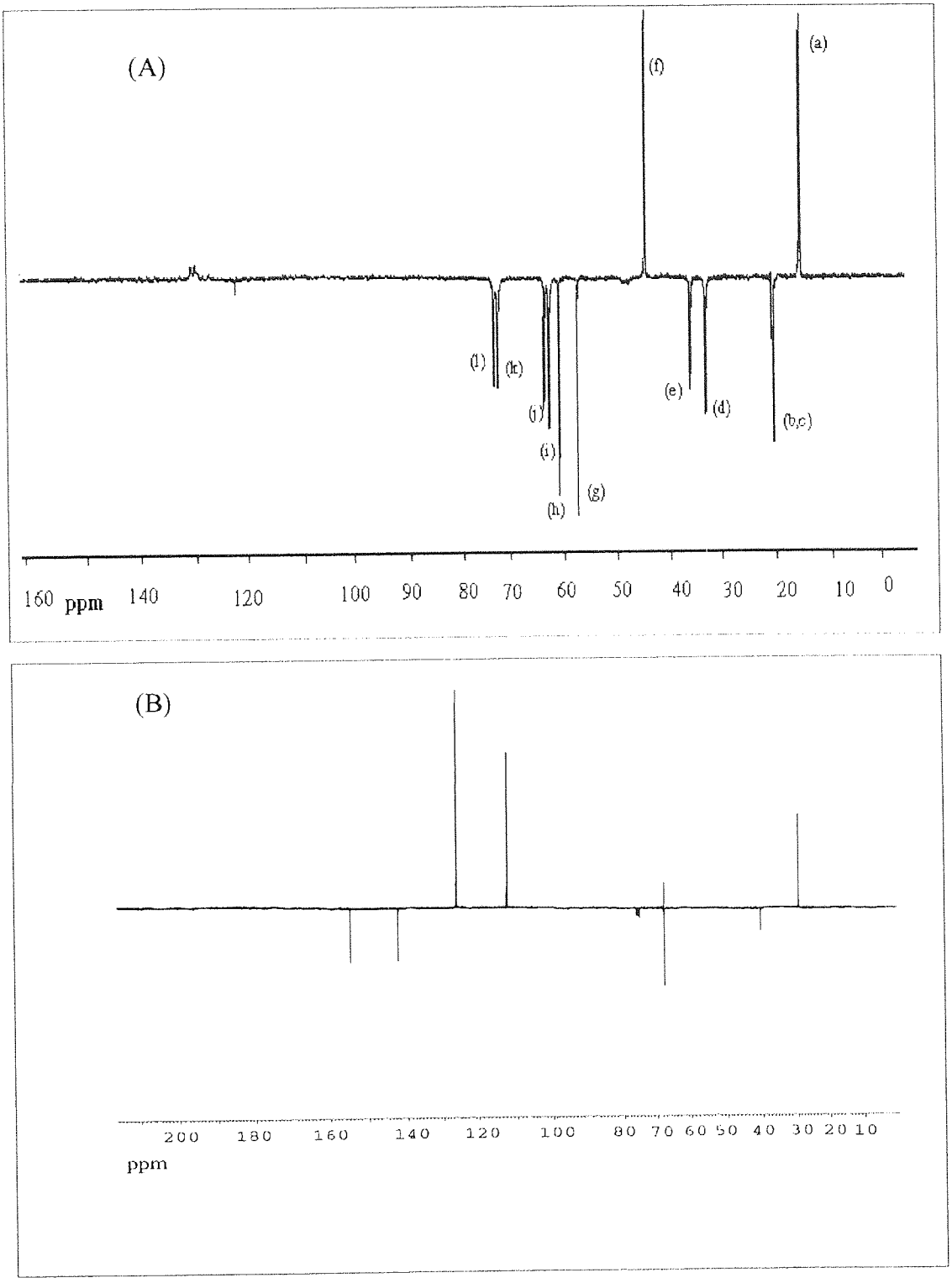

Figure 7.7 Carbon-13 NMR spectra of (A) WRB625 water-based latex and (B) a '9' type epoxy resin dissolved in $CDCl_3$

The peak assignments for the solvents and amines are given in Table 7.15. The peaks observed in the spectrum of the latex appear to be due to the solvents and the neutralising amine i.e. n-butanol, 2-butoxy ethanol and DMAE.

Using the spectra obtained from these components, the peaks in the carbon-13 NMR spectrum of the latex were assigned. The spectra were recorded using an attached proton test (APT) [213]. The direction of each signal as well as the peak assignments, are shown in Table 7.16.

Table 7.16. Carbon-13 NMR peak assignments for GEN1 latex

peak designation	chemical shift (ppm)	APT +/-	assignment
a	15.6	+	CH_3 from n-butanol and BCS
b	20.7	-	CH_2 from BCS
c	20.9	-	CH_2 from n-butanol
d	33.1	-	$CH_{2\ \text{from BCS}}$
e	36.1	-	CH_2 from n-butanol
f	42.8	+	CH_2 from DMAE
g	55.3	-	CH_2 from DMAE
h	58.8	-	CH_2 from DMAE
i	62.6	-	CH_2 from BCS
j	64.2	-	CH_2 from n-butanol
k	72.1	-	CH_2 from BCS
l	73.1	-	CH_2 from BCS

It was observed that the chemical shifts for DMAE changes upon addition of poly(acrylic acid). The peaks in the NMR spectra of the latex due to DMAE are similar to the spectrum of DMAE which has been neutralised with poly(acrylic acid). The NMR spectra of the aqueous solutions of DMAE are shown in Figure 7.8(a) and (b). Acetone-D_6 was used, in a glass capillary placed in the sample tube, to calibrate the instrument.

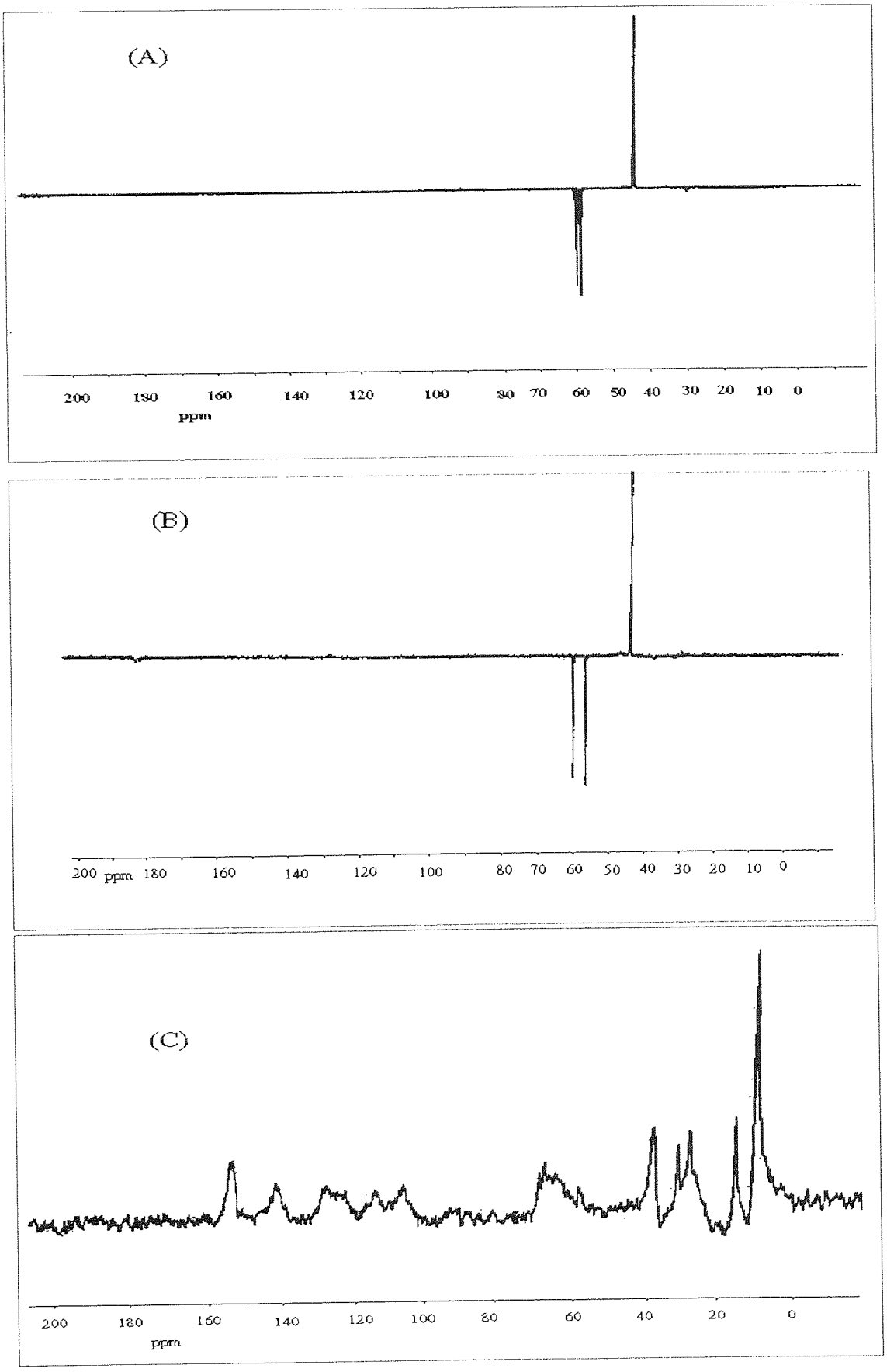

Figure 7.8 Carbon-13 NMR spectra of (A) DMAE in water, (B) DMAE neutralised with poly(acrylic acid) in water and (C) CP-MAS NMR spectrum of WRB625 latex recorded at -40^{0}C.

A CP/MAS carbon-13 NMR spectrum of the latex at a temperature of -40^{0}C was also recorded. The spectrum is shown in Figure 7.8(c). Under these conditions, peaks due to the aromatic carbon atoms with chemical shifts at 153.3, 140.9, 126.9 and 114.1 ppm can clearly be observed.

7.4 Infra-red Analysis

7.4.1 Introduction

FT-IR analyses of aqueous sodium hexanoate [164] indicates that there is a decrease in the asymmetric stretching frequency of the CH_3 group ($\nu_{as}CH_3$)and that of the CH_2 group ($\nu_{as}CH_2$) values with increasing concentration. The increase in concentration leads to a progressive increase in aggregation.

IR spectra of latex samples were recorded using both an ATR KRS5 liquid cell and a calcium fluoride fixed path length cell. A spectrum of the latex was also recorded after the solvents n-butanol and 2-butoxy ethanol had been extracted out into hexane.

IR spectra of the following samples were included in the analysis:

(a) PW1 dry film,

(b) DOW XZ86762 dry film ('9' type epoxy resin)

(c) DER331 (low molecular epoxy resin), and

(d) DER331 in solution.

The change in molecular environment in samples (a) through (d) should lead to increasing molecular mobility. This should correspond to a decrease in the position of $\nu_{as}CH_3$, if this system behaves in a similar manner to the sodium hexanoate system described above. The value of the $\nu_{as}CH_3$ in the latex spectrum could then be compared to the standard spectra.

7.4.2 Results

Four spectra of water and PW1 were recorded using 10, 100, 1000 and 10,000 scans using the ATR cell. Up to 1000 scans. the greater the number of scans the larger the signal-to-noise ratio. However it was observed that above 1000 scans there was no further improvement in the signal-to-noise ratio. Further experiments were therefore restricted to 1000 scans.

After spectral subtraction of water, the sample spectrum showed a high degree of noise outside the range 3100 to 800 cm^{-1}. This is due the strong water absorption in these regions. Between 3100 and 800 cm^{-1} a spectra similar to the non-volatile portion of the cast samples were obtained. However, water has a strong absorption band at 1650 cm^{-1} and after subtraction there is a degree of noise in the 1750 to 1650 cm^{-1} region. This tends to mask detail in the acrylic ester peak and because of this observation it was decided that all further studies would be carried out using the calcium fluoride cell.

For spectra obtained via transmission through the calcium fluoride cell 1000 scans were used. Figure 7.9(a) shows the IR spectrum of water and Figure 7.9(b) shows the IR spectrum of the latex PW1. Figure 7.10(a) shows the result of spectral subtraction of the water spectrum from that of the latex. The spectrum shows little noise in the ester carbonyl region. The spectrum, between 3200 and 1000 cm^{-1}, is similar to that obtained for a vacuum dried film of the latex (Figure 7.10(b)).

The C-H stretching frequencies from all the spectra were measured and are shown in Table 7.17. Values of $\nu_{as}CH_3$ for the epoxy resins, appear to follow the trend of decreasing wavenumber with increasing mobility. For the low molecular weight epoxy resin in solution, the frequency of the ν_{as} CH_3 band is 2969 cm^{-1}. This decreases to 2967 cm^{-1} for the pure sample, which is a liquid at room temperature, in the absence of solvents where the viscosity of the sample would be significantly higher. For a high molecular

weight epoxy resin, which would be solid at room temperature, the $\nu_{as}CH_3$ frequency was 2965 cm^{-1}. These shifts in frequency are much smaller than those observed for aqueous hexanoate [164]. The values of $\nu_{as}CH_3$ for the latex sample after solvent extraction and the dry film of the latex were 2965 cm^{-1} and 2966 cm^{-1}, respectively.

The values of $\nu_{as}CH_2$ appear to show an increase in frequency with decreasing mobility. In solution the value for the low molecular weight epoxy resin is 2927 cm^{-1}. In the absence of solvent this increases to 2928 cm^{-1} and the value for the high molecular weight DOW XZ86762 is 2932 cm^{-1}.

Table 7.17 IR C-H stretching frequencies: Epoxy resins

sample	wavenumber (cm^{-1})		
	CH_3 asym.	**CH_2 asym**	**CH_2 sym**
DOW XZ86762	2966	2932	2871
DER331 (liquid)	2967	2928	2872
DER331 (solution)	2969	2927	2873
PW1 (dry film)	2966	2933	2873
PW1 latex	2966	2940	2878
PW1 (D_2O)	2965	2938	2878
5% aq. n-butanol	2967	2942	2881
5% aq. BCS	2966	2942	2880
PW1 latex (extracted)	2965	2935	2874

The $\nu_{as}CH_3$ frequency for the latex samples appear to be greater than that of the dry latex films and pure epoxy resins. This was found to be due to the presence of the solvents n-butanol and 2-butoxy ethanol. After the solvents had been removed via extraction into hexane, the value of ν_{as}CH3 for the aqueous samples were similar to the dried polymer film i.e around 2935 cm^{-1}.

The values of $\nu_{as}CH_2$ show only minor changes with sample mobility. The levels of solvents in the initial and the extracted samples were determined using gas

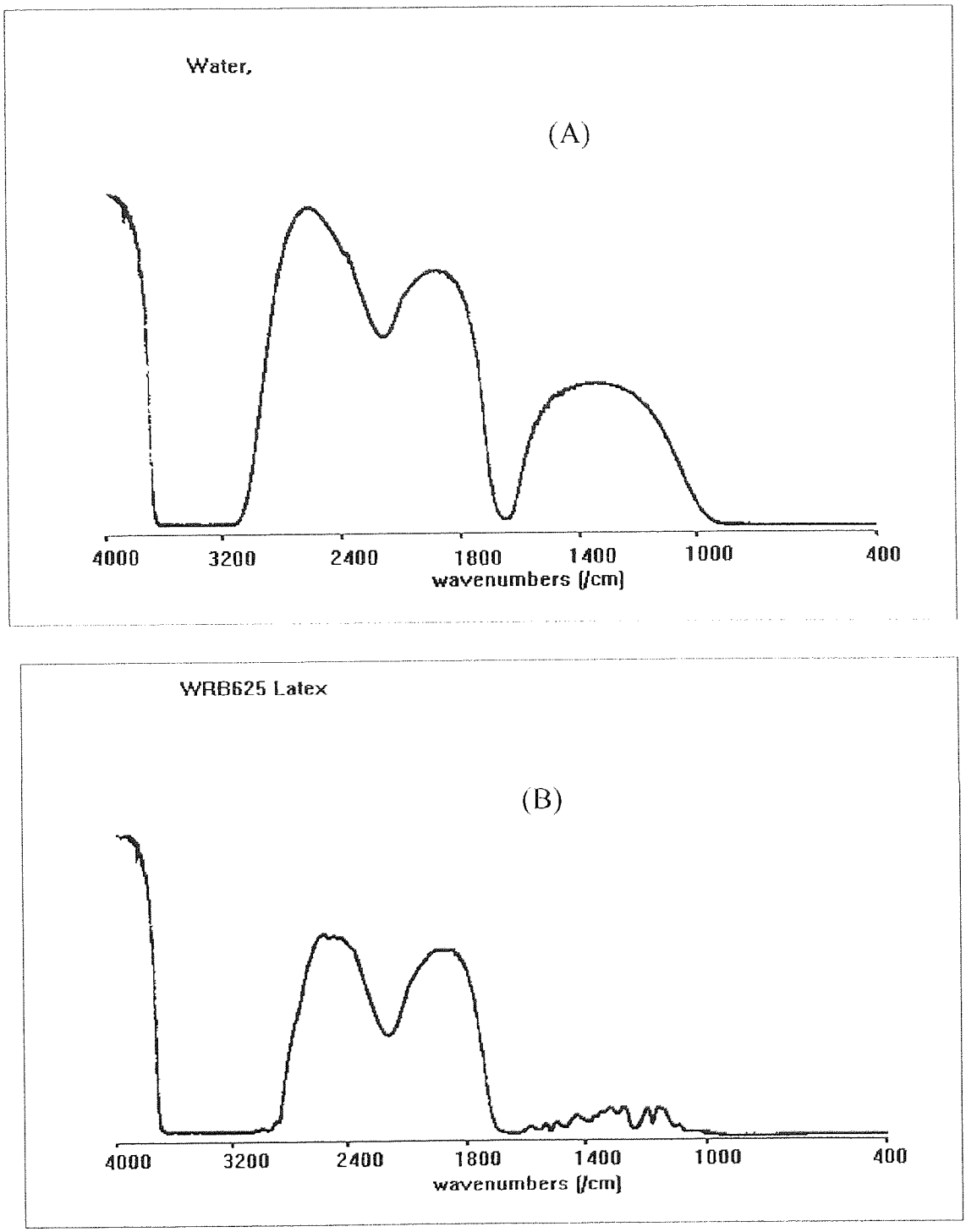

Figure 7.9 Transmission IR spectra of samples recorded in a calcium fluoride cell with a fixed path-length of 0.12 mm. (A) water only and (B) WRB625 latex.

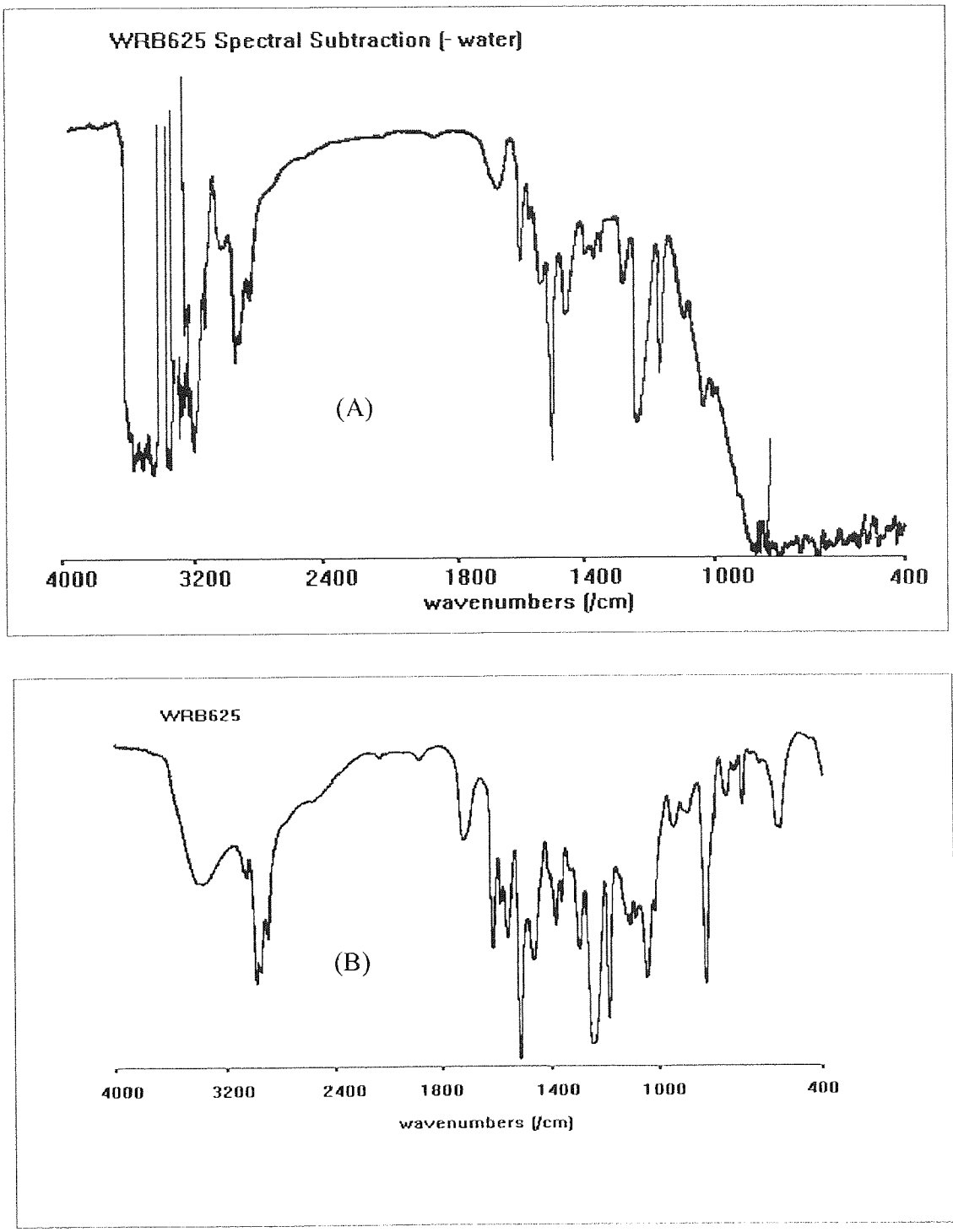

Figure 7.10 Transmission IR spectra of (A) WRB625 latex with a spectrum of water subtracted and (B) a dry film of WRB625

chromatography. The initial sample was found to contain 8.4% n-butanol and 11.2% 2-butoxy ethanol. After extraction into hexane the n-butanol and 2-butoxy ethanol levels in the latices were determined to be less than 0.1%.

7.5 Water-Soluble Polymer Studies

7.5.1 Determination of soluble polymer

It has been observed in this study that when DMAE is added, the latices increase in viscosity. These viscosity changes were measured as flow times through a suspended-level viscometer (refer to Chapter 7.2.2). To determine the cause of these effects, the level of water-soluble polymer present in the latices was measured as a function of the degree of neutralisation of the acid functional polymeric components.

Samples of the latices WRB624, WRB625, WRB626, WRB633 and PW1 (2 g) were diluted (25 cm^3) in de-ionised water and in a 2% solution of DMAE in water. The samples were centrifuged and the amount of soluble polymer in the aqueous layers were determined gravimetrically. The method for determining the amount of soluble polymer in the samples is described in Chapter 6.5. The repeated analysis of a single sample revealed an error of +/- 0.3%

The soluble polymer contents for the various latices are shown in Table 7.18. The soluble polymer content quoted in the table is the amount of polymer in the aqueous layer expressed as a percentage of the total polymer in the sample.

The sample 'PW1 +amino resin' contains added Cymel 303 amino resin (BIP Chemicals). The details of the preparation of these samples are shown in Chapter 6.2.2.

The soluble polymer contents show that for all samples, the addition of DMAE to the latex increases the amount of water-soluble polymer. For example, when WRB625 is diluted in water, the water-soluble polymer content is 29.8%. When the same sample is

diluted in the 2% aqueous DMAE solution, the soluble polymer content increases to 33.1%.

Table 7.18 Soluble Polymer Determinations

sample	diluent	soluble polymer (%)
WRB624	water	56.6
WRB624	2% aqueous DMAE	63.1
WRB625	water	29.8
WRB625	2% aqueous DMAE	33.1
WRB633	water	54.9
WRB633	2% aqueous DMAE	62.1
PW1	water	29.2
PW1	2% aqueous DMAE	30.8
PW1 + amino resin	water	29.6
PW1 + amino resin	2% aqueous DMAE	31.5

The soluble polymer content determinations also show that the higher the level of the acrylic component in the polymer, the higher the soluble polymer content. For example, WRB624 and WRB633 have a soluble polymer content in the region 55 to 65%. The epoxy to acrylic composition of both of these samples is 60:40. WRB625 and PW1 which have a composition of 80:20 epoxy to acrylic, have a soluble polymer content around 30%.

The soluble polymer content of the samples containing the amino resin is approximately 1.5 percentage points higher than those without the addition of this polymer. This suggests that the amino resin is soluble in water and, as will be shown later, the IR spectrum of the soluble polymer does indeed contain a higher level of amino component than the initial samples.

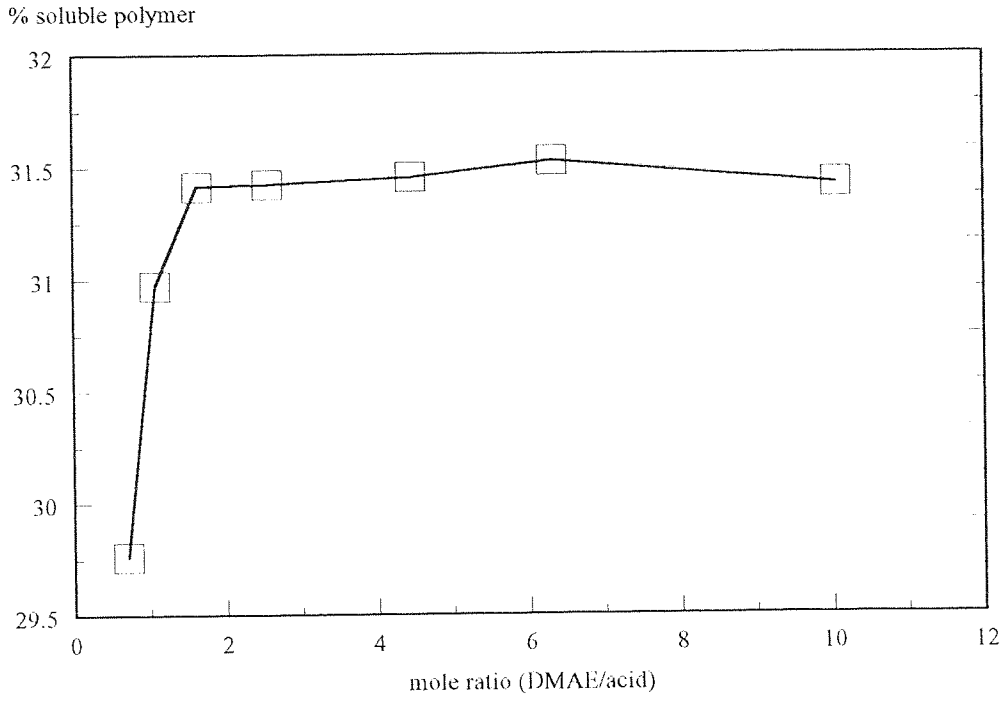

Figure 7.11 Graph showing effect of degree of neutralisation of acid groups with DMAE upon the level of soluble polymer in WRB625

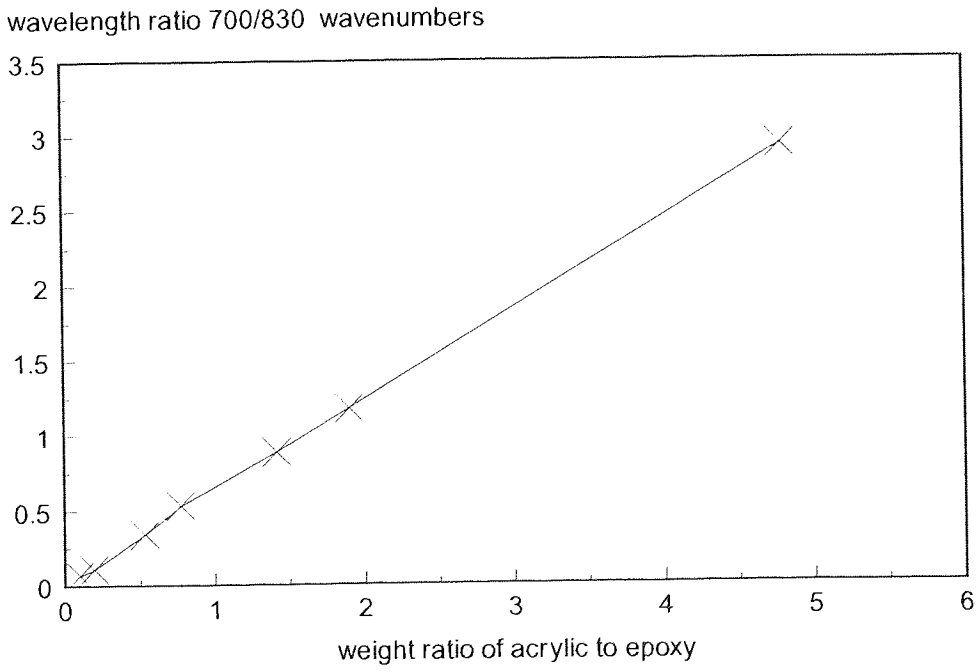

Figure 7.12 IR calibration data. Ratio of absorbances of peaks at 700 and 830 wavenumbers versus acrylic to epoxy ratio.

Samples of WRB625, diluted to a constant volume but with various concentrations of aqueous DMAE, were centrifuged to determine the level of soluble polymer as a function of the degree of neutralisation of the polymer acid groups. The details of the preparation of the samples and the pH measurements are described in Chapter 6.5. Chapter 7.2.2 details the effect of this addition of DMAE to the viscosity of the samples. The samples were prepared by taking aliquots (2 g) of the sample, adding various amounts of DMAE solution, and diluting with de-ionised water (25 cm^3). The volumes of DMAE solution added are shown in Table 7.19.

Table 7.19 Effect of Neutralisation upon Levels of Soluble Polymer

sample	volume of 2% aq. DMAE added (cm^3)	mole ratio DMAE/acid	soluble polymer (%)
WRB625 (1)	0	0.70	29.8
WRB625 (2)	1.0	1.08	31.1
WRB625 (3)	2.5	1.64	31.4
WRB625 (4)	5.0	2.57	31.4
WRB625 (5)	10.0	4.45	31.4
WRB625 (6)	15.0	6.32	31.5
WRB625 (7)	25.0	10.06	31.4

The levels of water-soluble polymer present in the latices with increasing neutralisation are shown in Table 7.19. The results indicate that the amount of soluble polymer increases with increasing levels of added DMAE up to the equivalence point. The results are shown graphically in Figure 7.12. This is a similar finding to that found for the effect of neutralisation upon particle size and viscosity (refer to Chapters 7.1.1 and 7.2.2). All of these properties increase with increasing neutralisation up to the neutral point and then remain constant with respect to further addition of DMAE.

7.5.2 Chemical composition of the separated layers using IR spectroscopy

(a) Introduction

The polymer composition of the soluble portion of the samples, obtained by centrifuging the diluted samples, were determined using Infra-red (IR) spectroscopy. A calibration graph, of epoxy to acrylic content versus the ratio of absorption bands at 830 cm^{-1} and 700 cm^{-1}, was constructed, after recording the IR spectra of known mixtures of epoxy and acrylic resins.

(b) Calibration

Mixtures of epoxy resin and an acrylic resin, the latter having the same composition as the monomer feed in the preparation of the graft polymer, were prepared. The polymers used were DOW XZ86762 (a 100% polymer content, '9' type epoxy resin) and the acrylic resin AT1140. The latter sample is an HSC experimental resin with a polymer content of 25% and a composition of methacrylic acid (65.0%), styrene (34.0%) and ethyl acrylate (1.0%). Table 7.20 shows the composition of each standard prepared.

Infra-red spectra of the various standards were recorded. Since the intensity of the ester carbonyl is effected by the presence of DMAE (refer to Chapter 5.1.3), it cannot be used to determine the level of acrylic resin in the samples. The ratio of the acrylic to styrene contents in all of the graft polymers is constant. For this reason the intensity of the peak at 700 cm^{-1}, due to the polystyrene component, can be used to determine the level of acrylic. The peak at 830 cm^{-1} is used to determine the level of epoxy.

Table 7.20 also shows the ratio of the 700 cm^{-1} to 830 cm^{-1} absorption bands. A plot of this absorption ratio against weight ratio is shown in Figure 7.12. The least-squares calculated values of the slope and intercept were 0.6091 and 0.0195 respectively, with a value of 0.9995 for the correlation coefficient.

Table 7.20 Preparation details of epoxy:acrylic polymer mixtures for IR calibration

mixture	ratio of acrylic to epoxy	700/830 cm^{-1} ratio
A	0.099	0.0696
B	0.193	0.1094
C	0.532	0.3410
D	0.773	0.5319
E	1.415	0.8865
F	1.899	1.1765
G	4.780	2.9240

(b) Sample analysis

IR spectra of the initial latex samples and the soluble portions, from the samples WRB625, WRB624, WRB633 and PW1 diluted in both water and 2% aqueous DMAE, were recorded. The ratio of the absorption values of peaks at 700 and 830 cm^{-1} were calculated. Using these ratios and the values of slope and intercept from the calibration curve, the composition of the polymer in the soluble layer was calculated (see Table 7.21).

The results indicate that there is a higher ratio of acrylic to epoxy in the soluble portion than in the initial sample. For example the acrylic content of the polymer present in the initial WRB624 latex is 29.0%. In the soluble portion, obtained by centrifuging, the acrylic content increases to 41.7%.

Table 7.21 Composition of soluble polymer determined using IR

sample	calculated % composition of acrylic polymer		
	initial latex	soluble polymer	
	aqueous	aqueous	2% DMAE
WRB624	29.1	41.7	44.5
WRB625	17.5	43.6	45.1
WRB633	32.8	44.9	45.4
PW1	18.1	39.5	43.7

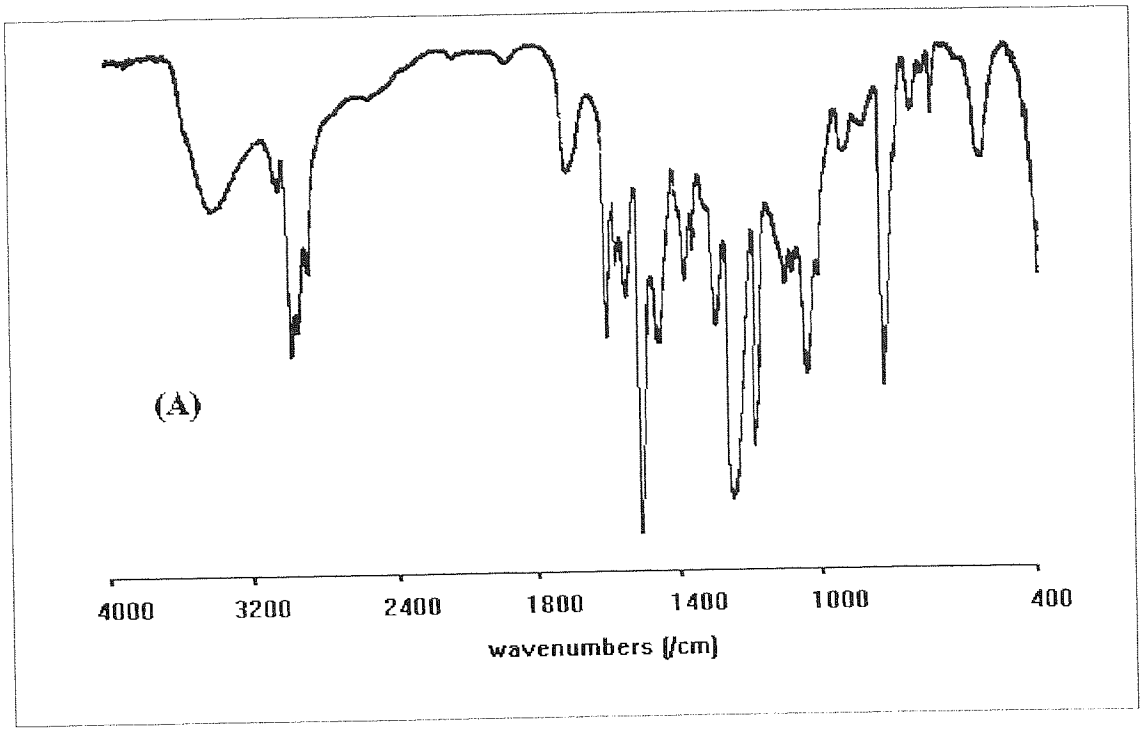

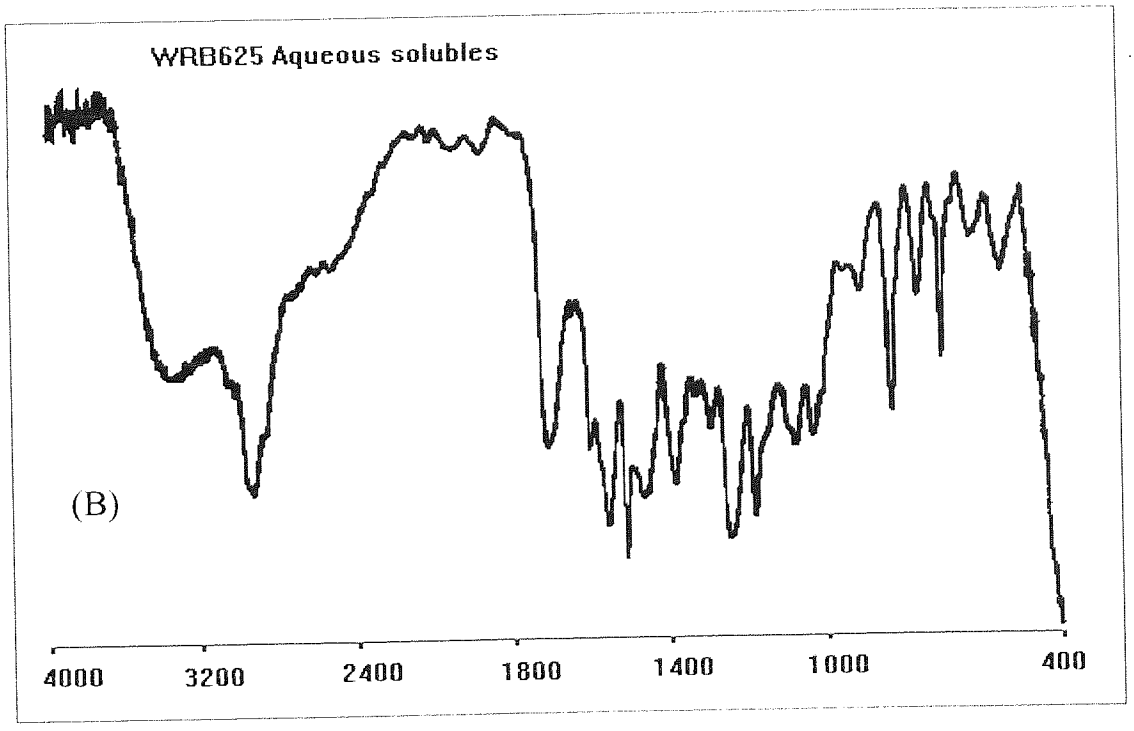

Figure 7.13. Transmission IR spectra of (A) a dry film of WRB625 cast from a latex and (B) a soluble portion of the latex obtained by centrifuging the sample.

No differences between the IR spectra of the soluble portions from the samples diluted in water and 2% aqueous DMAE solutions were observed. Figure 7.13 (a) shows the IR spectrum of the original WRB625 latex. Figure 7.13 (b) shows the spectrum of the soluble portion of the sample. Increases in both the carboxylic acid content (1700 cm^{-1}) and amino resin content (1550 cm^{-1}), relative to the epoxy component, can be observed.

7.5.3 Gel Permeation Chromatography analysis of the soluble polymer

GPC profiles of the initial latex and soluble portions from the latex WRB625 were recorded. The GPC profiles are shown in Figure 7.14(a). The molecular weight distribution analyses are shown in Table 7.22. The MWD values obtained for the epoxy-graft-acrylic polymer used to prepare the latex (WRB621) and epoxy resin prior to grafting (DLER100) are also shown in the table.

Table 7.22 MWD Results for the Initial Latex and Soluble Polymer.

sample	MWD values from GPC data			
	Mn	Mw	Mz	D
initial latex	7260	21000	51700	2.9
soluble portion	15900	48300	122000	3.1
WRB621	7230	21800	50400	3.1
DLER100	7160	20300	41200	2.8

The results indicate that the molecular weight of the polymer present in the latex is similar to that of the polymer prior to dispersion. The results of the GPC analyses also show that the molecular weight of the soluble portion is higher than that of the initial sample. The IR spectrum of the soluble polymer indicates that it contains a higher level of acrylic acid functional groups than the initial sample. These results support the earlier

assertion that the acrylic grafting is taking place on high molecular weight epoxy (see also Chapter 5.3.2.).

7.5.4 46900 latex

(a) The effect of pH on various physical characteristics

The 46900 formulation contains a phenolic resin as the cross-linking agent rather than the amino resin used in the GEN1 formulations. For further details of the composition of these latices refer to Chapter 3. Samples of 46900 water-based latex were diluted in a similar manner to that described previously i.e. the latex (2 g) was diluted to 25 cm^3 in either de-ionised water or in a 2% aqueous solution of DMAE. The samples were centrifuged and as before, the polymer contents of the initial sample and soluble layers were measured. Refer to Chapter 6.5 for details of the methods used. The results of these determinations are shown in Table 7.23.

Table 7.23 46900, Soluble Polymer Determinations.

sample	diluent	pH	% soluble polymer
46900	water	7.81	29.2
46900	2% DMAE	8.98	33.5

The results indicate that there is a higher level of soluble polymer present in the latex when diluted with DMAE i.e. the solution at higher pH, than in the latex diluted in water. For example, when the sample is diluted in water, 29.2% of the polymer is soluble. When the sample is diluted in aqueous DMAE solution the soluble polymer content increases to 33.5%. This increasing soluble polymer content with increasing pH is also observed with GEN1 type formulations. Refer to Chapter 7.5.1.

(b) Chemical composition

The latex known as 46900 (see Chapter 3.3 for details of the composition) contains a phenolic cross-linking polymer which is not easily observed in the IR spectrum in the presence of epoxy resin. Therefore, in order to compare the composition of the initial sample with that of the water-soluble portion, the technique of GPC was used. The only change to the instrument conditions, given in Chapter 5.4.1, was that the UV detector was set to monitor at 295 nm. This wavelength was chosen since the UV absorption for the phenolic component is greater than that of the epoxy component. This can be seen in Figure 5.10.

Analysis of the 46900 type latex, using GPC, reveals peaks due to both epoxy and phenolic components. The GPC profiles of the initial sample and the centrifuged soluble and insoluble portions are shown in Figure 7.14 (b), (c) and (d). The higher molecular weight epoxy component is seen to elute after approximately 13 minutes and the phenolic component elutes after 18 minutes.

Using the data handling software, the areas under the epoxy and phenolic peaks of the initial latex, soluble portion and the insoluble portion were measured. These peak areas are shown in Table 7.24.

Table 7.24 GPC Peak Area Data for Epoxy and Phenolic components in 46900 latex

sample	area under the peaks ($x10^6$)		
	epoxy	phenolic	total
initial	4.013	3.326	7.339
solubles	1.407	2.556	3.963
insoluble	3.166	1.669	4.835

There is insufficient data to calculate response factors using the simultaneous equation type calculations carried out in Chapters 5.5.4 and 5.5.5. However, the theoretical

composition for the 46900 sample is 80:20 epoxy to phenolic. The response factors (RF) for the epoxy and phenolic components can therefore be calculated by dividing the area under the peak for each component by the amount of that component known to be present in the initial 46900 sample. Using these response factors, the compositions of the soluble and insoluble polymers were determined to be 35.5% and 13.7%, respectively. The soluble portion from the centrifuged sample therefore contains a higher phenolic content (35.5%) than the initial sample (20%). It is also observed that the GPC profiles of the phenolic component present in the initial, soluble and insoluble portions are significantly different. This would suggests that various fractions of the phenolic are partitioning to different extents between the soluble and insoluble phases. The lower molecular weight fraction appears to be present at a higher concentration in the soluble portion.

Examination of GPC profiles of the ML97 phenolic resin at different UV wavelengths suggest that the polymer does not have the same chemical composition throughout the molecular weight range. GPC profiles at 245, 260, 280 and 295 nm are shown in Figure 7.15. There appear to be components, at low molecular weight, which absorb in the range 260 to 280 nm but not at 295 or 245 nm. It is this low molecular weight material which is more soluble in water than the higher molecular weight components.

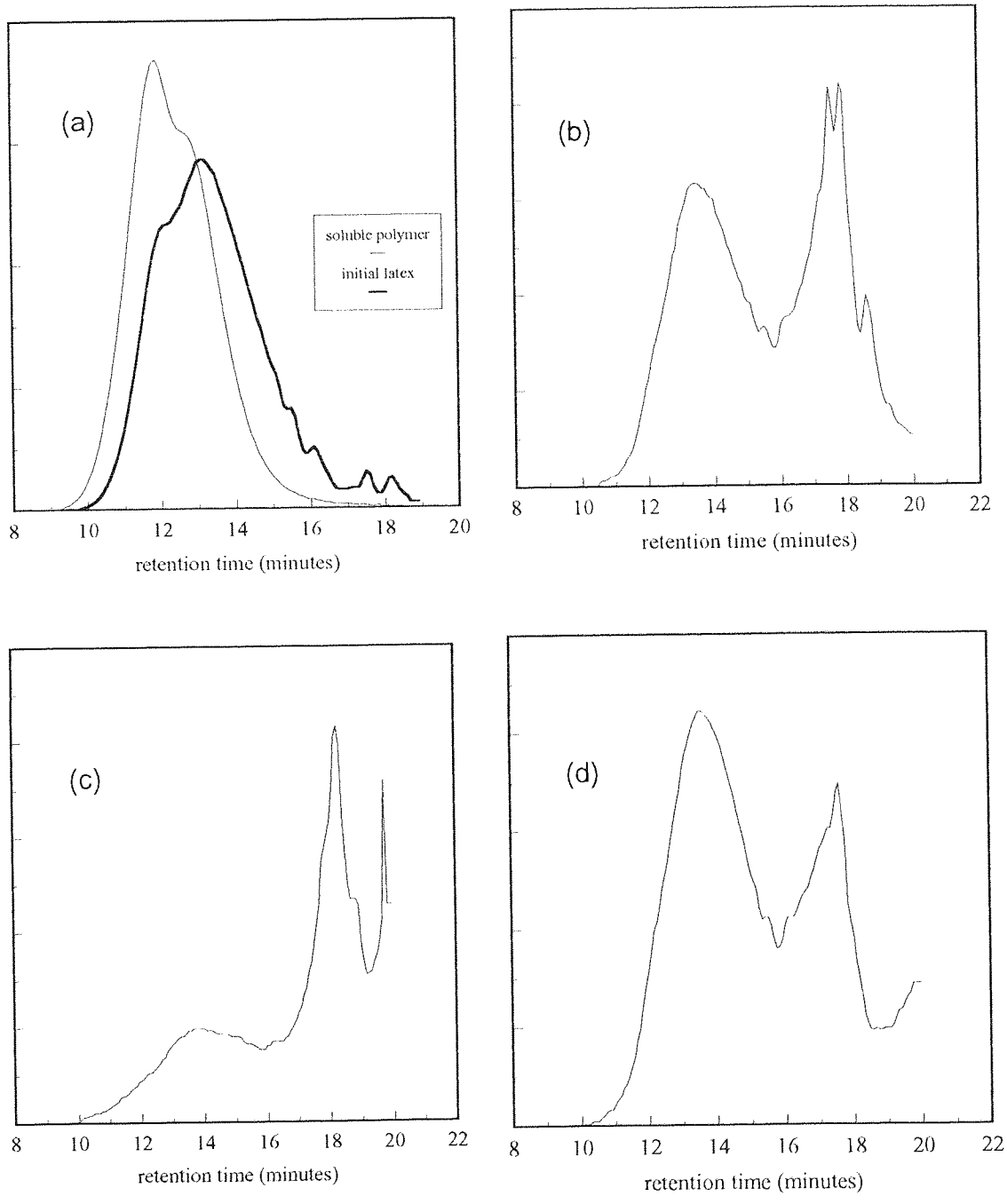

Figure 7.14. GPC profiles of (a) the initial WRB625 latex with the water-soluble polymer. GPC profiles of 46900 latex (contains phenolic cross-linker) (b) initial sample, (c) soluble and (d) insoluble portions.

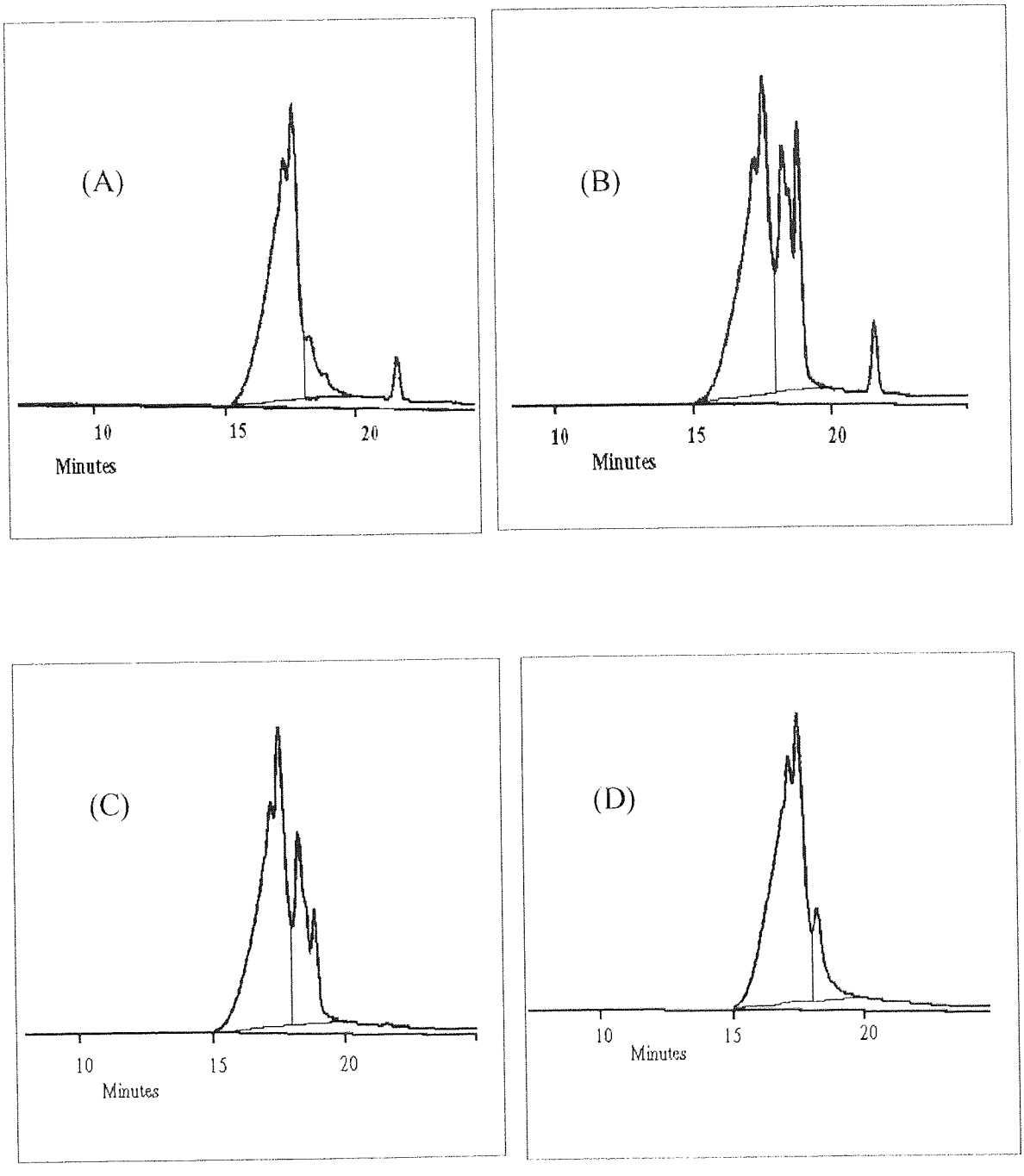

Figure 7.15. GPC profiles of phenolic resin ML97 recorded at four different wavelengths: (A) 245 nm, (B) 260 nm, (C) 280 nm and (D) 295 nm.

CHAPTER 8. FILM CHARACTERISATION: EXPERIMENTAL

8.1 Introduction

It had been reported previously [220] that the cured films produced from GEN1 type latices showed some structure when examined using transmission electron microscopy. When stained with osmium tetroxide, the micrographs of the films show unstained white circular domains surrounded by stained dark areas.

The method of analyses suggested in that earlier work was applied to the water-based latices WRB624, WRB625, WRB626 and WRB633. A description of these formulations is shown in Table 8.1. Details of the preparation of these samples are given in Chapter 3.

Table 8.1 Polymer formulations used in water-based latices

Latex number	base resin number	epoxy to acrylic ratio	degree of neutralisation
WRB633	WRB622	60:40	35%
WRB624	WRB622	60:40	70%
WRB625	WRB621	80:20	70%
WRB626	WRB623	90:10	70%

Two further formulations were produced. PW5, was prepared by dissolving WRB621 in organic solvents rather than dispersing it in water. The formulation had a similar polymer content to that of the latices. The sample also contained similar levels of n-butanol, 2-butoxy ethanol and DMAE. However the polymer was dissolved in 2-butanone rather than being dispersed in water. PW7 was a physical blend of epoxy and acrylic resins dissolved in the same solvents as PW5. The acrylic resin employed in this

formulation had an identical composition to the monomer feed used in the grafting process.

8.2. Application and curing conditions

The method of 'flood-spinning' was used to apply the latex samples to the tin-plate substrate. Flood-spinning is a technique used in the coatings industry whereby the sample is poured onto a flat square sheet and is rapidly spun. Excess sample is drawn off the edges by centrifugal force. Some control of the film weight/ film thickness is achieved by adjustment of the time that the sample if left spinning. The method was found to give reproducible film-weights and film thickness.

A typical procedure would be to apply approximately 25 cm^3 of the sample to the centre of a 15 cm square tin-plate panel placed in the flood-spinning apparatus. The lid is closed and the panel spun for approximately 30 seconds. The conditions are chosen to produce a film weight per unit area of approximately 1 mg cm^{-2}. It is difficult to check the film weight of a completely cured and cross-linked film. Therefore to check that the spin time for the given sample is giving the required film weight, the film is produced and partially cross-linked by placing the sample in an oven at 190^0C for 30 seconds. This removes all of the volatiles but does not cure the coating. The film weight can then be checked by weighing an area of the panel before and after removal of the coating by wiping with 2-butanone.

After the conditions have been established to produce a film with the correct film weight the applied panels were cured in a box oven set to 190^0C for 2 minutes.

8.3 Removal of films from substrate

8.3.1 Tin-plate

Mercury forms amalgams with many metals including tin. Notable exceptions include iron, cobalt and nickel.

An area of coated substrate, 2 cm square, was cut from the applied panel. An 'X' was scratched into the coating, penetrating to the metal surface, from the corners. A drop of mercury was then placed at the centre of the 'X'. After approximately 30 seconds the coated may be lifted off with forceps. The excess mercury was wiped from the film.

It should be noted that with highly cross-linked polymers the films were more difficult to remove from the substrate.

8.3.2 Aluminium

Aluminium dissolves in moderately concentrated hydrochloric acid to form hydrated aluminium chloride and hydrogen.

A 2 cm square of coated substrate was cut from the applied panel and dropped into a beaker containing 1:4 concentrated hydrochloric acid: water. It was found that after approximately 5 minutes all of the aluminium had dissolved.

8.4 TEM analysis

The films are vapour stained in osmium tetroxide prior to sectioning. Staining at this stage has little effect upon the final image but by pre-staining with osmium tetroxide, the film is easier to see after embedding in epoxy. The stained polymer films are embedded in an epoxy resin and silver sectioned. The sections were prepared using an ultra-microtome. Silver-section refers to the appearance of the film after sectioning. Silver-sections have a film thickness of 60 - 70 nm. The sections are then stained with methanolic uranyl acetate for 2 hours.

CHAPTER 9. FILM CHARACTERISATION: RESULTS

9.1 Introduction

Earlier work [220] indicated that, for a film based on a GEN1 water-based dispersion, structure could be observed when the samples were examined using transmission electron microscopy. Up until this time it was believed that the film was amorphous. The TEM image indicated the presence of white circular areas with stained circumferences. It was believed that the unstained white areas were due to epoxy domains surrounded by the acrylic resin. A structure, in fact, similar to that found in the latex.

9.2 Examination of films cast from latices

The sample preparation for this analyses described in this thesis is as follows:

1. Apply and cure the coating,
2. remove the coating using mercury amalgam (see Chapter 8.2),
3. stain the film with aqueous osmium tetroxide,
4. embed in epoxy resin, silver section and
5. fix with ethanolic uranyl acetate.

Work carried out at Birmingham University for the author indicated that maximum staining was achieved by vapour staining with osmium tetroxide for 24 hours prior to embedding and silver sectioning. After sectioning, the samples were stained with a solution of uranyl acetate in methanol (4%). It was also observed that the use of lead citrate, mentioned in the earlier report [220], had little effect upon the appearance of the final micrograph.

If the films are vapour stained with osmium tetroxide after sectioning an effect 'opposite' to that mentioned above arises i.e. dark circular domains each with a light circumference. This can be observed in Figure 9.1(a).

Films produced from the water-based latices WRB624, WRB625, WRB626 and WRB633 were all examined using TEM. The formulations and range of particle sizes measured from the micrographs are summarised in Table 9.1.

Table 9.1 Determined particle size range from TEM analysis of applied films

sample	epoxy: acrylic	degree of neutralisation	range of particle sizes (nm)
WRB625	80:20	70%	30 - 110
WRB624	60:40	70%	30 - 50
WRB633	60:40	35%	30 - 50
WRB626	90:10	70%	-

Figure 9.1(b) shows the micrograph of the WRB625 formulation and shows white areas surrounded by dark stained areas. The particle size range is 30 to 110 nm. No differences were observed between the sizes of particles in the latices WRB624 and WRB633. The particles observed from both samples had diameters in the range 30 to 50 nm. In both of the micrographs the amount of stained area relative to unstained area increased relative to that for WRB625. Both WRB624 and WRB633 have an acrylic content of 40% whereas WRB625 has an acrylic content of 20%. The result is consistent with the idea that it is the acrylic portion which is taking up the stain.

Figure 9.2(a) shows the micrograph of the film produced from the WRB626 latex. This micrograph is completely different from the micrographs obtained from the other films. The WRB626 micrograph does not show a regular structure. There are large

unstained areas plus some smaller areas surrounded by stained areas. There is apparently insufficient acrylic resin present to stabilise the micellar structure as the film begins to form.

9.3 Casting films from organic solvents

A formulation was prepared (PW5) which used the same base epoxy-g-acrylic polymer as WRB625 i.e. WRB621, an 80:20 epoxy:acrylic copolymer with 5% amino resin cross-linker, but which was dissolved, rather than dispersed, in an organic solvent mixture. The solvents chosen was mixture of n-butanol and 2-butoxy ethanol with sufficient 2-butanone to dissolve the polymer. The film was prepared in the same manner as that of the water-based dispersion. The resultant TEM image produced from this solvent cast formulation, see Figure 9.2(b) is different to that produced from the water-based formulation. The bulk of the film has a darker stain than that of the embedding medium. Rather than circular structures dark spots are observed and some possibly clustering. On the negative, the size of the 500 nm marker is 7.5 mm i.e. a magnification of 15,000. The diameter of the dark spots on the negative are less than 0.5 mm i.e. particle size of less than 33 nm.

A formulation, PW7, which was a blend of epoxy and acrylic resin, was also produced. The acrylic resin used has a monomer feed identical to that used in the grafting process in the epoxy-g-acrylic. The ratio of epoxy to acrylic polymers was 80:20 i.e. similar to WRB621. The polymer was dissolved in the same organic solvents to that used in PW5 i.e. a mixture of n-butanol, 2-butoxy ethanol and butanone. The micrograph did not show any fine structure.

(A)

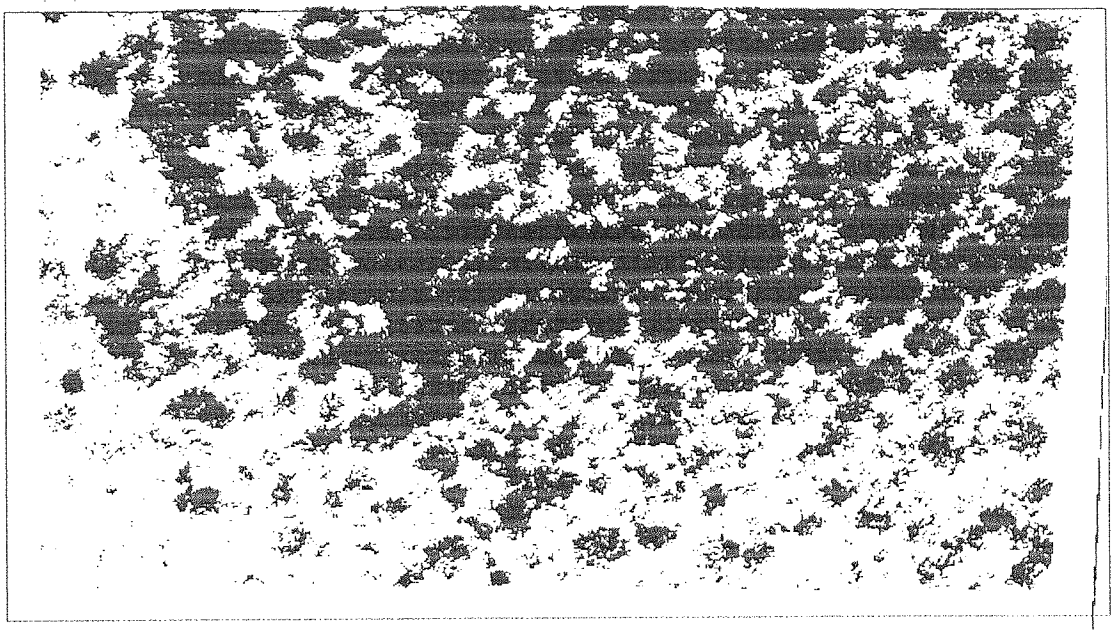

(B)

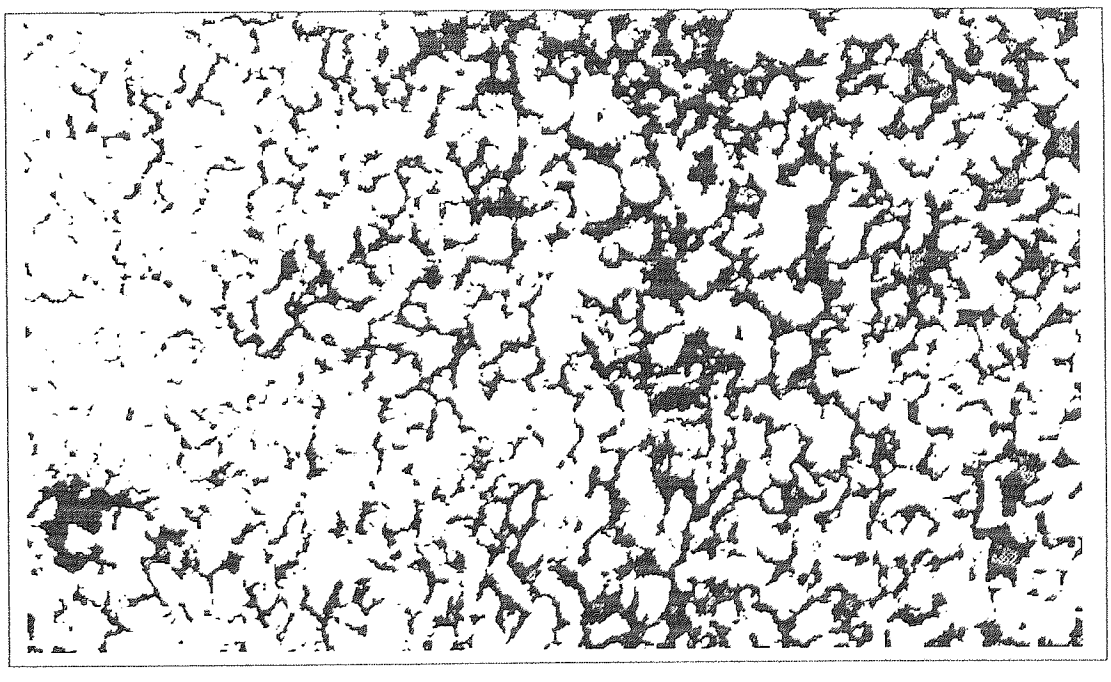

Figure 9.1 (A) TEM of WRB625 stained only with osmium tetroxide. The film produces an effect opposite to that observed in (B) a TEM of WRB625 stained with uranyl acetate.

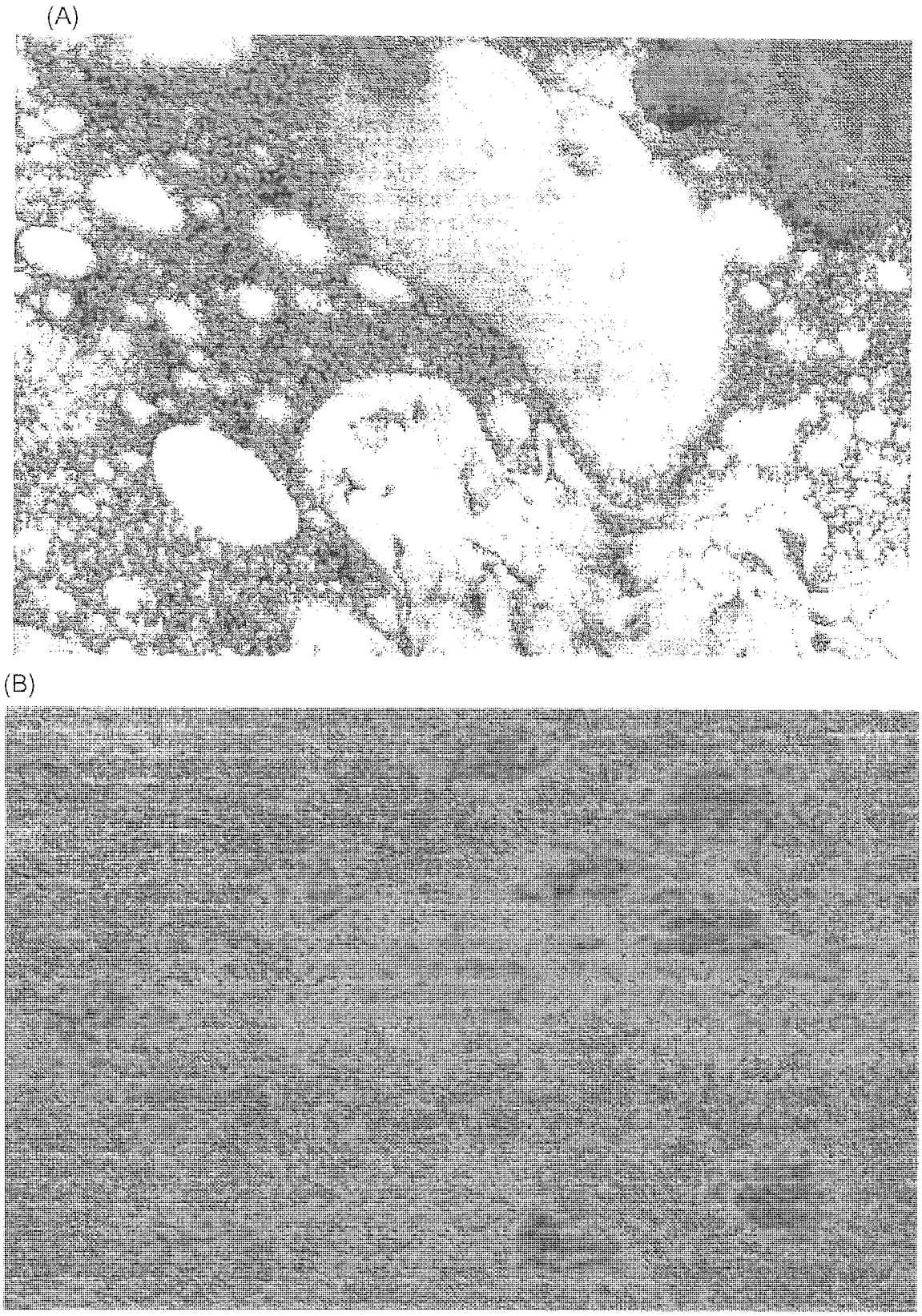

Figure 9.2 (A) TEM of a film produced from WRB626 (90:10 epoxy:acrylic). The micrograph shows large epoxy domains. This formulation produces a brittle film. (B) TEM of the film produced from a formulation similar to that of WRB625 (80:20 epoxy:acrylic) but is cast from organic solution rather than from a water-based dispersion.

CHAPTER 10. DISCUSSION

10.1 Determination of the degree of grafting

The techniques used to determine the levels of ungrafted epoxy resin, in the epoxy-graft-acrylic polymers, were: Soxhlet extractions using toluene and toluene/ 2-butanone blends, a liquid-liquid extraction procedure and by using a GPC technique which uses DMF as the mobile phase. See Chapter 5.3 for details of the extraction procedures and Chapter 5.5.7 for the GPC analysis. The levels of ungrafted epoxy in the epoxy-g-acrylic polymers and the level of extractable epoxy in the initial epoxy resins, determined using the techniques mentioned above, are shown in Table 10.1.

Table 10.1 Levels of Extractable Epoxy present in Samples determined using Soxhlet Extractions, Liquid-Liquid Extractions and by GPC

sample	level of extractable and ungrafted epoxy (%)			
	toluene Soxhlet	toluene/butan-2-one Soxhlet	liquid-liquid extraction	DMF GPC
Epikote 1007	99.9	99.9	99.9	99.7
DOW XZ86762	89.9	99.3	99.8	97.1
DER669	90.6	99.5	99.8	98.9
DLER100	91.1	99.1	99.3	96.5
WRB621	69.4	81.8	81.1	75.1
WRB622	47.5	58.3	55.5	60.5
WRB623	78.3	92.6	88.1	83.1

The results given in Table 10.1 suggest that the toluene Soxhlet extractions are giving lower than actual values for the level of ungrafted epoxy in the epoxy-g-acrylic polymers. This can be inferred from the results from the extraction of the '9' type epoxy resins, DLER100, DER669 and DOW XZ86762. The DLER100 is the base epoxy resin used to prepare all of the graft polymers. These '9' type epoxy resins have higher molecular

weight distributions than the '7' type Epikote 1007. The toluene Soxhlet is only dissolving approximately 90% of these polymers. Refer to Chapter 3.1 for details of epoxy resin nomenclature.

The molecular weight distribution of all epoxy and epoxy-g-acrylic polymers are shown in Table 10.3. Molecular weight distribution analyses were carried out on the original DLER100 base epoxy resin and the toluene Soxhlet soluble and insoluble portions. The MWD values, as determined using GPC, are shown in Table 10.2.

Table 10.2 MWD Results from the Toluene Soxhlet Extraction of DLER100

sample	Mn	Mw	Mz
initial	7510	21400	43900
solubles	3450	12500	24300
insolubles	51700	66700	85000

The Mn, Mw, and Mz values of the toluene Soxhlet soluble portion are significantly lower than those of the original DLER100 epoxy polymer. This indicates that the toluene Soxhlet is only extracting low molecular weight epoxy polymer from this '9' type epoxy resin. The molecular weight distribution i.e. Mw and Mz values, of this soluble portion is also higher than that of the '7' type epoxy resin Epikote 1007. The toluene Soxhlet would therefore be expected to dissolve the Epikote 1007 completely. It can be seen from Table 10.1 that the toluene Soxhlet is extracting 99.9% of the Epikote 1007 sample.

The Mw and Mz values for DER669 are only slightly lower than those values for DLER100. This would suggest that the DER669 would also not be extracted completely into toluene. Woo [5] determined that DER669 was completely extracted into a toluene

Soxhlet. It is apparent however that the batch of DER669 used by Woo was significantly lower in molecular weight than the batch used in this determination. The MWD distribution of the DER669 used by Woo was: Mn 1610, Mw 8050 and Mz 25200. The Mn and Mw values are lower than that of Epikote 1007 and therefore it is likely that a sample of DER669 with such a molecular weight distribution would be completely dissolved by a toluene Soxhlet.

Table 10.3 Molecular Weight Distribution Results from GPC Data

sample	Mn	Mw	Mz	D
DLER100	7510	21400	43900	2.9
WRB621	7570	23100	53900	3.1
WRB622	7510	23300	55800	3.1
WRB623	7530	22600	50700	3.1
Epikote 1007	3720	8770	15200	2.4
DER669	5720	18100	40900	3.2
DOW XZ86762	5640	17800	37400	3.2

Examination of the results for the determination of ungrafted epoxy resin given in Table 10.1 indicates that the toluene/ 2-butanone Soxhlet extractions are giving similar results to the liquid-liquid extraction. The largest discrepancy between the techniques is for the epoxy-g-acrylic sample WRB623. This formulation has an epoxy to acrylic ratio of 90:10. The toluene/ 2-butanone Soxhlet is extracting 92.6% of the epoxy present whilst the liquid-liquid extraction procedure is extracting 88.1% of the epoxy resin present. For all epoxy-graft-acrylic samples the liquid-liquid extraction process is extracting less epoxy resin than the Soxhlet process. The liquid-liquid extraction process involved two extractions from the sample. It is possible that, by increasing the number of liquid-liquid extractions per sample, the amount of extracted epoxy would increase to give a similar

results to the Soxhlet extraction process. Molecular weight distribution analysis, using GPC, was carried out on the soluble portion from the liquid-liquid extractions of the base polymer DLER100 and the epoxy-g-acrylic WRB621. The results are shown in Table 10.4.

Table 10.4 MWD Analysis of Samples Extracted using the Liquid-Liquid Extraction Procedure

sample	Mn	Mw	Mz
DLER100	7510	21400	43900
DLER100 organic layer	7430	20300	42500
WRB621	7570	23100	53900
WRB621 organic layer	5580	17600	39000

The MWD values obtained for the soluble portion of the base epoxy resin DLER100 are similar to those of the original sample. This gives confidence in interpreting the data for the epoxy-g-acrylic sample WRB621. The MWD values for the soluble portion of this sample are significantly lower than those of the epoxy resin used to prepare the graft polymer. This suggests that the acrylic is preferentially grafting onto high molecular weight epoxy polymer rendering it non-extractable into the organic phase. The GPC profiles of DLER100 and the liquid-liquid extract, shown in Figure 10.2(d), support these observations.

The levels of ungrafted epoxy, shown in Table 10.1, determined by GPC using DMF as the mobile phase, are slightly different to those values obtained using the Soxhlet and liquid-liquid extraction techniques. The difference in values between the techniques is approximately 5%. For the 80:20 and 90:10 epoxy to acrylic formulations, WRB621 and WRB623 respectively, the GPC technique is giving 5% lower levels of ungrafted epoxy.

For the 60:40 epoxy to acrylic formulation, WRB622, the GPC technique is giving a 5% higher level.

Examination of the GPC profile of DLER100 indicates the presence of a small early eluting peak. Figure 10.2(a) shows the GPC profiles of both base epoxy resin, DLER100, and the 80:20 composition graft polymer, WRB621, prepared from it. For the epoxy resin the early eluting peak has an area of approximately 3% of the total peak area. This peak may be due to either very high molecular weight material or partially cross-linked material. The major peak has a profile very similar to that of the GPC analyses carried out in THF. The GPC profile of the WRB621 sample has a significantly higher initial peak i.e. approximately 25% of the peak area. This peak is thought to contain all of the epoxy resin that has acrylic acid groups grafted onto it. The remainder is ungrafted epoxy resin. All of the profiles were obtained using a UV detector monitoring at 280 nm. At this wavelength the acrylic and styrene polymer components do not give a response on the detector. The level of ungrafted epoxy is taken to be the area of the second peak expressed as a percentage of the total. The detector responses at this wavelength, for the grafted and the ungrafted epoxy components, are assumed to be equal to one another.

10.2 Selective grafting onto high molecular weight epoxy resin

A number of techniques were used to confirm the suggestion by Woo [5] that grafting is taking place preferentially onto higher molecular weight epoxy resin. Two of the techniques involved selective detection and deconvolution of GPC profiles. For details of deconvolution of chromatograms refer to Chapter 5.5. One technique involved a GPC analysis where the mode of separation appeared not to be size exclusion. The other two techniques involved GPC analysis of polymer fractions separated using centrifugation of the latex and liquid- liquid extraction of the polymer.

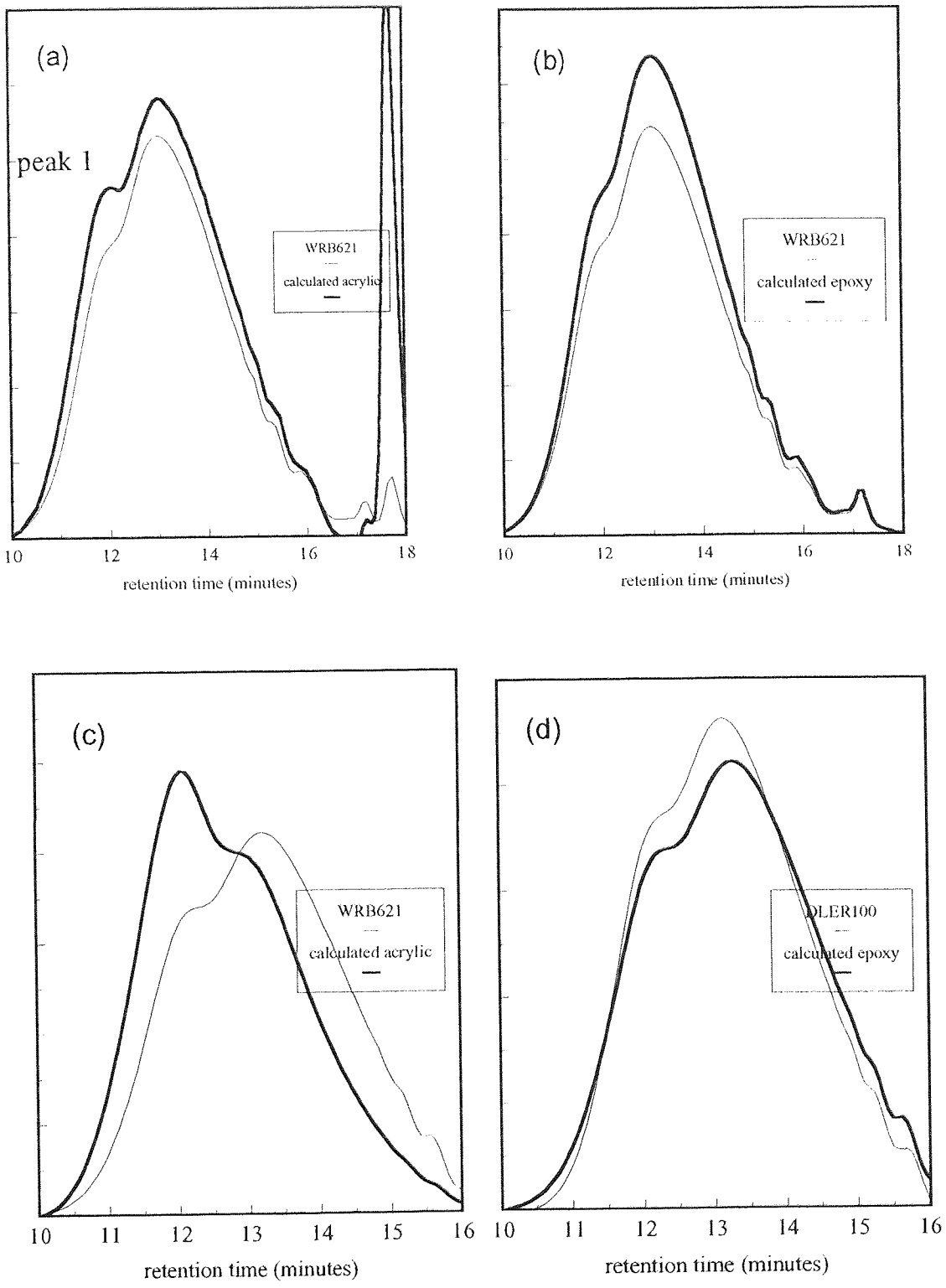

Figure 10.1 GPC profiles of WRB621 at 254 nm (a) super-imposed onto deconvoluted acrylic component, (b) super-imposed onto the deconvoluted epoxy component, (c) derivatised sample at 254 nm super-imposed onto acrylic component and (d) super-imposed onto deconvoluted epoxy component.

10.2.1 Selective detection and deconvolution of profiles

The two techniques used involved analysis of the samples using GPC with selective detection of the various polymeric components. This was followed by deconvolution of the profiles using the equations given in Chapter 5.5.1. The technique initially involves determining the response of each individual component of the sample on a number of detectors e.g. UV monitoring at 254 nm, UV monitoring at 280 nm and using a refractometer. This is followed by analysis of the sample and applying the equations to each data point collected. Using this approach, a point by point composition of the copolymer can be calculated. The second of the techniques involved prior derivatization of the acrylic acid component with NBDI (o-[p-nitrobenzyl]-N,N' [di-isopropyl] isourea) followed by a similar analysis using GPC.

The first of these techniques gave interesting but the least convincing results. Figure 10.1(a) shows the GPC profile of the epoxy-g-acrylic polymer WRB621 recorded under the conditions given in Chapter 4.4.2. Superimposed on the chromatogram is the calculated deconvoluted profile of the acrylic component. It is observed that there is a slight increase of the peak labelled 'peak 1' in the deconvoluted profile. This increase in the size of the peak is thought to be due to an increased concentration of acrylic component at the molecular weight corresponding to that elution time. If grafting is preferentially taking place on the high molecular weight portion of the epoxy, then the calculated epoxy component profile should indicate that it is lower molecular weight than the initial epoxy resin. Examination of Figure 10.1(b), which shows the deconvoluted epoxy profile from WRB621 super-imposed upon the DLER100 profile, shows the profiles to be similar. Therefore the technique described, when applied directly to the samples, is not sensitive enough to detect changes in composition of these type of materials.

If a similar analysis is carried out using samples which have been derivatized with NBDI, the deconvolution technique shows that the acrylic portion has a higher molecular

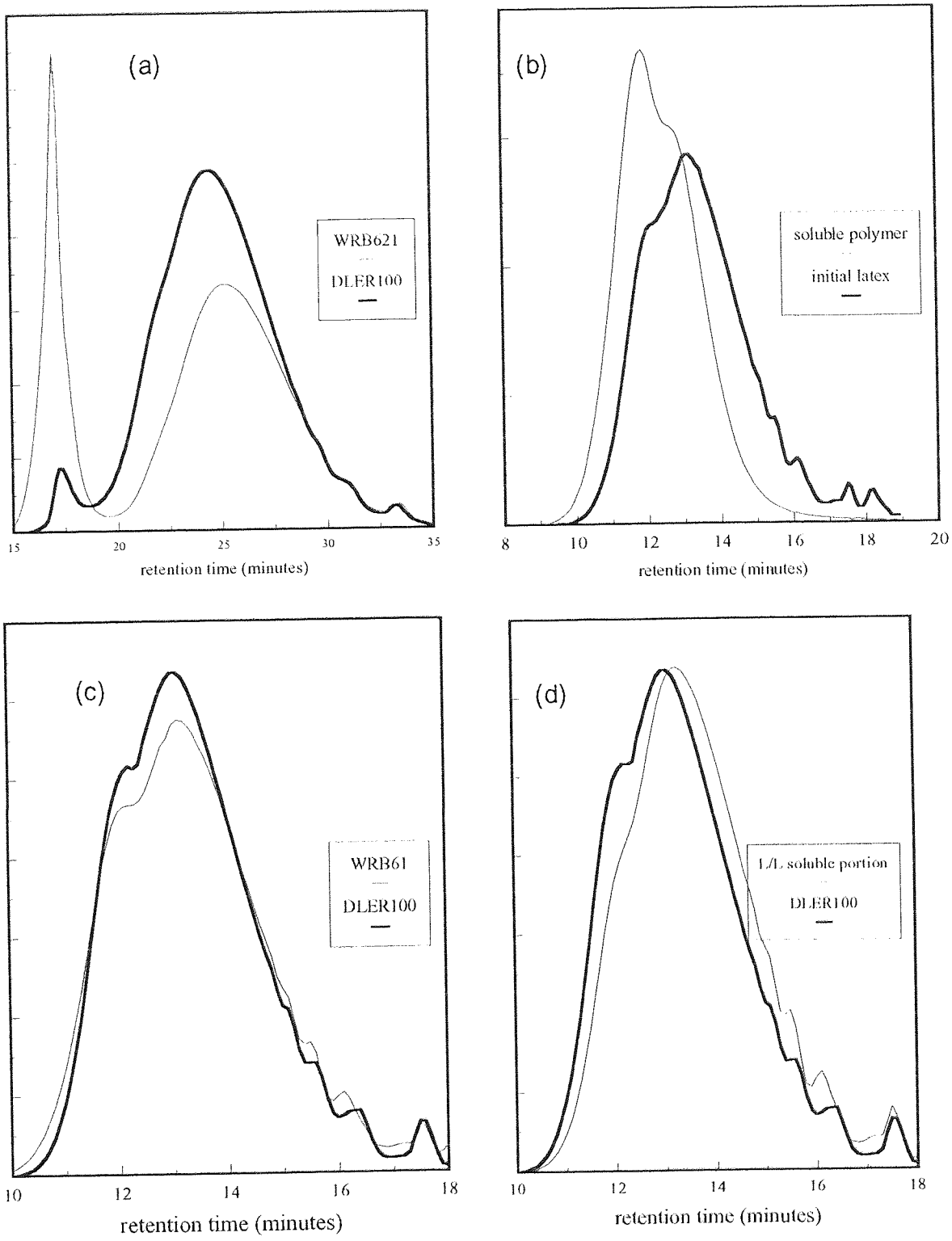

Figure 10.2 GPC profiles of (a) WRB621 and DLER100 using DMF as the mobile phase, (b) WRB625 latex with the soluble polymer obtained by centrifuging. DLER100 base epoxy resin with (c) WRB621 epoxy-graft- acrylic polymer and (d) THF solubles from the liquid-liquid extraction of WRB621

weight than the initial sample and that the epoxy portion has a lower molecular weight than the initial base-resin DLER100. Figure 10.1(c) shows the deconvoluted profile of the acrylic component super-imposed upon the initial epoxy-g-acrylic WRB621 profile. The deconvoluted profile has a shorter elution time and therefore has a higher molecular weight. Figure 10.1(d) shows a corresponding decrease in the molecular weight of the epoxy component compared to the original epoxy resin.

10.2.2 Non-size exclusion GPC separation

When dimethyl formamide is used as the eluent, in place of tetrahydrofuran, differences in the GPC profiles of both epoxy resin and epoxy-g-acrylic samples are observed. This difference appears as an early eluting peak, which is observed when DMF is used as the mobile phase but not when THF is used. For the epoxy resins the area of this peak, as a percentage of the total area, varies approximately between 0 and 3%. For the graft polymers the area of the initial peak depends upon the sample. The higher the graft level the greater the area of the peak. The area, as a percentage of the total, approximately corresponds to the values of grafted epoxy determined using solvent extraction techniques. This can be seen in Chapter 5.3. Since the profiles were obtained using the UV detector monitoring at 280 nm, a wavelength where the acrylic component does not respond, the GPC profile of the second peak, see Figure 10.2(a), is therefore due to epoxy only. This peak can be seen to elute significantly later from the column than the initial base epoxy resin and therefore has a lower molecular weight.

10.2.3 Solvent extraction

(a) Liquid-Liquid Extraction

The liquid-liquid extraction procedure, detailed in Chapter 5.3.2, involved extracting the acrylic containing components out of THF solution into a high pH aqueous

phase. The technique was applied to the graft polymers and a range of epoxy resins to ensure that preferential extraction did not occur. Figure 10.2(c) shows GPC profiles of the base epoxy resin DLER100 and the 80:20 epoxy-g-acrylic polymer WRB621. Figure 10.2(d) shows the GPC profile of the THF soluble portion and the profile of DLER100. The THF soluble portion elutes later from the column and is therefore lower molecular weight material.

(b) Centrifugation

The aqueous-soluble portion of the latex WRB625 was isolated by initially diluting the latex in water and then centrifuging the sample at 15,000 rpm for 30 minutes. Details of the procedure can be found in Chapter 6.5. IR spectra of the separated portions indicated that the aqueous soluble polymer contained a higher level of acrylic than the initial sample. See Chapter 7.5.2. GPC profiles of the soluble layer and the initial latex were recorded and are shown in Figure 10.2(b). The chromatograms were obtained using a UV detector monitoring at 280 nm, a wavelength where only the epoxy component will produce a response. The GPC profile of the aqueous soluble portion must therefore be due to grafted epoxy resin. The polymer elutes earlier from the GPC column than the initial latex and is therefore higher in molecular weight.

10.3 Particle Size Data

The size of the particles present in each latex were measured using transmission electron microscopy (TEM) and by using dynamic light scattering (DLS). Micrographs of the latices were obtained after initially diluting the latex samples in water and then drying the samples in an oven. The micrographs obtained are shown in Figures 7.3 (a) to (d). Particle sizes of the epoxy domains in the applied films of the latices were also measured using TEM. The sample preparation details are given in Chapter 8 and the micrographs are

shown in Chapter 9. The diameters of the particles were determined by measuring the particles on each micrograph divided by the magnification factor. The results from transmission electron microscopy and dynamic light scattering, are summarised in Table 10.5, where: D_n is the number-average particle diameter and D_w is the weight-average particle diameter both in units of nanometers (nm).

Table 10.5 Particle Diameters of Initial Latex Samples

sample	TEM (latex particles)		TEM (film) (nm)	DLS (nm)
	D_n (nm)	D_w (nm)		
WRB633	42.3	60.2	30-55	130
WRB624	38.5	53.2	30-55	390
WRB625	43.5	128.5	40-90	350
WRB626	31.6	156.7	-	220

The samples WRB633 and WRB624 have an identical polymer composition i.e. 60:40 epoxy to acrylic. The only difference is that the acrylic portion of WRB624 has been 70% neutralised with DMAE whereas WRB633 has been neutralised to 35%. The particle size data, using TEM, are similar for these two samples. The size of the epoxy domains in the applied films are also similar. However, the particle diameters from the DLS experiments for these two samples are significantly different. The measured particle size of WRB633 at 130 nm is the lowest value of the four latex samples whereas for WRB624 the measured particle size is highest at 390 nm. It is suggested that the TEM data represents the size of the epoxy core of the particle whereas the DLS determinations represent the hydrodynamic diameter. The diameter of this epoxy core appears only to depend upon the polymer composition and not the degree of neutralisation.

For silica based latices Killman et al [155] and Polverari [156] obtained good agreement between TEM and DLS data. However, in both cases, the size distribution of the latex particles were very narrow. Examination of the micrographs of the particles of WRB625 and WRB626 (80:20 and 90:10 epoxy to acrylic respectively) reveal a distribution of sizes. This is reflected in the weight-average diameters, shown in Table 10.5, which are between three and five times higher than the number-average diameters. The micrograph of the WRB626 particles, compared to WRB625, show a broader distribution of sizes i.e. a small number of large particles and a large number of small particles. This is reflected in a lower number-average and a higher weight-average particle diameter value. This can be seen in Figure 7.4 which shows histogram plots of the TEM data. The DLS data however suggests that the WRB625 particles are larger than the WRB626 particles.

The micrographs of the applied films of WRB624, WRB625 and WRB633 all show a narrow distribution of particle sizes. The applied film of WRB626 shows some very large epoxy structures. In fact this latex forms a very poor film with little strength. When the film is lifted off the substrate using mercury, see Chapter 8, the film disintegrates into small pieces. The latex also appears to be unstable and shows some settlement after a few weeks. This latex has an acrylic content of 10% which appears to be insufficient to stabilise the micellar structure and allow the formation of a film.

It is known from experiment, refer to Chapter 7.2, that the level of a neutralising amine present in the sample greatly influences the viscosity. To determine the effect of DMAE upon the particle size , the latices WRB624 and WRB633 were further examined after dilution in both water and a 2% aqueous solution of DMAE. The results are shown in Table 10.6. The diluents are shown in brackets in the sample column.

Table 10.6 Particle size data of samples diluted in water and 2% aqueous DMAE

sample	TEM (nm)		DLS (nm)
	D_n	D_w	
WRB624 (water)	36	44	390
WRB624 (DMAE)	33	43	320
WRB633 (water)	42	55	130
WRB633 (DMAE)	37	48	230

The results confirm the initial findings that the particle size, as measured using TEM, is unaffected by the presence of the DMAE. Using DLS, the particle size of WRB624 (60:40 epoxy to acrylic, 70% neutralised) appears to decrease slightly in the presence of DMAE. Whereas the particle size of WRB633 (60:40 epoxy to acrylic, 35% neutralised) significantly increases in the presence of DMAE.

The decrease in particle size of WRB624, from 390 nm to 320 nm, is due to the increased viscosity of the medium. For a given diffusion coefficient, as the viscosity of the medium increases the measured particle size will decrease (Stoke-Einstein equation [151]). The viscosity of water and 2% DMAE solution, measured as a flow time through the viscometer, were 78.3 seconds and 84.5 seconds respectively. A 10% solution, by weight, of sodium chloride in water had a similar viscosity to that of the DMAE solution. The flow time of this solution was 85.9 seconds. The particle size of the WRB624 sample measured in the sodium chloride solution was 330 nm i.e virtually identical to that obtained in a solution, of similar viscosity, of DMAE.

To study the effect of DMAE on the particle diameters of WRB633, various amounts of DMAE were added to a dilute solution of the latex in the light-scattering cell. The measured particle sizes are shown in Table 10.7.

Table 10.7 Effect of DMAE concentration upon the particle size of WRB633

moles of DMAE added (μmoles)	Acid/DMAE ratio	particle diameter (nm)
0	0.35	130
0.23	0.64	160
0.45	0.99	180
0.67	1.23	200
0.91	1.52	210
1.12	1.81	210
5.62	7.67	220

A plot of particle size versus DMAE/acid mole ratio is shown in Figure 7.2. The particle size appears to increase as the DMAE/acid ratio is increased to the equivalence point and then remains virtually constant as further DMAE is added. To determine the effect of the addition of a salt, to increase the ionic strength of the medium, upon the particle size of the latex, 1 μmole of sodium chloride was added to the WRB633 latex. The addition of sodium chloride to the latex did not produce any increase in the measured particle size. If acid e.g. dilute hydrochloric acid is added to the latex or is added to the latex to which DMAE has already been added, there is a decrease in the particle size. It is concluded that the changes in measured particle size, induced by the addition of either DMAE or acid, is due to neutralisation of the latex rather than to changes in the ionic strength of the medium.

10.4 Rheology and soluble polymer data

10.4.1. Initial samples

The composition and viscosities of the latices, prepared in Chapter 3.3.2, are shown in Table 10.8. The viscosity of these original formulations have been measured as a flow time through a BSS3 flow cup.

Table 10.8 Latex Composition and Flow-Time Viscosity

sample	epoxy/ acrylic	degree of neutralisation	Flow time (seconds)
WRB624	60:40	70%	225
WRB625	80:20	70%	76
WRB626*	90:10	70%	71
WRB633	60:40	35%	49

* Note: WRB626 was found to be unstable and settled out within two weeks of preparation.

Refering to Table 10.8 it can be sen that for a given acrylic acid content the greater the degree of neutralisation of that acid the higher the viscosity. Also, for a given degree of neutralisation the greater the acrylic acid content the higher the viscosity.

10.4.2 Diluted samples

In order to more accurately ascertain the effect of neutralisation upon viscosity the samples were diluted. Each sample (2 g) was diluted using either water (25 cm^3) or a 2% solution of DMAE in water (25 cm^3). Table 10.9 shows the viscosity of the samples as measured using a suspended level viscometer at 25^{0}C. The polymer content of the aqueous soluble portions, determined by centrifugation (see Chapter 7.5) and expressed as a function of total polymer, are also given in this table.

The flow times of water and 2% aqueous DMAE solution were measured as 78.3 seconds (+/- 0.2 seconds) and 84.4 seconds (+/- 0.2 seconds), respectively.

Table 10.9 Flow-Time Viscosities, expressed as seconds, of Latex and Soluble Portions Diluted in either water or 2% DMAE

sample	Flow-time of diluted sample, in seconds	% soluble polymer
WRB624 (aq.)	199	56.6
WRB624 (DMAE)	232	63.1
WRB625 (aq.)	139	29.8
WRB625 (DMAE)	156	33.1
WRB633 (aq.)	102	54.9
WRB633 (DMAE)	176	62.1
PW1 (aq.)	139	29.2
PW1 (DMAE)	157	30.8
PW2 + (aq.)	138	29.3
PW2 +(DMAE)	156	30.6

To further study the effect of the addition of DMAE to these samples, solutions of WRB625 (80:20 epoxy to acrylic) were prepared by diluting a stock solution of the latex in aqueous DMAE. See Chapter 7.2.2 for full details of the sample preparation.

Table 10.10 shows the mole ratio of DMAE to acrylic acid, the viscosity of the samples measured as flow times through the suspended-level viscometer and amounts of water-soluble polymer determined using centrifugation.

Table 10.10 Flow-Time Viscosity and Soluble Polymer Determinations as a function of Degree of Neutralisation

sample number	mole ratio DMAE/acid	corrected flow time (seconds)	% soluble polymer
WRB625 (1)	0.71	139.2	29.8
WRB625 (2)	1.08	151.1	31.1
WRB625 (3)	1.64	150.8	31.4
WRB625 (4)	2.57	150.5	31.4
WRB625 (5)	4.45	150.1	31.4
WRB625 (6)	6.32	149.3	31.5
WRB625 (7)	10.06	150.2	31.4

Table 10.10 shows that as the amount of DMAE added to the sample is increased up to the equivalence point, there is an increase in the viscosity of that sample and an increase in the level of soluble polymer. If further DMAE is added no further change to the viscosity or level of soluble polymer occurs.

Tthe viscosity of the latex, however, cannot solely depend upon the level of soluble polymer. Some other parameter must be at work. When diluted in water, WRB633 (60:40 epoxy to acrylic) has a lower flow time viscosity than WRB625 (80:20 epoxy to acrylic), i.e. 102 and 139 seconds respectively, but WRB633 has a higher level of soluble polymer i.e 54.9% and 29.8% respectively. The viscosity may also depend upon the charge density on the micelle e.g. the higher the charge density from a higher acid content, the higher the viscosity for a given degree of neutralisation.

For a given polymer composition, the amount of soluble polymer remains approximately constant with varying degrees of neutralisation, however the viscosity changes significantly. e.g. WRB624 is a 60:40 epoxy:acrylic formulation with 70% of the acid functionality neutralised with DMAE. It has a viscosity of 199 seconds and the amount of soluble polymer is 56.6%. WRB633 also is 60:40 epoxy:acrylic with 35% acid functionality neutralised. It has a much lower viscosity (102 seconds) but only a slightly lower soluble polymer content (54.9%) than that found for WRB624.

10.5 Latex stability and film morphology

Latices with compositions having epoxy to acrylic ratios of 60:40 and 80:20 appear to be very stable. Even after 12 months of storage following their preparation the viscosity of these formulations are virtually unchanged and there are no signs of a settlement layer. These formulations also produce coherent films with a regular fine structure as shown when examined using transmission electron microscopy. A micrograph of the film produced from WRB625 is shown in Figure 9.1. The latex with the

composition 90:10 epoxy to acrylic was not stable and produced a settlement layer after a number of weeks. This formulation did not produce a coherent film and when examined, using TEM, the film showed some fine structure, similar to that observed with the other formulations, but was dominated by large epoxy domains. See Figure 9.2(a). In the 90:10 formulation it would appear that there is insufficient acrylic to stabilise the micellar structure of the latex. It would therefore appear that to stabilise the latex and film morphology a minimum acrylic content of around 20% is required.

For the stable latices the close agreement between particle size determinations carried out on the latex and the domains observed in the film suggests that the micelles present in the latex are surviving through to and beyond film formation. This seems to be the case even though during stoving the temperatures experienced by the system are at least 100^{0}C above the melting points of the graft polymers.

When there is no micellar-type structure in the liquid sample e.g. a polymer dissolved in organic solvents, the micellar type morphology does not form during film formation although some phase separation does occur. This can be observed in the micrograph shown in Figure 9.2(b). The cast film used in the preparation of this micrograph was produced by initially dissolving formulation PW1 in tetrahydrofuran. The film was then produced by flood-spinning in a similar manner to that employed in the preparation of films produced from the aqueous samples. Details are given in Chapter 8. The film produced was coherent and was similar, in visual appearance, to the films produced from the aqueous samples

The references quoted concerning film formation (Chapter 2.4.2) suggest that particles must coalesce to form coherent films. The films examined here were cast from dispersions, show structure in the films and appear to be just as rigid as amorphous films formed from solvent based formulations.

11.1.1 Latex structure

Transmission electron micrographs, of both the latices and the films produced from those latices, indicate that the latex particles are spherical in shape. There is no evidence to support the idea that vesicle structures are present. The micrographs obtained show that the latex particles survive through to film formation and beyond. When present, vesicle structures can clearly be observed using TEM [216,217]

There is evidence to support the idea that the structure of the latex particles comprises of an epoxy core surrounded by an acrylic polymer. It was found that the hydrodynamic particle diameters, measured using dynamic light scattering, were always larger than values obtained for the particle core, measured using TEM. It is concluded that TEM gives a measure of the diameter of the epoxy core. Comparison of particle diameters obtained from DLS and TEM have been used to determine the hydrodynamic thickness layer (HLT) [156]. However, the particles used had a relatively narrow distribution. In this present study it is evident that the latex particles have a distribution of sizes making an accurate assessment of the HLT difficult.

There is also evidence that the latex is being stabilised by added amine (DMAE) by partial neutralising of the acid functional polymer attached to the epoxy core. Changes in ionic strength, by the addition of sodium chloride, have no effect upon the particle diameter. Addition of extra amine, further neutralising the acid functional polymer, increases the hydrodynamic particle diameter and has little effect upon the diameter of the epoxy core. As amine is added to the neutral point there is an increase in the level of soluble polymer, particle size, and viscosity, as measured through a suspended level viscometer. Beyond the neutral point no further changes are observed. The increase in

soluble polymer and interaction between the particles are both thought to contribute to the increase in viscosity. NMR spectra of the latices confirm that the acid functional polymer is being neutralised by the amine (DMAE). Addition of acid to the latex, neutralising the existing amine, reduces the hydrodynamic diameter.

11.1.2 Latex structure: Further studies

Further studies using light scattering should be carried out. Use of other algorithms e.g. CONTIN and DISCRETE [151] to determine particle size distributions. Measure actual intensities of scattered light using the static light scattering mode of the DLS700. Changes in particle diameter should correlate with changes in scattering intensity [216]. The data from the light scattering experiments should be compared with that obtained from TEM when producing modified latexes to obtain accurate data for the hydrodynamic layer thickness.

Use NMR to gain further information regarding the structure of the aqueous latex by measuring the diffusion of the various constituent polymeric components.

11.2.1 Polymer grafting studies

Studies carried out using GPC confirmed the suggestion [5] that grafting of acrylic polymer was taking place preferentially upon higher molecular weight epoxy resin.

GPC and solvent extraction studies determined, with some agreement, the level of grafted epoxy resin. The level of grafting was found to be lower than that expected [5]. The level of grafted epoxy resin, in an 80:20 epoxy:acrylic formulation, was determined to be approximately 75%.

There was difficulty in determining the site of grafting upon the epoxy chain and the level of ungrafted acrylic resin.

11.2.2 Polymer grafting: Further Studies

Further studies may involve chemometric analysis [219] of data generated from GPC profiles of polymer sample for example using principal component analysis to determine the number of components present and to calculate the MWD profiles of those components. Further NMR studies may involve identification of the location of the acrylic grafting site on the epoxy resin backbone.

Further solvent extraction techniques could be developed to determine the level of ungrafted acrylic resin present in the epoxy-graft-acrylic polymer.

APPENDICES

Appendix 1 NMR coupling constants for epoxy resins

Epikote 828 is a low molecular weight epoxy resin and its chemical structure is shown in Figure A1. The different types of proton are labelled 'a' through to 'h'.

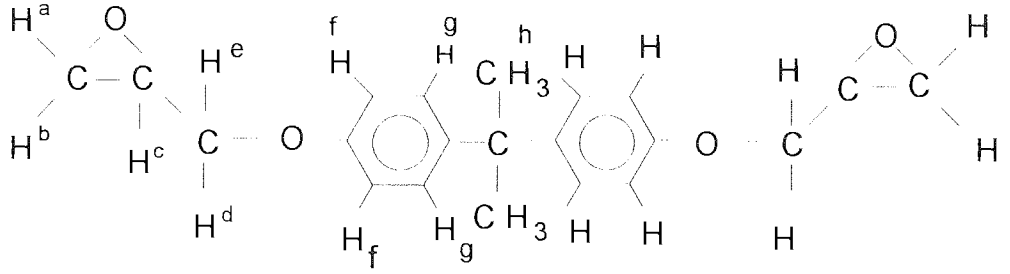

Figure A1 The structure of the epoxy resin Epikote 828 with the protons labelled for assignment of peaks in the proton NMR spectrum.

A proton NMR spectrum of the epoxy resin Epikote 828, dissolved in $CDCl_3$, is shown in Figure A2. The peak assignments are shown in Table A1. The chemical shift, in ppm, are relative to tetramethyl silane (TMS).

Table A1 Proton NMR Peak Assignments for the Epoxy Resin Epikote 828

chemical shift (ppm)	multiplicity	measured coupling constants (Hz)	integral	assignment (Figure 11.1)
1.6	singlet	none	3	methyl (h)
2.7	singlet, some structue	not measureable	1	methine (e)
2.9	singlet, some structue	not measureable	1	methine (d)
3.3	broad singlet	not measureable	1	methine (c)
3.9	doublet of doublets	(a) 12 and (b) 6	1	methine (a)
4.1	doublet of doublets	(a) 12 and (b) 3	1	methine (b)
6.8	doublet	10	2	aromatic (f)
7.1	doublet	10	2	aromatic (g)

A1.1 Discussion of Proton assignments

The spin-spin coupling values were measured from the spectrum. The interpretation of the spectra is as follows:

Spin-Spin coupling: Proton designated 'a'

The methine proton designated 'a' will split into a doublet of doublets with coupling constants equal to 12 Hz and 6 Hz due to the presence of protons 'b' and 'c' respectively.

Spin-Spin coupling: Proton designated 'b'

The methine proton designated 'b' will split into a doublet of doublets with coupling constants equal to 12 Hz and 3 Hz due to the presence of protons 'a' and 'c' respectively.

Spin-Spin coupling: Proton designated 'c'

The methine proton designated 'c' should show multiple splitting due to protons designated 'a', 'b', 'd' and 'e'. The fine structure of the splitting is not observed in the spectra.

Spin-Spin coupling: Proton designated 'd'

The methine proton signal designated 'd' should show a doublet of doublets due to the presence of protons 'e' and 'c'. There is only a hint of this splitting in the spectrum.

Spin-Spin coupling: Proton designated 'e'

The methine proton signal designated 'e' should show a doublet of doublets due to the presence of protons 'd' and 'c'. There is only a hint of this splitting in the spectrum.

Spin-Spin coupling: Aromatic Protons

Each of the aromatic protons is split into a doublet with a coupling constant of 12 Hz.

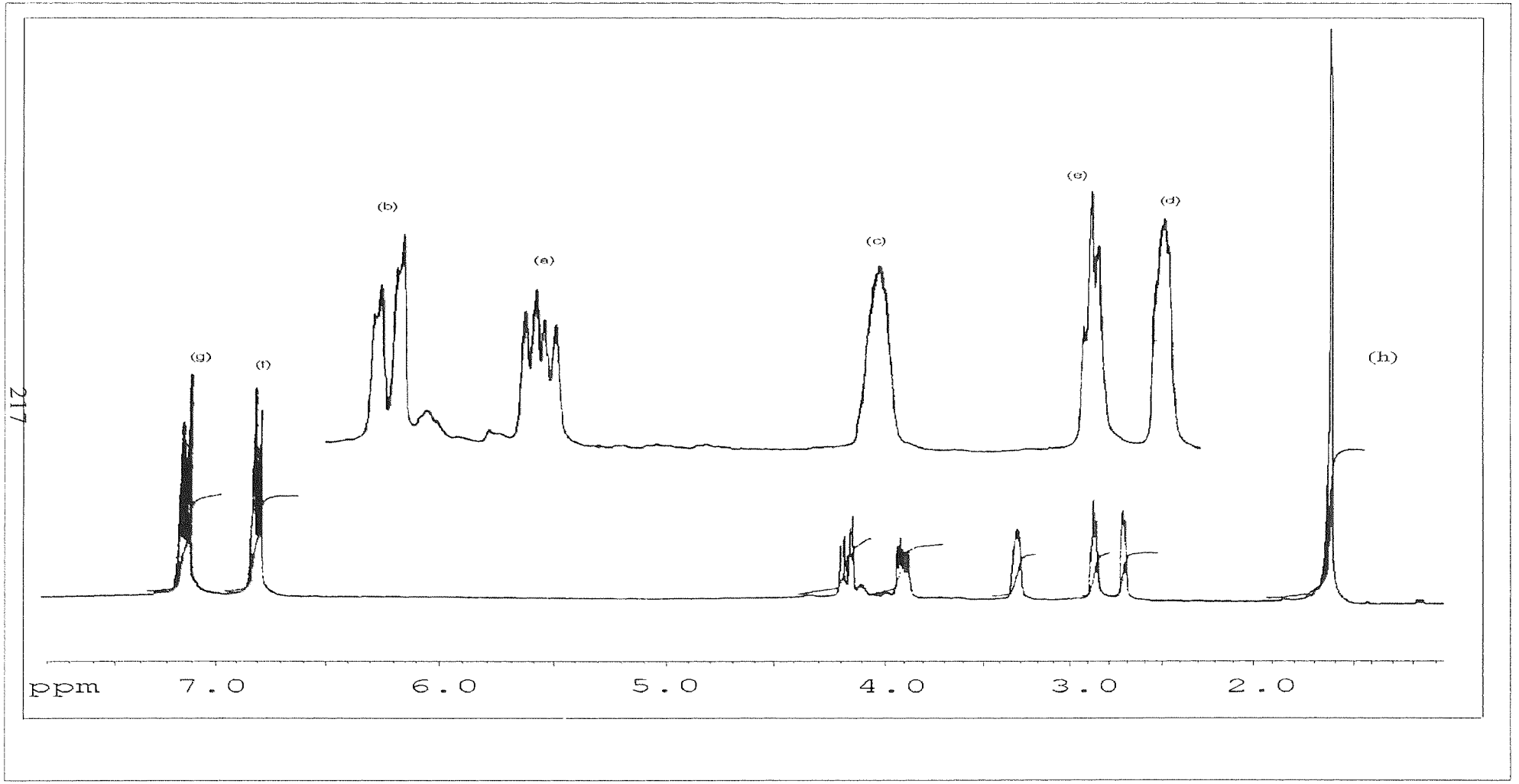

Figure A2 Proton NMR spectrum of Epikote 828

Appendix 2 Calculation of chemical shifts in substituted benzenes

The chemical structure of the repeat unit of an epoxy resin is shown in Table A3. For further information regarding the structure of epoxy resins, see Table 4.1. The same numbering system of carbon atoms is used to that used in Chapter 5.2.2 thus the aromatic carbon atoms are labelled '3' to '6'. Using the Wehrli and Wirthlin method [211] chemical shifts for the aromatic carbon atoms can be calculated. These calculated values will be compared to observed chemical shifts.

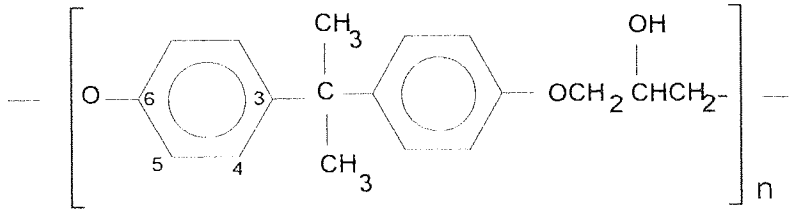

Figure A3 Chemical structure for the repeat unit of an epoxy resin.

The chemical groups closest in structure to the ether linkage and the dimethyl carbon structure quoted in the above literature were -C(CH_3) and -O(CH_3). Table A2 shows the magnitude in the change of chemical shift from the set initial value of 128.5 ppm.

Table A2 Effects of substitution on the chemical shifts for aromatic carbon atoms

R	C-1	ortho	meta	para
H	0.0	0.0	0.0	0.0
C(CH_3)	+22.4	- 3.1	-0.1	-2.9
O(CH_3)	+31.4	-14.1	1.0	-7.7

To calculate the chemical shift for the aromatic carbon atom labelled number 3, a value of 22.4 is added to the initial chemical shift value of 128.5 ppm. Hydrogen atoms ortho and meta to this carbon have no effect. A value of 7.7 is then subtracted from the total due to

the presence of the para- $O(CH_3)_3$ group. This gives a calculated chemical shift for the carbon atom labelled number 3 equal to 142.9 ppm. The observed chemical shift value is 132.2 ppm. Table A3 shows the calculated and observed chemical shifts for all the aromatic carbon atoms.

Table A3 Calculated and Observed Carbon-13 Chemical Shifts for the Aromatic Carbon Atoms in an Epoxy Resin

Carbon number	Effect of $-C(CH_3)_3$	Effect of $-OCH_3$	Total Effect	calculated ppm	observed ppm
3	+22.4	- 7.7	-14.4	142.9	143.2
4	- 3.1	+ 1.0	- 2.1	126.4	127.3
5	- 0.1	-14.4	-14.5	114.1	113.5
6	- 2.9	+31.4	+28.5	157.1	155.8

It can be seen from Table A3 that the observed chemical shifts of the aromatic carbon atoms are similar to the calculated values. The largest difference between the calculated and observed chemical shifts of 1.3 ppm is for the carbon atom labelled '6'.

Appendix 3 Matrix algebra operations on data

Matrices are used in this thesis to solve simultaneous equations generated from (a) GPC copolymer analysis, see Chapter 5.5.4, 5.5.5 and Appendix 6 and (b) curve fitting in both GPC MWD calibrations, see Chapter 5.4.2 and cumulant analysis in DLS experiments, see Appendix 8.

A3.1 Multiplication

$$\text{If } A = \begin{bmatrix} 3 & -1 & 2 \\ 0 & 4 & 1 \end{bmatrix} \quad \text{and} \quad B = \begin{bmatrix} 2 & 0 \\ 4 & 3 \\ 1 & -1 \end{bmatrix} \tag{A1}$$

$$\text{then } AB = \begin{matrix} a \\ b \end{matrix} \begin{bmatrix} 3 & -1 & 1 \\ 0 & 4 & 1 \end{bmatrix} \begin{bmatrix} c & d \\ 2 & 0 \\ 4 & 3 \\ 1 & -1 \end{bmatrix} = \begin{bmatrix} \Sigma ac & \Sigma ad \\ \Sigma bc & \Sigma bd \end{bmatrix} \tag{A2}$$

$$\text{but } BA = \begin{matrix} a \\ b \\ c \end{matrix} \begin{bmatrix} 2 & 0 \\ 4 & 3 \\ 1 & -1 \end{bmatrix} \begin{bmatrix} d & e & f \\ 3 & -1 & 2 \\ 0 & 4 & 1 \end{bmatrix} = \begin{bmatrix} \Sigma ad & \Sigma ae & \Sigma af \\ \Sigma bd & \Sigma be & \Sigma bf \\ \Sigma cd & \Sigma ce & \Sigma cf \end{bmatrix} \tag{A3}$$

i.e. the product has the same number of rows as the first matrix and the same number of columns as the second. For multiplication to be possible the first matrix must have the same number of columns as the second matrix has rows.

A3.2 Definitions

If M is equal to the following matrix:

$$M = \begin{bmatrix} a & b & c \\ d & e & f \\ g & h & i \end{bmatrix} \tag{A4}$$

then, M^t is the transposed matrix i.e.:

$$M^t = \begin{bmatrix} a & d & g \\ b & e & h \\ c & f & i \end{bmatrix} \qquad (A5)$$

and M^* is the adjoint matrix

$$M^* = \begin{bmatrix} A & -D & G \\ -B & E & -H \\ C & -F & I \end{bmatrix} \qquad (A6)$$

i.e. the elements in the transposed matrix have been replaced by cofactors. e.g the cofactor of the matrix element 'a' is 'A' which is calculated (ei)-(hf).

M^{-1} is the inverse matrix which is equal to the adjoint matrix divided by the determinant i.e. $M^*/|M|$, where $|M|$ is the determinant.

The determinant of 2x2 and 3x3 matrices are calculated as shown below.

For a 2x2 matrix , $\begin{bmatrix} a & b \\ c & d \end{bmatrix}$, the determinant is equal to (ad - bc)

For a 3x3 matrix there are two methods of finding the determinant. For the matrix M:

$$M = \begin{bmatrix} a_1 & b_1 & c_1 \\ a_2 & b_2 & c_2 \\ a_3 & b_3 & c_3 \end{bmatrix} \qquad (A7)$$

$$|M| = a_1(b_2c_3-c_2b_3) - b_1(a_2c_3-c_2a_3) + c_1(a_2b_3-b_2a_3) \qquad (A8)$$

also

$$|M| = ((a_2b_2-b_1a_2 \times a_1c_3-c_1a_3)-(a_1c_2-c_1a_2 \times a_1b_3-b_1a_3))/ a_1 \qquad (A9)$$

A3.3 Inversion

(a) 2x2 matrix

$$\text{if } A = \begin{bmatrix} a & b \\ c & d \end{bmatrix} \quad \text{then } A^{-1} = \frac{1}{|A|}\begin{bmatrix} d & -b \\ -c & a \end{bmatrix} \tag{A10}$$

(b) 3x3 matrix

$$\text{Let } A = \begin{bmatrix} a & b & c \\ d & e & f \\ g & h & i \end{bmatrix} \tag{A11}$$

Step 1: Transpose

$$A^t = \begin{bmatrix} a & d & g \\ b & e & h \\ c & f & i \end{bmatrix} \tag{A12}$$

Step 2: Calculate the Adjoint matrix i.e. replace elements with cofactors. The cofactor of element 'a', for example, is (ei-hf).

Step 3: divide by the determinant

A3.4 K matrix approach to multi-component analysis

The area (or response) (A) of a single component material, using a given detector, is equal to the response factor multiplied by its concentration i.e.

$$\mathbf{A} = \mathbf{KC} \tag{A13}$$

Therefore to determine the concentration, the concentration matrix **C** is calculated. The above equation must be rearranged to solve for **C**.

1. For a square **K** matrix $\mathbf{C} = \mathbf{K}^{-1}\mathbf{A}$ (A14)

2. For a non-square **K** matrix $\mathbf{C} = (\mathbf{K}^t\mathbf{K})^{-1}\mathbf{K}^t\mathbf{A}$ (A15)

or $\mathbf{C} = (\mathbf{K}^t\mathbf{K})^{-1}(\mathbf{K}^t\mathbf{A})$ (A16)

or $\mathbf{C} = \mathbf{K}^t(\mathbf{K}\mathbf{K}^t)^{-1}\mathbf{A}$ (but not $= (\mathbf{K}\mathbf{K}^t)^{-1}\mathbf{K}^t\mathbf{A}$) (A17)

For example, if four detectors were used to determine a three component mixture then **K** is a 4x3 matrix. $\mathbf{K}^t$ will therefore be a 3x4 matrix. $\mathbf{K}^t\mathbf{K}$ (and $(\mathbf{K}^t\mathbf{K})^{-1}$) will be 3x3 matrices. $(\mathbf{K}^t\mathbf{K})^{-1}\mathbf{K}^t$ will be a 3x4 matrix. **A** is a 4x1 matrix therefore the solution will be a 3x1 matrix.

A3.5 Over-determination

To minimise the effects of random errors the calculation can be over-determined. For example, if three measurements are made to determine the composition of a two component system[125].

Over determination will be used to calculate the composition of a two component mixture using GPC data from three detectors. For the experimental procedure see Chapter 4.4.2 and Chapter 5.5.2 for the data. The response factors for the epoxy and polystyrene components using the refractometer and UV detection at 254 nm and 280 nm are given in Table A4.

Table A4 Calculated GPC Response Factors for Epoxy and Polystyrene

polymer	response factor		
	UV 280 nm	UV 254 nm	RI
epoxy	663.36	158.85	8.05
polystyrene	4.38	85.64	7.92

The GPC peak areas for the mixture, obtained using the above detector configuration i.e. UV detector monitoring at 254 nm and 280 nm and using the RI detector, are given in Table A5.

Table A5 GPC Peak Area Data for the Epoxy/Polystyrene Mixture

sample	peak area (x 10^6)		
	UV 280 nm	UV 254 nm	RI
mixture	66.177	16.622	0.871

The response (or area) is equal to the response factor multiplied by the concentration or amount. This equation can be expressed in matrix form, where **A** is the column matrix of areas, **K** is the matrix of response factors and **C** is the matrix of analyte concentrations.

$$\mathbf{A} = \mathbf{KC} \tag{A18}$$

$$\begin{bmatrix} 66.18 \\ 16.62 \\ 0.871 \end{bmatrix} = \begin{bmatrix} 663.3 & 4.38 \\ 158.9 & 84.2 \\ 8.05 & 7.92 \end{bmatrix} \begin{bmatrix} C_1 \\ C_2 \end{bmatrix} \tag{A19}$$

To solve for **C**, then:

$$\mathbf{C} = (\mathbf{K}^t\mathbf{K})^{-1}(\mathbf{K}^t\mathbf{A}) \tag{A20}$$

$$\mathbf{K}^t\mathbf{K} = \begin{bmatrix} 663.3 & 158.9 & 8.05 \\ 4.38 & 84.2 & 7.92 \end{bmatrix} \begin{bmatrix} 663.3 & 4.38 \\ 158.9 & 84.2 \\ 8.05 & 7.92 \end{bmatrix} = \begin{bmatrix} 465280.9 & -16348.4 \\ -16348.4 & 7171.6 \end{bmatrix} \tag{A21}$$

$$\mathbf{K}^t\mathbf{A} = \begin{bmatrix} 663.3 & 158.9 & 8.05 \\ 4.38 & 84.2 & 7.93 \end{bmatrix} \begin{bmatrix} 66.18 \\ 16.62 \\ 0.871 \end{bmatrix} = \begin{bmatrix} 46545.1 \\ 1696.2 \end{bmatrix} \tag{A22}$$

$$\mathbf{C} = (\mathbf{K}^t\mathbf{K})^{-1}(\mathbf{K}^t\mathbf{A}) \tag{A23}$$

$$\mathbf{C} = \frac{1}{3.0695 \times 10^9} \begin{bmatrix} 7171.6 & -16348.4 \\ -16348.4 & 465280.9 \end{bmatrix} \begin{bmatrix} 46545.1 \\ 1696.2 \end{bmatrix} \tag{A24}$$

$$\mathbf{C} = \begin{bmatrix} C_1 \\ C_2 \end{bmatrix} = \begin{bmatrix} 0.0997 \\ 0.0092 \end{bmatrix} \tag{A25}$$

This gives a calculated composition of 91.6% epoxy and 8.4% polystyrene. The actual composition was 92.5 epoxy and 7.5% polystyrene.

Appendix 4 Equations used in multicomponent analysis

Calibration i.e. the determination of response factors, can be achieved by the measurement of the response or peak areas, monitored using the required detectors, of either single component standards of known concentration or of mixtures containing all of the components. If the latter approach is used the number of mixtures prepared should be equal to or greater than the number of components in the test sample. The equations necessary to calculate the response factors for two and three component systems, using standard mixtures, are given in the following sections.

A4.1 Two component system

(a) Calibration (using mixed standards)

To determine the composition of a two component sample, the sample must be analysed using two different detectors. Therefore, the response of each component on each detector must be measured. To achieve this two mixtures containing those two components are prepared and analysed using the two detectors. For a discussion of the errors which may be introduced at this stage refer to Appendix 5.

For the standard 'mixture 1' let the weight of component 1 be W_1, the weight of component 2 be W_2 and let the measured area/ response be A_1 using detector 1 and A_3 using detector 2.

For the standard 'mixture 2' let the weight of component 1 be W_3, the weight of component 2 be W_4 and let the measured area/ response be A_2 using detector 1 and A_4 using detector 2.

The measured response A_1 will be equal to the weight of component 1 multiplied by its response factor plus the weight of component 2 multiplied by its response factor. i.e.

$$A_1 = W_1K_1 + W_2K_2 \qquad (A26)$$

Similarly for measured response A_2

$$A_2 = W_3K_1 + W_4K_2 \quad (A27)$$

Rearrangement of equation 11.27 gives:

$$K_2 = (A_2 - W_3K_1)/ W_4 \quad (A28)$$

therefore: $$A_1 = W_1K_1 + W_2 (A_2 - W_3K_1)/ W_4 \quad (A29)$$

$$A_1W_4 = W_1K_1W_4 + W_2A_2 - W_2W_3K_1 \quad (A30)$$

$$K_1W_4W_1 - K_1W_2W_3 = A_1W_4 - W_2A_2 \quad (A31)$$

$$\mathbf{K_1 =(A_1W_4 - W_2A_2)/(W_1W_4 - W_2W_3)} \quad (A32)$$

Rearrangement of equation A26 gives:

$$K_1 = (A_1 - W_2K_2) / W_1 \quad (A33)$$

therefore: $$A_2 = W_4K_2 + W_3 (A_1 - W_2K_2)/W_1 \quad (A34)$$

$$A_2W_1 = W_4K_2W_1 + W_3A_1 - W_3W_2K_2 \quad (A35)$$

$$K_2W_4W_1 - K_2W_2W_3 = A_2W_1 - W_3A_1 \quad (A36)$$

$$\mathbf{K_2 = (A_2W_1 - W_3A_1) / (W_1W_4 - W_2W_3)} \quad (A37)$$

Similar response factors can be calculated for each of the two components on detector 2. i.e.

$$\mathbf{K_3 =(A_3W_4 - W_2A_4) / (W_1W_4 - W_2W_3)} \quad (A38)$$

and $$\mathbf{K_4= (A_4W_1 - W_3A_3) / (W_1W_4 - W_2W_3)} \quad (A39)$$

(b) Analysis

For the determination of a two component system using two detectors the response of each component using each detector is required. Let K_1 and K_2 be the response factors,

respectively, for components 1and 2 using detector 1 and let K_3 and K_4 be the response factors, respectively, for components 1and 2 using detector 2.

The total peak areas obtained from detectors 1 and 2 are A_1 and A_2, respectively. Each area is equal to the response factor of component 1 multiplied by its concentration plus the response factor of component 2 multiplied by its concentration.

Therefore:

$$A_1 = K_1W_1 + K_2W_2 \quad (A40)$$

$$A_2 = K_3W_1 + K_4W_2 \quad (A41)$$

These equations can be rearranged to give:

$$\mathbf{W_1 = (A_1K_4 - A_2K_2)/(K_1K_4 - K_2K_3)} \quad (A42)$$

$$\mathbf{W_2 = (A_1K_3 - A_2K_1)/(K_2K_3 - K_1K_4)} \quad (A43)$$

A4.2 Three component system

(a) Calibration using simultaneous equations

To determine the response factors of three components on three detectors, three mixtures of those components, in different proportions, should be prepared. The areas from the three mixtures, A_1, A_2 and A_3 are obtained from detector 1.

$$A_1 = W_1K_1 + W_2K_2 + W_3K_3 \quad (A44)$$

$$A_2 = W_4K_1 + W_5K_2 + W_6K_3 \quad (A45)$$

$$A_3 = W_7K_1 + W_8K_2 + W_9K_3 \quad (A46)$$

These equations can be re-arranged to solve for K_1, K_2 and K_3, namely,

$$K_1 = (A_3W_5E-A_2W_8E-A_2W_2F+A_1W_5F)/(W_1W_5F-W_4W_2F+W_7W_5E-W_4W_8E) \quad (A47)$$

$$K_2 = (A_3W_4D-A_2W_7D-A_2W_1C+A_1W_4C)/(W_2W_4C-W_1W_5C-W_5W_7D+W_4W_8D) \quad (A48)$$

$$K_3 =(A_3W_4A-A_2W_7A-A_2W_1B+A_1W_4B)/(W_3W_4B-W_1W_6B+W_4W_9A-W_6W_7A) \quad (A49)$$

where $A = W_1W_5 - W_2W_4$ $B = W_8W_4 - W_5W_7$ (A50)

$C = W_4W_9 - W_6W_7$ $D = W_1W_6 - W_3W_4$ (A51)

$E = W_2W_6 - W_3W_5$ $F = W_5W_9 - W_6W_8$ (A52)

The response factors of each component for the second and third detectors can be similarly calculated.

(b) Analysis

For a GPC experiment monitoring the MWD profile of a copolymer using 3 detectors e.g. UV at two wavelengths and RI the area contributions are as follows:

$$A_1 = W_1K_1 + W_2K_2 + W_3K_3 \quad (A53)$$

$$A_2 = W_1K_4 + W_2K_5 + W_3K_6 \quad (A54)$$

$$A_3 = W_1K_7 + W_2K_8 + W_3K_9 \quad (A55)$$

where W_i are the weight fractions of the three components, K_1,K_2 and K_3 are the response factors obtained using detector 1, K_4, K_5 and K_6 are the response factors obtained using detector 2 and K_7,K_8 and K_9 the response factors obtained using detector 3 and A_1 to A_3 are the detected areas from each of the 3 detectors. These equations can be rearranged to solve for W_1, W_2 and W_3.

$$\mathbf{W_1 = (A_3K_5U - A_2K_8U + A1K_5V - A_2K_2V)/(K_1K_5V - K_4K_2V + K_7K_5U - K_4K_8U} \quad (A56)$$

$$\mathbf{W_2 = (A_2K_7W - A_3K_4W - A_1K_4X + A_2K_1X)/(K_5K_1X - K_2K_4X + K_5K_7W - K_8K_4W)} \quad (A57)$$

$$\mathbf{W_3 = (A_3K_4Z - A_2K_7Z + A_1K_4Y - A_2K_1Y)/(K_3K_4Y - K_6K_1Y + K_9K_4Z - K_6K_7Z)} \quad (A58)$$

where $U = K_6K_2 - K_5K_3$ $V = K_9K_5 - K_6K_8$ (A59)

$W = K_3K_4 - K_6K_1$ $X = K_6K_7 - K_9K_4$ (A60)

$Y = K_8K_4 - K_5K_7$ $Z = K_5K_1 - K_2K_4$ (A61)

Worked examples

The validity of the above equations were tested by calculating the composition of a three component system. The peak areas 'A' and response factors 'K' were initially calculated assuming a polymer blend comprising of components 1 to 3 in a ratio 50 to 30 to 20, respectively. The response factors for these components, using three detectors, are given in Table A6.

Table A6 Response factors of components 1 to 3 used in the worked example

component/ detector	response factors		
	1	2	3
1	100 (K_1)	0 (K_2)	0 (K_3)
2	25 (K_4)	10 (K_5)	0 (K_6)
3	5 (K_7)	4 (K_8)	3 (K_9)

The areas detected on the three detectors are therefore:

$$A_1 = 50x100 = 5000 \quad \text{(A62)}$$

$$A_2 = 50x25 + 30x10 = 1550 \quad \text{(A63)}$$

$$A_3 = 50x5 + 30x4 + 20x3 = 430 \quad \text{(A64)}$$

Using the response factors given in Table A6 and the areas A_1 to A_3 calculated above, the weight fractions for the three components can be calculated.

First the constants U to Z will be calculated.

$U = K_6K_2\text{-}K_5K_3$ and $V = K_9K_5\text{-}K_6K_8$, therefore $U = 0$ and $V=30$. (A65)

$W = K_3K_4\text{-}K_6K_1$ and $X= K_2K_7\text{-}K_9K_4$, therefore $W= 0$ and $X= -75$. (A66)

$Y = K_8K_4\text{-}K_5K_7$ and $Z = K_5K_1\text{-}K_2K_4$, therefore $Y=50$ and $Z=1000$. (A67)

Using the constants, the values of W_1, W_2 and W_3 can be calculated:

$$W_1 = (A_3K_5U\text{-}A_2K_8U+A_1K_5V\text{-}A_2K_2V)/(K_1K_5V\text{-}K_4K_2V+K_7K_5U\text{-}K_4K_8U) \quad \text{(A68)}$$

$$\mathbf{W_1 = (0\text{-}0+(5000x10x30)\text{-}0)/(100x10x30)\text{-}0+0\text{-}0} \quad \text{(A69)}$$

$$\mathbf{W_2 = 150000/30000 = 50} \quad \text{(A70)}$$

$$W_2 = (A_2K_7W\text{-}A_3K_4W\text{-}A_1K_4X+A_2K_1X)/(K_5K_1X\text{-}K_2K_4X+K_5K_7W\text{-}K_8K_4W) \quad \text{(A71)}$$

$$W_2 =(0\text{-}0\text{-}(5000x25x\text{-}75)+(1550x100x\text{-}75))/((10x100x\text{-}75)\text{-}0+0\text{-}0) \quad \text{(A72)}$$

$$\mathbf{W_2 = -2250000/\ -75000 = 30} \quad \text{(A73)}$$

$$W_3 = (A_3K_4Z\text{-}A_2K_7Z+A_1K_4Y\text{-}A_2K_1Y)/(K_3K_4Y\text{-}K_6K1Y+K_9K_4Z\text{-}K_6K_7Z) \quad \text{(A74)}$$

W_3= (430x25x1000)-(1550x5x1000)+(5000x25x50)-(1550x100x50)/(0-0+75000-0)

(A75)

$$\mathbf{W_3 = 150000/75000 = 20} \quad \text{(A76)}$$

The calculated values of W_1, W_2 and W_3 are 50, 30 and 20 are equal to their initial values.

(c) Calibration of a three component system using inverse matrices

For a GPC experiment monitoring the MWD profile of a copolymer using 3 detectors the area contributions are as follows:

$$A_1 = W_1K_1 + W_2K_2 + W_3K_3 \quad (A77)$$

$$A_2 = W_1K_4 + W_2K_5 + W_3K_6 \quad (A78)$$

$$A_3 = W_1K_7 + W_2K_8 + W_3K_9 \quad (A79)$$

where W_i are the weight fractions of the 3 components, K_1 to K_3 are the response factors using detector 1, K_4 to K_6 are the response factors using detector 2 and K_7 to K_9 the response factors using detector 3 and A_1 to A_3 are the detected areas from each of the three detectors.

Equations A77 to A79 can be expressed in matrix form:

$$\begin{bmatrix} W_1 & W_2 & W_3 \\ W_4 & W_5 & W_6 \\ W_7 & W_8 & W_9 \end{bmatrix} \begin{bmatrix} K_1 \\ K_2 \\ K_3 \end{bmatrix} = \begin{bmatrix} A_1 \\ A_2 \\ A_3 \end{bmatrix} \quad (A80)$$

This can be written as:

$$\mathbf{WK=A} \quad (A81)$$

where W is the square matrix containing the weight fraction data and K and A are the column matrices containing the response factor and area data, respectively.

The response factors i.e. K can be calculated by solving the rearranged matrix:

$$\mathbf{K = W^{-1}A} \quad (A82)$$

(d) Analysis of a three component system using inverse matrices

For the analysis step i.e. the determination of W in equation A81, values of K have been determined and values of A are measured by experiment. Therefore equation A81 can be rearranged to give:

$$\mathbf{W = K^{-1}A} \quad (A83)$$

Worked example

In this worked example the same numbers will be used as in the previous example. The three component system will consist of components 1, 2 and 3 in a ratio of 50 to 30 to 20. The response factors for these components on three detectors are given in Table A6.

The matrix **A=KW** is therefore:

$$\begin{bmatrix} A_1 \\ A_2 \\ A_3 \end{bmatrix} = \begin{bmatrix} K_1 & K_2 & K_3 \\ K_4 & K_5 & K_6 \\ K_7 & K_8 & K_9 \end{bmatrix} \begin{bmatrix} W_1 \\ W_2 \\ W_3 \end{bmatrix} \qquad \text{(A84)}$$

To solve for W the matrix equation A83 must be solved. To invert the K matrix, the original matrix is (1) transposed (2) elements replaced by their cofactors and (3) divided by the determinant.

The original matrix K is equal to:

$$\mathbf{K} = \begin{bmatrix} 100 & 0 & 0 \\ 25 & 10 & 0 \\ 5 & 4 & 3 \end{bmatrix}, \text{ the transposed matrix is therefore } \mathbf{K}^t = \begin{bmatrix} 100 & 25 & 5 \\ 0 & 10 & 4 \\ 0 & 0 & 3 \end{bmatrix} \qquad \text{(A85)}$$

To complete the inversion of matrix K the cofactors of the elements K_1 to K_9 are calculated:

$k_1 = +(K_5K_9-K_8K_6) = 30$ $\quad k_2 = -(K_4K_9-K_7K_6) = -75$ $\quad k_3 = +(K_4K_8-K_7K_5) = 50$

$k_4 = -(K_2K_9-K_8K_3) = 0$ $\quad k_5 = (K_1K_9-K_7K_3) = 300$ $\quad k_6 = -(K_1K_8-K_2K_7) = -400$

$k_7 = +(K_2K_6-K_5K_3) = 0$ $\quad k_8 = -(K_1K6-K_4K3) = 0$ $\quad k_9 = +(K_1K_5-K_4K2) = 1000$

The determinant, refer to Appendix 3, is equal to:

$$|K| = 100x(10x3-0x4)-0+0 = 3000 \qquad \text{(A86)}$$

therefore, to solve $\mathbf{W}=\mathbf{K}^{-1}\mathbf{A}$:

$$\begin{bmatrix} W_1 \\ W_2 \\ W_3 \end{bmatrix} = \frac{1}{3000} \begin{bmatrix} 30 & 0 & 0 \\ -75 & 300 & 0 \\ 50 & -400 & 1000 \end{bmatrix} \begin{bmatrix} 5000 \\ 1550 \\ 430 \end{bmatrix} = \begin{bmatrix} 50 \\ 30 \\ 20 \end{bmatrix} \qquad \text{(A87)}$$

The calculated values of W_1, W_2 and W_3 are 50, 30 and 20, which are equal to their initial values.

A4.3 Four component systems

Four-by-four matrices have been used to solve quadratic equations for GPC molecular weight distribution calibration curves. Although four-component systems were not evaluated in this thesis the following describes how to conduct such an analysis.

Firstly, the 4x4 matrix is inverted. This is achieved by (1). transposing rows and columns (2). replacing each element with its cofactor and (3). dividing by the determinant. Steps 2 and 3 are more complex for a 4x4 matrix than a 3x3 matrix.

Let the 4x4 matrix be represented as follows:

$$\mathrm{M} = \begin{bmatrix} a_1 & b_1 & c_1 & d_1 \\ a_2 & b_2 & c_2 & d_2 \\ a_3 & b_3 & c_3 & d_3 \\ a_4 & b_4 & c_4 & d_4 \end{bmatrix} \quad \mathrm{M}^t = \begin{bmatrix} a_1 & a_2 & a_3 & a_4 \\ b_1 & b_2 & b_3 & b_4 \\ c_1 & c_2 & c_3 & c_4 \\ d_1 & d_2 & d_3 & d_4 \end{bmatrix} \quad \mathrm{M}^* = \begin{bmatrix} A_1 & A_2 & A_3 & A_4 \\ B_1 & B_2 & B_3 & B_4 \\ C_1 & C_2 & C_3 & C_4 \\ D_1 & D_2 & D_3 & D_4 \end{bmatrix} \qquad \text{(A88)}$$

where $\mathbf{M}^t$ is the transposed matrix and $\mathbf{M}^*$ is the adjoint matrix i.e. matrix replaced by cofactors. The cofactors are calculated as follows:

$$A_1 = [b_2(c_3d_4-c_4d_3)-b_3(c_2d_4-c_4d_2)+b_4(c_2d_3-c_3d_2)] \qquad \text{(A89)}$$

$$A_2 = -[b_1(c_3d_4-c4d_3)-b_3(c_1d_4-c_4d_1)+(b_4(c_1d_3-c_3d_1)] \qquad \text{(A90)}$$

etc.

The determinant is calculated in a number of steps:

$$|M| = (a_1)^2 \begin{bmatrix} a_1b_2 - b_1a_2 & a_1c_2 - a_2c_1 & a_1d_2 - a_2d_1 \\ a_1b_3 - a_3b_1 & a_1c_3 - a_3c_1 & a_1d_3 - a_3d_1 \\ a_1b_4 - a_4b_1 & a_1c_4 - a_4c_1 & a_1d_4 - a_4d_1 \end{bmatrix} = \begin{bmatrix} \alpha_1 & \alpha_2 & \alpha_3 \\ \alpha_4 & \alpha_5 & \alpha_6 \\ \alpha_7 & \alpha_8 & \alpha_9 \end{bmatrix} \qquad \text{(A91)}$$

i.e. let $\alpha_1 = (a_1b_2 - b_1a_2)$ etc.

$$|M| = (a_1)^2 \times \alpha_1 \times \begin{bmatrix} \alpha_1\alpha_5 & \alpha_1\alpha_6 \\ \alpha_1\alpha_8 & \alpha_1\alpha_9 \end{bmatrix} \qquad \text{(A92)}$$

Worked example

The four area response values will be calculated assuming a four component polymer comprising of component 1 to 4 in the ratio 50:30:15:5 respectively. The response factors of the four components using four detectors are given in Table A7.

Table A7 Response factors of components 1 to 4 in the worked example

detector	response factors			
	component 1	component 2	component 3	component 4
1	10	5	0	0
2	20	15	10	0
3	15	5	4	2
4	5	4	3	1

The areas can be calculated using the equation;

$$A_i = \Sigma(K_{ij})W_j \qquad \text{(A93)}$$

where i = detector 1 to 4 and j = component 1 to 4.

therefore:

$$A_1 = (50x10) + (30x5) + 0 + 0 \qquad = 650 \qquad \text{(A94)}$$

$$A_2 = (50x20) + (30x15) + (15x10) + 0 \qquad = 1600 \qquad \text{(A95)}$$

$$A_3 = (50x15) + (30x5) + (15x4) + (5x2) \qquad = 970 \qquad \text{(A96)}$$

$$A_4 = (50x5) + (30x4) + (15x3) + (5x1) \qquad = 420 \qquad \text{(A97)}$$

By introducing these area values and response factors into the matrix equations the composition of the polymer blend can be calculated.

$$\begin{bmatrix} A_1 \\ A_2 \\ A_3 \\ A_4 \end{bmatrix} = \begin{bmatrix} K_1 & K_2 & K_3 & K_4 \\ K_5 & K_6 & K_7 & K_8 \\ K_9 & K_{10} & K_{11} & K_{12} \\ K_{13} & K_{14} & K_{15} & K_{16} \end{bmatrix} \begin{bmatrix} W_1 \\ W_2 \\ W_3 \\ W_4 \end{bmatrix} \qquad \text{(A98)}$$

the vector W is required i.e $\mathbf{W}=\mathbf{K}^{-1}\mathbf{A}$, where

$$\mathbf{K} = \begin{bmatrix} 10 & 5 & 0 & 0 \\ 20 & 15 & 10 & 0 \\ 15 & 5 & 4 & 2 \\ 5 & 4 & 3 & 1 \end{bmatrix} \qquad \text{(A99)}$$

Therefore:

$$\mathbf{K}^t = \begin{bmatrix} 10 & 20 & 15 & 5 \\ 5 & 15 & 5 & 4 \\ 0 & 10 & 4 & 3 \\ 0 & 0 & 2 & 1 \end{bmatrix} \quad \mathbf{K}^* = \begin{bmatrix} 0 & 10 & 50 & -100 \\ 90 & -20 & -100 & 200 \\ -135 & 55 & 50 & -100 \\ 45 & -135 & 0 & 450 \end{bmatrix} \qquad \text{(A100)}$$

The following is an example of the calculation of a cofactor in a 4x4 matrix,

$$K_1 = b_2(c_3d_4-c_4d_3)-b_3(c_2d_4-c_4d_2)+b_4(c_2d_3-c_3d_2)$$

$$= 15x(4x1-2x3) - 10x(5x1-4x2) + 0x(5x3-4x4) = 0 \qquad \text{(A101)}$$

In calculating the determinant, the values of α_1 to α_9 (see equation A91) are as follows:

$$\begin{vmatrix} \alpha_1 & \alpha_2 & \alpha_3 \\ \alpha_4 & \alpha_5 & \alpha_6 \\ \alpha_7 & \alpha_8 & \alpha_9 \end{vmatrix} = \begin{vmatrix} 50 & 100 & 0 \\ -25 & 40 & 20 \\ 15 & 30 & 10 \end{vmatrix} \qquad \text{(A102)}$$

The determinant |M| is calculated to be 450. The column matrix W can now be calculated.

$$\begin{bmatrix} W_1 \\ W_2 \\ W_3 \\ W_4 \end{bmatrix} = \frac{1}{450} \begin{bmatrix} 0 & 10 & 50 & -100 \\ 90 & -20 & -100 & 200 \\ -135 & 55 & 50 & -100 \\ 45 & -135 & 0 & 450 \end{bmatrix} \begin{bmatrix} 650 \\ 1600 \\ 970 \\ 420 \end{bmatrix} = \begin{bmatrix} 50 \\ 30 \\ 15 \\ 5 \end{bmatrix} \qquad \text{(A103)}$$

The calculated values of W_1, W_2, W_3 and W_4 are therefore 50, 30, 15 and 5 which are equal to their initial values.

Appendix 5 Errors in multicomponent analysis

A5.1 Source of Errors

(a) Calibration using standard mixtures

To determine the concentration of a given component in a mixture, using the peak area from a chromatographic separation, the response of that pure component on that detector i.e. the response factor, must be known. The response factor can be determined by the analysis of a known concentration standard. The response factor can also be determined by the analysis of standard mixtures monitored by a number of different detectors. To calculate the response factors of two components, monitored by a given detector, using the method of standard mixtures, two mixtures each containing those two components, should be prepared and analysed. Let the response or area for mixture 1 equal A_1 and the response for mixture 2 equal A_2. Then, as shown in Appendix 4:

$$A_1 = W_1K_1 + W_2K_2 \quad \text{and} \quad A_2 = W_3K_1 + W_2K_2 \qquad (A104)$$

where W_1 and W_2 are the weights of components A and B in mixture 1 and W_3 and W_4 are the weights of components A and B in mixture 2.

These equations can be solved for K_1 and K_2:

$$K_1 = (A_2W_2 - A_1W_4)/ (W_3W_2 - W_1W_4) \qquad (A105)$$

$$\text{and} \quad K_2 = (A_2W_1 - A_1W_3)/(W_1W_4 - W_2W_3) \qquad (A106)$$

It can be seen that as W_3W_2 approaches W_1W_4 ie W_3W_2/W_1W_4 equals unity, the denominator will approach zero. Also, as A_2W_2 approaches A_1W_4 and A_2W_1 approaches A_1W_3 the numerators will approach zero.

To determine the effect of a deliberate error, introduced into one of the component weights, upon the calculated response factor, actual values of component weights and response factors will be introduced into the above equations. Values for A_1 and A_2 may then be calculated. A value for one of the response factors e.g. K_2 can be re-calculated after introducing a fixed error in one of the sample weights. In the following examples the areas have been calculated assuming a value of 0.1000 g for W_1. However if the weight actually measured was 0.0990 g then a value of K_{2error} can be calculated.

Example 1.

In this first example the weights of components A and B in mixture 1 are W_1 = 0.1000 g and W_2 = 0.0050 g. The weights of component A and B in mixture 2 are W_3 = 0.0900 g and W_4 = 0.0055 g. If the values of K_1 and K_2 are set to 500 and 5 respectively values for A_1 and A_2 can be calculated, see Table A8. It will be observed that the values obtained by multiplying W_1 by W_2 will be similar to that of W_3 multiplied by W_4. This results of the value for W_1W_4-W_2W_3 to be low, 0.0001. It will also be observed that since K_1 is significantly larger than K_2 and the weight of A in both mixtures is larger than the weight of component B, the value for A_2W_1-A_1W_3 is also low. Using the above values for the component weights, except introducing the error into W_1 (0.099 g for W_1), the value of K_2 can be calculated.

Table A8 Error analysis: Example 1

K_1	K_2	A_1	A_2	W_1W_4-W_2W_3	A_2W_1-A_1W_3	K_2calc.
500	5	50.025	45.0275	0.0001	0	-471.2

The calculated value for K_2 is therefore -471.2 instead of the correct value of 5. This error has been introduced by a 1% error in weight of one of the standard mixtures.

Example 2.

By changing the ratio of the weights in the two standards, the error in K_2 due to a an error in W_1 can be reduced. This example is similar to the first, however the weight of component B in mixture 2 i.e. W_4 has been increased ten times. In this second example the weights of components A and B in mixture 1 are W_1 = 0.1000 g and W_2 = 0.0050 g. The weights of component A and B in mixture 2 are W_3 = 0.0900 g and W_4 = 0.050 g. Values for W_1W_4-W_2W_3 and A_2W_1-A_1W_3 are both increased.

Table A9 Error Analysis: Example 2

K_1	K_2	A_1	A_2	W_1W_4-W_2W_3	A_2W_1-A_1W_3	$K2_{calc.}$
500	5	50.025	45.2575	0	0.02	-5

The calculated value of K_2 is now -5.0 instead of the correct value +5.0. The error has been reduced, compared to that obtained in the previous example, by choice of standard weights in the mixture but the error is still unacceptable large.

Example 3.

It can also be shown that the effect of the weighing errors upon the calculated response factors can be reduced by control, possibly by selection of UV wavelength, of the magnitude of the response factors. In this third example the weights of components A and B in mixture 1 are W_1 = 0.1000 g and W_2 = 0.0050 g. The weights of component A and B in mixture 2 are W_3 = 0.0900 g and W_4 = 0.050 g. In this third example the value of K_1 has been reduced from 500 to 50. The value for (A_2W_1-A_1W_3) remains the same as in example 2 but the value for (W_1W_4-W_2W_3) has increased by a factor of 10.

Table A10 Error Analysis: Example 3

K_1	K_2	A_1	A_2	W_1W_4-W_2W_3	A_2W_1-A_1W_3	K_2calc.
50	5	5.025	4.75	0.0455	0.02	4

The calculated value of K_2 is now 4.0 which is much closer to the set value of 5.0. It can therefore be seen that by optimising the weight ratios of the components in the mixture and by selection of response factors, the errors introduced into the calibration may be reduced. This topic will be further studied in Appendix 5.

(b) Calibration using single standards

In this approach the calibration step is carried out by preparing separate solutions of the two components. Errors in the calculated response factors will arise from errors in weighing and from errors in the measurement of peak areas.

Since the value of the response factor K is calculated by dividing the response or area by the weight sample, a 1% error in sample weight will produce a 1% error in response factor. The amounts of standard weighed should therefore be high enough so as not to introduce significant weighing errors. For example if the amount weighed was 0.0050 g, but the error in the balance was 0.0005 g then the error in the calculated response factor would 10%.

A5.2 Error Minimisation

The equations used to calculate weight fractions of a two component system from GPC peak areas and response factors are as follows:

$$W_1 = (A_1K_4\text{-}A_2K_2)/(K_1K_4\text{-}K_2K_3) \qquad \text{(A107)}$$

and $$W_2 = (A_1K_3\text{-}A_2K_1)/(K_2K_3\text{-}K_1K_4) \qquad \text{(A108)}$$

Inspection of the equations suggest that if the denominator approaches zero i.e. when $K_1/K_2 = K_3/K_4$ any errors in the response factors will produce large errors in the calculated weight fractions. Thus the error can be reduced when $K_1>K_2$ (or $K_2>K_1$) and $K_4>K_3$ (or $K_3>K_4$). A means of predicting errors in weight fractions due to errors in response factors is required such that if response factors can be altered, for example, by selection of wavelength if a tuneable UV detector is used, values may be chosen to minimise or at least reduce the potential error. The term 'sum of errors' is introduced.

(a) Sum of errors: Two-component system

Errors in each of the four response factors will produce a compound error in the calculated weight fraction. The sum of the individual errors in the calculated weight ratio due to the individual errors in the response factors will be termed the 'sum of errors'. The error term used will be a percentage value i.e.

$$\text{Error}_i = \left[\frac{\text{actual - calculated composition}}{\text{actual composition}} \right] \text{x } 100 \qquad \text{(A109)}$$

The sum of errors will also be seen to depend upon composition.

Example 1

For a two component system analysed using two detectors, let the response factors for components A and B using detector 1 be K_1 and K_2. Similarly, let the response factors for components A and B using detector 2 be K_3 and K_4. Let the response factors are set where $K_1>K_2$ and $K_4>K_3$. e.g. $K_1 = 500$, $K_2 = 5$, $K_3 = 10$ and $K_4 = 100$ and let the composition of the sample be 50:50. Using these values for sample composition and

response factors, the areas obtained from detector I and detector 2, A_1 and A_2, can be calculated. Thus:

$$A_1 = (50x500) + (50x5) = 25250 \qquad (A110)$$

$$A_2 = (50x10) + (50x100) = 5500 \qquad (A111)$$

The composition of the system could be back calculated from the areas A_1 and A_2, the response factors K_1 to K_4 and the equations given above. If, however, an error was introduced into one of the response factor values an erroneous value for the weight fraction would result. If a value of 505 instead of 500 (1% error) was used for K_1, the calculated weight fraction would be:

$$W_{1err} = \left[\frac{(5500x5) - (25250x100)}{(5x10) - (505x100)} \right] = 49.504 \qquad (A112)$$

Therefore the error in W_1 is:

$$\text{Error} = \left[\frac{50 - 49.505}{50} \right] x\ 100 = 0.991\% \qquad (A113)$$

The weight fractions for W_1 can be similarly calculated by introducing errors, at 1%, into the remaining response factors. These errors are then added together. Similarly the sum of errors for W_2 can be calculated.

Table A11 Sum of Errors for a Two-Component System. Example 1

error	calculated W_1	calculated W_2
K_{1error}	0.99	0.10
K_{2error}	0.01	0.00
K_{3error}	0.00	0.10
K_{4error}	0.01	0.99
Total	1.01	1.91

The sum of errors in the calculation of composition for this example is 2.2%. Therefore by optimisation of response factors errors may be minimised. We shall see in the next example that if response factors are not correctly chosen errors may increase.

Example 2

In this example $K_1>K_2$ but $K_3>K_4$. i.e. $K_1 = 500$, $K_2 = 5$, $K_3 = 200$ and $K_4 = 100$. This is unlike the previous example where $K_1>K_2$ and $K_3<K_4$. The sum of errors for this example can be similarly calculated.

Table A12 Sum of Errors for a Two-Component System. Example 2

error	**calculated W_1**	**calculated W_2**
K_{1error}	1.010	2.020
K_{2error}	0.101	0.020
K_{3error}	0.020	2.041
K_{4error}	0.010	1.010
Total error	1.051	4.902

By not carefully selecting the response factors the error has increased from approximately 2% to around 6%.

Example 3

It can also be shown that the composition of the sample will effect the sum of errors value. Using the same response factors as those employed in the second example but using a composition of 80:20, the sum of errors was calculated.

Table A13 Sum of Errors for a Two-Component System. Example 3

error	calculated W_1	calculated W_2
K_{1error}	1.010	8.081
K_{2error}	0.003	0.020
K_{3error}	0.020	8.165
K_{4error}	0.003	1.010
Total	1.036	17.28

It can be seen that the error has increased to 18%.

From the previous three examples it has been demonstrated that, to reduce the potential for error for the determination of composition of a two component system, one of the components should have the highest response on the one detection system but the lowest response on the other detector. Also the component with the lowest response factor should be present in the greatest concentration.

(b) Sum of errors: Three-component system

The sum of errors for a three component system can be similarly calculated. Response factors for the three components using three different detectors are required. For this example the response factors for the components: epoxy, polystyrene and poly(methyl methacrylate) will be used when monitoring is carried out using UV detection at 280 nm and 254 nm and using the differential refractometer. The values are taken from Table 5.31.

Table A 14 Response Factors for a Three-Component System

detector	epoxy	polystyrene	poly (methyl methacrylate)
UV, 280 nm	658.1 (K_1)	4.5 (K_2)	0.0 (K_3)
UV, 254 nm	158.6 (K_4)	80.0 (K_5)	0.0 (K_6)
refractometer	8.0 (K_7)	7.5 (K_8)	3.8 (K_9)

The sum of errors for this three component system can be calculated in a similar fashion to that described for the two-component system. An error of 1% is introduced into each of the response factors and the error in calculated composition is summed. The errors in the calculated weight fractions caused by the individual errors in the response factors along with the total errors are shown in Table A15. The composition of the polymer mixture used in the calculation is 80:15:5 epoxy: poly(methyl methacrylate): polystyrene.

Examination of the preceding analysis indicated that the largest errors in the weight fraction calculations are caused by the error in the K_1, K_4 and K_7 response factors. Further calculations show that if the error in those response values alone could be reduced to 0.1%, the errors in the calculation of W_1, W_2 and W_3 would reduce to 0.6%, 8.1% and 5.6% respectively which are significantly less than the values shown in Table A15.

Table A15 Sum of Errors for a Three-Component System

source of 1% error	**% error in weight fractions**		
	W_1	**W_2**	**W_3**
K_1error	0.42	32.49	8.58
K_2error	0.00	0.01	0.00
K_3error	0.00	0.01	0.00
K_4error	1.36	32.97	18.23
K_5error	0.04	1.05	0.58
K_6error	0.00	0.00	0.00
K_7error	1.63	1.63	9.21
K_8error	0.09	0.09	0.53
K_9error	0.15	0.09	0.84
total error	3.69	68.4	37.99

Appendix 6 Calculation of MWD calibration curves

To calibrate the GPC column, the retention time of a number of known molecular weight, narrow distribution, polystyrene standards were measured. See Chapter 5.4.2. The retention times and peak molecular weights (Mp) are listed in Table A16.

Table A16 GPC Retention Times of Polystyrene Molecular Weight Standards

peak molecular weight (Mp)	retention time (minutes)
675000	9.66
165085	10.68
127000	10.91
82565	11.44
34500	12.35
10000	13.86
5100	14.82
2464	15.78
950	17.00
162	19.12
toluene	20.46

Using this data linear, second and third order regression analyses were carried out.

(a) Linear regression

The equation for the data would be:

$$\log (Mp) = B_1 X + B_0 \qquad (A114)$$

where (Mp) is the peak molecular weight, B_1 is the slope, B_0 is the intercept and X is the retention time in seconds. Values of B_0 and B_1 can be calculated by solving a pair of simultaneous equations:

$$nB_0 + \Sigma X_i B_1 = \Sigma Y_i \qquad (A115)$$

$$\Sigma X_i B_0 + \Sigma X_i^2 B_1 = \Sigma X_i Y_i \qquad (A116)$$

where; n is the number of data points, X is the retention time and Y is the log of the peak molecular weight.

Values of ΣX_i, ΣY_i, ΣX_i^2 and $\Sigma X_i Y_i$ are calculated and substituted into the above equations. Table A17 shows all of the calculated values. The equations to solve for B_0 and B_1 are therefore:

$$10B_0 + 8137.2B_1 = 41.89188 \quad \text{(A117)}$$

$$8137.2B_0 + 6930412.2B_1 = 32206.945 \quad \text{(A118)}$$

Solving these equations gives values of the intercept (B_0) and the slope (B_1)

slope = -0.00608803, intercept = 9.143139395

(b) Second order regression

A second order equation is of the type:

$$Y = B_0 + B_1X + B_2X^2 \quad \text{(A119)}$$

Values of B_0, B_1 and B_2 can be calculated by solving three simultaneous equations.

$$nB_0 + \Sigma X_iB_1 + \Sigma X_i^2B_2 = \Sigma Y_i \quad \text{(A120)}$$

$$\Sigma X_iB_0 + \Sigma X_i^2B_1 + \Sigma X_i^3B_2 = \Sigma Y_iX_i \quad \text{(A121)}$$

$$\Sigma X_i^2B_0 + \Sigma X_i^3B_1 + \Sigma X_i^4B_2 = \Sigma Y_iX_i^2 \quad \text{(A122)}$$

These simultaneous equations can be represented by the matrix form **BX=Y**, where **B** is the column matrix containing B_0, B_1 and B_2, **X** is the square matrix containing values of n and X^m (where m= 1 to 4) and **Y** is the column matrix containing Y data. To solve for **B** the **X** matrix must be inverted. Values of ΣX_i, ΣY_i, ΣX_i^2, ΣX_i^3, ΣX_i^4, ΣX_iY_i and $\Sigma X_i^2Y_i$ are calculated and substituted into the above equations. See Table A17. The **X** matrix is therefore:

$$\mathbf{X} = \begin{bmatrix} 10.0 & 8137.2 & 6930421.2 \\ 8137.2 & 6930421.2 & 6.16651\text{x}10^{9} \\ 6930421.2 & 6.16651\text{x}10^{9} & 5.71\text{x}10^{12} \end{bmatrix} \qquad \text{(A123)}$$

The above matrix will be identical to its transposed form. The cofactors are then calculated. See Appendix 3 for the method of the calculation of cofactors.

$$\mathbf{X}^{*} = \begin{bmatrix} 1.546859\text{x}10^{18} & -3.727\text{x}10^{15} & 2.1474\text{x}10^{12} \\ -3.727\text{x}10^{15} & 9.0693\text{x}10^{12} & -5.2709\text{x}10^{9} \\ 2.1474\text{x}10^{12} & -5.2709\text{x}10^{9} & 3090188.2 \end{bmatrix} \qquad \text{(A124)}$$

The coefficients can now be calculated:

$$\begin{bmatrix} B_0 \\ B_1 \\ B_2 \end{bmatrix} = \left[K^{-1}\right] \begin{bmatrix} \Sigma Y_i \\ \Sigma Y_i X_i \\ \Sigma Y_i X_i^2 \end{bmatrix} = \begin{bmatrix} 10.57963 \\ -9.616\text{x}10^{-3} \\ 2.070\text{x}10^{-6} \end{bmatrix} \qquad \text{(A125)}$$

The coefficients describing the second order equation are:

$B_0 = 10.547561$ (A126)

$B_1 = -0.009535$ (A127)

$B_2 = 2.02\ \text{x}10^{-6}$ (A128)

(c) Third order regression

A third order equation is of the type:

$$Y = B_0 + B_1X + B_2X^2 + B_3X^3 \qquad \text{(A129)}$$

The application of the method of least squares leads to the following equations:

- $$nb_0 + \Sigma X_i b_1 + \Sigma X_i^2 b_2 + \Sigma X_i^3 b_3 = \Sigma Y_i \quad \text{(A130)}$$
- $$\Sigma X_i b_0 + \Sigma X_i^2 b_1 + \Sigma X_i^3 b_2 + \Sigma X_i^4 b_2 = \Sigma X_i Yi \quad \text{(A131)}$$
- $$\Sigma X_i^2 b_0 + \Sigma X_i^3 b_1 + \Sigma X_i^4 b_2 + \Sigma X_i^5 b_3 = \Sigma X_i^2 Y_i \quad \text{(A132)}$$

$$\Sigma X_i^3 b_0 + \Sigma X_i^4 b_1 + \Sigma X_i^5 b_2 + \Sigma x_i^6 b_3 = \Sigma X_i^3 Y_i \quad \text{(A133)}$$

Values of ΣX_i, ΣY_i, ΣX_i^2, ΣX_i^3, ΣX_i^4, ΣX_i^5, ΣX_i^6, $\Sigma X_i Y_i$, $\Sigma X_i Y_i^2$ and $\Sigma X_i Y_i^3$ are calculated and substituted into the above equations. See Table A17.

$$10b_0 + 8137.2b_1 + 6930412.2b_2 + 6.16651x10^9 b_3 = 41.89188 \quad \text{(A134)}$$

$$8137.2b_0 + 6930412.2b_1 + 6.16651x10^9 b_2 + 5.71x10^{12} b_3 = 32206.945 \quad \text{(A135)}$$

$$930412.2b_0 + 6.16651x10^9 b_1 + 5.71x10^{12} b_2 + 5.4749x10^{15} b_3 = 25839921 \quad \text{(A136)}$$

$$6.16651x10^9 b_0 + 5.71x10^{12} b_1 + 5.4749x10^{15} b_2 + 5.407x10^{18} b_3 = 2.1657x10^{10} \quad \text{(A137)}$$

Values of b_0, b_1, b_2 and b_3 can be solved using a 4x4 matrix.

$$\mathbf{X} = \begin{bmatrix} 10 & 8137.2 & 6930421.2 & 6.16651x10^9 \\ 8137.2 & 6930421.2 & 6.16651x10^9 & 5.71x10^{12} \\ 6930421.2 & 6.16651x10^9 & 5.71x10^{12} & 5.4749x10^{15} \\ 6.16551x10^9 & 5.741x10^{12} & 5.4749x10^{15} & 5.407x10^{18} \end{bmatrix} \quad \text{(A138)}$$

This transposed matrix will be identical to that above. The cofactors can then be calculated.

$$\mathbf{X}^* = \begin{bmatrix} 9.1905x10^{33} & -3.317x10^{31} & 3.881x10^{28} & -1.475x10^{25} \\ -3.317x10^{31} & 3.881x10^{28} & -1.475x10^{25} & 5.3821x10^{22} \\ 3.881x10^{28} & -1.475x10^{25} & 5.3821x10^{22} & -6.367x10^{19} \\ -1.475x10^{25} & 5.3821x10^{22} & -6.367x10^{19} & 2.4455x10^{16} \end{bmatrix} \quad \text{(A139)}$$

The inverse of the original matrix is calculated by dividing the above matrix by the determinant. See Appendix 3 for the calculation of a determinant of a 4-by-4 matrix.

The coefficients B_0, B_1, B_2 and B_3 can then be calculated.

$$\begin{bmatrix} B_0 \\ B_1 \\ B_2 \\ B_3 \end{bmatrix} = \left[K^{-1}\right] \begin{bmatrix} \Sigma Y_i \\ \Sigma Y_i X_i \\ \Sigma Y_i X_i^2 \\ \Sigma Y_i X_i^3 \end{bmatrix} = \begin{bmatrix} 18.739418 \\ -0.0392428 \\ 3.7385\text{x}10^{-5} \\ -1.358\text{x}10^{-8} \end{bmatrix} \qquad \text{(A140)}$$

The equation describing the MWD calibration curve is therefore:

$$\log Mw = 18.739418 - 0.039428RT + 3.7385\text{x}10^{-5}RT^2 - 1.358\text{x}10^{-8}RT^3 \qquad \text{(A141)}$$

where RT is the retention time in seconds.

Table A17. Calculation of ΣY_i, ΣX_i, ΣX_i^2, ΣX_i^3, ΣX_i^4, ΣX_i^5, ΣX_i^6, $\Sigma X_i^2 Y_i$, $\Sigma X_i^3 Y_i$, $\Sigma X_i Y_i$ and ΣY_i^2

	Log Mp (Y)	Retention time (X)	X_i^2	X_i^3	X_i^4	X_i^5	X_i^6	$X_i^2Y_i$	$X_i^3Y_i$	X_iY_i	Y_i^2
	5.8293038	579.6	335936.1	1.9471e8	1.1285e11	6.541e13	3.791e16	1.958e6	1.135e9	3378.66	33.98
	5.2177076	640.8	410624.6	2.6312e8	1.6861e11	1.081e14	6.924e16	2.214e6	1.373e9	3343.51	27.224
	5.1038037	654.6	428501.1	2.8050e8	1.8361e11	1.202e14	7.868e16	2.186e6	1.432e9	3340.95	26.05
	4.916796	686.4	471144.9	3.2339e8	2.2198e11	1.524e14	1.046e17	2.317e6	1.590e9	3374.89	24.18
	4.5378191	741.0	549081.0	4.0687e8	3.0149e11	2.234e14	1.655e17	2.492e6	1.846e9	3362.52	20.59
	4.0000000	831.6	691558.5	5.7510e8	4.7825e11	3.977e14	3.307e17	2.766e6	2.300e9	3362.40	16.00
	3.7075702	889.6	790676.6	7.0307e8	6.2517e11	5.559e14	4.943e17	2.931e6	2.607e9	3296.77	13.75
	3.3916407	946.8	896430.2	8.4874e8	8.0359e11	7.608e14	7.204e17	3.040e6	2.878e9	3211.20	11.503
	2.9777236	1020.0	1040400.0	1.0612e9	1.0824e11	1.104e15	1.126e18	3.098e6	3.160e9	3037.28	8.867
	2.2909515	1147.4	1316067.8	1.5098e9	1.732e12	1.987e15	2.280e18	2.908e6	3.336e9	2534.76	4.882
total	41.89	8137.2	6930421.2	6.1665e9	5.71e12	5.475e15	5.407e18	2.584e6	2.166e10	32206.95	187.01

Appendix 7 Particle size data using TEM: Raw data

A7.1 TEM examination of latices diluted in water

The water-based latices WRB624, WRB625, WRB626 and WRB633 were examined using transmission electron microscopy to determine the particle size of the micelles. Samples of WRB624 and WRB633 were also examined after dilution in a 2% aqueous solution of dimethyl amino ethanol (DMAE). Each of the samples were diluted by approximately 1000 times in either deionised water or DMAE solution. A drop of each solution was placed onto a Formvar coated copper grid. Most of the drop was removed by absorbing it onto the edge of a paper tissue. The grids were then dried at room temperature under vacuum for 5 minutes. Each grid was then examined using a transmission electron microscope and three areas were photographed. The number of particles on each photograph was counted.

The diameter of each particle was calculated by measuring a feature on the negative and then measuring the same feature on the print.

The enlargement factor between the negative and the photograph could then be calculated. The particle diameter on the print is multiplied by the magnification factor on the print and by the enlargement factor. This was carried out for all particles on each print.

Table A18 shows the number of particles per particle diameter. The diameter of the particles on each micrograph could only be measured to the nearest millimetre. Each millimetre on the micrograph corresponded to 6 nm actual particle diameter. A spreadsheet was used to calculate the number- (D_n) and weight-average (D_w) colloid particle diameters. The calculations used were as follows:

$$D_n = \Sigma(d_i \times n_i)/N \qquad \text{(A142)}$$

and

$$D_w = (3x\ \Sigma(n_i V_i^2)/2x(4\pi\Sigma(n_i V_i))^{1/3}) \qquad \text{(A143)}$$

Table A18 Number of Particle per Particle size for Latices diluted in Water

Particle diameter (nm)	Number of particles per particle size			
	WRB624	WRB625	WRB626	WRB633
12	6	0	12	5
18	8	32	98	14
24	43	68	93	45
30	40	55	97	81
36	49	17	56	63
42	57	22	40	78
48	40	5	14	61
54	28	10	12	42
60	8	12	4	40
66	2	6	4	17
72	2	6	2	11
78	0	3	1	5
84	0	8	0	5
90	0	4	1	1
96	0	1	0	0
102	0	5	0	0
108	0	4	0	0
114	0	1	0	0
120	0	4	0	0
126	0	2	0	0
132	0	0	0	0
138	0	0	0	0
144	0	1	2	0
150	0	1	1	0
156	0	1	0	0
162	0	1	1	0
168	0	0	0	0
174	0	0	0	0
180	0	0	0	0
186	0	0	0	0
192	0	1	0	0
204	0	0	1	0
264	0	0	1	0
Total	284	270	440	468

where d_i is the diameter of each particle, n_i is the number of each particle, N is the total number of particles and V_i is the volume of each particle.

The calculated number average and weight average particle diameters are shown in Table 7.8.

A7.2 Latices diluted in water and 2% aqueous DMAE

The particle size determinations were repeated following dilution in either deionised water or 2% aqueous DMAE. The diameter of the particles in the prints were calculated using methods described in the previous section. See Table A19. The magnification on this set of prints was slightly different than the previous experiment and one millimetre measured on the micrographs corresponded to a particle diameter of 7 nm.

Table A19 Number of Particles per Particle size of latices

Particle diameter (nm)	Number of particles per particle size			
	WRB624		WRB633	
	water	aq. DMAE	water	aq. DMAE
7	1	1	0	0
14	5	11	2	7
21	30	24	15	15
28	41	28	27	24
35	127	62	30	42
42	89	39	58	33
49	31	18	43	27
56	13	3	24	8
63	3	1	18	1
70	0	0	6	0
77	0	0	0	0
Total	340	187	223	157

The calculated number average and weight average particle diameters are shown in Table 7.9.

Appendix 8 Calculation of particle size from raw data

The particle size of the polystyrene sulphonate standard was determined using data generated from the display of the plot of the autocorrelation function. The DLS 700 software was run in the 'windows' environment and a bitmap file of the autocorrelation function plot was created. Figure A4a shows the plot of the autocorrelation function, Gn, versus time in units of micro-seconds, imported into MS Windows as a 'bit-map' file from the DLS700 software. The pixel x, y coordinates were converted into the autocorrelation function (Gn) and time (microseconds) respectively. This data was then entered into a spreadsheet (Lotus 1-2-3). Figure A4b shows the plot of (ln Gn) versus micro-seconds. From the autocorrelation function (Gn), ln(Gn-1) was calculated. Using the linear regression function built into the spreadsheet the slope of the graph (ln(Gn-1)) versus time was calculated.

The slope of the graph was determined to be 0.00135 $(\mu s)^{-1}$. The value of the autocorrelation function is equal to the slope divided by 2 [215] hence:

$$G = \text{slope}/2 = (0.00135 \times 10^6)/2 = 674.9714\ s^{-1} \qquad \text{(A144)}$$

The diffusion coefficient can be calculated using the following equation [151]:

$$D = G/K^2 \qquad \text{(A145)}$$

where $K = \text{scattering vector} = 4\pi n \sin(\theta/2)/\lambda$ (A146)

n = refractive index of the solvent (1.33)

λ = wavelength of incident radiation (632.8 nm)

and θ = scattering angle (90^0)

Therefore:

$$K = (4\pi \times 1.33 \times \sin(45^0))/632.8\times10^{-9} = 1.868 \times 10^7\ m^{-1} \qquad (A147)$$

and $$D = 674.9741/(1.868 \times 10^7)^2 = 1.9 \times10^{12}\ m^2s^{-1} \qquad (A148)$$

The particle diameter can then be calculated from the Stokes-Einstein equation:

$$D = kT/(6\pi\eta r) \qquad (A149)$$

where k = Boltzman constant (1.38×10^{-23} J K^{-1} $molecule^{-1}$),

T = temperature (292.8 K),

and η = viscosity (1.006×10^{-3} cps for water at 298 K)

Therefore:

$$r = (1.38 \times10^{-23} \times 292.8) / (6\pi \times 1.006\times10^{-3} \times 1.9\times10^{12}) = 110.4\ nm \qquad (A150)$$

The particle diameter is therefore calculated to be 220.8 nm.This result agrees favourably with the quoted diameter of 212 nm for this standard and the value of 220 nm determined using the DLS700 software.

Table A22(a) and (b) shows a print-out of the spreadsheet used to carry out the above calculation of particle size.

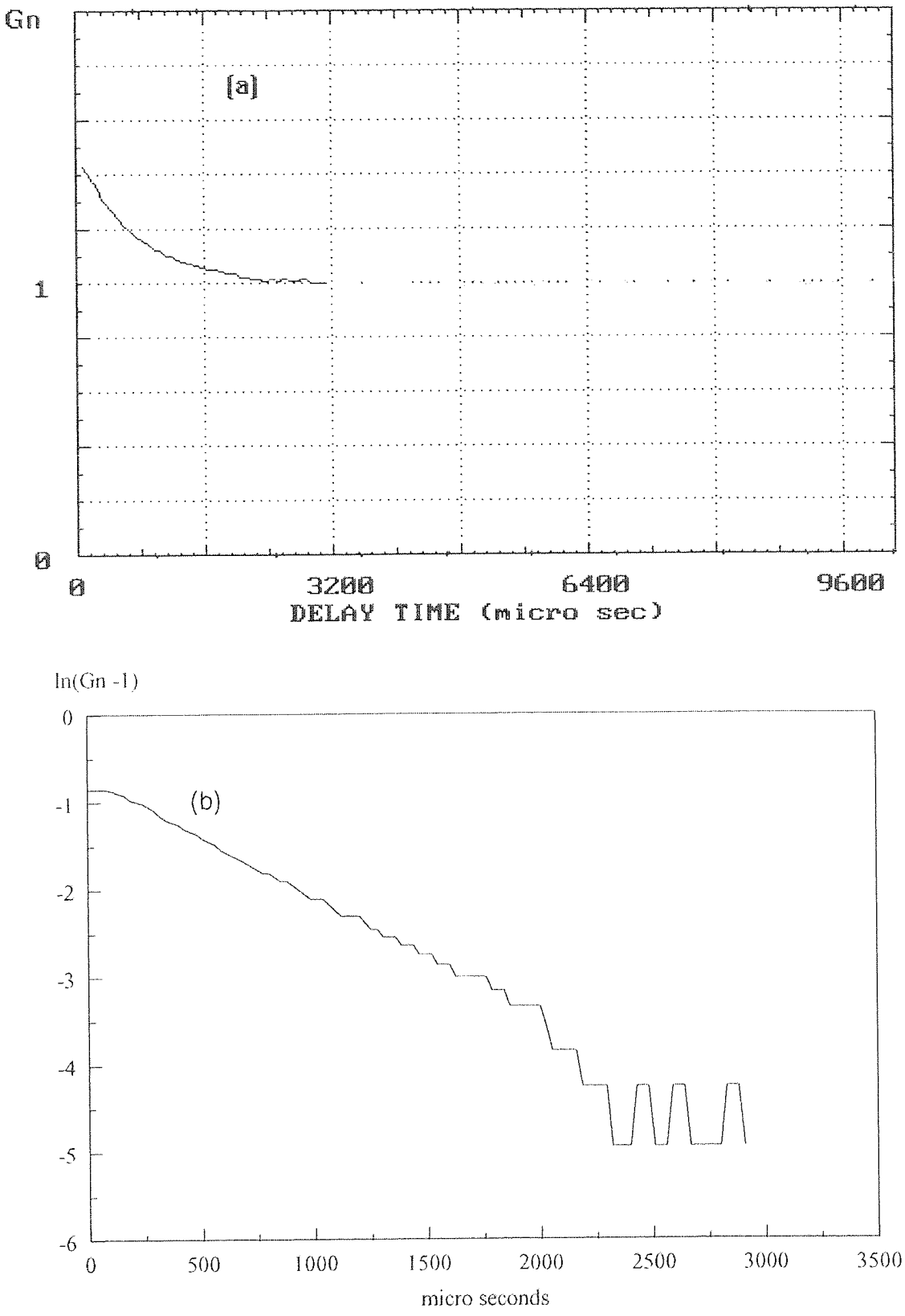

Figure A4 (a) Plot of the autocorrelation function from the data from the particle size standard. The image was imported into the MS Windows environment using the 'copy' and 'paste' commands. (b) ln plot of the autocorrelation function plotted from Lotus 1-2-3.

Table A20(a) DLS Spreadsheet data sheet

A	A	B	C	D	E	F
17	X cursor	micro secs	Y cursor	Gn	Gn - 1	ln (Gn - 1)
18	100	0	98	1.4285714	0.4285714	-0.847298
19	101	26.6667	98	1.4285714	0.4285714	-0.847298
20	102	53.3334	98	1.4285714	0.4285714	-0.847298
21	103	80.0001	98	1.4285714	0.4285714	-0.847298
22	104	106.6668	99	1.4214286	0.4214286	-0.864105
23	105	133.3335	101	1.4071429	0.4071429	-0.898591
24	106	160.0002	102	1.4	0.4	-0.916291
25	107	186.6669	105	1.3785714	0.3785714	-0.971351
26	108	213.3336	106	1.3714286	0.3714286	-0.990399
27	109	240.0003	107	1.3642857	0.3642857	-1.009817
28	110	266.667	109	1.35	0.35	-1.049822
29	111	293.3337	111	1.3357143	0.3357143	-1.091495
30	112	320.0004	114	1.3142857	0.3142857	-1.157453
31	113	346.6671	116	1.3	0.3	-1.203973
32	114	373.3338	117	1.2928571	0.2928571	-1.22807
33	115	400.0005	118	1.2857143	0.2857143	-1.252763
34	116	426.6672	120	1.2714286	0.2714286	-1.304056
35	117	453.3339	121	1.2642857	0.2642857	-1.330725
36	118	480.0006	122	1.2571429	0.2571429	-1.358123
37	119	506.6673	124	1.2428571	0.2428571	-1.415282
38	120	533.334	125	1.2357143	0.2357143	-1.445135
39	121	560.0007	126	1.2285714	0.2285714	-1.475907
40	122	586.6674	128	1.2142857	0.2142857	-1.540445
41	123	613.3341	129	1.2071429	0.2071429	-1.574347
42	124	640.0008	130	1.2	0.2	-1.609438
43	125	666.6675	131	1.1928571	0.1928571	-1.645806
44	126	693.3342	132	1.1857143	0.1857143	-1.683546
45	127	720.0009	133	1.1785714	0.1785714	-1.722767
46	128	746.6676	134	1.1714286	0.1714286	-1.763589
47	129	773.3343	135	1.1642857	0.1642857	-1.806148
48	130	800.001	135	1.1642857	0.1642857	-1.806148
49	131	826.6677	136	1.1571429	0.1571429	-1.8506
50	132	853.3344	137	1.15	0.15	-1.89712
51	133	880.0011	137	1.15	0.15	-1.89712
52	134	906.6678	138	1.1428571	0.1428571	-1.94591
53	135	933.3345	139	1.1357143	0.1357143	-1.997203
54	136	960.0012	140	1.1285714	0.1285714	-2.051271
55	137	986.6679	141	1.1214286	0.1214286	-2.108429
56	138	1013.3346	141	1.1214286	0.1214286	-2.108429
57	139	1040.0013	141	1.1214286	0.1214286	-2.108429
58	140	1066.668	142	1.1142857	0.1142857	-2.169054
59	141	1093.3347	143	1.1071429	0.1071429	-2.233592
60	142	1120.0014	144	1.1	0.1	-2.302585
61	143	1146.6681	144	1.1	0.1	-2.302585
62	144	1173.3348	144	1.1	0.1	-2.302585
63	145	1200.0015	144	1.1	0.1	-2.302585
64	146	1226.6682	145	1.0928571	0.0928571	-2.376693
65	147	1253.3349	146	1.0857143	0.0857143	-2.456736
66	148	1280.0016	146	1.0857143	0.0857143	-2.456736
67	149	1306.6683	147	1.0785714	0.0785714	-2.543747
68	150	1333.335	147	1.0785714	0.0785714	-2.543747
69	151	1360.0017	147	1.0785714	0.0785714	-2.543747
70	152	1386.6684	148	1.0714286	0.0714286	-2.639057
71	153	1413.3351	148	1.0714286	0.0714286	-2.639057
72	154	1440.0018	148	1.0714286	0.0714286	-2.639057
73	155	1466.6685	149	1.0642857	0.0642857	-2.744418
74	156	1493.3352	149	1.0642857	0.0642857	-2.744418
75	157	1520.0019	149	1.0642857	0.0642857	-2.744418
76	158	1546.6686	150	1.0571429	0.0571429	-2.862201
77	159	1573.3353	150	1.0571429	0.0571429	-2.862201
78	160	1600.002	150	1.0571429	0.0571429	-2.862201

Table A20(b) DLS Spreadsheet data sheet

A	A	B	C	D	E	F
79	161	1626.6687	151	1.05	0.05	-2.995732
80	162	1653.3354	151	1.05	0.05	-2.995732
81	163	1680.0021	151	1.05	0.05	-2.995732
82	164	1706.6688	151	1.05	0.05	-2.995732
83	165	1733.3355	151	1.05	0.05	-2.995732
84	166	1760.0022	151	1.05	0.05	-2.995732
85	167	1786.6689	152	1.0428571	0.0428571	-3.149883
86	168	1813.3356	152	1.0428571	0.0428571	-3.149883
87	169	1840.0023	152	1.0428571	0.0428571	-3.149883
88	170	1866.669	153	1.0357143	0.0357143	-3.332205
89	171	1893.3357	153	1.0357143	0.0357143	-3.332205
90	172	1920.0024	153	1.0357143	0.0357143	-3.332205
91	173	1946.6691	153	1.0357143	0.0357143	-3.332205
92	174	1973.3358	153	1.0357143	0.0357143	-3.332205
93	175	2000.0025	153	1.0357143	0.0357143	-3.332205
94	176	2026.6692	154	1.0285714	0.0285714	-3.555348
95	177	2053.3359	155	1.0214286	0.0214286	-3.84303
96	178	2080.0026	155	1.0214286	0.0214286	-3.84303
97	179	2106.6693	155	1.0214286	0.0214286	-3.84303
98	180	2133.336	155	1.0214286	0.0214286	-3.84303
99	181	2160.0027	155	1.0214286	0.0214286	-3.84303
100	182	2186.6694	156	1.0142857	0.0142857	-4.248495
101	183	2213.3361	156	1.0142857	0.0142857	-4.248495
102	184	2240.0028	156	1.0142857	0.0142857	-4.248495
103	185	2266.6695	156	1.0142857	0.0142857	-4.248495
104	186	2293.3362	156	1.0142857	0.0142857	-4.248495
105	187	2320.0029	157	1.0071429	0.0071429	-4.941642
106	188	2346.6696	157	1.0071429	0.0071429	-4.941642
107	189	2373.3363	157	1.0071429	0.0071429	-4.941642
108	190	2400.003	157	1.0071429	0.0071429	-4.941642
109	191	2426.6697	156	1.0142857	0.0142857	-4.248495
110	192	2453.3364	156	1.0142857	0.0142857	-4.248495
111	193	2480.0031	156	1.0142857	0.0142857	-4.248495
112	194	2506.6698	157	1.0071429	0.0071429	-4.941642
113	195	2533.3365	157	1.0071429	0.0071429	-4.941642
114	196	2560.0032	157	1.0071429	0.0071429	-4.941642
115	197	2586.6699	156	1.0142857	0.0142857	-4.248495
116	198	2613.3366	156	1.0142857	0.0142857	-4.248495
117	199	2640.0033	156	1.0142857	0.0142857	-4.248495
118	200	2666.67	157	1.0071429	0.0071429	-4.941642
119	201	2693.3367	157	1.0071429	0.0071429	-4.941642
120	202	2720.0034	157	1.0071429	0.0071429	-4.941642
121	203	2746.6701	157	1.0071429	0.0071429	-4.941642
122	204	2773.3368	157	1.0071429	0.0071429	-4.941642
123	205	2800.0035	157	1.0071429	0.0071429	-4.941642
124	206	2826.6702	156	1.0142857	0.0142857	-4.248495
125	207	2853.3369	156	1.0142857	0.0142857	-4.248495
126	208	2880.0036	156	1.0142857	0.0142857	-4.248495
127	209	2906.6703	157	1.0071429	0.0071429	-4.941642
128	210	2933.337	158	1	0	ERR
129	211	2960.0037	158	1	0	ERR
130	212	2986.6704	158	1	0	ERR
131	213	3013.3371	158	1	0	ERR
132	214	3040.0038	158	1	0	ERR
133	215	3066.6705	158	1	0	ERR
134	216	3093.3372	158	1	0	ERR
135	217	3120.0039	158	1	0	ERR
136	218	3146.6706	158	1	0	ERR
137	219	3173.3373	158	1	0	ERR
138	220	3200	158		0	0

ABBREVIATIONS

46900	Water dispersible formulation containing phenolic resin
BCS	2-butoxy ethanol
CP/MAS	Cross polarisation/ magic angle spinning
DLS	Dynamic light scattering
DLER100	'9' type epoxy resin prepared by HSC research laboratories
DMAE	dimethylaminoethanol
DOW XZ86762	Commercial '9' type epoxy resin
DPP	4,4'-isopropylidene diphenol
epoxy resin	reaction product of epichlorohydrin and DPP
Epoxy-graft-acrylic	polymer produced by reacting acrylic monomers onto an epoxy resin [5]
GEN 1	water dispersible formulation [5]
GPC	Gel permeation chromatography
HLT	Hydro-dynamic layer thickness
MWD	Molecular weight distribution
NBDI	(o-[p-nitrobenzyl]-N,N' [diisourea])
PW1, PW2	epoxy-graft-acrylic formulations based on GEN1
TEM	transmission electron microscopy
WRB621, 622, 623	epoxy-graft-acrylic formulations
WRB624, 625, 626, 633	water dispersible latices

REFERENCES

1. Statutory Instrument, 1988, no. 1657, Health and Safety. 'The Control of Substances Hazardous to Health regulations 1988'. ISBN 011 087 657 1.

2. 'Modified epoxy resins, processes for making and using same and substrates coated therewith' U.K. Patent 1,585,486, SCM Corp., (1977)

3. Robinson P.V., 'Design of water reducible polymers for use in food contact applications', J. Ctg Tech., **53**, 23-30, (1981)

4. Evans J.M., Ting V.W., 'Modified epoxy resins, processes for making and using same and substrates coated therewith' U.S. Patent 4,212,781, SCM Corp., (1980)

5. Woo J.T.K., Ting V., Evans J., Marcinko R., Carlson G., Ortiz C., 'Synthesis and characterisation of water-reducible graft epoxy copolymers' J.Ctg. Tech., **54**, 41-55, (1982)

6. 'Graft polymer compositions of terminated epoxy resin, processes for making and using same, and substrates coated therewith' U.S. Patent 1,585,487, SCM Corp., (1977)

7. Ting V.W., 'Aqueous dispersion polymerisation process and product' U.K. Patent 2,046,767, SCM Corp., (1977)

8. Ting V.W., 'Polymerisation process and product' U.S. Patent 4,285,847, SCM Corp., (1981)

9. Ting V.W., 'Polymer compositions and their production' European Patent 0,017,911, SCM Corp., (1980)

10. Ting V.W.,Woo J.T.K., Marcinko R.M., 'Base for a graft polymer, novel graft polymer composition, solvents and water-reducible coatings incorporating the novel graft polymers and processes' U.S. Patent 4,399,241, SCM Corp., (1983)

11. Winner P.P., 'Aqueous polymeric blends' U.S. Patent 4,487,861, SCM Corp., (1984)

12. Patzschke H.P., Luettenberg A., Schlinsog H.J., Bogdan W., 'Water-borne thermo-setting coatings' Ger.Offen., 3,601,560, Herberts, (1987)

13. Owens P.M., 'Stabilised aqueous epoxy acrylic coatings containing Zinc Oxide and C-4 alkylated urea dispersants' U.S. patent 4,703,071, Glidden Corp., (1987)

14. Ting V.W., Marcinko R.M. 'Aqueous epoxy ester emulsions' U.S. Patent 480,058, SCM Corp., (1984)

15. Georglas N., 'Water-dilutable coating composition and its use for coating ontainers' Ger.Offen., 3,446,178, Inmont, (1985)

16. Brown G.L., Spencer A.T., 'Aqueous coating composition comprising self-emulsfiable ester of epoxy and acid containing addition polymer' U.S. Patent 4,547,535, SCM Corp., (1985)

17. Chu S.C., Spencer A.T., 'Aqueous coatings comprising dispersible epoxy resin acid polymer ester and diluent polymer' U.S. Patent 4,446,258, Mobil, (1984)

18. Seiler H.K., Sommerfeld E.G., 'Electrocoating with water-borne compositions made from epoxy resin, a polymeric acid and a tertiary amine' U.S.Patent 4,3,03,488, du Pont, (1981)

19. Matthews J.F., Sommerfeld E.G., 'Water-borne coating composition made from epoxy resin, polymeric acid and tertiary amine' U.S. Patent 4,247,439, du Pont, (1981)

20. Chu S.C., Spencer A.T., McCarty W.H., 'Aqueous coating compositions' European Patent 0,116,225, Mobil, (1984)

21. Suzuki H. Kuno T., Yasuo Y., Okagami K., 'Epoxy resin-acrylic resin based aqueous coating compositions' U.K. Patent 2,068,967, Toyo, (1981)

22. Harper R.L., Obetz J.E., Steinmatz W.H., 'Water-borne coating composition made from Epoxy resin, polymer acid, amine and second polymeric acid' Int. Appl. WO/83/3613, du Pont, (1983)

23. Suzuki H., Kuno T., Yoshimura Y, Okugami K., 'Aqueous resin based coating composition', Fr. Demande 2,476,108, Toyo, (1981)

24. Suzuki H., Kuno T., Yoshimura Y, Okugami K., 'Aqueous resin coating compositions' Ger. Offen. 3,006,175, Toyo, (1981)

25. Winner P.P., Martino P.C., 'Aqueous self-curing polymeric blends' European Patent 0.096,197, SCM Corp, (1984)

26. Sekmakas K., Shah R., 'Copolymerisation in water soluble polyol with controlled reaction with the polyol and aqueous coatings containing the resulting solution' U.S. Patent 4,193,904, De Soto, (1980)

27. Christensen R.M., 'Coated metal surfaces and method of coating metal surfaces with aqueous resinous dispersions of epoxy and acrylic polymers', U.S. Patent 4,335,829, PPG, (1982)

28. Steinmetz W.H., 'Water-borne coating composition made from modified epoxy resin, polymeric acid and tertiary amine', U.S. Patent 4,302,373, du Pont, (1981)

29. Christensen R.M., Maska R., Dowbenko R., Hockswender T.R., ' Base-solubilised acrylic polymers and aqueous resinous dispersions of acrylic polymers and epoxy resins', U.S. Patent 4,289,674, PPG, (1981)

30. Sekmakas K., Shah R., 'Water soluble epoxy ester copolymers for interior can use', U.S. Patent 4,294,737, De Soto, (1981)

31. Sekmakas K., Shah R., 'Water soluble esters of epoxides for coating the interior of cans', Belg. Be 0,886,863 De Soto, (1981)

32. Perine D.R., Lucas P.A., 'Aqueous epoxy phosphate dispersions comprising n-butanol, n-hexanol and ethylene glycol monobutyl ether', U.S. Patent 4,316,922, Dow, (1982)

33. Winner P.P.,' Phosphate epoxy acrylic copolymers', U.S. Patent 4,600,754, SCM, (1986)

34. Winner P.P., Woo J.T.K., 'Aqueous self curing polymeric blends' U.S. Patent 4,487,860, SCM, (1984)

35. Abbey K.J., 'One-package coreactive amino and oxirane polymers', U.S. patent 4,367,298, SCM Corp., (1983)

36. Abbey K.J., Erickson J.R., 'Epoxy modified emulsion polymers', U.S. Patent 4,522,962, SCM Corp., (1985)

37. Castteilucci N.T., Grunewalder J.F., 'Base solubilisation of an azole functional resin and electrodeposition of such solubilised resin' U.S. Patent 4,360,614, PPG Ind., (1982)

38. Shimp D.A., 'Soluble resinous products of polyepoxide-amine adducts and cyclic dicarboxylic acid anhydrides', U.S. Patent 4,176,221, Celanese (1979)

39. van Ipren R., van der Mark J.M., Kooijmans P.G., 'Preparation of cationic coating compositions for food and beverage can interiors', European patent, 0,261,715, (1985)

40. Hart T.J., Dowbenko R., Rotslaw M.R., van Buskirk E.J., Tetenbaum M.T., 'Resinous blends of epoxy and acrylic resins and their use in electro- deposition', U.S. Patent 4,605,476, PPG Ind., (1986)

41. Georglas N., Keaveney W.P., 'Water-borne epoxy-phenolic coating compositions', U.S. Patent 4,341,678, Inmont, (1982)

42. Shimp D.A., Hicks D.D., Graver R.B., 'Two component resin coating systems and compositions and coating processes using them', European Patent 0,024,914, Celanese, (1980)

43. Shimp D.A., 'Water reproducible coating composition', European Patent 0,065,860, Celanese, (1982)

44. Shimp D.A., 'Ether-ester water reducible coating compositions' U.S. Patent 4,360,613, Celanese, (1982)

45. Powers E.J., Walsh T.E., Stewart D.R., 'Water reducible epoxy based coating composition', U.S. Patent 4,452,929, Celanese, (1984)

46. G.L. Brown, Spencer A.T., 'Aqueous can coatings of improved impermeability', U.S. Patent 4,195,005, Mobil, (1980)

47. You-ling Fan, 'Improved vinyl or vinylidene chloride resin metal coating compositions; method for their production and articles coated therein', U.K. Patent 2,065,141, Union Carbide, (1981)

48. Martino P.C., 'Thermosetting emulsion polymers prepared by a two stage process and their coatings' European patent 0,256,391, Glidden, (1988)

49. Shelley R.R., 'Stable aqueous dispersions of mixed resins', European Patent 0,034,913, Celanese, (1980)

50. Alutto P.F., Drees P.A., 'Aqueous organic coatings for metal surfaces', U.S. Patent 4,222,919, Inmont, (1980)

51. Bovey F.A. 'The characterisation of polymers by nuclear magnetic resonance spectroscopy', ACS polymer preprints, **31**, 95-96, (1990)

52. Afremow L.C., 'An introduction to Nuclear Magnetic Resonance Spectroscopy and its applications in the coatings industry', J. Paint Tech., **40**, 503-521, (1968)

53. Sojka S.A., Moniz W.B., 'The curing of an epoxy resin as followed by carbon-13 NMR spectroscopy', J.Appl.Polym.Sci., **20**, 1977-1982, (1976)

54. Fischer A., Schlothauer K., Pfitzman A., 'Carbon-13 liquid- and solid-state nuclear magnetic resonance and infra-red studies of amine-cured epoxy resins', Polymer, **33**, 1370-1373, (1992)

55. Gallouedec F., Costa-Torro F, Lauprete F., Jasse B.. 'Fourier transform infra-red and ^{13}C-NMR spectroscopic characterisation of model epoxy networks',J.Appl. Polym.Sci., **47**, 823-832, (1993)

56. Woo J.T.K., Toman A.,'Water-based epoxy-acrylic graft copolymer', Progr. Org. Chem., **21**, 371-385, (1993)

57. Sterna L.L., Smith H.C., 'Applications of high temperature magic-angle spinning to the analysis of amorphous, insoluble polymers', J.Mag.Res, **79**, 528-533, (1988)

58. Hirst R.C., Grant D.M., Hoff R.E., Burke W.J., 'Structural study of phenol-formaldehyde polymers with proton magnetic resonance', J.Polym.Sci. Part A, **3**, 2091-2105, (1965)

59. Carothers J.A., Gipstein E., Fleming W.W., Tompkins T., 'Determination of the structural configuration of cresol-novalac resins by C-13 NMR Spectroscopy', J.Appl. Polym. Sci., **27**, 3449-3454, (1982)

60. Walker L.E., Dietz E.A., Wolfe R.A., Dannels B.F., Sojka S.A., 'Carbon-13 NMR of phenolic resins: Positional isomers of bis(hydroxybenzyl) phenols and tris(hydroxy) phenols', ACS Polymer Preprints, **24**, 177-178, (1983)

61. Fitzgerald E.A., Tadros S.P., Almeida R.F., Sienko G.A., Honda K., Sariubbi T., 'Determination of methylene bridge type of mixed meta- and para-cresol formaldehyde novolaks by 13C-NMR spectroscopy', J.Appl.Polym.Sci., **45**, 363-370, (1992)

62. Woodbrey J.C., Higginbottom H.P., Culbertson H.M., 'Proton magnetic resonance study on the structures of phenol- formaldehyde resins', J.Polym.Sci. Part A, **3**, 1079-1106, (1965)

63. King P.W., Mitchell R.H., Westwood A.R., 'Structural analysis of phenolic resole resins', J.Appl.Polym.Sci., **18**, 1117-1130, (1974)

64. Dawbarn M., Ebdon J.R., Hewitt S.J., 'Examination of melamine- formaldehyde adducts by C-13 NMR', Polymer, **19**, 1309-1312, (1978)

65. Taylor R., Pragnell R.J., McLaren J.V., Snape C.E., 'Evaluation of NMR Spectroscopy for the quantitative characterisation of urea-formaldehyde resins', Talanta, **29**, 489-494, (1982)

66. Meyer B., Nunlist R., 'C-13 NMR identification of urea-formaldehyde resins', ACS Polymer Preprints, **22**, 130-131, (1981)

67. Maciel G.E., Szeverenyi N.M., Early T.A., Myers G.E., ' 13C NMR studies of solid urea-formaldehyde resins using Cross Polarisation and Magic Angle Spinning', Macromolecules, **16**, 598-604, (1983)

68. Ebdon J.R. , Heaton P.E., Huckerby T.N., O'Rourke W.T.S., Parkin J., 'Characterisation of urea- fomaldehyde and melamine- formaldehyde adducts and resins using 15N NMR Spectroscopy', Polymer, **25**, 821-825, (1984)

69. Yeagle M.L., 'Quantitative analysis of polymers by NMR', J. Paint Tech., **42**, 472-482, (1970)

70. Hvilsted S., Jorgensen N.U., 'Polyol structural elucidation in binder polyesters. 1. 13C NMR study of fundamental polyols in aliphatic and aromatic polyesters', Polymer Bulletin, **10**, 236-243, (1983)

71. Hvilsted S., 'C-13 NMR analysis of crosslinking sites in branched polyesters', Polymer Networks, 243-254, Elsevir, (1988)

72. Bovey F.A., Tiers G.V.D., Filipovich G., 'Polymer NSR Spectroscopy. I. The motion and configuration of polymer chains in solution', J. Polymer. Sci., **38**, 73-90, (1959)

73. Bovey F.A., Tiers G.V.D., 'Polymer NSR Spectroscopy. II. The high resolution spectra of methyl methacrylate polymers prepared with free radical and anionic initiators', J. Polymer Sci., **44**, 173-182, (1960)

74. Frisch H.L., Mallows C.L., Heatley F., Bovey F.A. 'On the stereoregularity of vinyl polymer chains. II'., Macromolecules, **6**, 533-537, (1968)

75. Kozluk T., Spychaj T., Hamielec A., 'Compositional analysis of styrene- acrylic acid copolymers by ^{1}H NMR', Makromol.Chem., **188**, 1951-1957, (1987)

76. McBrierty V.J., 'NMR Spectroscopy of polymers in the solid state', 397-428, Polymer Science, Pergamman, 1989

77. Cudby M.E.A., 'C-13 High resolution NMR in solids', European Spectroscopy news, **78**, 18-24, (1988)

78. Abraham R.J., Fisher J., Loftus P., 'Introduction to NMR Spectroscopy', Wiley, 1988

79. Kitamaru R., Horli F., Nakagawa M., 'Phase structure of lamellar crystalline polyethylene by solid state high resolution C-13 NMR: Detection of crystalline-amorphous interphase by H-1 spin decoupling', Polymer Preprints, **28**, 58, (1987)

80. Dickinson L.C., Chu C.W., Yang H., Chien J.C.W., 'Compatability and phase composition in blends of styrenic polymers with poly(2,6 dimethyl phenylene oxide) and with poly(vinyl methyl ether) by CP-MAS C-13 NMR', Polymer Preprints, **28**, 112, (1987)

81. Belfiore L.A. , Qin C., Pires A.T.N., Ueda E., 'Macromolecular phase behaviour via carbon-13 solid state NMR', Polymer Preprints, **31**, 170, (1990)

82. Periyasamy M., Ford W.T., 'CP-MAS C-13 NMR spectra of styrene-divinyl benzene copolymer networks', Proceedings of the ACS Div. of Polym. and Eng., **56**, 184-187, (1987)

83. Franses E.I., Miller W.G., 'Molecular motion and phase behaviour of a double- tail sulphonate surfactant by NMR', J. Colloid and Interface Science, **101**, 500-510, (1984)

84. Lyrela J.R., Economy J., Maresch G., Muhlebach A., Yannoni C.S., Fyfe C.A., 'Molecular motion in the monopolyesters of 4-hydroxybenzoic acid', Polymer Preprints, **30**, 534-535, (1989)

85. Gent M.P.N., Prestegard J.H., 'Nuclear Magnetic relaxation and molecular motion in phospholipid bilayer membranes', J. Magnetic Resonance, **25**, 243-262, (1977)

86. Masood A.K.M., Pethrick A., Barlow A.J., Kim M.G., Pliec R.P., Ladd J.A., Barraclough D., 'A comparison of the dielectric, acoustic, NMR and viscoelastic relaxation properties of supercooled liquids-cyclic carbonates', Advances in Molecular relaxation processes, **9**, 29-46, (1976)

87. Spraul M, 'Improvement for water suppression in 1H NMR', Bruker report, **1**, 9-13, (1988)

88. Yau W.W., Kirkland J.J., Bly D.D., 'Modern Size-Exclusion liquid chromatography', John Wiley and Sons, New York, 1979

89. Canales, 'Advanced calibration and calculations for size exclusion chromatography', Int.Lab., March, 38-48, (1990)

90. Grubisic Z., Rempp P., Benoit H,. 'A universal calibration for gel permeation chromatography', J.Polym.Sci., Polym.Lett., **5**, 753-759, (1967)

91. Rudin A., Hoegy H.L.W., 'Universal calibration in GPC'. J.Polym.Sci., A-1, **10**, 217-235, (1972)

92. Bianchi U., Peterlin A., ' Intrinsic viscosity of polymers of low molecular weight', J.Polym.Sci., A-2, **6**, 1759-1772, (1968)

93. Zinbo M., Parson J.L., 'Practical Gel Permeation Chromatographic column calibration for polymers', J.Chrom., **55**, 55-64, (1971)

94. Moore J.M., Physical Chemistry, Fifth Edition, Longman, (1987)

95. Glasstone & Lewis, Elements of Physical Chemistry, 2nd Edition Macmillan Press, (1976)

96. Riedl B.,Vohl M.J., Calve L., 'Molecular size and solvation of low molecular weight poly(ethylene oxide), J.Appl. Polym. Sci., **39**, 341-353, (1990)

97. Honma T., Tazaki M., 'Recent development in gel permeation chromatography and GPC-low-angle light scattering', Int. Polym. Sci. Tech., **15**, 56-62, (1968)

98. Haney M.A., Mooney C.E., Yau W., 'A new right angle laser light scattering detector for size exclusion chromatography in the triple detector configuration (SEC/RI-viscomter- LALLS)', Int. Labmate, **17**, 31-33, (1992)

99. Kasparkova V., Ommundsen E., 'Determination of molar mass and radius of gyration with on-line viscometer and multi-angle laser light scattering. High temperature characterisation of polystyrene', Polymer, **34**, 1765-1767, (1993)

100. Rinaudo M., Rochas C., 'Application of gel permeation chromatography to polyelectrolytes: Salt rejection mechanism and molecular weight distribution' J.Polym. Sci., Polym. Phys. Ed., **17**, 673-681, (1979)

101. Kim M.G., Amos L.W., Barnes E.E.. 'Study of the reaction rates and structures of a phenol-formaldehyde resol resin by carbon-13 NMR and gel permeation chromatography', Ind. Eng. Chem. Res., **29**, 2032-2037, (1990)

102. Malfait T., Slootmaekers D., Cauwelaert F.van,. 'High performance size exclusion chromatography of anionic polymers in aqueous solution', J.Appl.Polym. Sci., **39**, 571-581, (1990)

103. Guest M.J., Hancox N.L., 'Gel permeation chromatography techniques for the characterisation of polymeric materials with particular emphasis on epoxy resins and poly(methyl methacrylate)', Materials development division, AERE Harwell, ISBN 0-7058-0858-0

104. Eastmond G.C., Harvey L.W., 'The characterisation of polycarbonate containing graft copolymers and the kinetics of graft polymerisation', British Polym. J., **17**, 275-286, (1985)

105. Runyon J.R., Barnes D.E., Rudd J.F., Tung L.H., 'Multiple detectors for molecular weight and compositional analysis of copolymers by gel permeation chromatography', J.Appl.Polym. Sci., **13**, 2359-2369, (1969)

106. Chang F.S.C, 'Molecular weight analysis of block copolymer by gel permeation chromatography', J.Chromatog., **55**, 67-71, (1971)

107. Eastmond G.C., Parr K.J., Woo J., 'The synthesis of block copolymers:3. The use of functionalized polystyrene as a macroinitiator for free radical polymerisation' Polymer, **29**, 950-957, (1988)

108. Eastmond G.C., Grigo J., 'Formation of block copolymers by a combination of group transfer and free-radical polymerisations' J.Makromol.Chem., rapid commun., **7**, 375-379, (1986)

109. 'Investigation of compositional drift in a multi-component acrylic oligomer', McMaster Institute for polymer production technology, technical report 1986.

110. Teramachi S., Hasegawa A., Akatsuka M., Yamashita A., Takemoto N., 'Molecular weight distribution and correlation between chemical composition and molecular weight in a high conversion copolymer of styrene- methyl acrylate', Macromolecules, **11**, 1206-1210, (1978).

111. Meehan E., McConville J.A., Warner F.P., WilliamsA.G., 'Copolymer analysis using spreadsheet software' Polymer Laboratories poster, Pittsburgh Conference (1990)

112. Tompkins M.A., 'A stopped flow wavelength scanning system for HPLC' Int.Lab., March, 36-46, (1984)

113. Fielden P.R., 'Recent developments in LC detector technology' J.Chrom. Sci., **30**, 45-52, (1992)

114. Cahill J., Retzik M., 'A high performance photodiode array UV/Vis spectrophotometer' Int.Lab., May, 48-56, (1985)

115. Bunger H., Meister A., Otto M., 'Aromatic ring type analysis of complex hydrocarbon mixtures by high performance liquid chromatography with photo-diode array detection and curve resolution' J.Chromatogr., **520**, 383-389, (1990)

116. Yost R., Stoveken J., MacLean W., 'Positive peak indentifying in liquid chromatography using absorbance ratioing with a variable wavelength spectrophotometric detector' J.Chrom., **134**, 73-82, (1977)

117. Keller H.R. Massart D.L. 'Peak purity control in liquid chromatography with photodiode array detection by a fixed size moving window evolving factor analysis' Analytica Chimica Acta. **246**, 379-390, (1991)

118. Herman F.L., 'Tandem detectors to quantitate overlapping chromatographic peaks', Anal, Chem., **65**, 1023-1027, (1993)

119. Li J.B., Hillier E, Cotter R.L., 'A new programmeable multi-wavelength HPLC detector' J.Chrom. Sci., **23**, 446-449, (1985).

120. Wright A.G., Fell A., Berridge J.C., 'Computer aided optimisation with photodiode array detection in HPLC' Anal.Proc., **25**, 300-303, (1988)

121. Cladera A., Gomez E., .Estela J.M, V.Cerda., 'Multicomponent analysis of highly overlapped HPLC peaks using multiwavelength diode array detection', J.Chromatogr. Sci., **30**, 453-458, (1992)

122. Jurs P.C., Isenhour T.L., Wilkins C.L., ' BASIC programming for chemists; an introduction' Wiley Interscience, 1987

123. Vernin G., Channon M., 'Computer aids to chemistry'

124. Davies T., 'Chemometrics: software survey' Spectroscopy world, **6**, 33-34, (1991)

125. Bauman R.P., 'Absorption spectroscopy', Wiley, 1972

126. Crocombe R.A., Olsen M.L., Hill S.L., 'Quantitative Fourier transform infrared methods for real complex samples' Computerised quantitative infrared analysis Ed. G.L.McClure STP934 ASTM, 1987

127. Teramachi S., Hasegawa A., Shima Y., Akatsuka M., Nakajima M., 'Separation of styrene-methyl acrylate copolymer according to chemical composition using high- speed liquid chromatography' Macromolecules, **12**, 992-996, (1979)

128. Glockner G, Van den Berg J.H.M. 'Copolymer fractionation by gradient high-performance liquid chromatography' J.Chromatogr., **384**, 135-144, (1987)

129. Glockner G, 'Characterisation of chemically heterogeneous polymers using high performance liquid chromatography: A summary' J.Appl.Polym.Sci., Appl. Polym. Symp., **51**, 45-54, (1992)

130. Mori S. 'Determination of chemical composition and molecular weight distributions by high-conversion styrene-methyl methacrylate copolymers by liquid adsorption and size exclusion chromatography', Anal. Chem., **60**, 1125-1128, (1988)

131. Mori S. 'Dependence of ester type on the separation of styrene- acrylate and styrene- methacrylate copolymers by liquid adsorption chromatography', J.App. Polym. Sci., Appl. polym. Symp., **45**, 71-85, (1990)

132. Glockner G., Stickler M., Wunderlich W., 'Separation of stat-copoly (styrene /2-methoxyethyl methacrylate) samples according to composition by gradient high performance liquid chromatography' J.Appl.Polym.Sci., **37**, 3147-3161, (1989)

133. Sato H., Ogino K., Marou S., sasaki M., 'Separation of styrene-methacrylate copolymers by composition using normal and reversed phase high performance liquid chromatography', J.Polym.Sci.Part B:Polym Phys., **29**, 1073-1080, (1991)

134. van Doremaele G.H.J., Geerts F.H.J.M., ann de Meulen L.J., German A.L., 'Molar mass chemical composition distributions of styrene - methyl acrylate copolymers prepared by solution or emulsion polymerisation' Polymer, **33**, 1512-1518, (1992)

135. E.L.Johnson, R.Gloor, R.E.Majors, 'Coupled column chromatography employing exclusion and reversed phase: A potential general approach to sequential analysis', J.Chromatogr., **149**, 571-585, (1978)

136. Kato K., 'Osmium tetroxide fixation of rubber latices', J. Polym. Sci., Polym. Lett. Ed., **4**, 35-38, (1966)

137. Kato K., 'The Osmium tetroxide procedure for light and electron microscopy of ABS plastics', Polym. Eng. Sci., 7, p38-39, (1967)

138. Vitali R., Montani E., 'Ruthenium tetroxide as a staining agent for unsaturated and saturated polymers', Polymer, **21**, 1220-1222, (1980)

139. Dimonie V., 'Core-shell emulsion copolymerisation of styrene and acrylonitrile on polystyrene seed particles', J. Polym. Sci., **22**, 2198-2215, (1984)

140. Sundberg D.C., 'Morphology development of polymeric microparticles in aqueous dispersion- The role of interfacial thermodynamics' 19th Annual Short course 'Advances in Emulsion Polymerisation and latex technology' Lehigh University (1988)

141. Joseph E.G., Aguilera J.M., Houle J.R., 'The use of ruthenium trichloride/ aqueous clorox mixture as a staining agent in the morphological studies of styrene macromer containing acrylate', Polym. Preprints, **28**, (2), 345-346, (1987)

142. Vanderhoff J.W., DiStefano F.V., El-Aasser M.S., O'Leary R., Shaffer O.M., Visioli D.L., 'Inverse emulsion polymerisation of acrylamide: Polymerisation kinetics and process development' J. Dispersion Sci. and Tech., **5**, 323-363, (1984)

143. Vanderhoff J.W., Visioli D.L., El-Aasser M.S., 'Inverse emulsion polymerisation of acrylamide: anomalous behaviour of tetronic 1102 emulsifier' 19th Annual Short course 'Advances in Emulsion Polymerisation and latex technology' Lehigh University, 1988

144. Misra S.C., 'Batch and semi-continuous emulsion polymerisation of vinyl acetate-butyl acrylayte. I.', J.Polym. Sci., **21**, 2363-2382, (1983)

145. Bucknall C.B. 'Toughened plastics: Materials Science Series' Applied Science Publishers, 1977

146. Ishikawa S., Ishizu K., Fukotmii T., 'New staining technique for distinction between crystalline and amorphous parts in transmission electron microscopy of poly(tetrahydrofuran), Polymer Communications, **31**, 407-408, (1990)

147. Armes S.P., Aldissi M., ldzorek G.C., Keaton P.W., rowton L.J., Stradling G.L., Collopy M.T., Mccoll D.B., 'Particle size distributions of polypyrolle colloids', J. Coll.Int. Sci., **141**, 119-126, (1991)

148. Chen Y., Dimonie V., El-Aaasser M.S., 'Particle morphology in artificial composite latex systems', J.Appl. Polym. Sci., **46**, 691-707, (1992)

149. Smith S.D., DeSimone J.M., Huang H., York G., Dwight D.W., Wilkes G.L. McGrath J.E., 'Synthesis and characterisation of poly(methyl methacrylate)-g-poly (methyl siloxane) copolymers 1. Bulk and surface characterisation', Macromolecules, **25**, 2575-2581, (1992)

150. Koppel D.E.,'Analysis of macromolecular polydispersity in intensity correlation spectroscopy: The method of Cumulants' , J.Chem Phys., **57**, 4814-4820, (1972)

151. Schmitz K.S., 'Dynamic Light Scattering by macromolecules', Academic Press, 1990

152. Herrington T.M., Midmore B.R., 'Determination of rate constants for rapid coagulation of polystyrene microspheres using Photon Correlation Spectroscopy' J. Chem. Soc., Faraday Trans., **85**, 3529-3536, (1989)

153. Hemker D.J., Frank C.W., 'Dynamic Light scattering studies of the fractal aggregation of poly(methacrylic acid) and poly(ethylene glycol)', Macromolecules, **23**, 4404-4410, (1990)

154. Douglas S.J., Illum L., Davis S.S., Kreuter J., 'Particle size and distribution of poly(butyl-2-cyanacrylate) nanoparticles', J. Colloid and Interface Sci., **10**, 149-158, (1984)

155. Killman E., Sapuntzjis P., Maier H., 'Dynamic light scattering for characterisation of lattices', Makromol. Chem., Macromol.Symp., **61**, 42-58, (1992)

156. Polverari M, van de Ven T.G.M., 'Dynamic light scattering of suspensions of PEO-coated latex particles', Coll. & Surf. A:Physiochemical and engineering aspects, **86**, 209-228, (1994)

157. Mekras C.I., George M.H., Barrie J.A., 'Synthesis and characterisation of poly-(urethane-g-acrylic acid)s', Polymer, **30**, 745-751, (1989)

158. Haslam J., Willis H.A., 'Identification and analysis of Plastics', Iliffe Books Ltd, (1965)

159. An Infrared spectroscopy atlas for the coatings industry', Federation of societies for coatings technology, 4th Ed., (1991)

160. Hummel D., Scholl F.K., 'Infra-red analysis of Polymers, resins and additives. An atlas', Carl Hanser, Munich, (1972)

161. Computerised Quantitative Infrared analysis. Ed. G.L.McClure, ASTM, (1987)

162. Fourier transform infrared spectroscopy in colloid and interface sciecne. Ed. D.R. Schering. ACS, (1991)

163. Chittur K.K. 'FTIR spectroscopy/ATR studies of protein adsorption in flowing systems' J.Coll.Int.Sci., **111**, 419-433, (1986)

164. Umemura J., Cameron D.G., Mantsch H.H., 'FTIR study of micelle formation in aqueous sodium n-hexanoate solutions', J.Phys.Chem., **84**, 2272-2277, (1980)

165. Cosgrove T., Prestidge C.A., King S.M., Vincent B., 'Fourier Transform infrared spectroscopy and Monte Carlo studies on the dynamics of physisorbing and chemisorbing polymers', Langmuir, **8**, 2206-2209, (1992)

166. Cable K.M., Moore R.B., ' FTIR investigations of ionic interactions in perfluoro-sulphonate ionomers containing hydrophobic counterions', Polymer preprints, **33**, April, (1992)

167. Kornum L.O. 'Evaporation and water-dilutable coatings', J.Oil Col.Chem. Assoc., **63**, 103-123, (1980)

168. Dodin M.G. 'Kinetics of solvent desorption from poly(vinyl alcohol) films', J.Coat. Tech., **53**, 41-49, (1981)

169. Hensen W.A., Taber D.A., Bradford E.B., 'Mechanism of film formation of latex paint', Ind.Eng. Chem., **45**, 735-739, (1953)

170. Dillon R.E., Matheson L.A., Bradford E.B., 'Sintering of synthetic latex particles', J.Coll.Int.Sci., **6**, 108-117, (1951)

171. Brown G.L., 'Formation of films from polymer dispersions', J.Polym.Sci, **22**, 423-434, (1956)

172. Voyutski S.S., 'Amendment to the papers by Bradford, Brown, and co-workers: 'concerning mechanism of film formation from high polymer dispersions', J.Polym.Sci., **32**, 528-530, (1958)

173. Sheetz D.P., 'Formation of films by drying of latex', J.Appl.Polym.Sci., **9**, 3759-3773, (1965)

174. Vanderhoff J.W., Tarkowski H.L., Jenkins M.C., Bradford E.B. 'Theoretical considerations of the interfacial forces involved in the coalescence of latex particles', J. Macromol. Chem., **1**, 361, (1966)

175. Eckersley S.T., Rudin A., 'Mechanism of film formation from polymer latexes', J.Coatings Tech., **62**, 89-100, (1990)

176. Winnik M.A., Wang Y., Haley F., 'Latex film formation at the molecular level: The effect of coalescing aids on polymer diffusion', J.Coatings Tech., **64**, 51- 61, (1992)

177. Wang Y., Zhao C., Winnik M.A., 'Molecular diffusion and latex film formation: An analysis of direct nonradiative energy transfer experiments', J.Chem. Phys., **93**, 2143-2153, (1991)

178. Dobler F., Pith T., Lambla M., Holl Y., 'Coalescence mechanisms of polymer colloids, 1. coalescence under the influence of particle-water interfacial tension' J.Coll.Int.Sci., **152**, 1-11, (1992)

179. Dobler F., Pith T., Lambla M., Holl Y., 'Coalescence mechanisms of polymer colloids, 2. coalescence with evaporation of water', J.Coll.Int.Sci., **152**, 12-21, (1992)

180. van Dent A., te Nijenhuis K., 'Turbidity study of thi process of film formation of polymer particles in drying thin films of acrylic latices', J.Coll.Int.Sci., **150**, 97-114, (1992), 806-821, (1992)

181. Chevalier Y., Pichot C., Graillat C., Joanicot M., Wong K., Maquet J., Linder P., Cabane B., 'Film formation with latex particles', Colloid Polym. Sci., **270**, 806-821, (1992)

182. Ellgood B., 'Recent advances in vinylidene chloride copolymers for surface coatings', J.Oil Col.Chem.Assoc., **68**, 164-169, (1985)

183. Myers R.R, Schultz R.K., 'Acrylic latex film formation in the critical temperature range', J.Appl.Polym.Sci., **8**, 755-764, (1964)

184. Coa T., Xu Y., Wang Y., Chen X., Zheng A., 'Effects of monomer feed methods in emulsion polymerizations and hydrophilicity of monomers on morphology of latex particles and their minimum film forming temperatures', Polym. Internat., **32**, 153-158, (1993)

185. Devon M.J., Gardon J.L., Roberts G., Rudin A., 'Effects of core-shell latex morphology on film forming behaviour', J.Appl.Polym.Sci., **39**, 2119-2128, (1990)

186. Morgan L.W., 'Multifeed emulsion polymers: The effects of monomer feed sequence and the use of seed emulsion polymers', J.Appl.Polym.Sci., **27**, 2033-2042, (1982)

187. Matsuo M., Sagae S., Asai H., 'Fine structures of styrene-butadiene block copolymer films cast from toluene solution', Polymer, **10**, 79-87, (1969)

188. Bates F.S., Berney C.V., Cohen R.E., 'Microphase structure of solvent-cast diblock copolymers and copolymer-homopolymer blends containing spherical microdomains', Macromolecules, **16**, 1101-1108, (1983)

189. Glauert A.M. 'Epoxy resins: An update on their selection and use'. Microcopy and Analysis, 15-20, (1991)

190. Lewis P.R., Price C., 'Morphology of ABA block polymers',Nature, **223**, 494-495, (1969)

191. Lewis P.R., Price C., 'The morphology of (styrene)x,(butadiene)y,(styrene)x block copolymers', Polymer, **12**, 258-271, (1971)

192. Lewis P.R., Price C., 'Electron microscopy of sym-SBS block polymers', Polymer, **13**, 20-26, (1972)

193. Kanig G., Neff N., 'Ein Neues kontrastierverfahren fur die elektron-mikroskopische untersuchung von saure- und ester-gruppenhaltigen polymersystemen', Colloid and Polym. Sci., **253**, 29-31, (1975)

194. Misra S.C., Pichot C., El-Aasser M.S., Vanderhoff J.W., 'Effect of emulsion polymerisation process on the morphology of vinyl acetate-butyl acrylate copolymer latex films', J. Polym. Sci., Polym. lett. Ed., **17**, 567-572, (1979)

195. Misra S.C., Pichot C., El-Aasser M.S., Vanderhoff J.W. , 'Batch and semi-continuous emulsion polymerisation copolymerisation of vinyl acetate-butyl acrylate II', J. Polym. Sci., **21**, 2383-2396, (1983)

196. Kanig G., 'Ein neues kontrastierverfahren fur die elekronmikroskopische untersuchung von polyathylen', Kolloid-Z. u.Z Polymere, **251**, 787-783, (1973)

197. Kanig G., 'Neue elektronenmikroskopische untersuchung uber die morphologie von polyathylenen', Prog. Colloid & Polym. Sci., **57**, 176-191, (1975)

198. Kanig G., 'Sichtbarmachung der feinsruktur von getemperten polyathylenproben durch kurzzeitontrastierung direkt bei der tempertemeratur', Colloid Polym. Sci., **255**, 1005-1007, (1977)

199. Voight-Martin I.G., 'Use of electron microscopy to obtain quantitative information about the melting behaviour of branched polyethylene' J. Polym. Sci., Polym Phys. Ed., **18**, 1513-1522, (1980)

200. Djerassi C., Engle R.R., 'Oxidations with ruthenium tetroxide', J. Am. Chem.Soc., **75**, 3838-3840, (1953)

201. Berkowitz L.M., Rylander P.N., 'Use of ruthenium tetroxide as a multi- purpose oxidant, J. Am. Chem. Soc., **80**, 6682-6684, (1958)

202. Trent J.S., Scheinbaum J.I., Couchman P.R., 'Electron microscopy of PS/ PMMA and rubber modified polymer blends: Use of ruthenium tetroxide as a new staining agent', J. Polym. Sci., Polym. Lett. Ed., **19**, 315- 319, (1981)

203. Trent J.S., Scheinbaum J.I., Couchman P.R., 'Ruthenium tetroxide staining of polymers for electron microscopy' Macromolecules, **16**, 589-598, (1983)

204. Vanderhoff J.W., Dimonie V. El-Aasser M.S., Klein A., 'Emulsion copolymerisation of azeotropic styrene- acrylonitrile monomer mixture in polystyrene seed latices', Makromol. Chem. Suppl., **10/11**, 391-402, (1985)

205. Joseph E.G. , Aguilera J.M., Houle J.R., 'The use of ruthenium trichloride/ aqueous clorox mixture as a staining agent in the morphological studies of styrene macromer containing acrylate', Polym. Preprints, **28(2)**, 345-346, (1987)

206. Feng D., Wilkes G.L., 'The structure-property behaviour of free radical synthesized PDMS-PS block polymers', Polym. Preprints, **28(2)**, 238-239, (1987)

207. Hobbs S.Y., Watkins V.H., Russell R.R., 'TEM studies of polymer blends stained with mercuric trifluoracetate' J. Polym. Sci., Polym. Phys. Ed., **18**, 393-395 (1980)

208. Lindeburg K.A.H., Johansson M, Bertilsson H.E., 'Effects of the addition of a multi-block copolymer to an incompatible blend' Plastics Rubber Proccessing and Applications, **14**, 195-202, (1990)

209. Shell UK publication, polymer data, (1977)

210. Koike T., 'Determination of glass transition temperature from dielectric analysis of a series of epoxide oligomers', J.Appl.Polym.Sci., **45**, 901-907, (1992)

211. Wehrli F.W., Wirthlin T.W., 'Interpretation of Carbon-13 NMR spectra',Heydon and Sons, (1967)

212. Hiemenz P.C., 'Principles of colloid and surface chemistry', Marcel Dekker, second edition, (1986)

213. Williams K.R., King R.W., 'The Fourier transform in chemistry-NMR', J. Chem. Ed., **67**, 93-105, (1990)

214. Garcia-Rubio L.H., 'The effect of composition, sequence length and tacticity on the UV absorption analysis of styrene copolymers in solution', J. Appl. Polym. Sci., **27**, 2043-2052, (1982)

215. Dynamic Light Scattering Photometer, DLS700 Operation Manual (Hardware version) Otsuka Electronics Company Ltd. (now available through Polymer Laboratories, Church Stretton, England)

216. Edwards K., Almgren M., 'Solubilization of Lecithin vesicles by $C_{12}E_8$', J. Coll. Interface Sci., **147**, 1-21, (1991)

217. Kaler E.W., Murthy A.K., Rodriguez B.E., Zasadzinski J.A.N., 'Spontaneous vesicle formation in aqueous mixtures of single-tailed surfactants' Science, **245**, 1371-1374, (1989)

218. Brennan D., 'Morphology of liners for Can Coating', ICI Packaging Coating Internal report, (1990)

219. Wright P., Beevers M., 'Multicomponent analysis using GPC', 206th ACS National meeting Chicago Il, August 22-27, (1993)